

NUMERICAL STUDY OF STRAIN RATE EFFECTS ON STRESS STRAIN

RESPONSE OF SOILS.

A thesis presented

for the degree of Doctor of Philosophy

in the Faculty of Engineering of the University of London

by

JOSE CARLOS ZIOLKOWSKI

B.Sc. Eng, M. Sc..

Department of Civil Engineering

Imperial College of Science and Technology

London,

October - 1984

To Riva and our parents.

ACKNOWLEDGEMENTS

The work described in this thesis has been carried out in the Soil Mechanics Section of the Civil Engineering Department, Imperial College, London. This thesis would not have been possible without the kind help of several people. The author wishes to thank Dr. P.R.Vaughan, interim head of the Soil Mechanics Section, when this research began in 1979, and later head of the section Prof. J. B. Burland, for taking interest in my work and for allowing it to be carried out in the academic environment of the Imperial College of Science and Technology. The author wishes to thank the Brazilian Government and the Conselho Nacional de Pesquisa (CNPq) for the financial support given.

The author would very much like to express his sincere gratitude to the extraordinary person, Dr. A. Skinner, appointed supervisor to this research, for his immense kindness, patience and understanding, particularly for supporting the author in every circumstance during the long period of contact. A great deal of help, encouragement, equilibrium and confidence was received from him during the course of this research to which the author is greatly in debt. Much useful help and constructive suggestions were given by Prof. J. B. Burland, David Potts, David Hight, Richard Jardine, and Dr. S. Cavoudinis.

Special thanks to Eileen Gibbs, Lou Spall, Fred Evans, Steven Ackerley and all the staff of the Soil Laboratory for the most friendly reception during tea time for during those years.

David Toll, a person whom the author greatly admires for his

experience, for his nature, devoted friendship, who made life in England more enjoyable and most of all easier, for his prompt and unscrupulous help in all matters and for the devotion of a great deal of his precious time painstakingly going through the whole thesis, suggesting, contributing and correcting the English use of language. There are no words to express the author's gratitude for what he has done in contributing to the completion of this thesis.

The author very much appreciated the valuable discussion and suggestion from his many colleagues in the Soil Mechanics Section, T. de Campos, M. Chandler, A. Fourie, L. Lemos, M. Martins, J. Maswoswe, S. Shibuya, M. Takahashi, D. Rinaldis, L. Costa-Filho, F. Lupini, P. Martins, and M. Symes, J. Hellings, E. Ovando-Shelley, M. Maccarini.

Malcom Clark, who made himself always available whenever help was required, specially when it concerned equations and computing, which the author greatly appreciated.

The author also wishes to thank his colleagues, U. Trueb, D. Bates, N. Agelidis, from the Structure section of Imperial College, for their help, discussion, and advice in computing method and finite elements affairs. Many thanks are due to Mrs Majorie Carter, Mrs. Kay Crooks and Ms. Stringer for their assistance in the library. Thanks are also due to Mr. H. Catanhede, for his friendship, willingness to help and for undertaking the task of draughting the figures for this thesis, work of a craftsman, and whose help was indispensable.

The author also wishes to extend his thanks to Prof. E. Osvaldo Cruz, representative of the Brazilian Institution CNPq here in London for his tireless support during the completion of this thesis.



Last, but not least, the author would like to thank Riva for her continuous encouragement throughout the research programme, for her uninterrupted and tireless assistance in typing the draft manuscript, and in making several of the drawings included in the report. Her support is most appreciated and valued by the author.

ABSTRACT

A discussion of consolidation of saturated clay is presented. The governing differential equations are reached using the concepts of continuum mechanics of a mixture, where one phase represents the deformable clay skeleton, and the other represents the pore fluid which fills the pores of the skeleton. A geometrically non-linear-system and a elasto-viscoplastic-plastic material are accounted for. For the geometrically non-linearity the up-dated Lagrange method is applied. Two independent yield surfaces have been used to describe the viscoplastic- plastic constitutive relationship, and an associative and/or a non-associative flow rule have been assumed.

Darcy's law for a deformable skeleton and a permeability matrix dependent on the void ratio have been taken into account.

An algorithm based on finite element discretization and numerical integration in time is adopted for the numerical treatment of the transient process. The finite element type chosen is a variable eight noded isoparametric one where the same number of nodes for displacement and pore water pressure have been adopted. A semi-implicit type method for time integration is used. For each time and/or load step a tolerable equilibrium condition is achieved iteratively to take into account the material and geometric non-linearities.

A sample of numerical examples have been calculated to show the

general abilities of the computer program.

Key words - Consolidation, finite elements, plasticity, creep, large deformation.

CONTENTS

## CHAPTER I - INTRODUCTION

I.1 - Need for More Realistic Analysis.....	1
I.2 - Purpose of this Research.....	2
I.3 - Original Characteristics.....	3
I.4 - Summary of the Contents and Scope of this Research.....	4

## CHAPTER II - PHENOMENOLOGICAL CONCEPTS

II.1 - Introduction.....	7
II.2 - Consolidation Phenomena.....	8
II.3 - Initial Settlement.....	9
II.4 - Primary Consolidation.....	10
II.5 - Secondary Consolidation.....	11
II.6 - Terminology.....	12
II.7 - Basic Principles: Discussion.....	13

## CHAPTER III - CONSOLIDATION THEORY : BRIEF SURVEY

III.1 - Introduction.....	16
III.2 - Basic Characteristics and Applicability.....	16
III.3 - Non-Consistent Theory: Brief Discussion.....	18

III.4 - Self Consistent Theory: Biot's Theory.....	20
III.5 - Continuum Theory Approach.....	21
III.6 - Solution Methods.....	23
CHAPTER IV - CONTINUOUS MECHANICS OF MIXTURE REVIEW	
IV.1 - Introduction.....	24
IV.2 - Body Motion.....	25
IV.3 - Independent Variables.....	27
IV.4 - Strain Definitions.....	30
IV.5 - Strain Invariants.....	35
IV.6 - Compatibility Conditions.....	40
IV.7 - Force Distribution, Mass Density, Internal Energy Density...	42
IV.8 - Global Balance Law.....	43
IV.9 - Local Balance Laws.....	46
IV.10 - Definition of Stress.....	49
1. Stress Vector.....	49
2. Stress Tensor.....	51
CHAPTER V - VARIATIONAL METHOD	
V.1 - Introduction.....	60
V.2 - A Brief Survey of Different Approaches.....	61

V.3 - Principle of Virtual Work.....	65
--------------------------------------	----

#### CHAPTER VI - FIELD EQUATION IN INCREMENTAL FORM

VI.1 - Introduction.....	69
--------------------------	----

VI.2 - Velocity Increment.....	73
--------------------------------	----

VI.3 - Strain Increment.....	74
------------------------------	----

VI.4 - Stress Increment.....	76
------------------------------	----

VI.5 - Stress-Strain Increment Relationship for the Solid Skeleton.	78
---	----

VI.6 - Stress-Strain Increment Relationship for the Fluid Phase and Darcy Law.....	81
---	----

VI.7 - Bernoulli's Theorem - Darcy's Law.....	83
---	----

VI.8 - Total Lagrange Formulation.....	85
--	----

VI.9 - Updated Lagrange.....	88
------------------------------	----

VI.10 - Linearization of Equilibrium Equations.....	90
---	----

#### CHAPTER VII - FINITE ELEMENT SOLUTION

VII.1 - Introduction.....	93
---------------------------	----

VII.2 - Finite Element Solution.....	93
--------------------------------------	----

VII.3 - Finite Element Matrices.....	95
--------------------------------------	----

VII.4 - Numerical Integration.....	99
------------------------------------	----

VII.5 - Equilibrium Iteration.....	101
------------------------------------	-----

## CHAPTER VIII - CONSTITUTIVE LOCAL STRESS-STRAIN RELATIONSHIPS

VIII.1 - Preliminaries.....	107
VIII.2 - Brief Description of Soil Properties.....	108
VIII.2.1 - Soil Properties in the Quasi-Static Region.....	111
1. Triaxial Test Conditions.....	111
2. Third Stress Invariant.....	125
VIII.2.2 - Properties of the Material in the Kinematic Region.....	131
1. Speculative Introduction.....	131
2. Failure Envelope Line.....	132
3. Peak Strength, Pore Water Pressure Generation.....	133
VIII.2.3 - Effect of the Strain Rate on the Stress-Strain Relationship Based on the Elasto-Plastic Theory.....	136
1. First Yielding.....	136
2. Shape of the Yield Locus and Plastic Potential.....	136
3. Elastic Constants.....	137
VIII.2.4 - Material Behaviour for Rates Smaller than the Quasi-Static One.....	138
VIII.3 - Brief Comments on Various Attempts.....	139
VIII.3.1 - Elasticity- Viscoelasticity.....	140
VIII.3.2 - Hyper and Hypoelasticity-Visco-Hyperelasticity.....	142
VIII.3.3 - Hypo-Elasticity.....	142

VIII.3.4 - Elasto-Plasticity.....	144
VIII.3.5 - Elasto-Viscoplasticity Endochronic Theory.....	155
VIII.3.6 - Viscoelastic-Plastic and Viscoelastic-Viscoplastic Models.....	156
VIII.3.7 - Elastic-Viscoplastic-Plastic Model.....	159
VIII.3.8 - Elasto-Plastic Kinematics Hardening Model.....	161
VIII.3.9 - Elasto-Viscoplastic Kinematic Hardening Model.....	163
VIII.4 - Explicitly Local Constitutive Stress-Strain Relationship.	164
1. Elasto-Viscoplastic Kinematics.....	165
2. Elasto-Viscoplastic Kinematics- Vanishing elastic region.	173
3. Elasto-Viscoplastic-Plastic Model.....	178
4. Constitutive Law in Stiffness Form.....	179
5. Yield and Potential Surfaces Form.....	181
6. Practical Application of the Models.....	201
 CHAPTER IX - SAMPLE SOLUTIONS	
IX.1 - Introduction.....	234
IX.2 - Static Linear Analysis.....	236
IX.2.1 - General.....	236
IX.2.2 - One-dimensional Test.....	237



IX.2.3 - Two-dimensional Problem.....	248
IX.2.4 - Axi-symmetric Load on Finite Layer.....	251
IX.2.5 - Creep Effect.....	253
IX.3 - Static Non-linear Analysis.....	255
IX.3.1 - General.....	255
IX.3.2 - Linear Material Non-linear Geometry Analysis.....	257
IX.3.3 - Elasto Perfectly Plastic Material and Non-linear Geometry	257
IX.3.4 - Elasto-plastic Material and Linear Geometry.....	259
IX.3.5 - Non-linear Geometry and Creep Influence.....	262
CHAPTER X - CONCLUDING REMARKS	
X.1 - General Results.....	265
X.2 - Future Developments.....	268
APPENDIX A - A BRIEF SUMMARY OF MATHEMATIC BACKGROUND.....	A1
APPENDIX B - GEOMETRIC TRANSFORMS IN DEFORMATION - AREA AND VOLUME.	B1
APPENDIX C - EXPLICIT STIFFNESS MATRICES.....	C1
APPENDIX D - MATRICES OF ELASTIC CONSTANTS.....	D1
APPENDIX E - REFERENCES.....	E1

NOTATIONS AND LIST OF SYMBOLS

Both indicial notation and matrix notation have been used in this report. Notations from classical continuum mechanics will be used unchanged as far as possible.

Tensors are to a great extent treated as dyadics implying that the specification of a coordinate system is conveniently avoided. However, tensor equations and scalar equations are also given in a component form with indices. The summation convention is used if not otherwise specified in the text. Equations containing physical variables are often given in a matrix form, which is convenient for programming purposes. Although, notation and symbols are explained as they appear in the text for the first time, some explanation will be made in a general list of symbols and notations.

The right subscript in the roman characters  $i, j, k$ , etc denote variation of the index over a range of values 1, 2, and 3. The greek index  $\alpha$  denote variation over a range of values 1 and 2. The left superscript define the configuration of the body to which the variable is referred to. The left subscript define which independent variable describe the function. In the case of two left subscript the first refers to the independent variable and the second refers to the reference frame (deformed and undeformed frame).

Latin Letters:

$A$  -Generalized point, Constant.

$\bar{A}$  -Constant.

$a$  -Identity matrix, Ordinate of the bound or yield surface.

$a_i$  -Vector position.

$a^0$  -Ordinate of the yield surface.

$a^s$  -Ordinate of the surface  $f^S$ .

$\bar{a}_i$  -Interpolation function.

$ac$  -Acceleration.

$B$  -Domain, Strain displacement matrix, Constant.

$\bar{B}$  -Constant.

$b$  -Third invariant function of Lode angle, Ordinate of the surface  $f^S$ .

$b_i$  -Vector position, Unit vector in the direction of gravity.

$b_\beta$  -Elipse semi-axes length.

$C$  -Stiffness matrix, Constant

$C_i$  -Constant.

$C_u$  -Shear strength in compression.

$C_{ue}$  -Shear strength in extension.

$C_p$  -Peak strength in compression.

$C^{ep}$  -Elasto-plastic flexibility matrix.

$\bar{C}$  -Constant.

$c_{ij}$  -Deformation tensor

$c_{ijkl}$  -Stiffness matrix

${}^j c_{ijkl}$  -Jauman's stiffness matrix.

$c$  -Lagrange multiplier, Ordinate of the surface  $f^S$ .

$C_{v1}$  -1-D coefficient of consolidation.

$C_{v3}$  -3-D coefficient of consolidation.

$c_\beta$  -The proper numbers.

$D$  -Linear elastic matrix, Transformed permeability matrix, Stiffness matrix, Constant.

$\bar{D}$  -Constant.

$D^{ep}$  -Elasto-plastic stiffness matrix.

$d$  -Angle between the stress rate direction and the normal to the yield surface, Ordinate of the surface  $f^S$ .

$\det$  -Determinant.

$div$  -Divergent.

$d r$  -Differential of the vector  $r$ .

$E$  -Elastic modulus, Gradient of interpolation function matrix, Lagrange multiplier, Constant.

$\bar{E}$  -Constant.

$e_{ij}$  -Strain tensor.

$e$  -Simplified notation of the strain tensor  $e_{ij}$ , Void ratio, Neper

number.

$e^p$  -Plastic void ratio.

$e_1, e_2, e_3$  -Principal strain components.

$\bar{e}_{ij}$  -Deviator strain tensor.

$\bar{e}$  -Simplified notation of the deviator strain tensor  $\bar{e}_{ij}$ .

$e_{klm}$  -Alternative tensor.

$F$  -Force vector, Constant, Ratio between the quasi-static yield surface and the reference quasi-static yield surface.

$f$  -Force by unit of total volume mixture, Generalized scalar function.

$f_{xy}$  -Compressive (positive) strain in the x direction.

$f^s$  -General yield surface, Plastic potential or bounding surfaces.

$f_R^2$  -Reference quasi-static yield surface.

$G$  -Finite element matrix.

$G_s$  -Shear modulus.

$g$  -Generalized scalar function, Plastic potential.

$g_i$  -General shape function on the  $\pi$ -plane.

$g_{xy}$  -Expansive (negative) strain in the y direction.

$H$  -Finite element matrix.

$H_p$  -Hardening parameter at a point on the yield surface.

$H_{p0}$  -Maximum hardening parameter.

$H_R$  -Hardening parameter at a point on the bounding surface.

$\bar{H}$  -Scalar function.

$h$  -Hydraulic head, Vector of creep law (function of stresses and time).

$I$  -Component of unit vector constant.

$I_1, I_2, I_3$  -Strain invariant.

$\bar{I}_1, \bar{I}_2, \bar{I}_3$  -Deviatoric strain invariant.

(i) -Indicate iteration i.

$J$  -Jacobian.

$J_1, J_2, J_3$  -Stress invariant.

$J_m$  -First stress invariant of the translated stresses.

$J_3$  -Third deviatoric stress invariant of the translated stress.

$\bar{J}_1, \bar{J}_2, \bar{J}_3$  -Deviatoric stress invariant.

$j$  -Approximate determinant of J.

$K$  -Permeability matrix.

$K_{ij}$  -Permeability matrix.

$K_L$  -Finite element matrix.

$K_{NL}$  -Finite element matrix.

$K_R$  -Hardening parameter at a point on the bounding surface.

$k$  -Constant ratio of the second deviatoric stress invariant to the

first invariant, hardening parameter.

$L$  -Finite element matrix, Generalized geometric transformation, 1-D sample length.

$l_{kl}$  -Infinitesimal strain tensor, interpolation function.

$m$  -Number of finite element, Mass.

$m_v$  -Coefficient of compressibility.

$N$  -Finite element matrix.

$n_b$  -Value of  $\eta$  at ordinate  $b$  on the surface  $f^S$ .

$n_c$  -Value of  $\eta$  at ordinate  $c$  on the surface  $f^S$ .

$n_k$  -Components of unit normal vector.

$n_{1k}, n_{2k}, n_{3k}$  -Principal directions.

$P$  -Generalized point, Generalized point on the yield surface.

$P_{fc}$  -Mean stress at failure in compression.

$P_{fe}$  -Mean stress at failure in extension.

$P_{ij}$  -Viscous stress tensor.

$p$  -Pore-Pressure, Mean stress.

$p_0$  -Initial pore water pressure.

$q$  -Function of the second invariant of stresses.

$R$  -Vector of boundary conditions, Generalized point at bounding surface.

$r$  -General variable, Distance between two points.

- $S_a$  -Tangent at ordinate a of surface  $f^S$ .
- $\bar{S}_a$  -Tangent at ordinate a of surface  $f^S$  for  $\theta = \pi/6$ .
- $S_c$  -Tangent at ordinate c of surface  $f^S$ .
- $\bar{S}_c$  -Tangent at ordinate c of surface  $f^S$  for  $\theta = \pi/6$ .
- $\bar{S}_0$  -Tangent at ordinate a of surface  $f^S$ .
- $s$  -Element area.
- $T$  -Generalized transformation symbol, Transformation matrix.
- $T_1$  -1-D time factor.
- $T_3$  -3-D time factor.
- $t$  -Time.
- $tol$  -Tolerance
- $tr$  -Trace.
- $U$  -Dimensionless pore water pressure.
- $u_i$  -Displacement vector.
- $v$  -Velocity.
- $w$  -Settlement.
- $w_{kl}$  -Infinitesimal rotation tensor.
- $w^f$  -Total settlement.
- $x$  -Position vector.



Greek Letters:

$\alpha^P$  -Integration constant, Translated tensor.

$\alpha_{ij}$  -Translated tensor.

$\alpha_{II}$  -Spherical component of the translated tensor.

$\bar{\alpha}_{ij}$  -Deviatoric components of the translated tensor.

$\beta$  -Constant, Integration constant, Rate function parameter, Stress rate direction.

$\gamma_f$  -Pore fluid unit weight.

$\Delta$  -Increment.

$\delta$  -Virtual increment, Transformed distance between a point on the yield surface and the conjugate on the bounding surface.

$\delta_{kl}$  -Kronecker Delta.

$\delta_i$  -Distance between two points in distinct surfaces.

$\delta_0$  -Maximum distance between two points in distinct surfaces (material memory)

$\epsilon$  -Strain vector, Internal energy density.

$\epsilon^e$  -Elastic strain tensor.

$\epsilon^{vp}$  -Visco-plastic strain tensor.

$\epsilon_v$  -Volumetric strain component.

$\epsilon_q$  -Deviatoric strain component.

$\epsilon^p$  -Plastic strain tensor.

$\epsilon_{ij}$  -Linear strain tensor, Part of the strain tensor function of linear terms of displacement increment.

$\eta$  -Ratio of the second deviatoric invariant to the first invariant.

$\eta_{ij}$  -Part of the strain tensor function of non-linear terms of displacement increment.

$\theta_i$  -Lode angle of strain.

$\theta_j$  -Lode angle of stress.

$k$  -Compressibility constant.

$k_{ij}$  -Constants.

$\Lambda$  -Creep function (function of time).

$\lambda$  -Stretch of line segment, Compressibility constant, Constant.

$\mu$  -Constant.

$\nu$  -Poisson ratio

$\xi_k$  -Finite element interpolation function.

$\bar{\xi}_0$  -Ratio between two ordinates of the general surface  $f^S$  for  $\theta = \pi/6$  .

$\bar{\xi}_1$  -Ratio between two ordinates of the general surface  $f^S$  for  $\theta = \pi/6$  .

$\bar{\xi}_2$  -Ratio between two ordinates of the general surface  $f^S$  for  $\theta = \pi/6$  .

$\pi$  -Constant.

$\rho$  -Mass density.

$\sigma$  -Stress tensor.

$\sigma_{kl}$  -Stress tensor.

$\sigma_{(n)}$  -Force per unit of surface of the mixture.

$\sigma_m$  -First stress invariant.

$\bar{\sigma}$  -Second deviator stress invariant, Second deviator stress invariant of the translated stress.

$\bar{\sigma}_+$  -Second deviator stress invariant for  $\theta = \pi/6$  .

$\bar{\sigma}_{ij}$  -Deviator stress tensor.

$\bar{\sigma}_k$  -Traction vector.

$\tau_k$  -Generalized tensor field, Vector function.

$\Phi$  -Friction angle, Creep function (function of stresses).

$\chi$  -Constant.

$\psi$  -Vector function, Generalized function, Finite element interpolation function.

$\Omega$  -Complementary energy function.

$\omega$  -General surface.

$\vartheta$  -Volume.

Script Letters and Miscellaneous Symbols:

$\mathcal{E}$  -Internal energy.

$\mathcal{K}$  -Kinematic energy.

$U_{\xi}$  -General energy source.

$\mathcal{W}$  -Rate of work for force and couples.

$\times$  -Cross product symbol.

$\cdot$  -Scalar product symbol.

$\frac{d}{dt}$  or  $\cdot$  -Material time derivative.

$\nabla$  -Gradient operator.

$\frac{\partial}{\partial x_k}$  -Space differentiation.

$\frac{\partial}{\partial t}$  -Time derivative.

$\mathcal{T}$  -Indicate Transport.

$\theta_1$  -Angle between the tangent at the general surface  $f^S$  and the axes direction, for  $\theta = \pi/6$ .

$\theta_2$  -Angle between the tangent at the general surface  $f^S$  and the axes direction, for  $\theta = \pi/6$ .

## CHAPTER I

### INTRODUCTION

#### I.1 The Need for More Realistic Analysis

In engineering practice the requirement for analysis of the mechanical behaviour of clays has always been a challenge for the engineer. After Terzaghi's pioneering work (1925,1943) an enormous amount of literature has been dedicated to this subject, and a lot has been done. From a broad point of view, the modelling technique employed in predicting the mechanical behaviour of clays should take into account the most flexible boundary conditions (static and dynamic analysis for periodic and non-periodic loading conditions), the consolidation phenomena, the effect of geometry change, the material non-linearity, the time effect on the material properties and multidimensional effects.

The need for such an analysis can be appreciated if one considers for example the problem of predicting the effect of changing the hydraulic equilibrium in an aquifer confined by a clay layer. Such non-equilibrium conditions may arise from ground water discharge, tunnelling in rock or soil beneath the aquifer, or from a change of the infiltration characteristics of the surface in urban environments. These problems can involve a significant amount of pore-pressure decrease beneath the clay which yields consolidation until hydraulic

equilibrium is achieved. Obviously a reliable prediction of the resulting non-uniform settlement, which may cause serious damage to a building standing on the surface, can not be achieved if the major mechanical concerns described previously are not taken into account.

Although innumerable analytical consolidation problems has been considered for specific circumstances, there has been no evidence of a case, which has yet taken into account these major mechanical characteristics . In fact most of existing analytical consolidation theories in engineering practice assumes an isotropic linear material with geometric linearity, static and fixed boundary conditions and one-dimensional straining and pore-water flow. There is an urgent need for the development of more appropriate models.

Although much has been achieved in this direction there is still a lot which needs to be done, especially in the area concerning the modelling of material properties which has not yet been definitely nor satisfactorily solved.

### I.2 Purpose of this Research

The main aim of this research is to describe the consolidation process of saturated clay which embodies all the features mentioned in the previous section, except for the cyclic and dynamic loading, and to provide a solution procedure for the appropriate governing partial differential equations resulting from the general equation of motion for a mixture of two continua.

The model proposed here provides a tool for computation of settlement,

lateral movement, stresses, pore-pressure and the failure stresses , creep, etc... for any static non-periodic loading path-time programme with variable geometry in an unified manner. If the failure stresses are known the safety factor can be estimated for the specified loading path-time programme.

Based on the finite element method a relatively flexible computer program has been implemented. The computer results should be observed with due attention to the reliability of the input data concerning whether the material model (based on data obtained in simplified laboratory conditions with disregard for some important material properties) is representative of the field conditions, the difficulty in obtaining true values for the constitutive parameters and initial stresses and, also the uncertainty over the laboratory precision.

### I.3 Original Characteristics

To the author's knowledge some features concerning consolidation analysis are original in this work:

- 1) Application of total Lagrange and up-dated Lagrange method to describe the governing equation of the consolidation problem and the use of up-dated Lagrange in the finite element consolidation problem.
- 2) The proposition of a general elasto-viscoplastic non-associated model which can be simplified to almost any known elasto-viscoplastic model and can be calibrated to almost any experimental results. The advantage is that, apart from embodying the usual more rigid models, it also allows the engineer to accommodate more soil features, which

are not possible in other models.

3) The use of an elasto-viscoplastic-plastic constitutive model which allows consolidation at large displacement to occur simultaneously.

#### I.4 Summary of the Contents and Scope of this Research

In Chapter II, clay characteristics are broadly described together with the usual concepts, principles and terminology concerning the consolidation problem.

In Chapter III, a very brief description of the main approaches used for modelling the consolidation phenomena, with particular emphasis on the distinction between non-consistent and consistent theories. References to the continuum mechanics approach are also made.

In Chapter IV a very compact and solid review of the equation of motion for a mixture of continua is described where nothing is left unjustified. Every single equation being based on previously established ones. The Euler and Lagrange methods are both considered and when pertinent the various interrelations between variables from one approach to the other are included. No restriction at all, apart from disregarding the acceleration effect, is made to this formulation. In this chapter the equation of motion for the mixture is obtained in the local reference frame as a function of Euler and Lagrange variables and is then converted to a global reference frame.

A brief description of the variational method is considered in Chapter V. In this chapter, the principle of virtual work to represent the



equilibrium equations and an integral form of the continuity equation are included.

In Chapter VI the conditions required for frame-indifference constitutive equations and permeability matrix are discussed in detail. Various constitutive equations and permeability matrices are postulated and the geometric transformation to be applied to the postulated property to satisfy the frame indifferent principle are deduced for the most fundamental stress and strain rate definitions.

The Darcy law for large displacement is also included. Additionally a more convenient form of the total Lagrange and up-dated Lagrange consolidation theories for finite element application are presented. Finally the required transformation of these non-linear theory to an approximated linear one is introduced.

The system of approximated linear equations presented in Chapter VI are discretized for a finite element solution in Chapter VII. All the finite element matrices are presented for the Lagrange and up-dated Lagrange methods. Numerical integration in space and time is briefly discussed. Also the equilibrium iteration scheme, the calculation procedure and convergence conditions are presented.

In Chapter VIII a local stress-strain relationship review is presented. Fundamental experimental results proving the inapplicability of the Rendulic principle (one of the basic assumptions of the critical state theory) are presented. It is interesting to note that even for isotropic kaolin it does not seem to be applicable.

In this chapter two distinct constitutive model for the solid skeleton are described. One based upon the elastic-viscoplastic kinematic approach and the other upon the elasto-viscoplastic-plastic kinematic approach. In the first model the shape of yield surface and plastic potential can be assumed as functions of the initial conditions and the past history of stress and also of the strain or stress rate. Also, the hardening parameter can be assumed as an independent function of plastic strain and either strain or stress rate. In the second model an inviscid behaviour is accounted for within the concept of critical state and the viscid behaviour is accounted for by means of an appropriate creep law. Although cyclic loading is not discussed in this report the effect of this kind of action could be included. Consequently liquefaction due to growth in pore-pressure is beyond the scope of this report.

The computer program, its construction and versatility is briefly described in Chapter IX. A sample solution illustrating the accuracy and flexibility of the program is presented. The response to the variation of the parameters is studied too.

Concluding remarks and suggestions for future research in the area of consolidation with related problems are found in Chapter X.

Four appendices containing information to support the main text are included. That is to say, mathematical background, explicit finite element matrices, the general elasticity matrix and references to literature.

## CHAPTER II

### PHENOMENOLOGICAL CONCEPTS

#### II.1 Introduction

From the physical microscopic model point of view, clay is inherently a multi-phase system consisting of a mineral phase, known as the mineral skeleton, plus fluid phases, denominated pore fluids. The clay particles consist of crystalline particles, mainly silicate molecules. The mechanical properties of the skeleton are affected by aggregates, which are formed from clay particles linked together by physico-chemical forces. Oxides or organic molecules may also be present, giving special features to the mechanical properties of the clays.

Since the solid particles are, in most cases, surrounded by water ions, they do not touch each other directly.

The distribution of particles in the aggregates as well as the way in which the aggregates attach to each other, form what is called the soil structure.

The structure, which greatly depends on the environment of sedimentation, reflects the mechanical properties of clays.

For example, in marine clays the aggregates are large and dense and are arranged in such a way that produces large pores. In lacustrine clays, however, the aggregates are comparatively small and the skeleton is compact giving a smaller porosity.

## II.2 Consolidation Phenomena

From the mechanical point of view clay is a deformable porous medium. During Geological history, clay, in situ, has always been pre-stressed and pre-deformed. This initial state of stresses equilibrates forces acting over the soil mass. Such forces are usually gravitational forces and percolation forces, created by natural flow conditions.

When a layer of clay is subjected to an additional surface load, a field of deformation occurs. If this load is instantaneously applied, partly initial and partly time-dependent settlements will occur. The concept of instantaneous loading is an idealized assumption, and it is only used for the sake of simplicity. Also, when this time dependent process is induced by a change in pore-pressure, no such initial settlement will occur in saturated clay soil .

Usually, consolidation settlement is defined as the phenomenon caused by a time-dependent volume change in the soil skeleton. It is, however, convenient to point out here that volume change without deviatoric strain does not occur in practice, and the water flow takes place, in general, in three directions.

Although in the standard oedometer test the straining and water flow takes place vertically only, the stress state changes in a particular

way in triaxial conditions, so, it is common to interpret the field consolidation settlements for almost any stress-path, from the axial displacement obtained oedometer test .

Also the consolidation phenomenon is usually divided into a main part called "primary consolidation" which is followed by a secondary part named "secondary consolidation". Such classification of consolidation is due to the fact that the process as observed in the early days of experimentation, an oedometer test results, was considered composed by two different physical processes. A different approach will be discussed later in this chapter.

### II.3 Initial Settlement

The initial settlements are caused by recoverable and irrecoverable deformations. If the clay is normally consolidated or slightly overconsolidated, irrecoverable deformation will dominate, for active loading increment. Obviously, recoverable-irrecoverable deformation generally occurs with volume change of the soil skeleton (swelling or contraction).

From a physical point of view, clay is often assumed to be initially incompressible. The validity of this assumption, however, requires that the clay must be saturated and pore water and solid particles must be considered incompressible. In practice, the latter assumptions are quite reasonable whilst the former is not always valid.

It is clear, then, that if the above assumptions hold, the incompressibility condition of the system is in fact a direct

consequence of the assumption that the deformation takes place under the constraints of undrained conditions. This does not imply, however, that there will be no local flow of pore water through the clay pores. Within the framework of a theoretical continuum model for clay, the incompressibility condition can be verified. In this idealized model, however, nothing is required to be said about the individual compressibilities of the soil particles and the fluid. The difficult task involved in including individual compressibilities is encountered in the definition of the load sharing among the different phases.

#### II.4 Primary Consolidation Process

The main feature of the primary consolidation process is the transient flow of pore water, followed by a field of deformation of the solid skeleton. It is widely accepted that the flow is governed by the water pressure gradient introduced by loading. The process is usually treated as quasi-dynamic because acceleration effects are considered negligible both in the soil skeleton and in the pore water.

For pulsing loads like wave loads in offshore engineering or for shock loads from deformations, however, inertia effects must be included.

The rate of change of water flow from a unit of bulk volume equals the rate of skeleton volume change during deformation. This latter remark comes from the continuity matter assumptions in the consolidation theory formulation.

The deformation field in a consolidation process continues until a

state of hydraulic equilibrium is achieved or failure of the clay mass occurs due to uncontrolled growth of deformations. For constant boundary conditions a stable process have the deformation field theoretically the process is asymptotic in time, though, in practice a certain finite time is required to finish the process.

It is usually assumed that the hydraulic equilibrium (steady state flow or no flow) corresponds to zero volumetric strain rate, which, if no creep(or relaxation) is included, the constitutive properties of the clay skeleton, is equivalent to zero effective volumetric stress rate.

The steady state will occur when the excess pore pressure boundary conditions are non-homogeneous, while no flow conditions are present when these boundary conditions are homogeneous.

### II.5 Secondary Consolidation

Secondary Consolidation is usually thought of as the process which follows the primary one. It is characterized by the continuation of settlement in the oedometer test after pore pressures have apparently dissipated. The physical character of the secondary consolidation process has not quite been satisfactorily investigated and, hence, is not fully explained. It is believed, however, that the secondary process presented by the deformation of clay skeleton are of viscous type and a large literature has been dedicated to visco-elastic or visco-elasto-plastic creep in soils.

In practice it has been observed that the viscous effect appears in

all soil but is particularly significant for normally consolidated clay. There has been some disagreement about the achievement of rupture state by creep (Bishop,1966) . However, it is believed that creep rupture may occur under certain conditions (Mitchell, 1976).

### II.6 Terminology

The distinction between primary and secondary consolidation is traditional in Soil Mechanics. Both processes however, are simultaneous during the entire deformation process. One possible physical interpretation of this phenomena, is that the volume change caused by the flow conditions breaks the local equilibrium of the soil structure, which can not find its new local equilibrium configuration instantaneously. Accompanying the dissipation of pore pressure and volume changes(due to what is known as primary consolidation) additional volume and hydraulic gradient changes are introduced due to the accomodation of particles on the way to their final local equilibrium. These interactive processes occur until no flow occurs. As a matter of fact it goes on even after no noticeable flow is recorded.

Following the same argument, towards the end of the process when hydraulic equilibrium is achieved, the rate of accomodation of particles has been reduced to a level where deformation can occur without any considerable change in hydraulic gradient, and consequently causing no noticeable fluid flow. Flow however must occur otherwise the solid particles themselves have to suffer change in volume, which is unlikely.



In this thesis the term consolidation will be use to describe the more involved process mentioned above. In other words the rate of deformation (both volumetric and deviatoric parts) is controlled partly by the constitutive law governing the diffusion and partly by the rheology of the soil skeleton , where both phenomena interact throughout the whole process.

### II.7 Basic Principles: Discussion

In an analysis of the consolidation process some principles must be adopted before obtaining a final result from the computation. Some basic priciples are presented and commented on briefly. They are as much as possible in agreement with the physical observation discussed above.

The formulation has to be founded in the classical concepts of mechanics. The distribution of the various quantities in space and time are formulated with the support of the Continuum Mechanics Model.

Although it is well known from the microscopical observations of soil that the microstructure to some extent has a random constitution which results in discontinuities within the soil mass, a two phase continuous medium is assumed.

As mentioned previously, this internal characteristic may to a large extent govern the macrophysical behaviour of clay during the entire process of deformation. Even yield processes occuring in normally consolidated clay may be explained by the propagation of small local structure colapse.

Also the physical characteristics of soil material contained within an infinitesimal volume element are considered to be the same as those determined experimentally from measurements on samples with finite dimensions.

Secondly, the effective stress principle is assumed. This principle, first postulated by Terzaghi (1923), means that the effective stresses in the soil skeleton and the pore water pressure are considered as partial stresses, which are assumed to act in the entire bulk volume. In addition, skeleton deformations are only due to the effective stresses. Because pore water viscosity is neglected in the equations of motion, (although not neglected in the flow relations) the pore water stress is considered to be isotropic, i.e., independent of the flow velocity gradients.

A third feature concerns the loading procedure. For explicit formulation of governing equations it is considered that the load (at least for most theories) is instantaneously applied. The accuracy of such an idealization should be judged in conjunction with permeability and compressibility properties of the soil skeleton. In fact, consolidation and creep occurs even during the construction stage, which means that in cases where the permeability is not small and the viscosity is not very large, the time dependent processes during loading can not be neglected.

A fourth feature concerns the geometry change during the consolidation process. Again for explicit formulations the governing equation of consolidations is assumed to retain its initial geometric configuration during the whole process of deformation. This

idealization may be applied in cases when the soil compressibility is relatively small but when very compressible material, (as is usually true of normally consolidated clay) is analysed, such assumptions may provide extremely crude results.

A fifth feature concerns the proper choice of constitutive models. The main constitutive characteristic of the clay skeleton is that it can accommodate recoverable and irrecoverable deformations. The actual classification of these deformations into elastic, plastic or viscous remains yet to be achieved.

It is indeed recommendable to think of the constitutive characteristic of a constitutive model as being reflected by recoverable and irrecoverable deformations, whose actual value depends on the strain rate of deformation. Depending on prior anisotropic stresses in the soil mass, material anisotropy will be induced (which effects the constitutive relations). Even loading-unloading stress-paths on initially isotropic material still produces remarkable effects on the constitutive law (the Hysteresis effect).

According to the observations pointed out previously one would be discouraged from searching for a simple model to represent the constitutive model for soil.

### CHAPTER III

#### CONSOLIDATION THEORY : BRIEF SURVEY

##### III.1 Introduction

No attempt has been made to go into details of the entire development of the consolidation theories, but entire books have been dedicated to the matter (Zaretskii, 1967).

The intention here is to emphasize the main points of the constitution of multi-dimensional self-consistent models.

Although the well known non self-consistent one dimensional theories have played a great role in practical calculations since the birth of soil mechanics, only brief comments will be made on them.

The term non self-consistent is applied in this thesis to those theories where total equilibrium and strain compatibility are not satisfied.

##### III.2 Basics Characteristics and Applicability

A number of theories for the theoretical treatment of the consolidation of soil have been presented in the literature. Many of

these theories, however, are restricted to conditions which are characterized by the explicit solution technique to be employed. Many of the older theories are characterized by properties which seriously affect their applicability.

In particular it is frequently assumed that the strain and flow conditions are uni-dimensional. Only under certain rather idealized circumstances do calculations based on these hypotheses give accurate results.

It is implicitly assumed in the one dimensional theories that differential settlement within the soil mass can not occur.

Most engineering loading produce differential settlement which is at variance with the uni-dimensional theories.

Most consolidation models, whatever the soil skeleton constitution, do not satisfy the basic requirement of equilibrium and continuity conditions , i.e., they provide the calculation of pore-pressure but not the effective stresses. The convenient consolidation equation is obtained from the continuity equation under the assumption of certain strain and flow conditions. Such models are said to be non self-consistent.

The imposed strain conditions do not coincide with those corresponding to the effective stress field assumed in most of engineering practice, especially in the inelastic range where the disagreement may be substantial.

Also in most practical circumstances, for example when pore pressure

redistribution takes place, the assumption of constant total stress imposed by most non-consistent theories may seriously affect the effective and pore-pressure calculations and consequently the strain distribution.

The stress distribution is often obtained by evaluating the total stress directly. Particularly in the plain strain situation it is common to assume an infinite half-plane loaded with a surface load while the clay is assumed to be an elastic isotropic solid. Even rougher stress estimates are frequently used. Such estimates are obtained under the assumption that the vertical stress beneath the centre of a uniform load decreases hyperbolically with the depth underneath the load surface. A slightly improved formula was proposed by Frohlick (1933), who also provided the estimation of stresses off the centre line of a circular load.

It seems that not many comparisons between the practical application and the self-consistent theory has been made. A problem for which non-consistent theory seems to give acceptable results is consolidation by means of vertical drains, particularly when the water flow will be radially towards a cylindrical drain resulting in a one dimensional flow equation in radial coordinates, and the strain is assumed to be uniform and vertical only.

### III.3 Non-Consistent Theory : Brief Discussion

The most well known one-dimensional theory is that by Terzaghi (1943). In this theory excess pore pressure is evaluated by a parabolic differential equation of the heat conduction type. Within the same

basic assumptions , the generalization of this theory was first suggested by Rendulic (1936) and it is known as Biot's pseudo-theory (see Schiffman et al (1964))

Few versions of the Terzaghi-Rendulic theory has been presented for particular problems. A two dimensional variation is used in ground water hydrology for the analysis of aquifers. The variation of the hydraulic head is assumed to be horizontal and strain is assumed to be vertical .

Although distortion can occur in the Terzaghi theory the change in effective stress is assumed to be zero initially. Obviously, this assumption is very crude from the engineering practice point of view, apart from seeming inconsistent. A slight modification was introduced by Skempton and Bjerrum (1957), who assumed that the initial pore pressure is not equal to the total vertical stress. In this way they provided a tentative attempt to avoid the assumption of zero lateral strain imposed in the one-dimensional theory. In such a case non-zero initial settlement is obtained.

Rheological effects in one dimensional problems were introduced by Taylor and Merchant(1940), Tan (1957), see also McNabb (1960) and Gibson et al (1961). In Taylor's theory, for example, the soil skeleton is assumed to behave as a Kelvin body, while in Tan's theory a Maxwell type solid is considered.

In these theories primary and secondary consolidation are assumed to occur simultaneously. However, they have been restricted to linear models.

Consolidation theories where non-linear rheological effects are considered were introduced by Schiffman (1959), Murayama and Shibata (1958) and Abdel-Hady and Hervin (1966). Schiffman (1959) proposed a linear elastic and constant viscous effect. In the Murayama and Shibata (1958) and Abdel-Hady and Hervin (1966) both viscous and elastic effects are considered to be non-linear. A discussion of Murayama and Shibata's model can be found in the Rheology of Soil Mechanics (1964). Many other models were introduced, each combining different arrangements of springs, dashpots, and friction bodies.

#### III.4 Self Consistent Theory : Biot's Theory

The self consistent theories are those where equilibrium and compatibility conditions are fully satisfied. This is the case for Biot's theory. In the first formulation Biot (1941a and 1941b) a linear isotropic soil skeleton and linear permeability were assumed. The resulting theory was completely linear and uncoupled. Later refinements were presented in a series of papers by Biot (1941b, 1955, 1956). The displacement of the soil skeleton and pore-pressure became coupled to the governing differential equations. The principle of effective stress was also introduced. Further, a fluid strain parameter was considered, but unfortunately this is not convincingly supported from the continuum mechanics point of view.

There is no need to go into further details about Biot's theory here. A comprehensive study is due to Sandhu (1968), and a comparison of the self-consistent and pseudo theory was presented by Schiffman et al (1964). Verruijt (1968) introduced an additional derivation of the governing equations of consolidation to include partly saturated



soils.

### III.5 Continuum Theory Approach

In spite of the consistency of Biot's theory and its degree of generality it still contains some inconveniences.

A part from the restrictions discussed before, the finite deformation is not included in the equilibrium equation.

Many conceptual difficulties are encountered in expand this theory to consider non-saturated mass, finite deformations, water viscosity effects in the equation of motion, etc.... These conceptual difficulties can be reduced if a theory of a mixture of many media is used. A comprehensive discussion of mixture theory for a many phase material was presented by Bowen (1976), where two approaches are discussed. The first of these approaches was introduced by Green and Atkins(1964) in the discussion of diffusion of a fluid through an elastic porous solid. In this approach the continuity equation (conservation of mass) and the linear momentum equation for the mixture were proposed as postulates.

The second, somewhat different approach was given by Green and Naghdi (1965), in which the basic equations were derived from an energy balance equation for the mixture. It is necessary to postulate such an equation if one wants to take thermodynamic effects into account. Also in this case an entropy production inequality has to be postulated, as used by Green and Naghdi in their previous paper. If the thermodynamic effect is neglected, the two approaches come to the same result. By

making use of the same approach, Green and Steel (1966) treated the special case of Newtonian fluid flow through an elastic porous medium, while Crochet and Naghdi (1966) extended the analysis to a non-Newtonian fluid.

For a discussion of this later paper see Sandhu (1968) who first applied the mixture theory to clay.

An important point which comes from these approaches is the proposition of a generalized Darcy Law for a compressible solid skeleton. A different approach, however, can be used to arrive at a generalized Darcy Law. Some authors introduced a diffusive dynamic force conjugated with the diffusion velocity. Others such as Tabaddor and Little (1971) arrived at the generalized Darcy Law by rewriting the equation of motion under the constraint of the fluid being incompressible and assuming that the so called intrinsic permeability is small.

With appropriate assumptions in the mixture theory it converts to Biot's theory. However, the whole transformation process is interpreted as transient, or quasi-dynamic, i.e. the equilibrium equations are obtained from the equation of motion. Also, the principle of effective stress is automatically satisfied.

In this thesis, however, the Biot theory can not be used, because it is only valid for the linear case. In the next chapter the mixture theory will be used to obtain the equation of motion for the soil mass. The Darcy Law is then obtained by postulating the mass continuity for all parts of the body and independently for each phase.

### III.6 Solution Methods

A great number of solutions for one dimensional consolidation problems have been provided, by both analytical and numerical methods. The choice between one method and the other strongly depend on the characteristics and complexity of the problem.

General methods of analytical solution have been developed in terms of stress and displacement functions (Biot 1956b). A stress function formulation was used by Josseling de Jong (1957) to treat axisymmetric boundaries, while Macnamee and Gibson (1960a) developed a solution for plane strain and axisymmetric problems by means of displacement function formulations.

There is a great number of closed form solutions for the consolidation problem, and discussion of these is out of the scope of this thesis (for detailed discussion see Zaretskii, 1967)). Numerical methods have been used almost exclusively in solving multi-dimensional problems, and the finite element method is frequently adopted to discretize the space domain while finite difference is assumed when the time domain is discretized.

A brief discussion of the analysis of consolidation using the finite element method is given in text books such as Desai and Abel (1972) and Zienkiewicz (1977). In the following chapters of this thesis all developments concerning the techniques of solving the consolidation problem by finite element are fully discussed.

CHAPTER IVCONTINUOUS MECHANICS OF MIXTURE REVIEWIV.1. Introduction

The purpose of this chapter is to formulate a consistent System of Equilibrium and Continuity Equations to act as a model for the non-linear consolidation problem. Two systems of equations are presented, one as a function of the Euler variable and the other as a function of the Lagrange variable. In subsequent chapters, however, the Lagrange approach prove to be more convenient for the application purpose in question.

The compact notation utilized made it possible to present the major features of the entire formulation in a relatively short chapter.

The mathematical descriptions were built up, step by step, from the basic concepts of Continuous Mechanics, all subsequent passes always being based on previously established ones. Firstly the Lagrange strain tensor is defined as a function of the Green deformation tensor and the Euler strain tensor as a function of the Cauchy deformation tensor. From these definitions the various interrelations are deduced. In the same section relations between the strain vector and deformation vector are presented in a general form. Also the most general expressions for the Lagrange and Euler tensor as functions of

the infinitesimal strain tensor are deduced. The definition of strain invariants is introduced either as a function of the deviatoric strain tensor or as a function of the natural strain tensor.

Next the Global and Local Balance Laws, and their restrictions are presented. Under the assumption of the validity of these laws, one continuity equation as function of the Euler variables and one as function of the Lagrange variables are deduced.

By using the equation of balance of momentum the local stress vector and tensor are defined. Applying the balance of linear momentum law locally the first law of Cauchy Law (equation of motion of deformable body) is obtained, associated with its jump conditions.

To transform these equations to a fix reference frame the definition of the Piola-Kirchhoff pseudo stresses (either defined by unit of underformed area or by unit of deformed area) are introduced as functions of the Euler stress tensor. Thus the equation of motion in a reference frame can then be established.

Finally, the stress invariants either as function of deviatoric stress tensor or as function of the natural stress tensor are given.

#### IV.2 Body Motion

The mathematical description of motion requires, necessarily, the utilization of a convenient frame of reference.

In most physical problems, particularly in soil mechanics, it is

sufficient to adopt a fixed system of reference attached to the earth motion.

Imagine a physical body with different phases (especially with two phases), in continuous motion, in such way that it experiences different positions and time in order to satisfy the requirements of equilibrium. Let any of these states be defined as a body configuration.

In Figure IV.2.1 a body in three different equilibrium configurations is presented. The first configuration is any previously known configuration or the initial configuration (I.C.) defined by a domain  ${}^0B$ , bounded by a surface  ${}^0\omega$  and occupying a volume  ${}^0\upsilon$ . Any area element related to this configuration is written as  ${}^0s$ . The second is an actual configuration (A.C.) of the body which is defined by a domain  ${}^tB$ , bounded by the surface  ${}^t\omega$  and occupies a volume  ${}^t\upsilon$  and any area element referred to this configuration is represented by  ${}^ts$ . The previously known or initial configuration may be referred to as the configuration at time  $t=0$  whereas the actual configuration is that at time  $t$ .

The third configuration is any one after the second configuration. So, when configurations one and two are referred to only, the position vector will be represented by  $a_i^0$  and  $x_i^0$  respectively and when we refer to configurations 1,2 and 3 the position vector will be represented by  $a_i^0$ ,  $b_i^0$  and  $x_i^0$  respectively.

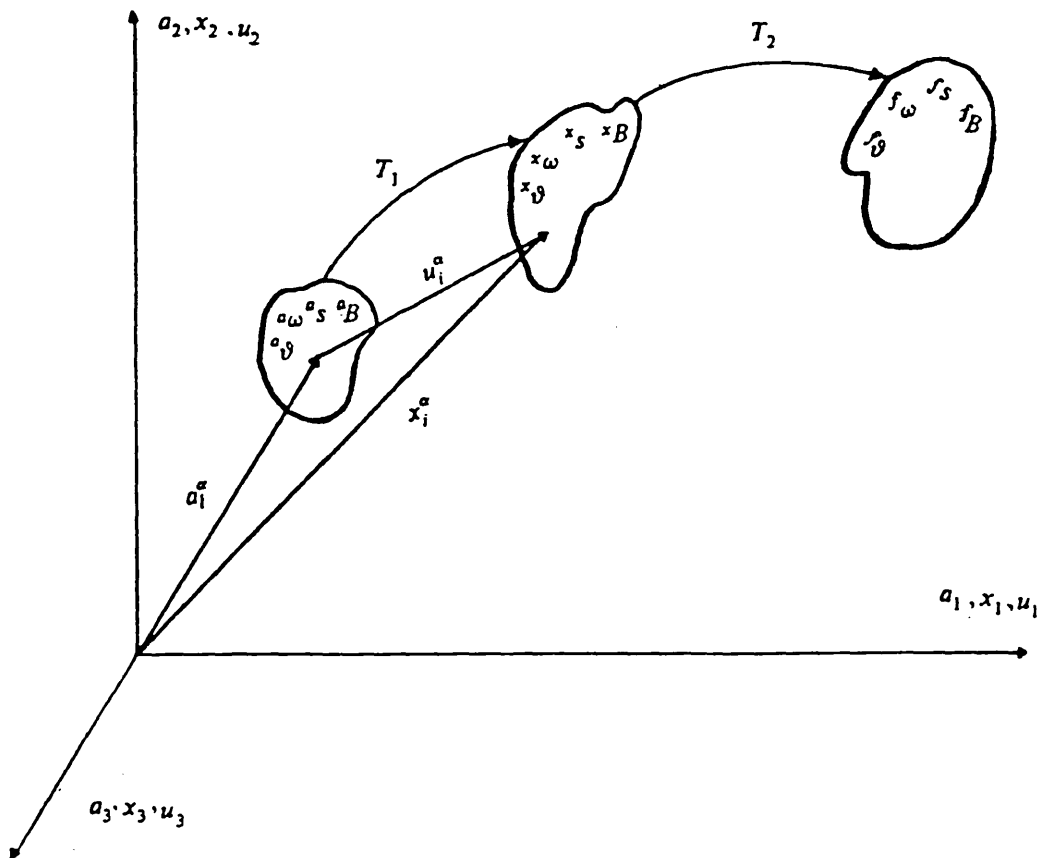


Figure IV.2.1

### IV.3 Independent Variables

From an initial configuration, a body, under the action of external loads, finds itself in dynamic equilibrium (or particularly quasi-static equilibrium) in an actual configuration. A description of this motion may be expressed in two ways: in a parametric form (refer to Figure IV.2.1)

$$(IV.3.1) \quad x_i^a = x_i^a(a_1^a, a_2^a, a_3^a, t) \quad \text{or} \quad x_k^a = x_k^a(a_k^a, t)$$

or,

$$(IV.3.3) \quad a_k^\alpha = a_k^\alpha(x_1^\alpha, x_2^\alpha, x_3^\alpha, t) \quad \text{or} \quad a_k^\alpha = a_k^\alpha(x_i^\alpha, t)$$

or, in a vector form

$$(IV.3.3) \quad x^\alpha = x^\alpha(a^\alpha, t), \quad a^\alpha = a^\alpha(x^\alpha, t)^1$$

where  $\alpha = 1 \text{ or } 2$  represents the material phases 1 and 2 respectively. In this thesis the material phase 1 is the same as the linear fluid phase of the body and the material phase 2 is the same as the non-linear solid phase of the body.

The equation (IV.3.1) means that any position point  $a^\alpha$  at initial configuration is found in a spatial position  $x^\alpha$  in an actual configuration. Inversely the equation (IV.3.3) states that the material point at time  $t$  occupying the spatial position  $x^\alpha$  may be traced back to its original position  $a^\alpha$ .

The transformation of equation (IV.3.1) into (IV.3.3) and conversely, is unequivocally determined if they are continuous, possess continuous first order partial derivatives and the Jacobian  $J$ , defined by

$$J = \det\left(\frac{\partial x_k^\alpha}{\partial a_j^\alpha}\right)$$

does not vanish in the neighbourhood of  $a_j^\alpha$ . Inversely, the same may be stated for  $J^{-1}$ .

In fact, the functions stated by equations (IV.3.1) and (IV.3.3) are considered to be continuous and differentiable to any order as required.



This hypothesis is known under the name of the "Axiom of Continuity", expressing the indestructibility of matter. No domain, which corresponds to a finite positive volume, can be deformed into a domain of zero or infinite volume. Motion represented by equations (IV.3.1) and (IV.3.3) therefore, transform any domain into another domain, any surface into another surface and any curve into another curve.

In practice, there are examples in which this axiom is violated. For example, the material may fracture or transmit shock waves or other kinds of discontinuities. Special attention must be given to these cases.

Referring to the Figure (IV.2.1) the representation of the position vector in the second configuration can be replaced by  $b$  and  $x$  can be used as the position vector for the third configuration, as explained before.

Therefore let  $T_1$  be the transformation from  $a_i^\alpha$  to  $b_i^\alpha$ , and  $T_2$  be the transformation from  $b_i^\alpha$  to  $x_i^\alpha$ , which can be written symbolically as  $b_i^\alpha = T_1 a_i^\alpha$  and  $x_i^\alpha = T_2 b_i^\alpha$ , respectively. Also the product  $T_2 T_1$  means the transformation from configuration  $a_i^\alpha$  to  $x_i^\alpha$ , that is,  $x_i^\alpha = T_2 T_1 a_i^\alpha$ . This product will be proper if the Jacobian, defined by  $\det(\partial x_i^\alpha / \partial a_j^\alpha)$ , is not infinite or zero. However, by the chain rule of differentiation

$$\frac{\partial x_i^\alpha}{\partial a_j^\alpha} = \frac{\partial x_i^\alpha}{\partial b_k^\alpha} \frac{\partial b_k^\alpha}{\partial a_j^\alpha}$$

may be written, so that by the property of product of determinants,

$$(IV.3.4) \quad J = \det\left(\frac{\partial x_i^\alpha}{\partial a_j^\alpha}\right) = \det\left(\frac{\partial x_i^\alpha}{\partial b_k^\alpha}\right) \det\left(\frac{\partial b_k^\alpha}{\partial a_j^\alpha}\right) = J_2 J_1.$$

Since neither  $J_1$  nor  $J_2$  vanishes or is infinite their product is neither zero nor infinite and the transformation  $T_2 T_1$  is proper.

Also, when the position vector  $x_i^\alpha$  is very close to  $b_i^\alpha$  the determinant of  $\partial x_i^\alpha / \partial b_k^\alpha$  may approximate to the first order terms as

$$(IV.3.5) \quad \det\left(\frac{\partial x_i^\alpha}{\partial b_k^\alpha}\right) = \delta_{ik} + \frac{\partial u_i}{\partial b_i} = J_2$$

To show this, take  $x_i^\alpha = b_i^\alpha + u_i^\alpha$  and evaluate  $\partial x_i^\alpha / \partial b_k^\alpha$  and then evaluate the determinant where the second order terms in  $u_i$  are neglected.

#### IV.4 Strain Definitions

In the following chapters any quantity, scalar, vector, or tensor referred to a configuration "a" will be denoted by a left superscript. For example, if "r" refers to a configuration "a" it will be written  ${}^a r$ . Also, when relevant, the independent variable of any quantity will be defined by a left subscript. The left subscript "a" means that the current quantity defined is a function of the Lagrange variable and the left subscript "x" means that the current quantity is a function of the Euler variable.

For example a quantity  ${}^x e$  is defined at configuration "x" and depends on the Lagrange variable.

In this text the particular concern is studying the strain state

variation when passing from the neighbourhood of point  $a^\alpha$  defined by the vector  $da^\alpha$  in  ${}^aB$  to a corresponding neighbourhood  $x$  defined by the vector  $dx^\alpha$  in  ${}^xB$  when finite deformation occurs. The transformation of such a vector  $da^\alpha$  into  $dx^\alpha$  is shown schematically in Figure IV.4.1.

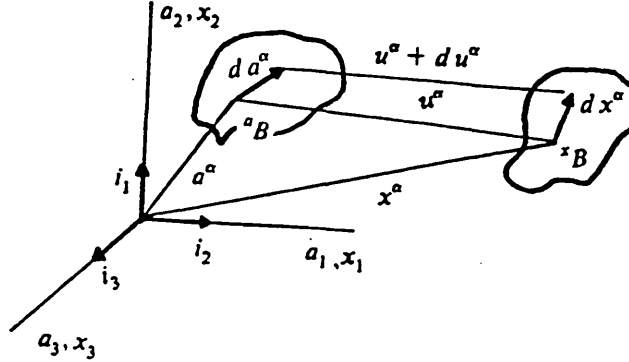


Figure IV.4.1

Making use of equations (A.4) and (A.6) it is possible to express the square of the arc length in  ${}^aB$  as a function of the variables in  ${}^xB$  as :

$$(IV.4.1) \quad (d^a r^\alpha)^2 = \delta_{kl} \frac{\partial a_k^\alpha}{\partial x_i^\alpha} \frac{\partial a_l^\alpha}{\partial x_j^\alpha} dx_i^\alpha dx_j^\alpha$$

conversely

$$(IV.4.2) \quad (d^x r^\alpha)^2 = \delta_{kl} \frac{\partial x_k^\alpha}{\partial a_i^\alpha} \frac{\partial x_l^\alpha}{\partial a_j^\alpha} da_i^\alpha da_j^\alpha$$

where

$$(IV.4.3) \quad x^c_{ij}{}^\alpha = \delta_{kl} \frac{\partial a_k^\alpha}{\partial x_i^\alpha} \frac{\partial a_l^\alpha}{\partial x_j^\alpha}, \quad a^c_{ij}{}^\alpha = \delta_{kl} \frac{\partial x_k^\alpha}{\partial a_i^\alpha} \frac{\partial x_l^\alpha}{\partial a_j^\alpha}$$

are, respectively, Cauchy's deformation tensor and Green's deformation

tensor

Note also that Cauchy's deformation tensor is a function of Euler's variable, whilst Green's deformation tensor is a function of Lagrange variable.

Lagrangian and Eulerian strain tensors are defined, respectively, by

$$(IV.4.4) \quad {}_a e_{kl}^{\alpha} = \frac{1}{2}({}_a c_{kl}^{\alpha} - \delta_{kl}) \quad {}_x e_{kl}^{\alpha} = \frac{1}{2}(\delta_{kl} - {}_x c_{kl}^{\alpha})$$

It is useful sometimes to have a relationship between Cauchy's deformation  ${}_x c_{ij}^{\alpha}$  tensor and Green's deformation  ${}_a c_{ij}^{\alpha}$  tensor, which is nearly the same as the relationship between Lagrangian's and Eulerian's strain tensors.

By making use of equations (IV.4.2), (A.3) and (IV.4.4); and similarly for equations (IV.4.1), (A.4) and (IV.4.4)

$$(IV.4.5) \quad (d^x r^{\alpha})^2 = 2{}_a e_{kl}^{\alpha} d a_k^{\alpha} d a_l^{\alpha} = 2{}_x e_{kl}^{\alpha} d x_k^{\alpha} d x_l^{\alpha}$$

may be written. From this and (A.6)

$$(IV.4.6) \quad {}_a e_{ij}^{\alpha} = {}_x e_{kl}^{\alpha} \frac{\partial x_k^{\alpha}}{\partial a_i^{\alpha}} \frac{\partial x_l^{\alpha}}{\partial a_j^{\alpha}}, \quad {}_x e_{kl}^{\alpha} = {}_a e_{ij}^{\alpha} \frac{\partial a_i^{\alpha}}{\partial x_k^{\alpha}} \frac{\partial a_j^{\alpha}}{\partial x_l^{\alpha}}$$

These equations also ensure that both  ${}_a e_{ij}^{\alpha}$  and  ${}_x e_{kl}^{\alpha}$  are second-order absolute tensors.

The strain tensors may also be expressed in terms of the displacement vector  $u^{\alpha}$  which extends from a material point in the I.C. to its spatial location at time  $t$  in the A.C., as shown schematically in

Figure (IV.4.1). From this Figure one may write:

$$(IV.4.7) \quad u^\alpha = x^\alpha - a^\alpha \quad \text{or} \quad u_k^\alpha = x_k^\alpha - a_k^\alpha$$

The displacement vector may be expressed in terms of its Lagrangian and Eulerian components  $u_k(a_i^\alpha, t)$  and  $u_i^\alpha(x_k^\alpha, t)$ .

By differentiating (IV.4.7) one may get:

$$(IV.4.8) \quad dx_k^\alpha = (\delta_{kl} + \frac{\partial u_k^\alpha}{\partial a_l^\alpha}) da_l^\alpha, \quad da_l^\alpha = (\delta_{lk} - \frac{\partial u_l^\alpha}{\partial x_k^\alpha}) dx_k^\alpha$$

By taking  $\partial x_k^\alpha / \partial a_l^\alpha$  and  $\partial a_l^\alpha / \partial x_k^\alpha$  from the above equation and substituting in (IV.4.4) one gets

$$(IV.4.9) \quad {}_x c_{kl} = \delta_{kl} - 2 {}_x e_{kl} = \delta_{kl} - \frac{\partial u_k^\alpha}{\partial x_l^\alpha} - \frac{\partial u_l^\alpha}{\partial x_k^\alpha} + \frac{\partial u_m^\alpha}{\partial x_k^\alpha} \frac{\partial u_m^\alpha}{\partial x_l^\alpha}$$

$${}_a c_{kl} = \delta_{kl} + 2 {}_a e_{kl} = \delta_{kl} + \frac{\partial u_k^\alpha}{\partial a_l^\alpha} + \frac{\partial u_l^\alpha}{\partial a_k^\alpha} + \frac{\partial u_m^\alpha}{\partial a_k^\alpha} \frac{\partial u_m^\alpha}{\partial a_l^\alpha}$$

which are the strain tensors Euler and Lagrange, respectively, in terms of the the linear and non-linear components of the displacement gradients.

The Lagrange strain tensor  ${}_a e_{kl}$  will be used a great deal in future chapters and its explicit expression can be found in the Appendix C.

The strain tensors, as well as the deformations tensors, are symmetric tensors, i.e.

$${}_a e_{kl} = {}_a e_{lk}, \quad {}_x e_{kl} = {}_x e_{lk}, \quad {}_a c_{kl} = {}_a c_{lk}, \quad {}_x c_{kl} = {}_x c_{lk}$$

if arranged in a matrix form as:

$$e_{kl} = \begin{pmatrix} e_{xx} & e_{xy} & e_{xz} \\ e_{yx} & e_{yy} & e_{yz} \\ e_{zx} & e_{zy} & e_{zz} \end{pmatrix}$$

which is a matrix symmetrical with respect to its main diagonal. The strain components  $e_{xx}, e_{yy}, e_{zz}$  displayed in the main diagonal are called normal strains, while the others are called shear strains. This symmetry is exploited a great deal to save an enormous amount of computer memory when programming deformable bodies.

Also often employed in linear theories of continua, are the infinitesimal strain tensors  ${}_a I_{kl}^\alpha$ ,  ${}_x I_{kl}^\alpha$  and infinitesimal rotation tensors  ${}_a W_{kl}^\alpha$ ,  ${}_x W_{kl}^\alpha$  defined by

$$(IV.4.10) \quad \begin{aligned} {}_a I_{kl}^\alpha &= \frac{1}{2} \left( \frac{\partial u_k^\alpha}{\partial a_l^\alpha} + \frac{\partial u_l^\alpha}{\partial a_k^\alpha} \right), & {}_x I_{kl}^\alpha &= \frac{1}{2} \left( \frac{\partial u_k^\alpha}{\partial x_l^\alpha} + \frac{\partial u_l^\alpha}{\partial x_k^\alpha} \right) \\ {}_a W_{kl}^\alpha &= \frac{1}{2} \left( \frac{\partial u_k^\alpha}{\partial a_l^\alpha} - \frac{\partial u_l^\alpha}{\partial a_k^\alpha} \right), & {}_x W_{kl}^\alpha &= \frac{1}{2} \left( \frac{\partial u_k^\alpha}{\partial x_l^\alpha} - \frac{\partial u_l^\alpha}{\partial x_k^\alpha} \right) \end{aligned}$$

also called symmetric part and anti-symmetric part of the infinitesimal strain tensor.

From (IV.4.10) it may be written

$$(IV.4.11) \quad \frac{\partial u_k^\alpha}{\partial a_l^\alpha} = {}_a I_{kl}^\alpha + {}_a W_{kl}^\alpha, \quad \frac{\partial u_k^\alpha}{\partial x_l^\alpha} = {}_x I_{kl}^\alpha + {}_x W_{kl}^\alpha$$

and substituting into equation (IV.4.9)

$$(IV.4.12) \quad {}_x c_{kl}^\alpha = \delta_{kl} - 2{}_x e_{kl}^\alpha = \delta_{kl} - 2{}_x I_{kl}^\alpha + ({}_x I_{mk}^\alpha + {}_x W_{mk}^\alpha)({}_x I_{ml}^\alpha + {}_x W_{ml}^\alpha)$$

$${}_a c_{kl}^\alpha = \delta_{kl} + 2{}_a e_{kl}^\alpha = \delta_{kl} + 2{}_a I_{kl}^\alpha + ({}_a I_{mk}^\alpha + {}_a W_{mk}^\alpha)({}_a I_{ml}^\alpha + {}_a W_{ml}^\alpha)$$

is obtained, and from which, in various physical situations, approximate expressions are obtained by dropping various combinations of products.

#### IV.5 Strain Invariants

It is of interest to determine, at a given point in the material body, the directions for which the stretch takes extreme values. Bearing in mind Figure (B.1) and defining  ${}^a n_k^a$  and  ${}^x n_k^a$  as the unit vectors along  $d a^a$  and  $d x^a$ , respectively,

$$(IV.5.1) \quad {}^a n_k^a = \frac{d a_k^a}{|d a^a|} = \frac{d a_k^a}{d a^a}, \quad {}^x n_k^a = \frac{d x_k^a}{|d x^a|} = \frac{d x_k^a}{d x^a}$$

where  $d a^a$  and  $d x^a$ , whose squares are defined by equations (IV.4.1) and (IV.4.2), respectively, are the length of  $d a^a$  and  $d x^a$ . The stretch  ${}^a \lambda^a = {}^a \lambda^a$  is the ratio of  $d x^a / d a^a$ . When it is considered as a function of  ${}^a n^a$ ,  ${}^a \lambda^a$  is written, and when it is considered as a function of  ${}^x n^a$ ,  ${}^x \lambda^a$  is written.

$$\text{So, (IV.5.2)} \quad {}^a \lambda^a = \frac{d x^a}{d a^a} = \left( {}_a c_{kl}^a {}^a n_k^a {}^a n_l^a \right)^{\frac{1}{2}}, \quad {}^x \lambda^a = \frac{d x^a}{d a^a} = 1 / \left( {}_x c_{kl}^a {}^x n_k^a {}^x n_l^a \right)^{\frac{1}{2}}$$

From (IV.5.2) it is clear that the normal components of  ${}_a c^a$  and  ${}_x c^a$  in the direction of  ${}^a n^a$  and  ${}^x n^a$  are, respectively, the square and the inverse square of stretches in these directions.

Now to obtain the direction for which the stretch takes extreme values the above equation must be differentiated in relation to  ${}^a n_m^a$ , where  ${}^a n_m^a$  is subject to the condition

$$(IV.5.3) \quad \delta_{kl} {}^a n_k^a {}^a n_l^a = 1$$

Using Lagrange's method of multipliers and introducing the inverse of (IV.4.4) it may be deduced that

$$(IV.5.4) \quad ({}_a e_{kl}^a - E \delta_{kl}) {}^a n_l^a = 0$$

where

$$(IV.5.5) \quad 2E^a = c^a - 1$$

and  $c^a$  is the unknown Lagrange multiplier.

Now solving (IV.5.4) for  ${}^a n_l^a$ . A nontrivial solution of this equation exists if the coefficient determinant vanishes, i.e.

$$(IV.5.6) \quad \det({}_a e_{kl}^a - {}_a e^a \delta_{kl}) = \begin{vmatrix} {}_a e_{xx}^a - {}_a e^a & {}_a e_{xy}^a & {}_a e_{xz}^a \\ {}_a e_{yx}^a & {}_a e_{yy}^a - {}_a e^a & {}_a e_{yz}^a \\ {}_a e_{zx}^a & {}_a e_{zy}^a & {}_a e_{zz}^a - {}_a e^a \end{vmatrix} = 0$$

Upon expanding this determinant, a cubic equation is obtained, known as the characteristic equation of the strain tensor:

$$(IV.5.7) \quad e^3 - I_1 e^2 + I_2 e - I_3 = 0$$

where  ${}_a e^a$  has been changed to  $e$  for simplicity.



The quantities  $I_1, I_2, I_3$  are known as the principal invariants of the strain tensor. These quantities remain invariant upon the transformation of coordinates. A second-order tensor  ${}^a e_{kl}^\alpha$  in  $\mathbb{R}^3$  possesses only three independent invariants, that is, all other invariants of  ${}^a e_{kl}^\alpha$  can be shown to be functions of the above three invariants.

The characteristic equation (IV.5.7) possesses three roots  ${}^a e_\xi^\alpha (\xi = 1, 2, 3)$  called principal strains. The coefficients  $I_1, I_2, I_3$  of the characteristic equation are the sums of the products of these roots taken one, two and three at a time, i.e.

$$I_1 = {}^a e_{kk}^\alpha = {}^a e_{xx}^\alpha + {}^a e_{yy}^\alpha + {}^a e_{zz}^\alpha \quad (\text{IV.5.8})$$

$$I_2 = {}^a e_{yy}^\alpha {}^a e_{zz}^\alpha + {}^a e_{zz}^\alpha {}^a e_{xx}^\alpha + {}^a e_{xx}^\alpha {}^a e_{yy}^\alpha - {}^a e_{yz}^\alpha {}^a e_{zy}^\alpha - {}^a e_{zx}^\alpha {}^a e_{xz}^\alpha - {}^a e_{xy}^\alpha {}^a e_{yx}^\alpha, \quad I_3 = \det {}^a e_{kl}^\alpha$$

The three linear equations (IV.5.4) determine a direction  ${}^a n_\xi^\alpha$  corresponding to each principal strain  ${}^a e_\xi^\alpha (\xi = 1, 2, 3)$ . If the principal strain is real and distinct, then the directions  ${}^a n_{1k}^\alpha, {}^a n_{2k}^\alpha$  and  ${}^a n_{3k}^\alpha$  are real and uniquely determined. By using equation (IV.5.4) and the symmetric property of the strain tensor, it may be proved that all principal strains are real.

Also the principal directions corresponding to two distinct principal strains may be proved to be orthogonal and, furthermore, it is always possible to find at a point  $a^a$  at least three mutually orthogonal directions for which the stretch takes the stationary values. However, the state of strain takes a particularly simple form when the reference frame is selected to coincide with the principal directions. In this case  ${}^a n_{lk}^\alpha = 0$  whenever  $l \neq k$ . It may be written  ${}^a n_{lk}^\alpha = \delta_{lk}$  and from (IV.5.4) it follows that

$$(IV.5.9) \quad {}_a e_{km}^{\alpha} = {}_a e_{\underline{m}}^{\alpha} \delta_{\underline{m}k}$$

where underscored indices are summed. That is, in matrix notation

(IV.5.9) leads to

$$(IV.5.10) \quad \begin{pmatrix} e_{xx} & e_{xy} & e_{xz} \\ e_{yx} & e_{yy} & e_{yz} \\ e_{zx} & e_{zy} & e_{zz} \end{pmatrix} = \begin{pmatrix} e_1 & 0 & 0 \\ 0 & e_2 & 0 \\ 0 & 0 & e_3 \end{pmatrix}$$

Where the superscript indices have been dropped, for simplicity.

Hence, the determination of principal directions and principal strains of a tensor  ${}_a e_{kl}^{\alpha}$  is equivalent to finding a rectangular frame of reference in which the matrix  $\|{}_a e_{kl}^{\alpha}\|$  takes the diagonal form, i.e. the principal strains are the normal components of the strain tensor, and the shear components of the strain tensor in the principal frame of reference vanish.

The usual procedure to solve the characteristic equation is by changing the dependent variable  $e_{ij}$  by

$$\bar{e}_{ij} = e_{ij} - \frac{1}{3} \delta_{ij} I_1$$

where the subscript has been dropped for simplicity.

Substituting the previous equation into equation (IV.5.7) one may have:

$$(IV.5.11) \quad \bar{e}^3 - T_2 \bar{e} - T_3 = 0$$

where the principal deviatoric strain invariants are:

$$(IV.5.12) \quad T_2 = 3I_1^2 - I_2 = \frac{1}{6} \left[ (e_{xx} - e_{yy})^2 + (e_{yy} - e_{zz})^2 + (e_{zz} - e_{xx})^2 + 6(e_{yz}^2 + e_{zx}^2 + e_{xy}^2) \right] = \frac{1}{2} \bar{e}_{ij} \bar{e}_{ij}$$

$$(IV.5.13) \quad T_3 = I_3 - I_2 I_1 + 2I_1^3 = \frac{1}{3} \bar{e}_{ij} \bar{e}_{ij} \bar{e}_{ij}$$

Since it is known that all roots of the equation (IV.5.11) are real and they can be found to be:

$$(IV.5.14) \quad \bar{e}_1 = \frac{2}{\sqrt{3}} T_2 \sin(\theta_1 + \frac{2}{3}\pi), \bar{e}_2 = \frac{2}{\sqrt{3}} T_2 \sin \theta_1, \bar{e}_3 = \frac{2}{\sqrt{3}} T_2 \sin(\theta_1 + \frac{4}{3}\pi)$$

where a trigonometric equation similar to (IV.5.11) was used to find the solutions (Nayak and Zienkiewicz, 1972) and

$$(IV.5.15) \quad \theta_1 = \frac{1}{3} \arcsin\left(\frac{3\sqrt{3}T_3}{2T_2^{\frac{3}{2}}}\right) = \arctan\left[\frac{2e_2 - e_1 - e_3}{\sqrt{3}(e_1 - e_3)}\right] \quad -\frac{\pi}{6} \leq \theta_1 \leq \frac{\pi}{6}$$

Hence for the three principal components of strain ( $e_1 \geq e_2 \geq e_3$ ) the expression

$$(IV.5.16) \quad \begin{aligned} e_1 &= \frac{2}{\sqrt{3}} T_2 \sin(\theta_1 + \frac{2}{3}\pi) + \frac{1}{3} I_1 \\ e_2 &= \frac{2}{\sqrt{3}} T_2 \sin \theta_1 + \frac{1}{3} I_1 \\ e_3 &= \frac{2}{\sqrt{3}} T_2 \sin(\theta_1 + \frac{4}{3}\pi) + \frac{1}{3} I_1 \end{aligned}$$

can be written.

In order to give a geometric interpretation to the strain transformation from the I.C. to the A.C. the following simplification is introduced.

In the principal triad the square of the arc length is given by

$$(d^x r^a)^2 = \delta_{kl} \frac{\partial x_k^a}{\partial a_i^a} \frac{\partial x_l^a}{\partial a_j^a} d a_i^a d a_j^a = \sum_{\beta} c_{\beta}^a (d a_{\beta}^a)^2$$

Where according to (IV.5.5)  $c_{\beta}^a = 1 + 2e_{\beta}^a$  are the proper numbers. For  $(d^x r^a)^2 = k^2$  fixed, the previous equation represents an ellipsoid called the strain ellipsoid of Cauchy. The stretches  ${}^{\beta}\lambda^a = {}^a\lambda^{\beta} = d^x r^a / d^a r^{\beta}$  along the principal axes of this ellipsoid are given by

$$(IV.5.17) \quad {}^{\beta}\lambda = k / d a_{\beta}^a = c_{\beta}^{\frac{1}{2}} = k / b_{\beta}$$

where  $b_{\beta}$  are the lengths of the semi-axes.

Geometrically speaking, the strain ellipsoid of Cauchy means that an originally spheric isotropic solid material in the I.C. becomes an ellipsoid in the A.C. with the semi-axes lying down in the principal strain directions and the stretch values are given by (IV.5.17). The reciprocity holds for the inverse transformation (Aris, 1962).

#### IV.6 Compatibility Conditions

In three-dimensional space the deformation tensor  $c_{kl}^a$  and the strain tensor  $e_{kl}^a$  each possess six components which are expressible in terms of three components  $u_k^a$  of the displacement vector, i.e.

$$(IV.6.1) \quad c_{kl}^{\alpha} = \delta_{kl} + 2e_{kl}^{\alpha} = \delta_{kl} + \frac{\partial u_k^{\alpha}}{\partial a_l^{\alpha}} + \frac{\partial u_l^{\alpha}}{\partial a_k^{\alpha}} + \frac{\partial u_m^{\alpha}}{\partial a_k^{\alpha}} \frac{\partial u_m^{\alpha}}{\partial a_l^{\alpha}}$$

Thus, given three  $u_k^{\alpha}$ , six  $c_{kl}^{\alpha}$  can be calculated. If, on the other hand six  $c_{kl}^{\alpha}$  or  $e_{kl}^{\alpha}$  are given, can a single-valued displacement field be found corresponding to this strain? It is clear that this requires the integration of six partial differential equations (IV.6.1) for the three unknowns  $u_k^{\alpha}$ . Unless certain integration conditions known as the compatibility conditions, are satisfied, this may not be possible.

One way of finding the compatibility conditions is through the elimination of  $u_k^{\alpha}$  from (IV.6.1) by partial differentiation. An alternative method is to use the theorem of Riemann (Eringen et al, 1974).

By using one of the two methods the compatibility conditions for  ${}_o e_{kl}^{\alpha}$  and  ${}_x e_{kl}^{\alpha}$  can be obtained. It may be written in terms of  ${}_x e_{kl}^{\alpha}$  as

$$(IV.6.2) \quad e_{kn,lm} + e_{lm,kn} - e_{km,ln} - e_{ln,km} - c_{rs}^{-1} \left[ (e_{kr,n} + e_{nr,k} - e_{kn,r}) \right. \\ \left. (e_{ls,m} + e_{ms,l} - e_{lm,s}) - (e_{kr,m} + e_{nr,k} - e_{km,r}) (e_{ls,n} + e_{ns,l} - e_{ln,s}) \right] = 0$$

Where  ${}_x$  and  ${}_o$  have been dropped for simplicity.

Also, when strains are small their products are dropped to obtain the compatibility conditions for the infinitesimal strain tensor.

#### IV.7 Force Distribution, Mass Density, Internal Energy Density

In the study of a one-phase continuum media, one is concerned with the manner in which forces are transmitted through a medium. At this stage, one is concerned specifically with two classes of forces. The first is the so-called external or body force distribution, distinguished by the fact that it acts directly on the distribution of matter in the specified domain, such as gravitation or electromagnetic forces. Accordingly, it is represented as a function of position and time and will be denoted by  $f(x_i, t)$ . This force is an intensity function and is generally evaluated per unit mass or per unit of volume of the material acted upon. The second is the internal or contact force which is to be regarded as acting on an element of volume through its bounding surface. If the element of volume has an external bounding surface, the specified force is called surface traction which is an intensity defined by unit of area, and is a function of the position  $x_i$ , time  $t$ , and the orientation  $n$  of the surface element, according to Cauchy's principle. They are denoted by  $\sigma_{(n)}(x_i, t)$ .

In the study of two-phase continua, the body force in each phase is defined in relation to the total volume of the media. They are denoted as  $f^1(x_i, t)$  and  $f^2(x_i, t)$  or simply  $f^a(x_i, t)$ . The internal force in each phase is defined per unit of total surface, instead of by unit of individual phase surfaces, which are denoted as  $\sigma_{(n)}^1(x_i, t)$  and  $\sigma_{(n)}^2(x_i, t)$  or simply  $\sigma_{(n)}^a(x_i, t)$ .

With these simplifications the two following identities hold for a volume element:

$$f(x_i, t) = f^1(x_i, t) + f^2(x_i, t) = f^a(x_i, t)$$

(IV.7.1)

$$\sigma_{(n)}(x_i, t) = \sigma_{(n)}^1(x_i, t) + \sigma_{(n)}^2(x_i, t) = \sigma_{(n)}^a(x_i, t)$$

Also in continuous mechanics the existence of continuous mass measure (mass density) and the internal energy density are postulated: (  $\rho, \epsilon$  )

The total mass  $m$  within a volume  $\vartheta$  is given by

$$(IV.7.2) \quad m = \int_{\vartheta} \rho d\vartheta, \quad \varnothing \leq \rho < \infty$$

and the total internal energy  $\mathcal{E}$  in the same volume is given by

$$(IV.7.3) \quad \mathcal{E} = \int_{\vartheta} \rho \epsilon d\vartheta$$

The expression for the mass and internal energy for each phase may be written in a similar way to the body force distribution, so,

$$(IV.7.4) \quad m = \int_{\vartheta} \rho d\vartheta = \int_{\vartheta} \rho^1 d\vartheta + \int_{\vartheta} \rho^2 d\vartheta = m^1 + m^2 = m^a \quad \varnothing \leq \rho^1, \rho^2 < \infty$$

and

$$(IV.7.5) \quad \mathcal{E} = \int_{\vartheta} \rho d\vartheta \epsilon d\vartheta = \int_{\vartheta} \rho^1 \epsilon^1 d\vartheta + \int_{\vartheta} \rho^2 \epsilon^2 d\vartheta = \mathcal{E}^1 + \mathcal{E}^2$$

#### IV.8 Global Balance Law

In continuous mechanics there are five laws which are postulated, irrespective of material constitution and geometry, each law having its own domain of applicability. These laws are restricted to relativistic speeds (for special relativity) and restricted in

relation to dimensions (for general relativity); also microscopic and quantum-mechanical phenomena can not be treated. They are valid for all bodies subject to thermomechanical effects. Because of the nature of the problem concerned, only four of these laws are presented (not the Entropy Law):

1. Law of Conservation of Mass: The total mass of a body is unchanged with motion, or

$$(IV.8.1) \quad \frac{d}{dt} \int_{\mathcal{V}} \rho d\mathcal{V} = \frac{d}{dt} \int_{\mathcal{V}} \rho^1 d\mathcal{V} + \frac{d}{dt} \int_{\mathcal{V}} \rho^2 d\mathcal{V} = 0$$

Where  $d/dt$  is the material time derivative. Also, the Law of Conservation of Mass may state that the initial mass of the body is the same as the total mass of the body at any other time, i.e.

$$(IV.8.1a) \quad \int_{\mathcal{V}^a} \rho d^a \mathcal{V} = \int_{\mathcal{V}^x} \rho d^x \mathcal{V}$$

By using the transformation law  $d^x \mathcal{V} = J d^a \mathcal{V}$  given by (B.3) this may be written as

$$(IV.8.1b) \quad \int_{\mathcal{V}^a} (\rho - \rho J) d^a \mathcal{V} = 0 \quad \text{or} \quad \rho - \rho J = 0$$

2. Balance of Linear Momentum: The time rate of change of momentum in a volume element is equal to the resulting force acting on it.

$$(IV.8.2) \quad \frac{d}{dt} \int_{\mathcal{V}} \rho v d\mathcal{V} = \oint_S \sigma_{(n)} ds + \int_{\mathcal{V}} \rho f d\mathcal{V} \quad \text{or, alternatively}$$

$$(IV.8.3) \quad \frac{d}{dt} \int_{\mathcal{V}} (\rho^1 v^1 + \rho^2 v^2) d\mathcal{V} = \oint_S \sigma_{(n)} ds + \oint_S \sigma_{(n)} ds + \int_{\mathcal{V}} (\rho^1 f^1 + \rho^2 f^2) d\mathcal{V}$$



3. Balance of Moment of Momentum : The time rate of change of moment of momentum is equal to the resultant forces and couples acting on the body . So,

$$(IV.8.4) \quad \frac{d}{dt} \int_V \rho^\alpha x_x^\alpha v^\alpha d\vartheta = \oint_S x_x^\alpha \sigma_{(n)}^\alpha ds + \int_V \rho^\alpha x_x^\alpha f^\alpha d\vartheta \quad \text{or, alternatively,}$$

$$(IV.8.5) \quad \frac{d}{dt} \int_V (\rho^1 x_x^1 v^1 + \rho^2 x_x^2 v^2) d\vartheta = \oint_S (x_x^1 \sigma_{(n)}^1 + x_x^2 \sigma_{(n)}^2) ds + \int_V (\rho^1 x_x^1 f^1 + \rho^2 x_x^2 f^2) d\vartheta$$

where the left-hand side is the time rate of the total moment of momentum about the origin. On the right-hand side the surface integral is the moment of the surface tractions about the origin, and the volume integral is the total moment of body forces about the origin.

4. Conservation of Energy: The time rate of the sum of Kinetic energy  $\mathcal{K}$  and internal energy  $\mathcal{E}$  is equal to the sum of the rate of work of all forces and couples  $w$  and all other energy  $u_\xi$  that enters and leaves the body per unit of time.

$$(IV.8.6) \quad \frac{d}{dt}(\mathcal{K} + \mathcal{E}) = w + \sum_\xi u_\xi$$

where,

$$\mathcal{E} = \int_V \rho \epsilon d\vartheta, \quad \mathcal{K} = \frac{1}{2} \int_V \rho v_x v d\vartheta, \quad w = \oint_S \sigma_{(n)}^x v ds + \int_V \rho f_x v d\vartheta.$$

the other energy  $u_\xi = (\xi=1, \dots, n)$  that enters and leaves the body may be thermal, eletromagnetic, chemical, physico-chemical or of some other origin.

### IV.9 Local Balance Laws

These laws are particularly important in establishing the equilibrium and the boundary conditions in continuum mechanics.

They are found by applying the global balance law established previously to the local conditions.

-Conservation of mass locally.

If the material time derivative of a volume integral defined by equation (A.26) is now applied to the equation of global conservation of mass given by (IV.8.1) where  $\psi = {}^x\rho$

$$(IV.9.1) \quad \int_{\vartheta-\omega} \left[ \frac{\partial {}^x\rho}{\partial t} + \text{div}({}^x\rho {}^xv) \right] d^x\vartheta + \int_{\omega} [{}^x\rho({}^xv - v)] \cdot {}^x n d^x s = \emptyset$$

or

$$(IV.9.2) \quad \int_{\vartheta-\omega} \left[ \frac{\partial {}^x\rho^1}{\partial t} + \text{div}({}^x\rho^1 {}^xv^1) \right] d^x\vartheta + \int_{\vartheta-\omega} \left[ \frac{\partial {}^x\rho^2}{\partial t} + \text{div}({}^x\rho^2 {}^xv^2) \right] d^x\vartheta + \int_{\omega} [{}^x\rho({}^xv - v)] \cdot {}^x n d^x s = \emptyset$$

can be written, where  ${}^x\rho {}^xv = {}^x\rho^1 {}^xv^1 + {}^x\rho^2 {}^xv^2$  defines the mean velocity  ${}^xv$ .

It is now postulated that all balance laws are valid independently for each part of the mixture and for every part of the body and discontinuity surfaces. Applied to equation (IV.9.2) this implies that the integrands of the integral must vanish independently. Thus in component form,

$$(IV.9.3) \quad \frac{\partial {}^x \rho}{\partial t} + \frac{\partial}{\partial x_k} ({}^x \rho {}^x v_k) = \frac{\partial {}^x \rho^1}{\partial t} + \frac{\partial}{\partial x_k} ({}^x \rho^1 {}^x v_k^1) = \frac{\partial {}^x \rho^2}{\partial t} + \frac{\partial}{\partial x_k} ({}^x \rho^2 {}^x v_k^2) = 0$$

$$(IV.9.4) \quad [{}^x \rho ({}^x v - \nu)] \cdot {}^x n = 0$$

These are the equations of local conservation of mass and the jump conditions.

Also, if the functional dependency  $x = x(a, t)$  in equation (IV.9.3) is changed it becomes,

$$(IV.9.5) \quad \frac{d {}^x \rho}{d t} + {}^x \rho \frac{\partial {}^x v_k}{\partial a_k} = \frac{d {}^x \rho^1}{d t} + {}^x \rho^1 \frac{\partial {}^x v_k^1}{\partial a_k} = \frac{d {}^x \rho^2}{d t} + {}^x \rho^2 \frac{\partial {}^x v_k^2}{\partial a_k} = 0$$

where equation (A.15) and,  ${}^x {}_a \rho = \rho(x(a, t)) = {}^x \rho(a, t)$  is made use of. Tracing back it is found,

$$(IV.9.6) \quad {}^x {}_a \rho = {}^x J^{-1} {}^a \rho(a, t) = {}^x J^{-1} {}^a \rho$$

It can also be written that  ${}^x v_k = v_k(x(a, t)) = {}^x v_k(a, t)$  which, traced back becomes

$$(IV.9.7) \quad {}^x v_k(a, t) i_k = \frac{\partial x_k}{\partial a_l} {}^a v_l(a, t) i_k = {}^x v_k(x, t) i_k$$

To write the jump conditions first note the relations between the exterior unit normal  ${}^x n$  at the deformed surface and  ${}^a n$  at the undeformed surface. From equation (B.2) one may have

$$(IV.9.8) \quad d {}^x s_k = {}^x J \frac{\partial a_l}{\partial x_k} d {}^a s_l$$

$$(IV.9.9) \quad x_{n_k} = d^{x_{s_k}} (d^{x_{s_1}} d^{x_{s_l}})^{\frac{1}{2}} = \frac{d^{x_{s_k}}}{d^{x_s}}, \quad a_n = d^{a_{s_k}} (d^{a_{s_1}} d^{a_{s_l}})^{\frac{1}{2}} = \frac{d^{a_{s_k}}}{d^{a_s}}$$

hence,

$$(IV.9.10) \quad x_{n_k} = x_J \frac{\partial a_l}{\partial x_k} a_{n_l} \frac{d^{a_s}}{d^{x_s}}$$

Using (IV.9.8)

$$(IV.9.11) \quad \frac{d^{a_s}}{d^{x_s}} = x_J^{-1} (c_{ln}^{-1} a_{n_l} a_{n_n})^{-\frac{1}{2}}$$

is obtained, thus

$$(IV.9.12) \quad x_{n_k} = (c_{ln}^{-1} a_{n_l} a_{n_n})^{-\frac{1}{2}} \frac{\partial a_m}{\partial x_k} a_{n_m}$$

Putting this into equation (IV.9.4) the material form of the jump conditions, are obtained

$$(IV.9.13) \quad \left[ {}^a \rho (x_{v_k} - x_{v_k}) \frac{\partial a_l}{\partial x_k} \right] a_{n_l} = \emptyset$$

Also, if phases 1 and 2 are submitted to an isochronic flow, i.e.  $\rho(a,t) = \text{constant}$ , the equation (IV.9.5) may be replaced by

$$(IV.9.14) \quad \frac{\partial}{\partial a_k} x_{v_k}^1 = \frac{\partial}{\partial a_k} x_{v_k}^2 = \frac{\partial}{\partial a_k} x_{v_k} = \emptyset$$

or

$$(IV.9.15) \quad \delta_{kl} \frac{\partial x_{v_k}^1}{\partial a_l} - \delta_{kl} \frac{\partial x_{v_k}^2}{\partial a_l} = \emptyset$$

If it is now postulated that equation (IV.9.15) vanishes independently for each phase and the solid and fluid phases are considered less

compressible than the soil skeleton, the following equation may be written:

$$(IV.9.15a) \quad \delta_{kl} \frac{\partial}{\partial a_i} ({}^x v_k^1 - {}^x v_k^2) - \delta_{kl} \frac{\partial {}^x v_k^2}{\partial x_j} = 0$$

which is another form of (IV.9.15).

The same argument can be used to get a similar equation equivalent to (IV.9.3).

#### IV.10 Definition of stress

##### 1. Stress Vector

To clearly define stress at a given point represented by the vector position  $x_i$  in A.C., a tetrahedron is considered adjacent to the surface  ${}^x s$  of the body. Consider a tetrahedron of volume  $\Delta^x \vartheta$  having three coordinate surfaces  $\Delta^x s_k$ .

By using the equation of balance of momentum (IV.8.2) and the mean value theorem for this tetrahedron, the following can be written

$$(IV.10.1.1) \quad \frac{d}{dt} ({}^x \rho^* {}^x v^* \Delta^x \vartheta) = {}^x \sigma_{(n)}^* \Delta^x s - {}^x \sigma_k^* \Delta^x s_k + {}^x \rho^* {}^x f^* \Delta^x \vartheta$$

where  ${}^x \rho^*$ ,  ${}^x v^*$ ,  ${}^x f^*$  are respectively, the values of  $\rho$ ,  $v$  and  $f$  at some interior point of the deformed tetrahedron and  ${}^x \sigma_{(n)}^*$  and  ${}^x \sigma_k^*$  are the values of  $\sigma_{(n)}$  on the deformed surface  $\Delta^x s$  and on coordinate surfaces  $\Delta^x s_k$ , Figure (IV.10.1),

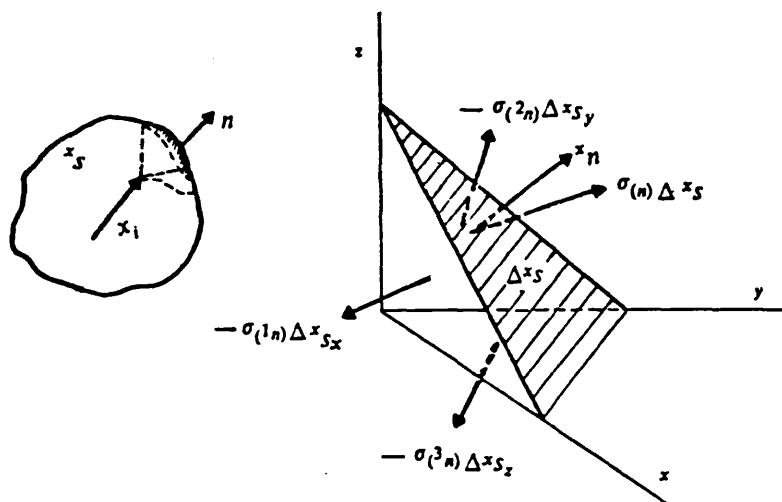


Figure IV.10.1

In the limit as  $\Delta\vartheta \rightarrow 0$  one has

$$(IV.10.1.2) \quad \lim_{\Delta\vartheta \rightarrow 0} \frac{d}{dt} ({}^x\rho \cdot {}^xv \cdot \Delta\vartheta) = {}^x\rho \cdot {}^xv \cdot d^x\vartheta + {}^xv \cdot \frac{d}{dt} \Delta\vartheta = {}^x\rho \cdot {}^xv \cdot d^x\vartheta$$

since the conservation of total mass equation (IV.8.1) ensures that  $\frac{d}{dt} \Delta\vartheta = 0$ . In the limit  $d^x\vartheta / d^x s \rightarrow 0$

$$(IV.10.1.3) \quad {}^x\sigma_{(n)} d^x s = {}^x\sigma_k d^x s_k$$

is obtained. Here  ${}^x\sigma_k$  is called the total stress vector at  $x$ .

similarly, if the balance of moment for a two phase material given by equation (IV.8.3) is used, the following is obtained

$$(IV.10.1.4) \quad {}^x\sigma_{(n)}^\alpha d^x s = {}^x\sigma_k^\alpha d^x s_k \quad \alpha = 1 \text{ or } 2$$

Bearing in mind the tetrahedron, the area vector  $d^x s$  is equal to the sum of the coordinate area vectors, i.e.

$$(IV.10.1.5) \quad d^x s = {}^x n d^x s = d^x s_k i_k$$

or

$$(IV.10.1.6) \quad d^x s_k = {}^x n_k d^x s$$

Introducing this into equation (IV.10.1.3) gives

$$(IV.10.1.7) \quad {}^x \sigma_{(n)} = {}^x \sigma_k {}^x n_k \quad \text{and} \quad {}^x \sigma_{(n)}^\alpha = {}^x \sigma_k^\alpha {}^x n_k^\alpha$$

From these it may be concluded that

$$(IV.10.1.8) \quad {}^x \sigma_{(-n)} = -{}^x \sigma_{(n)} \quad \text{and} \quad {}^x \sigma_{(-n)}^\alpha = -{}^x \sigma_{(n)}^\alpha$$

This means that the traction is a linear function of the normal and that the tractions acting at the opposite sides of a surface area are equal in magnitude and opposite in sign.

## 2. Stress Tensor

The stress tensor  $\sigma_{kl}$  is the  $l$ th component of the stress vector  $\sigma_k$  acting on the positive side of the  $k$ th coordinate surface.

$$(IV.10.2.1) \quad \sigma_k = \sigma_{kl} i_l$$

The positive components of  $\sigma_{kl}$  on the faces of a parallelepiped built on the coordinate surface are shown on Figure (IV.10.2). In order to avoid confusion only the stress components on two pairs of parallel coordinate surfaces have been shown. Note that when the

exterior normal of a surface is in the same direction as the coordinate axes perpendicular to the surface, the positive stress components on that surface are in the positive direction of the coordinates. Similarly, when the exterior normal is opposite in direction to the coordinate axes, the positive stress components are in the opposite direction to the coordinates.

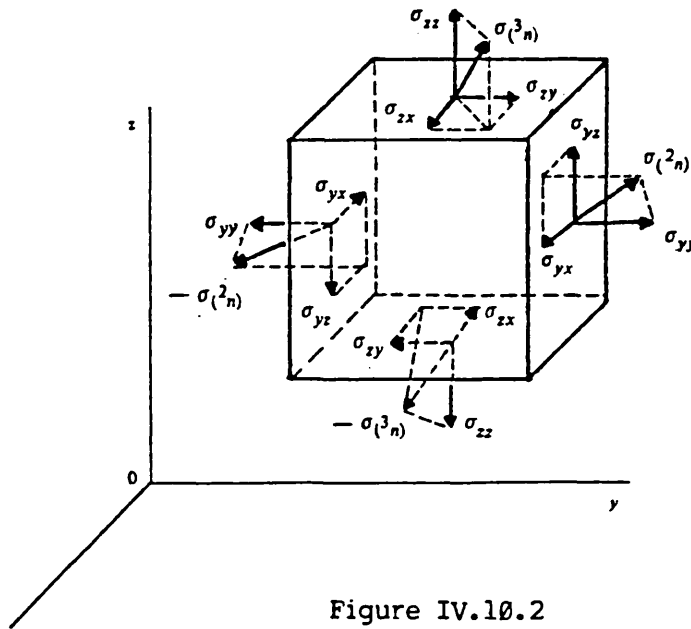


Figure IV.10.2

The components  $\sigma_{xx}$ ,  $\sigma_{yy}$ ,  $\sigma_{zz}$  are called normal stresses, and  $\sigma_{xy}$ ,  $\sigma_{yx}$ ,  $\sigma_{yz}$ ,  $\sigma_{zy}$  are called shear stresses.

Also the stress tensor may be arranged in a matrix form.

$$(IV.10.2.2) \quad \sigma_{kl} = \begin{pmatrix} \sigma_{xx} & \sigma_{xy} & \sigma_{xz} \\ \sigma_{yx} & \sigma_{yy} & \sigma_{yz} \\ \sigma_{zx} & \sigma_{zy} & \sigma_{zz} \end{pmatrix}$$

The traction is given by



$$(IV.10.2.3) \quad \sigma_{(n)} = \sigma_{ki} n_k i_i$$

directly from (IV.10.2.1) and (IV.10.1.7)

Another important property of the stress tensor is its symmetry. So, taking the equation of balance of linear momentum (IV.8.2) associated with equations (A.13) and (A.26) where  $\psi = \rho v$  and  $\tau_k = \sigma_k$ ,

$$(IV.10.2.4) \quad \int_{\mathcal{V}-\omega} \left[ \frac{\partial(\rho v)}{\partial t} + \frac{\partial}{\partial x_k} (\rho v v_k) - \frac{\partial \sigma_k}{\partial x_k} - \rho f \right] d\mathcal{V} + \int_{\omega} \left[ \rho v (v_k - \nu_k) + \sigma_k \right] n_k dS = 0$$

is obtained. If this is postulated for all parts of the body, the integrands vanish independently. Upon using (IV.9.3), this is simplified to

$$(IV.10.2.5) \quad \frac{\partial \sigma_k}{\partial x_k} + (f - \dot{v}) = 0 \quad \text{in} \quad \mathcal{V} - \omega$$

$$(IV.10.2.6) \quad \left[ \rho v (v_k - \nu_k) - \sigma_k \right] n_k = 0 \quad \text{on} \quad \omega$$

where

$$\dot{v} = \frac{\partial v}{\partial t} + \frac{\partial v}{\partial x_k} v_k$$

Equation (IV.10.2.5) is the first law of Cauchy expressing the local balance of momentum, and (IV.10.2.6) is the associated jump condition on the singular surface  $\omega$ .

Upon carrying (IV.10.1.7) into the equation of balance of moment of momentum (IV.8.4) and using (A.13) and (A.26) locally one obtains

$$(IV.10.2.7) \quad i_{k \cdot x} \sigma_k = 0 \quad \text{in} \quad \mathcal{V} - \omega$$

where the local laws of conservation of mass and balance of momentum (IV.9.3), (IV.9.4), (IV.10.2.5) and (IV.10.2.6) were used. The associate jump conditions for the moment of the momentum is satisfied identically.

When (IV.10.2.1) is used, (IV.10.2.7) gives

$$(IV.10.2.8) \quad \sigma_{kl} = \sigma_{lk}$$

thus, the necessary and sufficient condition for the satisfaction of the local balance of moment of momentum is the symmetry of the stress tensor.

- Piola-Kirchhoff stress tensor.

To find the equation of motion in a fix reference frame the stress tensor must be transformed from the local and deformed coordinate system to the original fix one. Thus, let  ${}^a_x \sigma_k$  be the stress at a spatial point  $x$  in the A.C. but referred (measured) by unit of area at  $a$  in the I.C. If  $d^x s$  and  $d^x s_k$  are, respectively, the area surface at  $x$  and the components of the area surface at  $x$  and  $d^a s_k$  are the area components, when tracing back the components of the area surface at  $x$  to the initial configuration, the following equation can be written

$$(IV.10.2.9) \quad \sigma_{(x_n)} d^x s = {}^x_x \sigma_k d^x s_k = {}^x_a \sigma_k d^a s_k$$

where  $x_n$  is the normal of the area element at  $x$  .

By making use of the equation (B.2)

$$(IV.10.2.10) \quad {}^x\sigma_k = J^{-1} \frac{\partial x_k}{\partial a_l} {}^a\sigma_l, \quad {}^a\sigma_l = J \frac{\partial a_l}{\partial x_k} {}^x\sigma_k$$

can be written, where  ${}^x\sigma_k$  is the stress vector defined at  $x$  by unit of deformed area and  ${}^a\sigma_l$  is the stress vector defined at  $x$  by unit of undeformed area.

To represent the components the Piola-Kirchhoff pseudo stresses  ${}^a\sigma_l$  and  ${}^a\sigma_{kl}$  are introduced and defined by

$$(IV.10.2.11) \quad {}^a\sigma_l = {}^x\sigma_{lm} \cdot i_m$$

where  ${}^x\sigma_{lm}$  is the  $m$ th scalar component of the stress vector  ${}^x\sigma_l$ , obtained on the deformed axes. Now, tracing back to the undeformed axis,  ${}^a\sigma_{ln}$  is found with the effect of the inverse transformation  $\partial a_n / \partial x_m$  (the same explanation was used in arriving at equation (A.5)). Or,

$$(IV.10.2.12) \quad {}^x\sigma_{lm} = {}^a\sigma_{ln} \frac{\partial x_m}{\partial a_n} \quad \text{and} \quad {}^a\sigma_l = {}^a\sigma_{ln} \frac{\partial x_m}{\partial a_n} i_m$$

so that by (IV.10.2.10) one can write

$$(IV.10.2.13) \quad {}^x\sigma_{ln} = J \frac{\partial a_l}{\partial x_k} {}^x\sigma_{kn}, \quad {}^x\sigma_{kn} = J^{-1} \frac{\partial x_k}{\partial a_l} {}^a\sigma_{ln} = J^{-1} \frac{\partial x_k}{\partial a_l} \frac{\partial x_m}{\partial a_n} {}^a\sigma_{km}$$

$$(IV.10.2.14) \quad {}^a\sigma_{ln} = {}^x\sigma_{lm} \frac{\partial a_n}{\partial x_m} = J \frac{\partial a_l}{\partial x_k} \frac{\partial a_n}{\partial x_m} {}^x\sigma_{km}$$

Thus, to obtain the stress tensor  ${}^a\sigma$  (defined at A.C. but measured by unit of surface at I.C. and at the coordinate system at I.C.) as

function of  ${}^x_{xx}\sigma$  (defined at A.C., measured by unit of surface at A.C. and at the deformed coordinate at A.C.) the transformation given by equation (IV.10.2.14) should be used. Transformation among  ${}^x_{aa}\sigma$ ,  ${}^x_{ax}\sigma$  and  ${}^x_{xx}\sigma$  can also be obtained, from the same equation.

Now, substituting (IV.10.2.10) into (IV.10.2.5) and using (A.11), (IV.8.16)

$$(IV.10.2.15a) \quad \frac{\partial {}^x_{aa}\sigma_k}{\partial a_j} + {}^x_{aa}\rho({}^x_{aa}f - {}^x_{aa}v) = 0$$

is obtained, which is the Cauchy's equation of motion in the reference frame. For component representation (IV.10.2.11) is introduced into (IV.10.2.15a) or (IV.10.2.14) into (IV.10.2.15a) and two different forms of the equation of motion are obtained:

$$(IV.10.2.15b) \quad \frac{\partial {}^x_{ax}\sigma_{kj}}{\partial a_k} + {}^a\rho({}^x_{aa}f_k - {}^x_{aa}v_k) = 0$$

$$(IV.10.2.15c) \quad \frac{\partial ({}^x_{aa}\sigma_{kj} \partial x_i / \partial a_j)}{\partial a_k} + {}^a\rho({}^x_{aa}f_k - {}^x_{aa}v) = 0$$

Cauchy's second law of motion follows from  $\sigma_{ki} = \sigma_{ik}$  and using (IV.10.2.13), too. Also using  $\sigma_{ki} = \sigma_{ik}$  another two different forms are obtained,

$$(IV.10.2.15d) \quad {}^x_{ax}\sigma_{kj} \frac{\partial x_i}{\partial a_k} = {}^x_{ax}\sigma_{ki} \frac{\partial x_j}{\partial a_k}$$

$$(IV.10.2.15e) \quad {}^x_{aa}\sigma_{kj} = {}^x_{aa}\sigma_{jk}$$

To write the jump conditions in the reference frame, equations (IV.10.1.2), (IV.10.2.10) are introduced into equation (IV.10.2.6) to find

$$(IV.10.2.15f) \quad \left[ {}^a \rho_a^x \vartheta (x_\nu - x_a^{\nu k}) \frac{\partial a_l}{\partial x_k} - x_a^{\sigma l} \right] a_{n_l} = 0$$

Finally, it may be possible to express equations (IV.10.2.13) in relation to the infinitesimal strain tensor  $l_{kl}$  and infinitesimal rotation tensor  $w_{kl}$ . By using (IV.4.8) and (IV.4.10) the following can be written

$$(IV.10.2.16) \quad \frac{\partial a_k}{\partial x_l} = \delta_{kl} - l_{kl} - w_{kl}$$

Introducing this into equation (IV.10.2.13), equations

$$(IV.10.2.17) \quad {}^a \sigma_{kl} \approx \delta_{mn} x^m \sigma_{nl} - w_{mn} x^m \sigma_{nl}$$

$$(IV.10.2.18) \quad {}^a \sigma_{kl} \approx \delta_{ln} \sigma_{kn} - w_{ln} \sigma_{kn} - w_{nk} \sigma_{nl} + w_{ml} w_{mn} \sigma_{kn}$$

are obtained where it has been assumed that  $l_{kl}$  is small compared to 1 and  $j = 1 + l_{kk}$  as given by (IV.3.5)

#### -Principal Directions of Stress: invariants of the stress tensor

Now that the concept of stress in the vector and tensor form has been established, this tensor can be expressed by the theorems demonstrated in the Strain Definitions section. In particular, it can be shown (on the basis that the law of transformation for the normal stress tensor is analogous to that for strain tensor) that for every point in a body after deformation there exists three mutually perpendicular surfaces on which all shear stresses are zero, and on which normal stresses assume stationary values. By reasoning analogous to that in the strain section, it may be shown that a similar characteristic equation for

the stress tensor can be obtained. Following the same procedure as used for the characteristic equation of strain, the three roots of the characteristic equation of stress may give the principal stress tensor:

$$\sigma_1 = \frac{2}{\sqrt{3}} J_2 \sin\left(\theta_J + \frac{2}{3}\pi\right) + J_1$$

$$(IV.10.2.19) \quad \sigma_2 = \frac{2}{\sqrt{3}} J_2 \sin\theta_J + J_1, \quad \sigma_1 \geq \sigma_2 \geq \sigma_3$$

$$\sigma_3 = \frac{2}{\sqrt{3}} J_2 \sin\left(\theta_J + \frac{4}{3}\pi\right) + J_1$$

$$(IV.10.2.20) \quad J_1 = \frac{1}{3}(\sigma_{xx} + \sigma_{yy} + \sigma_{zz}) = \frac{1}{3}\sigma_{kk}$$

$$(IV.10.2.21) \quad J_2 = \sigma_{xx}\sigma_{yy} + \sigma_{yy}\sigma_{zz} + \sigma_{zz}\sigma_{xx} - \tau_{yz}^2 - \tau_{zx}^2 - \tau_{xy}^2 = \frac{1}{2}\sigma_{ij}\sigma_{ij}$$

$$(IV.10.2.22) \quad \bar{\sigma}_{ij} = \sigma_{ij} - \frac{1}{3}\delta_{ij}\sigma_{kk}$$

$$(IV.10.2.23) \quad J_2 = 3J_1^2 - J_2 = \frac{1}{6}\left[(\sigma_{xx} - \sigma_{yy})^2 + (\sigma_{yy} - \sigma_{zz})^2 + (\sigma_{zz} - \sigma_{xx})^2 + 6(\tau_{yz}^2 + \tau_{zx}^2 + \tau_{xy}^2)\right] = \frac{1}{2}\bar{\sigma}_{ij}\bar{\sigma}_{ij}$$

$$(IV.10.2.24) \quad J_3 = J_3 - J_2 J_1 + 2J_1^3 = J_3 + J_2 J_1 - J_1^3 = \frac{1}{3}\bar{\sigma}_{ij}\bar{\sigma}_{ij}\bar{\sigma}_{ij}$$

$$(IV.10.2.25) \quad \theta_J = \frac{1}{3} \arcsin\left(-\frac{3\sqrt{3}}{2} \frac{J_3}{J_2^3}\right) = \arcsin\left[\frac{2\sigma_2 - \sigma_1 - \sigma_3}{\sqrt{3}(\sigma_1 - \sigma_3)}\right], \quad -\frac{\pi}{6} \leq \theta_J \leq \frac{\pi}{6}$$

The stresses invariants  $J_1$ ,  $J_2$  and  $\theta_J$  given by the previous equations, together with the strain invariants  $I_1$ ,  $I_2$ ,  $\theta_I$  given by equation (IV.5.12) are to play, in future, an important role in the

definition of local stress-strain relationship.

CHAPTER VVARIATIONAL METHODV.1 Introduction

The consolidation problem will be adequately represented by a system of differential equations with its respective boundary and/or side conditions.

It is well known that, except for simple cases, it is impossible to find a closed form solution to these equations which in addition must satisfy the boundary conditions. Another alternative is to seek an approximate method of solution.

Because of the possibility of using the finite element method for numerical solutions, a consistent variational approach is therefore required. The variational method consists in replacing the system of continuous equations by an equivalent global statement, which accepts approximate functions as its solutions. The continuous equations are usually transformed in a functional by an energy theorem. A functional may be defined as a special type of function where the independent variables are one or more unknown functions.

By transforming the continuous equations into a functional, it is always necessary to find the conditions which these unknown functions must satisfy in order to make the functional a stationary point, usually the minimum. It may be shown that a functional has a



minimum stationary point when its integrand satisfies the Euler-Lagrange equations, as well as the boundary and side conditions (Washizu (1968)).

It is well known that the particular choice of approximated function characteristic of the finite element method, imply substantial advantages.

The discussion of the method of solution, and applicability of the finite element method has been published in a number of publications, see for example Naylor (1981), Zienkiewicz (1972), Cook (1974) and Smith (1982). In the first text book the applications of many important problems in soil mechanics are discussed, and a mathematical analysis of the method is given by Strang and Fix (1973).

Another alternative to the finite element method is the boundary element method, Banerjee and Butterfield (1979) , in which approximations are introduced only on the boundary. With the aid of a fundamental solution, the differential equations are reformulated as integral equations. Evidently, the method would be powerful in combination with the finite element method to account for the effect of semi-infinite regions occurring frequently in soil mechanics problems. The application to the consolidation problem still remains for the future, and is beyond the scope of this thesis.

## V.2 A Brief Survey of Different Approaches

Although in this thesis the transformation of the continuous field equations into finite element equations is reached by means of virtual

work rate definition, a brief description of previous formulations is presented

Many formulations have previously been discussed in relation to the case of complete linear problems, i.e., linearity is assumed both in kinematics and in the material constitution. The latter restriction is, however, not essential when different functionals are discussed.

In the case of linear kinetics a number of approaches which can be used to reach the finite element equations are possible.

One of the first approaches was introduced by Christian and Boehmer (1968,1969) , who solved a sequence of fictitious undrained problems. After load is added in a time interval, the pore pressure and displacement field generated are evaluated for the undrained case. The pore pressure generated is then used in the continuity equation to evaluate the rate of volumetric deformation. Keeping the rate constant during the next step, one easily obtains an additional volumetric strain increment. For each known total volumetric strain a new set of displacement and pore pressure are obtained at the end of the time step. The method may be seen as a forward Euler Scheme with successive application of Reisner's variational principle, as the continuity equation is a constraint condition (stepwise incompressibility during each time-step).

Following an approach established by Gurtin (1964) for linear initial value problems like heat conduction and viscoelasticity, Sandhu (1968) solved a pseudo-variational problem (stationary point), where the associate functional contains convolution products in the time domain. In practice the method can be shown to be equivalent to a semi-

discrete method, with Crank-Nicholson's finite difference scheme in the time domain. Explicit results of the linear problem for plane strain and plane flow have been presented by Sandhu and Wilson (1969), who used 6 noded isoparametric elements, where displacement and pore-pressure are approximated in the same manner.

Similar variational principles have been suggested for related coupled problems, Sandhu and Pister (1970), and an extension to non-linear problems and mixed formulations have been made by Sandhu (1976). No practical applications have, however, as far as the author knows, been presented for the latter cases.

Using similar methods to those previously described (Galerkins method in the space domain and Crank-Nicholson's finite difference scheme in the time domain) Hwang et al (1971) obtained a solution for the linear case. Taking advantage of the decay in the process they work with logarithmic time increments.

A mixed formulation of the linear problem based on the variation of an extended functional corresponding to the Hu-Washizu's variational principle in elasticity was proposed by Yokoo et al (1976). Independent variables are displacements, strains, effective stresses, excess pore pressures, hydraulic gradient, and diffusion velocities. Restricting themselves to the ordinary theory with displacement and excess pore pressures as unknown, which in fact may also be considered as mixed theory, Yokoo et al (1976) present results for the case of the load growing from zero linearly to a final value during a finite time. All unknowns are assumed to be zero initially. For a linear theory the continuous loading approach requires more than one solution step which is contrary to the initial loading approach. On the other

hand, this disadvantage disappears at the extension of such non-linear models for which an initial loading approach requires an incremental loading technique, while the algorithm for the continuous loading approach will be unchanged in principle. Of course, the continuous loading may well be motivated by physical reasons, i.e., consolidation effects during loading should not be neglected. This type of approach is adopted in this thesis.

Yokoo et al (1974) used the discontinuous loading approach also. In their work it was considered, that in such a case, i.e., consolidation following undrained deformation, approximations of the excess pore pressure have to be discontinuous in time.

A totally different approach was used by Booker (1974). The field equations are made explicitly independent of time by a Laplace transformation. Such a transformation yields an eigenvalue-problem in the Laplace transform space. An approximation for the finite element method provided a discrete approach with associated eigenfunctions in terms of nodal unknown values. The approximate transforms are expanded in terms of their discrete points, i.e. the eigenvalues, and are finally inverted. Solutions have been presented mainly for isotropic linear elasticity and isotropic permeability.

A more simple approach for non-linear kinematics was presented by Carter, Booker and Small (1979) where the equilibrium equations were treated by the principle of virtual displacement in rate form and the continuity equation described by an equivalent of integral form, also in rate form. The use of the principle of virtual work approach is supported by the fact that this principle reflects the condition of equilibrium, which makes it valid for linear and non-linear problems.

Also, it may be shown that this principle satisfies the Galerkin process which makes it correspond to a functional.

Finally the Crank-Nicholson finite difference scheme in time was used. Their formulation, however, used an Euler approach which is different to the so called total Lagrange and updated Lagrange method assumed in this thesis. In the next chapter it will be shown that the updated Lagrange approach yields a symmetric finite element equation whilst the Euler approach makes the finite element equation non-symmetric, and inconvenient.

### V.3 Principle of Virtual Work

In this section, integral equations representing the equilibrium equation and also the continuity equation are presented. In particular the principle of virtual displacement is applied to the total equilibrium and an integral form of continuity equation is used to link both phases.

Principle of Virtual Displacement: Considering an deformable body which moves continuously in space, the principle of virtual displacement assumes that a distinct equilibrium configuration exists in the very close neighbourhood of the current equilibrium configuration. If at a particular configuration (the equilibrium position at time  $t$ ) a virtual displacement  $\delta u_k$  is imposed, the body moves virtually to an adjacent equilibrium configuration, associated with time  $t + \Delta t$ . See Figure V.3.1.

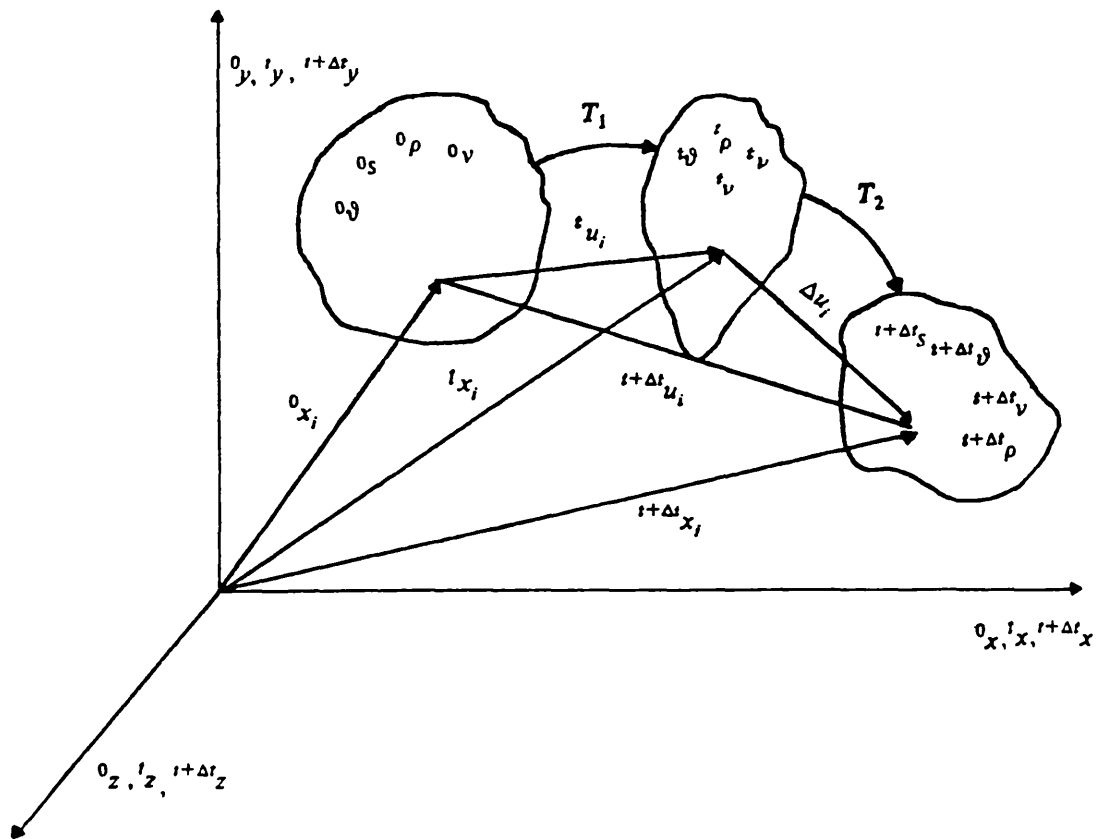


Figure V.3.1.

Using this assumption, the principle of virtual displacement requires:

$$(V.3.1) \quad \int_{1+\Delta t \vartheta} {}^{1+\Delta t} \sigma_{ij} \delta {}^{1+\Delta t} e_{ij}^2 {}^{1+\Delta t} d\vartheta = {}^{1+\Delta t} R$$

where  ${}^{1+\Delta t} R$  is the external virtual work expression for isochronic flow. However for compressible and/or viscous fluid the quantity  ${}^{1+\Delta t} e_{ij}^2$  can be substituted by  ${}^{1+\Delta t} e_{ij}^1 + {}^{1+\Delta t} e_{ij}^2$ .

$$(V.3.2) \quad {}^{1+\Delta t} R = \int_{1+\Delta t s} {}^{1+\Delta t} \bar{\sigma}_k \delta u_k {}^{1+\Delta t} ds + \int_{1+\Delta t \vartheta} {}^{1+\Delta t} \rho {}^{1+\Delta t} f_k \delta u_k {}^{1+\Delta t} d\vartheta$$

Note that this principle is an equilibrium requirement being valid, of course, for both linear/non-linear problems and also for a body under non-conservative external forces.

In equations (V.3.1) and (V.3.2)  $\delta u_k$  is a virtual variation of the current displacement components  ${}^{t+\Delta t}u_k$  and  $\delta_{t+\Delta t}e_{ij}$  are the corresponding variations in strain, i.e.

$$\delta_{t+\Delta t}e_{ij} = \delta \frac{1}{2} \left( \frac{\partial u_i}{\partial t+\Delta t x_j} + \frac{\partial u_j}{\partial t+\Delta t x_i} \right)$$

Equations (V.3.1) and (V.3.2) may be proved to be equivalent to the field equations (IV.10.2.5) and (IV.10.2.6).

Integral Form of the Continuity Equation Based on the same argument and using the same assumptions used to establish the principle of virtual displacement, an integral equation equivalent to the continuity equation can be derived. One simple way to obtain such an equation is by means of Galerkin Method or even by physical reasoning. Such an equation may be written as:

$$(V.3.3) \quad \int_{t+\Delta t \Omega} \delta_{ij} ({}_{t+\Delta t}e_{ij}^1 - {}_{t+\Delta t}e_{ij}^2) \delta {}^{t+\Delta t}\sigma_{ij}^1 {}^{t+\Delta t}d\vartheta + \int_{t+\Delta t \Omega} \delta_{ij} ({}_{t+\Delta t}e_{ij}^2) \delta {}^{t+\Delta t}\sigma_{ij}^2 {}^{t+\Delta t}d\vartheta = 0$$

where 
$$\dot{e}_{ij}^\alpha = \frac{1}{2} \left( \frac{\partial v_i^\alpha}{\partial t+\Delta t x_j} + \frac{\partial v_j^\alpha}{\partial t+\Delta t x_i} \right), \quad \alpha = 1 \text{ or } 2$$

is the rate of deformation of the fluid phase derived from the field velocity of the fluid phase when  $\alpha = 1$ , and is the rate of deformation

derived from the field velocity of the solid skeleton when  $\alpha = 2$  .  
 And

$\delta_{ij}$  is the Kronecker Delta,

${}^{t+\Delta t}\sigma_{ij}^1$  is the virtual variation of stress for the fluid phase,

${}^{t+\Delta t}\sigma_{ij}^2$  is the virtual variation of stress for the solid skeleton.

Note that equations (V.3.1) and (V.3.3) cannot be solved directly since the configuration at time  $t + \Delta t$  is unknown. One way to overcome this inconvenience and arrive at a solution is to refer all variables for this current configuration to a previously known one. Any previously known configuration can be chosen.

However, usually, the choice lies between two different approaches, namely, total Lagrange and updated Lagrange approaches. In fact a third approach could be used - the so-called Euler approach - but this formulation makes the stress - strain law definition inconvenient for finite element applications, since it leads to a non-symmetric stress - strain law from a geometric point of view.

Both total Lagrange and updated Lagrange method will be developed in the next chapter by transforming the equations (V.3.1), (V.3.2) and (V.3.3) accordingly.



CHAPTER VIFIELD EQUATION IN INCREMENTAL FORMVI.1 Introduction

In the previous chapter the principle of virtual work was established in rate form. These principles are now made use of to formulate the governing equation of consolidation in rate form. Two systems of integral equations will be reached, one by the so called total Lagrange formulation and the other by the so called updated Lagrange formulation.

Although these approaches have been used when establishing the field equations for other kind of problems, they have not yet been explicitly applied to the Consolidation problem.

However, before introducing these treatments, the various rate definitions of the variables involved are summarised.

Firstly, the velocity vector measured in the deformed and undeformed frame of reference and the various definitions of strain rate and stress rate are given. Detailed treatment showing their interrelationship are also presented.

Next, the various stress-strain relationships are introduced as well as the linear combinations between them. Also the Bernoulli theorem and Darcy's Law for the finite deformation conditions are included.

After the basic definitions , by making use of the principle of virtual work for the equilibrium equation and the integral form of the continuity equation, the general incremental form of the consolidation equations are reached by the use of total Lagrange and updated Lagrange methods.

Finally, after linearization, it can be seen that the total Lagrange Formulation exhibits a system of non-symmetric equations while the updated Lagrange formulation provides a system of equations which still maintains its symmetry. As the Euler approach also provides a non-symmetric system of equations (Carter et al 1979), the previous conclusion makes the updated Lagrange formulation the best choice for the solution technique.

A fourth option could be used where the solid skeleton is treated by the total Lagrange formulation, while the fluid equation is treated by the Euler formulation. This approach was used by Argyris (1981) to analyse incompressible viscous flow through solid media.

This option is not discussed here but its deduction follows the same procedure presented in this chapter.

To formulate the incremental theory it is essential to define rate of strain, velocity and stress rate. However, instead of rate of strain, velocity and stress rate, the strain increment, velocity increment and stress increment, will be used.

Firstly, the loading path of the solid body problem is divided into a number of equilibrium states. Figure VI.1.1 shows schematically three

of these equilibrium configurations.

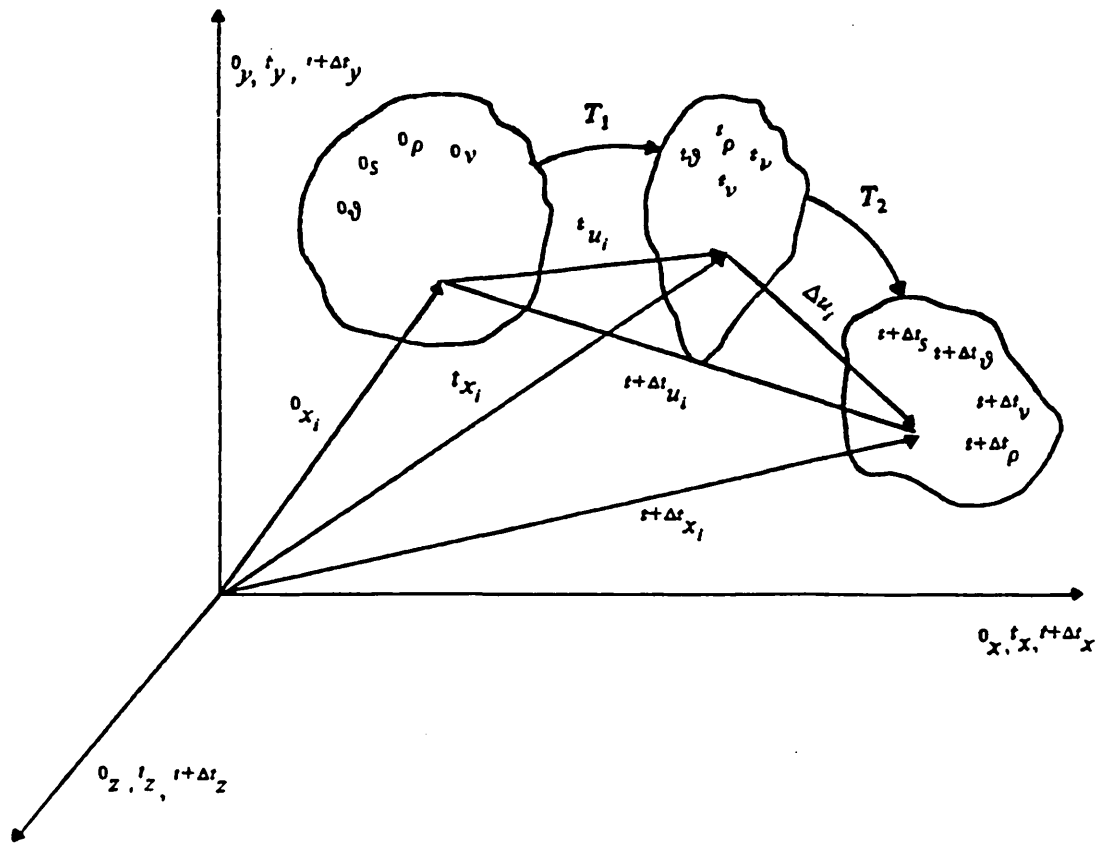


Figure VI.1.1

In the first configuration all variables are known and referred to as:

Time	$\emptyset$	or	$\emptyset$
Volume	${}^0\vartheta$	or	${}^a\vartheta$
Area	${}^0s$	or	${}^as$
Generalized point	${}^0P({}^0x, {}^0y, {}^0z)$	or	${}^aP$
Position vector	${}^0x_i$	or	${}^ax_i$
Velocity vector	${}^0v^a$	or	${}^av^a$
Pore pressure	${}^0p$	or	${}^ap$

In the second configuration all variables are known and referred as:

Time	$t$	or	$t$
Area	${}^t s$	or	$b_s$
Volume	${}^t v$	or	$b_v$
Generalized point	${}^t P({}^t x, {}^t y, {}^t z)$	or	$b_P$
Position vector	${}^t x_i$	or	$b_{x_i}$
Velocity vector	${}^t v^\alpha$	or	$b_{v^\alpha}$
Displacement vector	${}^t u$	or	$b_u$
Pore pressure	${}^t p$	or	$b_p$

The third configuration is one step away from configuration two where the variables are unknown and would be referred to as:

Time	$t + \Delta t$	or	$t + \Delta t$
Area	${}^{t+\Delta t} s$	or	$x_s$
Volume	${}^{t+\Delta t} v$	or	$x_v$
Generalized point	${}^{t+\Delta t} P({}^{t+\Delta t} x, {}^{t+\Delta t} y, {}^{t+\Delta t} z)$	or	$x_P$
Position vector	${}^{t+\Delta t} x_i$	or	$x_{x_i}$
Velocity vector	${}^{t+\Delta t} v^\alpha$	or	$x_{v^\alpha}$
Displacement vector	${}^{t+\Delta t} u$	or	$x_u$
Pore Pressure	${}^{t+\Delta t} p$	or	$x_p$

Referring to Figure VI.1.1

$$(VI.1.1) \quad {}^t x_i = {}^0 x_i + {}^t u_i, \quad {}^{t+\Delta t} u_i = {}^t u_i + \Delta u_i$$

$$(VI.1.2) \quad {}^{t+\Delta t} x_i = {}^0 x_i + {}^{t+\Delta t} u_i = {}^0 x_i + {}^t u_i + \Delta u_i$$

$$(VI.1.3) \quad {}^t v_i^\sigma = \frac{\Delta u_i^\sigma}{\Delta t} \Big|_t, \quad {}^{t+\Delta t} v_i^\sigma = \frac{\Delta u_i^\sigma}{\Delta t} \Big|_{t+\Delta t}, \quad \Delta v_i^\sigma = \frac{\Delta u_i^\sigma}{\Delta t}$$

$$(VI.1.4) \quad {}^{t+\Delta t} v_i^\sigma = {}^t v_i^\sigma + \Delta v_i^\sigma, \quad {}^{t+\Delta t} v_i^1 - {}^{t+\Delta t} v_i^2 = {}^t v_i^1 - {}^t v_i^2 + \Delta v_i^1 - \Delta v_i^2$$

can be written.

Sometimes a variable may also be referred to in one configuration but measured in relation to another. In this case it would be written, say, for stress tensor as  ${}_b^a \sigma_{kl}$  (or alternatively  ${}_t^0 \sigma_{kl}$ ), or for strain  ${}_a^t e_{kl}$  (or alternatively  ${}_0^{t+\Delta t} e_{kl}$ ) meaning, respectively, that the stress tensor is defined at geometry "a" but measured using geometric dimensions at "b", (or the stress tensor is defined at time  $\emptyset$  but measured by the geometric dimensions at time t); the strain tensor is defined at geometric configuration "x"  $x({}^{t+\Delta t} x_i)$  but measured using the geometric dimensions at "a" ( ${}^0 x_i$ ), (or, the strain tensor is defined at time  $t + \Delta t$  but measured using the geometric dimensions at time  $\emptyset$ ).

## VI.2 Velocity Increment

By using the expression (IV.9.7) the velocity components V (measured at current configuration "b" which has undergone a transformation  $\partial b_k / \partial a_j$  in relation to the referential configuration "a") may be written as a function of the velocity components measured at "a" as,

$$(VI.2.1) \quad {}^b v_k = \frac{\partial a_k}{\partial b_j} {}^b v_j$$

If the body experiences additional movement from its equilibrium position at "b" to another equilibrium position at "x" and also the reference frame suffers a transformation  $\partial x_i / \partial b_j$ , the velocity components in this new equilibrium position may be related to:

$$(VI.2.2) \quad ({}^b v_j + \Delta {}^x v_j) = \frac{\partial b_j}{\partial x_i} ({}^x v_i + \Delta {}^x v_i)$$

and the velocity components viewed from the initial reference frame "a" may be expressed:

$$(VI.2.3) \quad ({}^b v_k + \Delta {}^x v_k) = \frac{\partial a_k}{\partial b_j} ({}^b v_j + \Delta {}^x v_j) = \frac{\partial a_k}{\partial b_j} \frac{\partial b_j}{\partial x_i} ({}^x v_i + \Delta {}^x v_i)$$

or the incremental components of the vector velocity may be related to each other:

$$(VI.2.4) \quad \Delta {}^x v_k = \frac{\partial a_k}{\partial b_j} \Delta {}^x v_j = \frac{\partial a_k}{\partial b_j} \frac{\partial b_j}{\partial x_i} \Delta {}^x v_i = \frac{\partial a_k}{\partial x_i} \Delta {}^x v_i$$

### VI.3 Strain Increment

By using expression (IV.4.9) the Lagrange strain tensor  ${}^b e_{kl}$  at "b" but measured at "a" and the Lagrange strain tensor  ${}^x e_{kl}$  at "x" but measured at "a" may be written as

$$(VI.3.1) \quad 2 {}^b e_{kl} = \frac{\partial {}^a u_k}{\partial a_j} + \frac{\partial {}^a u_l}{\partial a_k} + \frac{\partial {}^a u_m}{\partial a_k} \frac{\partial {}^a u_m}{\partial a_j}$$

$$(VI.3.2) \quad 2 {}^x e_{kl} = \frac{\partial ({}^a u_k + \Delta u_k)}{\partial a_j} + \frac{\partial ({}^a u_l + \Delta u_l)}{\partial a_k} + \frac{\partial ({}^a u_m + \Delta u_m)}{\partial a_k} \frac{\partial ({}^a u_m + \Delta u_m)}{\partial a_j}$$

From these equations,

$$(VI.3.3) \quad 2\Delta_a^x e_{kl}^\alpha = \left( \delta_{ll} + \frac{\partial u_i}{\partial a_l} \right) \frac{\partial(\Delta u_i)}{\partial a_k} + \left( \delta_{lk} + \frac{\partial u_i}{\partial a_k} \right) \frac{\partial(\Delta u_i)}{\partial a_l} + \frac{\partial(\Delta u_i)}{\partial a_k} \frac{\partial(\Delta u_i)}{\partial a_l}$$

is readily obtained, and where  ${}^x e_{kl}^\alpha = {}^b e_{kl}^\alpha + \Delta_a^x e_{kl}^\alpha$  and  $\Delta_a^x e_{kl}^\alpha$  is the increment strain tensor from "b" to "x" but measured as a function of the geometric dimension at "a".

Also, the Lagrange strain increment  $\Delta_b^x e_{kl}^\alpha$  at "x" but measured at "b" can be written as:

$$(VI.3.4) \quad 2\Delta_b^x e_{kl}^\alpha = \frac{\partial(\Delta u_k^\alpha)}{\partial b_l^\alpha} + \frac{\partial(\Delta u_l^\alpha)}{\partial b_k^\alpha} + \frac{\partial(\Delta u_i^\alpha)}{\partial b_k^\alpha} \frac{\partial(\Delta u_i^\alpha)}{\partial b_l^\alpha}$$

Note that the  $\lim_{x \rightarrow b} \Delta_b^x e_{kl}^\alpha$  may be found to be the deformation rate which is defined by the material time derivative of the expression (A.4), where (A.22) is used. Also note that the  $\lim_{x \rightarrow a} \Delta_a^x e_{kl}^\alpha$  may be found to be the material derivative of the Lagrange strain tensor, which may be found by taking the material time derivative of (A.4) where (A.22) and (A.5) are used. Consequently, the relationship between the two limits may be readily found to be approximately,

$$(VI.3.5) \quad \Delta_a^x e_{kl}^\alpha = \frac{\partial b_i^\alpha}{\partial a_k^\alpha} \frac{\partial b_j^\alpha}{\partial a_l^\alpha} \Delta_b^x e_{ij}^\alpha, \quad \Delta_b^x e_{ij}^\alpha = \frac{\partial a_k^\alpha}{\partial b_i^\alpha} \frac{\partial a_l^\alpha}{\partial b_j^\alpha} \Delta_a^x e_{kl}^\alpha$$

It is convenient to breakdown the expression of the strain increment into linear and non-linear terms in  $\Delta u_i$ , so,

$$(VI.3.6) \quad \Delta_x^x e_{kl}^\alpha = \Delta_a^x \epsilon_{kl}^\alpha + \Delta_a^x \eta_{kl}^\alpha$$

where the first part of the expression on the righthand side contains linear terms and the latter contains nonlinear terms.

#### VI.4 Stress Increment

By using the expression (IV.10.2.14) the Kirchhoff stress tensor  ${}^b_a\sigma_{kl}$  at "b" may be written as a function of the Euler stress tensor  ${}^b_b\sigma_{ij}$  at "b". So,

$$(VI.4.1) \quad {}^b_a\sigma_{kl} = {}^bJ^{-1} \frac{\partial b_i^\alpha}{\partial a_k^\alpha} \frac{\partial b_j^\alpha}{\partial a_l^\alpha} {}^b_b\sigma_{ij}$$

where  ${}^b_a\sigma_{kl}$  is written instead of  ${}^b_{aa}\sigma_{kl}$  and  ${}^b_b\sigma_{ij}$  instead of  ${}^b_{bb}\sigma_{ij}$ .

The Kirchhoff stress tensor  ${}^x_a\sigma_{kl} = {}^b_a\sigma_{kl} + \Delta {}^x_a\sigma_{kl}$  at "x" measured at "a" may also be written as a function of the Euler stress tensor defined as  ${}^x_b\sigma_{ij} = {}^b_b\sigma_{ij} + \Delta {}^x_b\sigma_{ij}$ , so,

$$(VI.4.2) \quad {}^x_a\sigma_{kl} + \Delta {}^x_a\sigma_{kl} = {}^xJ^{-1} \frac{\partial x_i^\alpha}{\partial a_k^\alpha} \frac{\partial x_j^\alpha}{\partial a_l^\alpha} ({}^b_b\sigma_{ij} + \Delta {}^x_b\sigma_{ij})$$

Also the Kirchhoff stress tensor  ${}^x_b\sigma_{kl} = {}^b_b\sigma_{kl} + \Delta {}^x_b\sigma_{kl}$  at "x", but defined at "b", may be defined as a function of the Euler stress tensor at "x" becoming

$$(VI.4.3) \quad {}^x_b\sigma_{kl} + \Delta {}^x_b\sigma_{kl} = {}^xJ_2^{-1} \frac{\partial x_i^\alpha}{\partial a_k^\alpha} \frac{\partial x_j^\alpha}{\partial a_l^\alpha} ({}^b_b\sigma_{ij} + \Delta {}^x_b\sigma_{ij})$$

Combining the expression (VI.4.2) and (VI.4.3) and using the equation (IV.3.4) and (VI.4.1)



$$(VI.4.4) \quad \Delta_b^x \sigma_{ij} = {}^b J^{-1} \frac{\partial b_i^\alpha}{\partial a_k^\alpha} \frac{\partial b_j^\alpha}{\partial a_l^\alpha} \Delta_a^x \sigma_{kl}$$

is obtained, where  $\Delta_b^x \sigma_{ij}$  is called the Truesdell stress increment tensor.

The relationship between the Truesdell stress tensor and the Euler stress tensor may be derived from (VI.4.3) if relations (IV.3.5), (VI.4.1), (VI.4.3) are used. So,

$$(VI.4.5) \quad \Delta_b^x \sigma_{ij}^\alpha = \Delta_x^x \sigma_{ij}^\alpha - {}^b \sigma_{ik}^\alpha \Delta_b^x w_{kj} - {}^b \sigma_{jn}^\alpha \Delta_b^x w_{ni} - {}^b \sigma_{il}^\alpha \Delta_b^x \epsilon_{jl} - {}^b \sigma_{jl}^\alpha \Delta_b^x \epsilon_{il} + {}^b \sigma_{ij}^\alpha \Delta_b^x \epsilon_{ll}$$

where

$$\Delta_b^x w_{ij} = \frac{1}{2} \left[ \frac{\partial(\Delta u_j^\alpha)}{\partial b_i^\alpha} - \frac{\partial(\Delta u_i^\alpha)}{\partial b_j^\alpha} \right]$$

Note that  ${}^x \sigma_{kl}$  basically differs from  ${}^x \sigma_{ij}$  by a rigid body rotation.

The expression (VI.4.5) may also be obtained by taking the material time derivative of (IV.10.2.14)2 with similar simplifications.

Finally, the Jaumann stress increment tensor will be defined. Consider that a small rectangular parallelepiped in equilibrium with the Euler stress tensor  ${}^b \sigma_{ij}$  has undergone an incremental motion to find its new equilibrium position under the Euler stress tensor  ${}^b \sigma_{ij} + \Delta_x^x \sigma_{ij}$ .

Intuitively, therefore, the stress tensor at this new position may be defined approximately as the Euler stress tensor minus a rigid body rotation, so, in a matricial form,

where 
$$[\delta^b \sigma + \Delta^j \sigma] = [\delta^b \sigma + \Delta^x \sigma] + [L][\delta^b \sigma + \Delta^x \sigma][L]^T$$

$$(VI.4.6) \quad [L] = \begin{pmatrix} 0 & \Delta_b^x w_{12} & -\Delta_b^x w_{31} \\ -\Delta_b^x w_{12} & 0 & \Delta_b^x w_{23} \\ \Delta_b^x w_{31} & \Delta_b^x w_{23} & 0 \end{pmatrix}$$

Neglecting terms of products of a higher order, the Jaumann stress tensor increment can be expressed by

$$(VI.4.7) \quad [\Delta^j \sigma] = [\Delta^x \sigma] + [\delta^b \sigma][\Delta_b^x w]^T + [\Delta_b^x w][\delta^b \sigma]$$

or

$$\Delta^j \sigma_{ij} = \Delta^x \sigma_{ij} - \delta^b \sigma_{il} \Delta_b^x w_{lj} - \delta^b \sigma_{jl} \Delta_b^x w_{li}$$

as function of the Euler stress increment tensor.

Also, by combining equation (VI.4.7) with equation (VI.4.5) the relationship between the Truesdell stress tensor increment and the Jaumann stress tensor increment can be obtained:

$$(VI.4.8) \quad \Delta_b^x \sigma_{ij}^a = \Delta^j \sigma_{ij}^a - \delta^b \sigma_{il}^a \Delta_b^x \epsilon_{jl} - \delta^b \sigma_{jl}^a \Delta_b^x \epsilon_{il} + \delta^b \sigma_{ij}^a \Delta_b^x \epsilon_{ll}$$

### VI.5 Stress-Strain Increment Relationship for the Solid Skeleton

Material indifference principle: Quantities which depend only on the orientation of the reference frame, which is given by  $[L]$ , and not on the other aspects of the motion of the reference frame (such as its translation) are said to be indifferent (Stokes' Hypothesis). Under

this hypothesis indifferent quantities are, except for rotation, independent of the reference frame. Scalars, vectors and tensors, are transformed according to,

$$(VI.5.1) \quad {}^a f = {}^x f, \quad {}^a v = L {}^x v, \quad {}^a T = L {}^x T L^T$$

The constitutive equations (for example the stress - strain increment relationship) represents an intrinsic response of the material. This response must be seen to be the same for all observers, as otherwise it would not be intrinsic to the material.

Now considering that the rate of strain of a body may be represented by pure rate of stretching along three mutually perpendicular axes, plus the rate of rotation of these three axes and choosing to observe this body from a reference frame which is moving and rotating with these axes, all that is left to see is the rate of stretching along the three axes

If the rate of stretching is the material response under the stress rate, which may be written symbolically as  ${}^x \dot{\tau} = g({}^x \dot{E})$  for the rotating axes, the material response viewed from the fixed axes must be written as

$$(VI.5.2) \quad {}^a \dot{T} = L \left[ g({}^x \dot{E}) \right] L^T$$

to be seen as invariant.

However, transformations are not always as simple as those stipulated by the Stokes' Hypothesis. A more general transformation for the stress tensor than the one stipulated by equation (VI.5.1) may be, for

example, represented by equations (VI.4.4) or (VI.4.5).

So, the principle of material indifference may be postulated more generally as: The response of the material is the same for all observers independently of the kind of transformation suffered by the material.

Next postulating the stress strain incremental relationship for the solid skeleton.

One of the most natural assumptions may be to postulate the relationship between  ${}^x_b\sigma_{ij}^a$  and  $\Delta_b^x e_{ij}$  or  ${}^x_b\sigma_{ij}^a$  and  $\Delta_b^x \epsilon_{ij}$  in the following form

$$(VI.5.3) \quad \Delta_b^x \sigma_{ij} = {}^x_b c_{ijkl} \Delta_b^x e_{kl} \quad \Delta_b^x \sigma_{ij} = {}^x_b c_{ijkl} \Delta_b^x \epsilon_{kl}$$

Naturally, in these equations,  ${}^x_b c_{ijkl}$  may include the effect of the past history of the material. Particularly, for one purpose, the stress increment are the effective stress increment and the strain increment are the total strain increment for the solid.

If (VI.5.3) is the intrinsic response of the material, a proper transformation to be applied to  ${}^x_b c_{ijkl}$  may be deduced to obtain the relationship between  $\Delta_a^x \sigma_{ij}$  and  $\Delta_a^x \epsilon_{kl}$ . So, with the aid of equations (VI.3.5)2, (VI. 4.4) and (VI.5.3)

$$(VI.5.4) \quad \Delta_a^x \sigma_{ij} = {}^x_a c_{ijkl} \Delta_a^x e_{kl} \quad \text{or} \quad \Delta_a^x \sigma_{ij} = {}^x_a c_{ijkl} \Delta_a^x \epsilon_{kl}$$

may be written, where

$$(VI.5.5) \quad \frac{x}{a} c_{ijkl}^{\alpha} = b_j \frac{x}{b} c_{pqrs}^{\alpha} \frac{\partial a_i^{\alpha}}{\partial b_p^{\alpha}} \frac{\partial a_j^{\alpha}}{\partial b_q^{\alpha}} \frac{\partial a_k^{\alpha}}{\partial b_r^{\alpha}} \frac{\partial a_l^{\alpha}}{\partial b_s^{\alpha}}$$

An alternative natural assumption may be to postulate the relationship between  $\Delta^j \sigma_{ij}$  and  $\Delta_b^x \epsilon_{kl}^{\alpha}$  as the intrinsic property of the material, or,

$$(VI.5.6) \quad \Delta^j \sigma_{ij} = {}^j c_{ijkl}^{\alpha} \Delta_b^x \epsilon_{kl}^{\alpha}$$

The equation (VI.5.6) has been used frequently in the theoretical development and analysis of elasto-plastic problems.

If equation (VI.5.6) is postulated as material intrinsic property, then the relationship between  $\Delta_b^x \sigma_{ij}$  and  $\Delta_b^x \epsilon_{kl}^{\alpha}$  may be derived if equations (VI.4.8) and (VI.5.6) are combined. So,  ${}^x c_{ijkl}^{\alpha}$  to be used in (VI.5.3) is given by

$$(VI.5.7) \quad \frac{x}{b} c_{ijkl}^{\alpha} = {}^j c_{ijkl}^{\alpha} - \frac{b}{b} \sigma_{ik}^{\alpha} \delta_{jl} - \frac{b}{b} \sigma_{jk}^{\alpha} \delta_{il} + \frac{b}{b} \sigma_{ij}^{\alpha} \delta_{kl}$$

Also with the aid of (VI.5.5) and (VI.5.6) an expression may be found for  ${}^x c_{ijkl}^{\alpha}$  to be used in (VI.5.4), so,

$$(VI.5.8) \quad \frac{x}{a} c_{ijkl}^{\alpha} = b_j \frac{\partial a_i^{\alpha}}{\partial b_p^{\alpha}} \frac{\partial a_j^{\alpha}}{\partial b_q^{\alpha}} \frac{\partial a_k^{\alpha}}{\partial b_r^{\alpha}} \frac{\partial a_l^{\alpha}}{\partial b_s^{\alpha}} \left[ {}^j c_{pqrs}^{\alpha} - \frac{b}{b} \sigma_{pr}^{\alpha} \delta_{qs} - \frac{b}{b} \sigma_{qr}^{\alpha} \delta_{ps} + \frac{b}{b} \sigma_{pq}^{\alpha} \delta_{rs} \right]$$

## VI.6 Stress-Strain Increment Relationship for the Fluid Phase and Darcy Law

If the stress system is such that an element of area always experiences a stress normal to itself and this stress is independent

of the orientation, the stress is called hydrostatic. All fluid at rest exhibits this stress behaviour. This means that for any normal  $n$ ,  $n \cdot \sigma$  is always proportional to  $n$  and furthermore, the constant of proportionality is independent of  $n$ . Writing this constant as  $-p$ ,

$$(VI.6.1) \quad n_i \sigma_{ij} = -pn_j$$

This equation means, however, that any vector is a characteristic vector of  $\sigma$  which must therefore be spherical. Thus

$$(VI.6.2) \quad \sigma_{ij} = -p\delta_{ij}$$

For a compressible fluid at rest,  $p$  may be identified with the pressure of classical thermodynamics. On the assumption that there is local thermodynamic equilibrium even when the fluid is in motion this concept of stress may be held. For an incompressible fluid the thermodynamic, or more correctly thermostatic, pressure cannot be defined except as the limit of pressure in a sequence of compressible fluids. It may be seen that it has to be taken as an independent dynamic variable

A general stress tensor may always be written as

$$(VI.6.3) \quad \sigma_{ij} = -p\delta_{ij} + P_{ij}$$

where  $P_{ij}$  is called the viscous stress tensor, and is a function of the fluid velocity.  $P_{ij}$  vanishes for a hydrostatic stress field, an incompressible Newtonian fluid and perfect fluids.

When  $\sigma_{ij}$  is defined as in (VI.6.3) the transformation required to be applied to ensure the frame indifference is similar to the ones stipulated for the solid skeleton. In this work, only the case of an incompressible Newtonian fluid is considered.

### VI.7 Bernoulli's Theorem - Darcy's Law

The Bernoulli theorem establishes the value of the total energy carried by a fluid particle at each instant of its movement over a stream line. For different flow conditions this energy equation assumes different functions.

For a particular barotropic laminar flow the energy function "h" is a time constant given by unit of weight as,

$$h = p/\gamma_f + x_i b_i$$

Where  $p$  is the hydrostatic pressure

$b_i$  is the unit vector in the direction of gravity according to the adopted reference frame

$\gamma_f$  is the unit weight of the pore fluid

$h$  is called hydraulic head.

The Darcy Law relates the fluid velocity with the hydraulic gradient. So, the natural way to define the Darcy Law is to define it in a reference frame which moves and deforms as the soil skeleton does. Thus, postulating

$$(VI.7.1) \quad \Delta_x^x(v_i^1 - v_i^2) = {}^x K_{ij} \frac{\partial \Delta h}{\partial x_j}$$

then transforming by using (VI.2.4) to obtain the relationship between  $\Delta_b^x(v_i^1 - v_i^2)$  and  $\partial\Delta h/\partial b_j$  as,

$$(VI.7.2) \quad \Delta_b^x(v_i^1 - v_i^2) = {}_b^x K_{ij} \frac{\partial\Delta h}{\partial b_j} \quad \text{where}$$

$$(VI.7.3) \quad {}_b^x K_{ij} = \frac{\partial b_i}{\partial x_j} K_{lm} \frac{\partial b_m}{\partial x_j} \quad \text{which}$$

is the proper transformed permeability matrix to be used in (VI.7.2).

The same postulated permeability matrix is viewed from a reference frame "a", as

$$(VI.7.4) \quad {}_a^x K_{ij} = \frac{\partial a_i}{\partial x_j} K_{lm} \frac{\partial a_m}{\partial x_j}$$

to be used in

$$(VI.7.5) \quad \Delta_a^x(v_i^1 - v_i^2) = {}_a^x K_{ij} \frac{\partial\Delta h}{\partial a_j}$$

An alternative assumption may be to postulate the relationship between  $\Delta_b^x(v_i^1 - v_i^2)$  and  $\partial\Delta h/\partial a_j$  as the intrinsic permeability of the material. Thus,

$$(VI.7.6) \quad \Delta_b^x(v_i^1 - v_i^2) = {}_b^x K_{ij} \frac{\partial(\Delta h)}{\partial a_j}$$

If this is postulated then the relationship between  $\Delta_b^x(v_i^1 - v_i^2)$  and  $\partial\Delta h/\partial a_j$  defines  ${}_b^x K_{ij}$  which may be obtained with the aid of (VI.7.4), as



$$(VI.7.7) \quad {}^x K_{ij} = \frac{\partial a_i}{\partial b_l} {}^x K_{lm} \frac{\partial a_m}{\partial b_j}$$

### VI.8 Total Lagrange Formulation

In the total Lagrange formulation all variables in equations (V.3.1), (V.3.2) and (V.3.3) are referred to the initial configuration.

The applied forces in equation (V.3.2) are evaluated by using the following expression:

$$(VI.8.1) \quad {}_{i+\Delta t}^{i+\Delta t} \bar{\sigma}_k d s = {}_0^{i+\Delta t} \bar{\sigma}_k^0 d s$$

$$(VI.8.2) \quad {}_{i+\Delta t}^{i+\Delta t} \rho \int_{i+\Delta t} {}^{i+\Delta t} f_k d \vartheta = {}_0^{i+\Delta t} \rho \int_0 {}^{i+\Delta t} f_k^0 d \vartheta$$

where it is assumed that the direction and magnitude of the forces  ${}_0^{i+\Delta t} \bar{\sigma}_k$  and  ${}_0^{i+\Delta t} \rho \int_0 {}^{i+\Delta t} f_k^0 d \vartheta$  are independent of the specific configuration at time  $t + \Delta t$ . That means,  ${}_{i+\Delta t}^{i+\Delta t} \bar{\sigma}_k = {}_0^{i+\Delta t} \bar{\sigma}_k$  and  ${}_{i+\Delta t}^{i+\Delta t} \rho \int_{i+\Delta t} {}^{i+\Delta t} f_k = {}_0^{i+\Delta t} \rho \int_0 {}^{i+\Delta t} f_k^0$ .

However, if the traction  ${}_{i+\Delta t}^{i+\Delta t} \bar{\sigma}_k$  is dependent on the deformation, a convenient computational form of the expression (IV.10.2.10) must be used.

The equation of virtual displacement (V.3.1) in terms of the Cauchy stresses and the infinitesimal virtual strain must be transformed by means of equation (IV.4.6) and (IV.10.2.14) to give:

$$(VI.8.3) \quad \int_{i+\Delta t} {}_{i+\Delta t}^{i+\Delta t} \sigma_{ij} \delta_{i+\Delta t} e_{ij}^2 d \vartheta = \int_0 {}_0^{i+\Delta t} \sigma_{ij} \delta_0 e_{ij}^2 d \vartheta$$

for isochronic fluid flow.

Also, the integral form of the continuity equation given by (V.3.3) may be transformed by means of expressions (VI.3.5)2 and (IV.10.2.14)2 to give:

$$(VI.8.4) \quad \int_{t+\Delta t, \mathcal{V}} \delta_{ij} ({}_{t+\Delta t} e_{ij}^1 - {}_{t+\Delta t} e_{ij}^2) \delta^{t+\Delta t} \sigma_{ij}^1 d\vartheta + \int_{t+\Delta t, \mathcal{V}} \delta_{ij} ({}_{t+\Delta t} e_{ij}^2) \delta^{t+\Delta t} \sigma_{ij}^2 d\vartheta =$$

$$\int_{\mathcal{V}_0} \delta_{ij} ({}_0^{t+\Delta t} e_{ij}^1 - {}_0^{t+\Delta t} e_{ij}^2) \delta_0^{t+\Delta t} \sigma_{ij}^1 d\vartheta + \int_{\mathcal{V}_0} \delta_{ij} ({}_0^{t+\Delta t} e_{ij}^2) \delta_0^{t+\Delta t} \sigma_{ij}^2 d\vartheta = \emptyset$$

where incremental strain has been replaced in (VI.3.5)2 by strain rate, and

$$(VI.8.5) \quad {}_0^{t+\Delta t} e_{ij}^\alpha = \frac{1}{2} \left( \frac{\partial \vartheta_k^\alpha}{\partial a_k} \frac{\partial x_k^\alpha}{\partial a_i} + \frac{\partial \vartheta_k^\alpha}{\partial a_k} \frac{\partial x_k^\alpha}{\partial a_j} \right),$$

and

$${}_0^{t+\Delta t} e_{ij}^\alpha = \frac{d}{dt} ({}_0^{t+\Delta t} e_{ij}^\alpha)$$

By relating expressions (VI.8.1), (VI.8.2) and (VI.8.3) with equations (V.3.1) and (V.3.2) ; and by relating expression (VI.8.4) with (V.3.3) two expressions may be obtained,

$$(VI.8.6) \quad \int_{\mathcal{V}_0} ({}_0^{t+\Delta t} \sigma_{ij}^1 + {}_0^{t+\Delta t} \sigma_{ij}^2) \delta_0^{t+\Delta t} e_{ij}^2 d\vartheta = {}^{t+\Delta t} R$$

$$(VI.8.7) \quad \int_{\mathcal{V}_0} \delta_{ij} ({}_0^{t+\Delta t} e_{ij}^1 - {}_0^{t+\Delta t} e_{ij}^2) \delta_0^{t+\Delta t} \sigma_{ij}^1 d\vartheta + \int_{\mathcal{V}_0} \delta_{ij} ({}_0^{t+\Delta t} e_{ij}^2) \delta_0^{t+\Delta t} \sigma_{ij}^2 d\vartheta = \emptyset$$

where

$$(VI.8.8) \quad {}^{t+\Delta t} R = \int_{\mathcal{V}_0} {}_0^{t+\Delta t} \sigma_k \delta \Delta u_k d\mathcal{V} + \int_{\mathcal{V}_0} \rho_0 {}_0^{t+\Delta t} f_k \delta \Delta u_k d\mathcal{V}$$

The expression (VI.8.6) represents the equilibrium equation for the body in the configuration at time  $t + \Delta t$  but referred to the

configuration at time  $\theta$ . The expression (VI.8.7) represents the continuity equation for the body in the configuration at time  $t + \Delta t$  but referred to the configuration at time  $\theta$ . In expression (VI.8.6)  ${}^t_0 \sigma_{ij}^{t+\Delta t}$  was replaced by  ${}^t_0 \sigma_{ij}^1 + {}^t_0 \sigma_{ij}^2$ .

Since the stresses  ${}^t_0 \sigma_{ij}^1$ ,  ${}^t_0 \sigma_{ij}^2$ , and strains  ${}^t_0 \epsilon_{ij}^1$ , are unknown for solution purposes, the following incremental decompositions are used.

$$(VI.8.9) \quad {}^t_0 \sigma_{ij}^{t+\Delta t} = {}^t_0 \sigma_{ij}^1 + \Delta_0^x \sigma_{ij}^1$$

$$(VI.8.10) \quad {}^t_0 \sigma_{ij}^2 = {}^t_0 \sigma_{ij}^2 + \Delta_0^x \sigma_{ij}^2$$

$$(VI.8.11) \quad {}^t_0 \epsilon_{ij}^{t+\Delta t} = {}^t_0 \epsilon_{ij}^1 + \Delta_0^x \epsilon_{ij}^1$$

$$(VI.8.12) \quad {}^t_0 \epsilon_{ij}^2 = {}^t_0 \epsilon_{ij}^2 + \Delta_0^x \epsilon_{ij}^2$$

where  ${}^t_0 \sigma_{ij}^1$ ,  ${}^t_0 \sigma_{ij}^2$  and  ${}^t_0 \epsilon_{ij}^1$ ,  ${}^t_0 \epsilon_{ij}^2$  are the known second Piola-Kirchhoff stresses for the fluid phase when  $\alpha = 1$ , for the solid skeleton when  $\alpha = 2$  and the Green-Lagrange strains in the configuration at time  $t$ . It follows from equations (VI.8.9), (VI.8.10), (VI.8.11) and (VI.8.12) that

$$\delta {}^t_0 \sigma_{ij}^{t+\Delta t} = \delta \Delta_0 \sigma_{ij}^\alpha \quad \text{and} \quad \delta (\Delta_0^{t+\Delta t} \epsilon_{ij}^1) = \delta \Delta_0 \epsilon_{ij}^1$$

where  $\Delta_0 \epsilon_{ij}^1$  is defined by equation (VI.3.3),  $\Delta_0 \sigma_{ij}^2$  is defined by equation (VI.5.4) and  $\Delta_0 \sigma_{ij}^1$  is defined by equation (VI.6.2).

Equation (VI.8.3) may now be written as:

$$(VI.8.13) \quad \int_{\mathfrak{v}} {}_0 c_{ijkl} \Delta_0 e_{kl}^2 \delta \Delta_0 e_{ij}^2 d\vartheta + \int_{\mathfrak{v}} {}_0' \sigma_{ij}^1 \delta \Delta_0 \eta_{ij}^2 d\vartheta + \int_{\mathfrak{v}} {}_0' \sigma_{ij}^2 \delta \Delta_0 \eta_{ij}^2 d\vartheta \\ + \int_{\mathfrak{v}} \Delta_0 \sigma_{ij}^1 \delta \Delta_0 e_{ij}^2 d\vartheta = {}^{t+\Delta t} R - \int_{\mathfrak{v}} {}_0' \sigma_{ij} \delta \Delta_0 \epsilon_{ij}^2 d\vartheta$$

Similarly, equation (VI.8.4) leads to:

$$(VI.8.14) \quad \int_{\mathfrak{v}} \left( \frac{\partial b_m}{\partial a_i} + \frac{\partial \Delta u_m}{\partial a_i} \right) {}_0 K_{mi} \frac{\partial h}{\partial a_i} \delta \frac{\partial(\Delta p)}{\partial a_i} d\vartheta - \int_{\mathfrak{v}} \delta_{ij} \frac{d}{dt} ({}^{t+\Delta t} \sigma_{ij}^2) \delta \Delta p^0 d\vartheta = \emptyset$$

where equations (VI.8.5), (VI.3.3), (IV.10.2.14), (IV.4.6)2, (VI.6.2), (VI.7.5) and (VI.8.12) have been used and,

$$(VI.8.15) \quad h = \frac{1}{\gamma_w} p + \bar{h}, \quad \bar{h} = x_k \cdot i_k$$

where  $i_k$  is the direction of gravity in relation to the fixed reference frame adopted.

### VI.9 Updated Lagrange

In the updated Lagrange formulation all variables in equations (V.3.1), (V.3.2) and (V.3.3) are referred to the previously known configuration (configuration at time  $t$ ). By a similar procedure, as used to derive the equation for the total Lagrange formulation equation (V.3.1) may be written in this case, as

$$(VI.9.1) \quad \int_{\mathfrak{v}} ({}^{t+\Delta t} \sigma_{ij}^1 + {}^{t+\Delta t} \sigma_{ij}^2) \delta {}^{t+\Delta t} \epsilon_{ij}^1 d\vartheta = {}^{t+\Delta t} R$$

where  ${}^{t+\Delta t} \sigma_{ij}^\alpha$  are the components of the second Piola-Kirchhoff stress tensor and  ${}^{t+\Delta t} \epsilon_{ij}^\alpha$  are the components of the Green-Lagrange strain tensor from the configuration at time  $t$  to the configuration at time  $t + \Delta t$  and referred to the configuration at time  $t$ .

Since deformation is considered not to affect external loading,  ${}^{t+\Delta t}R$  is evaluated as in total Lagrange formulation.

Also, equation (V.3.3) may be transformed to give,

$$(VI.9.2) \quad \int_{\mathcal{V}} \delta_{ij} ({}^{t+\Delta t}e_{ij}^1 - {}^t e_{ij}^2) \delta {}^t \sigma_{ij}^1 d\vartheta + \int_{\mathcal{V}} \delta_{ij} ({}^{t+\Delta t}e_{ij}^2) \delta ({}^{t+\Delta t}\sigma_{ij}^2) d\vartheta = 0$$

The incremental decomposition of stress, strain and velocity used in this case is,

$$(VI.9.3) \quad {}^t \sigma_{ij}^\alpha = {}^t \sigma_{ij}^\alpha + \Delta {}^x \sigma_{ij}^\alpha$$

$$(VI.9.4) \quad {}^t e_{ij}^\alpha = \Delta {}^x e_{ij}^\alpha$$

$$(VI.9.5) \quad {}^t v_i = {}^t v_i(x(t))$$

where  ${}^t \sigma_{ij}^\alpha$  are the components of the Cauchy stress tensor for fluid and the soil skeleton, and  $\Delta {}^x \sigma_{ij}^\alpha$  are the components of the second Piola-Kirchhoff stress increment tensor referred to the configuration at time  $t$ . The expression for  ${}^t \sigma_{ij}^\alpha$  is given by equation (VI.3.4)

As in the case of the total Lagrange formulation, equations (VI.9.1) and (VI.9.2) may be written as,

$$(VI.9.6) \quad \int_{\mathcal{V}} r_{ijkl} \Delta {}^x e_{kl}^2 \delta \Delta {}^x e_{ij}^2 d\vartheta + \int_{\mathcal{V}} {}^t \sigma_{ij}^1 \delta \Delta {}^x \eta_{ij}^2 d\vartheta + \int_{\mathcal{V}} {}^t \rho_{ij}^2 \delta \Delta {}^x \eta_{ij}^2 d\vartheta + \int_{\mathcal{V}} \Delta {}^x \sigma_{ij}^1 \delta \Delta {}^x e_{ij}^2 d\vartheta = {}^{t+\Delta t}R - \int_{\mathcal{V}} {}^t \rho_{ij} \delta \Delta {}^x e_{ij}^2 d\vartheta$$

$$(VI.9.7) \quad \int_{\mathcal{V}} \left( \delta_{mi} + \frac{\partial \Delta {}^x u_m}{\partial b_i} \right) {}^x K_{mi} \frac{\partial h}{\partial b_i} \delta \frac{\partial (\Delta p)}{\partial b_i} d\vartheta - \int_{\mathcal{V}} \delta_{ij} \frac{d}{dt} ({}^{t+\Delta t} e_{ij}^2) \delta \Delta p d\vartheta = 0$$

where  $h$  is as already defined.

### VI.10 Linearization of Equilibrium Equations

It should be noted that the system of equations (VI.8.13), (VI.8.14) and (VI.9.6), (VI.9.7) are, theoretically, equivalent and provided the appropriate constitutive equations are used, both equations yield identical solutions. However, it will be seen that the finite element matrices established for solutions are, of course, different.

The solution of the system of equations (VI.8.13), (VI.8.14) and (VI.9.6), (VI.9.7) cannot be evaluated directly, since they are non-linear in the displacement increments. An approximate solution can be obtained by assuming that in equation (VI.8.13)  $\delta\Delta_0 e_{ij}^2 = \delta\Delta_0 \epsilon_{ij}^2$  and in equation (VI.9.6)  $\delta\Delta_r \epsilon_{ij}^2 = \delta\Delta_r \epsilon_{ij}^2$

This means that, in addition to using

$$\delta\Delta_0 e_{ij}^2 = \delta\Delta_0 \epsilon_{ij}^2 \quad \text{and} \quad \delta\Delta_r \epsilon_{ij}^2 = \delta\Delta_r \epsilon_{ij}^2$$

respectively, the incremental constitutive relations employed are,

$$\Delta_0 \sigma_{ij}^2 = c_{ijkl} \Delta_0 \epsilon_{kl}^2 \quad \text{and} \quad \Delta_r \sigma_{ij}^2 = r_{ijkl} \Delta_r \epsilon_{kl}^2$$

Also, the following tensors

$$\left(\frac{\partial b_m}{\partial a_i} + \frac{\partial \Delta u_m}{\partial a_i}\right) \quad \text{and} \quad \left(\delta_{mi} + \frac{\partial \Delta_i u_m}{\partial b_i}\right)$$

may be simplified respectively to  $\frac{\partial b_m}{\partial a_i}$  and  $\delta_{mi}$  to avoid non-linear terms  $\Delta u_m \Delta h$ .

Equation (VI.8.13) and (VI.8.14) may then be written as

$$(VI.10.1) \quad \int_{\mathfrak{V}} {}_0 c_{ijkl} \Delta_0 \epsilon_{kl} \delta \Delta_0 \epsilon_{ij} {}^0 d\vartheta + \int_{\mathfrak{V}} (-\delta_{ij} {}^i \rho_p + {}^i \sigma_{ij}) \delta \Delta_0 \eta_{ij} {}^0 d\vartheta \\ + \int_{\mathfrak{V}} -\delta_{ij} \Delta_0 p \delta (\Delta_0 \epsilon_{ij}) {}^0 d\vartheta = {}^{i+\Delta} R - \int_{\mathfrak{V}} (-\delta_{ij} {}^i \rho_p + {}^i \sigma_{ij}) \delta (\Delta_0 \epsilon_{ij}) {}^0 d\vartheta$$

$$(VI.10.2) \quad \int_{\mathfrak{V}} \frac{\partial b_m}{\partial a_i} {}_0 K_{mi} \frac{\partial_0 h}{\partial a_i} \delta \frac{\partial (\Delta_0 p)}{\partial a_i} {}^0 d\vartheta - \int_{\mathfrak{V}} \delta_{ij} \frac{d}{dt} ({}^{i+\Delta} \sigma_{ij}) \delta \Delta_0 p {}^0 d\vartheta = \emptyset$$

and equations (VI.9.6) and (VI.9.7) leads to,

$$(VI.10.3) \quad \int_{\mathfrak{V}} {}^i c_{ijkl} \Delta_i \epsilon_{kl} \delta \Delta_i \epsilon_{ij} {}^i d\vartheta + \int_{\mathfrak{V}} (-\delta_{ij} {}^i \rho_p + {}^i \sigma_{ij}) \delta \Delta_i \eta_{ij} {}^i d\vartheta \\ + \int_{\mathfrak{V}} -\delta_{ij} \Delta_i p \delta (\Delta_i \epsilon_{ij}) {}^i d\vartheta = {}^{i+\Delta} R - \int_{\mathfrak{V}} (\delta_{ij} {}^i \rho_p + {}^i \sigma_{ij}) \delta (\Delta_i \epsilon_{ij}) {}^i d\vartheta$$

$$(VI.10.4) \quad \int_{\mathfrak{V}} \delta_{mi} {}^i K_{mi} \frac{\partial_i h}{\partial b_i} \delta \frac{\partial (\Delta_i p)}{\partial b_i} {}^i d\vartheta - \int_{\mathfrak{V}} \delta_{ij} \frac{d}{dt} ({}^{i+\Delta} \sigma_{ij}) \delta \Delta_i p {}^i d\vartheta = \emptyset$$

where  $\sigma_{ij}^1 = -\delta_{ij} p$ ,  $\Delta \sigma_{ij}^1 = -\delta_{ij} (\Delta p)$ ,  $\sigma_{ij}^2 = \sigma_{ij}$ ,  $\Delta \sigma_{ij}^2 = \Delta \sigma_{ij}$ ,  $\epsilon_{ij}^2 = \epsilon_{ij}$ ,  $\Delta u_i^2 = \Delta u_i$

After the linearization, equation (VI.10.3) and (VI.10.4) will be seen to be still symmetric while equation (VI.10.1) and (VI.10.2) will no longer be symmetric. In the next chapter, these equations are going to

be transformed into a more convenient form and used in finite element method. Then, the symmetry and the non-symmetry characteristic of the resulting field equations obtained by the updated and total Lagrange method will be clearer.



## CHAPTER VII

### FINITE ELEMENT SOLUTION

#### VII.1 Introduction

In this chapter the system of incremental equations representing consolidation, obtained in the previous chapter, are transformed for the finite element method.

Although both formulations, total Lagrange and updated Lagrange, must arrive at the same solution, the finite element equations will be seen to be quite different. Both formulations are presented explicitly but only the updated Lagrange is actually used in the programming form.

Following the presentation of finite element matrices, the numerical integration schemes, equilibrium iteration and convergence criteria are briefly discussed.

#### VII.2 Finite Element Solution

The two systems of equations (VI.10.1), (VI.10.2) and (VI.10.3), (VI.10.4) represent, respectively, the total Lagrange and updated Lagrange formulations of a geometric non-linear consolidation problem, where one may consider the constitutive stress-strain

relationship and permeability matrix, dependant on the history of the soil stresses.

A general solution for these equations is impossible unless an approximate method is used.

Here, a numerical method of solution is presented by means of the finite element technique.

In the total Lagrange formulation the approximate equilibrium and continuity equations to be solved are, in matrix form:

$$(VII.2.1) \quad \int_{\Omega_0} \delta(\Delta_0 \epsilon)^T {}_0 C \Delta_0 \epsilon^0 d\vartheta + \int_{\Omega_0} \delta(\Delta u)^T \nabla^T {}'_0 \sigma \nabla(\Delta u)^0 d\vartheta - \int_{\Omega_0} \delta(\Delta_0 \epsilon)^T a \Delta_0 p^0 d\vartheta = {}^{t+\Delta t} R - \int_{\Omega_0} \delta(\Delta_0 \epsilon)^T {}'_0 \bar{\sigma}^0 d\vartheta$$

$$(VII.2.2) \quad \int_{\Omega_0} \delta(\Delta_0 p)^T \nabla^T {}_0 T^T {}_0 K \nabla h^0 d\vartheta + \int_{\Omega_0} \delta(\Delta_0 p)^T a^T \frac{d}{dt} ({}_0 \epsilon)^0 d\vartheta = \emptyset$$

whereas in the updated Lagrange formulation they are:

$$(VII.2.3) \quad \int_{\Omega} \delta(\Delta_t \epsilon)^T {}_t C \Delta_t \epsilon^t d\vartheta + \int_{\Omega} \delta(\Delta u)^T \nabla^T {}'_t \sigma \nabla(\Delta u)^t d\vartheta - \int_{\Omega} \delta(\Delta_t \epsilon)^T a \Delta_t p^t d\vartheta = {}^{t+\Delta t} R - \int_{\Omega} \delta(\Delta_t \epsilon)^T {}'_t \bar{\sigma}^t d\vartheta$$

$$(VII.2.4) \quad \int_{\Omega} \delta(\Delta_t p)^T \nabla^T {}_t T^T {}_t K \nabla h^t d\vartheta + \int_{\Omega} \delta(\Delta_t p)^T a^T \frac{d}{dt} ({}_t \epsilon)^t d\vartheta = \emptyset$$

where  $a^T = (1,1,1,0,0,0)$  and  $a^T = (1,1,0,1)$  (axisymmetric case)  $\nabla^T = \left(\frac{\partial}{\partial a_1}, \frac{\partial}{\partial a_2}, \frac{\partial}{\partial a_3}\right)$

$$(VII.2.5) \quad {}_0R = \int_{\sigma_s} \delta(\Delta u)^T {}_0\bar{\sigma}^0 ds + \int_{\sigma_v} \delta(\Delta u)^T {}_0\bar{F}^0 d\vartheta$$

The equations (VII.2.1), (VII.2.2) and (VII.2.3), (VII.2.4) are linear equations in incremental displacement and pore-pressure for total Lagrange and updated Lagrange formulations, respectively. The derivation of matrices corresponding to a single isoparametric element are given since the assembling procedure is standard .

### VII.3 Finite Element Matrices

In the isoparametric element solution the coordinates, displacement and pore-pressure are interpolated using

$$(VII.3.1) \quad a_i = \sum_{k=1}^m \xi_k a_i^k, \quad b_i = \sum_{k=1}^m \xi_k b_i^k, \quad x_i = \sum_{k=1}^m \xi_k x_i^k$$

$$(VII.3.2) \quad {}^t u_i = \sum_{k=1}^m \xi_k {}^t u_i^k, \quad \Delta u_i = \sum_{k=1}^m \xi_k \Delta u_i^k = \psi_u \Delta u_i^k, \quad i = 1, 2, 3$$

$$(VII.3.3) \quad p = \sum_{k=1}^m \xi_k {}^t p^k, \quad \Delta p = \sum_{k=1}^m \xi_k \Delta p^k = \psi_p \Delta p^k$$

$a_i^k, b_i^k, x_i^k$  are the coordinates of the nodal point  $k$  corresponding to direction  $i$  at time  $0, t$  and  $t + \Delta t$ , respectively;  ${}^t u_i^k, {}^t p^k$  are

defined similarly to  $b_i^k$ ;  $\xi_k$  is the interpolation function corresponding to nodal point  $k$ ; and  $m$  is the number of nodal points of the element.

Using equations (VII.3.1), (VII.3.2), (VII.3.3) to evaluate the displacement and pore-pressure derivatives required in the integrals, equations (VII.2.1) and (VII.2.2) become, respectively, for a single element,

$$(VII.3.4) \quad ({}^i_0K_L + {}^i_0K_{NL})\Delta_0 u^k - {}^i_0L \Delta_0 p^k = {}^{i+\Delta t}R - {}^i_0F$$

$$(VII.3.5) \quad -{}^i_0H \frac{d}{dt} {}_0 u^k - {}^i_0G {}_0 p^k = {}^i_0N$$

where  ${}^i_0K_L$ ,  ${}^i_0K_{NL}$ ,  ${}^i_0L$ ,  ${}^i_0H$ ,  ${}^i_0G$ ,  ${}^i_0F$ ,  ${}^i_0N$ ,  ${}^{i+\Delta t}R$  thus obtained are defined as:

$${}^i_0K_L = \int_{\Omega_0} {}^i_0B_L^T C {}^i_0B_L {}^0 d\vartheta \quad {}^i_0K_{NL} = \int_{\Omega_0} {}^i_0B_{NL}^T {}^i_0\sigma {}^i_0B_{NL} {}^0 d\vartheta \quad {}^i_0L = \int_{\Omega_0} {}^i_0B_L^T a {}^i_0\psi_p {}^0 d\vartheta$$

$${}^i_0B_L = {}^i_0B_{L\varnothing} + {}^i_0B_{L1} \quad {}^i_0H = \int_{\Omega_0} {}^i_0\psi_p^T a^T {}^i_0B_L {}^0 d\vartheta = {}^i_0L^T$$

$${}^i_0G = \int_{\Omega_0} {}^i_0\psi_p^T \nabla^T {}^i_0T^T {}^i_0K \nabla {}^i_0\psi_p {}^0 d\vartheta = \int_{\Omega_0} {}^i_0E^T {}^i_0D {}^i_0E {}^0 d\vartheta, \quad {}^i_0E = \nabla {}^i_0\psi_p, \quad {}^i_0D = {}^i_0T^T {}^i_0K$$

$${}^tF = \int_{\mathfrak{V}} {}^tB_L^T {}^t\bar{\sigma}^0 d\mathfrak{V} \quad {}^{t+\Delta t}R = \int_{\mathfrak{S}} {}^t\psi_u^T \bar{\sigma}^0 dS + \int_{\mathfrak{V}} {}^t\psi_u^T f^0 d\mathfrak{V}$$

$${}^tN = \int_{\mathfrak{V}} {}^t\psi_p^T \nabla^T {}^tT^T {}^tK \nabla {}^t\bar{H}^0 d\mathfrak{V} = \int_{\mathfrak{V}} {}^tE^T {}^tD \nabla {}^t\bar{H}^0 d\mathfrak{V}$$

In the above equations  ${}^tB_L$  and  ${}^tB_{NL}$  are linear and non-linear strain displacement transformation matrices respectively.  ${}^tB_{L\emptyset}$ , due only to incremental displacement;  ${}^tB_{L1}$ , due to initial displacement and incremental displacement, is called the initial displacement stiffness matrix;  ${}^tB_{NL}$ , due to initial stresses and incremental displacement is also called the initial stress stiffness matrix;  ${}^tC$  is the incremental material property matrix;  ${}^t\sigma$  is a matrix of 2nd Piola-Kirchhoff stresses;  ${}^t\bar{\sigma}$  is a vector of these stresses;  $\psi_u$  is the interpolation function for displacement within the element;  $\psi_p$  is the interpolation function for pore-pressure within the element;  ${}^tK$  is the permeability matrix for a pore-pressure increment;  ${}^tT$  is a transformation matrix which depends on the initial displacement;  $\bar{\sigma}$  is the prescribed total traction vector;  $f$  is the dead weight by unit volume;  ${}^t\bar{H}$  is a scalar depending on the direction of gravity relative to the adopted reference frame;  $\nabla$  and  $a$  have already been defined. All matrix elements correspond to the configuration at time  $t$  and are defined with respect to the configuration at time  $\emptyset$ .

Similarly, the finite element equations in the updated Lagrange formulation may be found to be:

$$(VII.3.6) \quad ({}^iK_L + {}^iK_{NL})\Delta_i u^k - {}^iL \Delta_i p^k = {}^{i+\Delta}R - {}^iF$$

$$(VII.3.7) \quad -{}^iH \frac{d}{dt} u^k - {}^iG_i p^k = {}^iN$$

where

$${}^iK_L = \int_{\mathcal{V}} {}^iB_L^T C {}^iB_L d\vartheta, \quad {}^iK_{NL} = \int_{\mathcal{V}} {}^iB^T \rho {}^iB_{NL} d\vartheta$$

$${}^iH = \int_{\mathcal{V}} {}^i\psi_p^T a^T {}^iB_L d\vartheta = {}^iL^T, \quad {}^iL = \int_{\mathcal{V}} {}^iB_L^T a {}^i\psi_p d\vartheta \quad {}^iB_L^T = {}^iB_L \emptyset$$

$${}^iG = \int_{\mathcal{V}} {}^i\psi_p^T \nabla^T {}^iT^T {}^iK \nabla {}^i\psi_p d\vartheta = \int_{\mathcal{V}} {}^iE^T {}^iD {}^iE d\vartheta, \quad {}^iE = \nabla {}^i\psi_p, \quad {}^iD = {}^iT^T {}^iK$$

$${}^{i+\Delta}R = \int_{\mathcal{S}} {}^i\psi_u^T \bar{\sigma} d s + \int_{\mathcal{V}} {}^i\psi_u^T f d\vartheta, \quad {}^iF = \int_{\mathcal{V}} {}^iB^T \bar{\sigma} d\vartheta$$

$${}^iN = \int_{\mathcal{V}} {}^i\psi_p^T \nabla^T {}^iT^T {}^iK \nabla {}^i\bar{H} d\vartheta = \int_{\mathcal{V}} {}^iE^T {}^iD \nabla {}^i\bar{H} d\vartheta$$

It should be noted that all integrals from equation (VII.3.4) until now are functions of the natural element co-ordinate and that the volume integrations are performed using a co-ordinate change from cartesian to natural co-ordinates.

The explicit form of the previous defined finite element equations are presented in the Appendix C.

#### VII.4 Numerical Integration

Time integration - equations (VII.3.5) and (VII.3.7) contain the material time derivative of the nodal displacement points which are unknown. The time integration of these equations is impossible to evaluate exactly. So, an approximate procedure is required.

Let a typical time integral have the following approximation:

$$(VII.4.1) \quad \int_t^{t+\Delta t} p^k dt = \alpha \Delta t {}_t^k p^k + (1-\alpha) \Delta t {}_{t+\Delta t}^{t+\Delta t} p^k = ({}_t^k p^k + \beta \Delta t {}_t^k p^k) \Delta t$$

and

$$\beta = 1 - \alpha$$

where  $\alpha$  may vary from 0 to 1.

$\alpha = 1/2$  linear variation in time

$\alpha = 0$  fully explicit method

$\alpha = 1$  fully implicit method

In order to ensure a stable calculation procedure, it is necessary to adopt  $1/2 \leq \alpha \leq 1$  (Booker and Small -1974).

Now evaluating the integration over time of equation (VII.3.5) with the aid of equation (VII.4.1)

$$(VII.4.2) \quad -{}^i_0H \Delta_0 u^k - \beta \Delta t {}^i_0G \Delta_p p^k = {}^i_0N \Delta t + \Delta t {}^i_0G {}^i_0 p^k$$

is obtained. A similar procedure may be used to integrate equation (VII.3.7) for the updated Lagrange formulation to find

$$(VII.4.3) \quad -{}^iH \Delta_i u^k - \beta \Delta t {}^iG \Delta_p p^k = {}^iN \Delta t + \Delta t {}^iG {}^i p^k$$

Finally re-writing equations (VII.3.4) and (VII.3.5) in the following form:

$$(VII.4.4) \quad \begin{pmatrix} ({}^i_0K_L + {}^i_0K_{NL}) & -{}^i_0L \\ -{}^i_0L^T & -\beta \Delta t {}^i_0G \end{pmatrix} \begin{pmatrix} \Delta_0 u^k \\ \Delta_0 p^k \end{pmatrix} = \begin{pmatrix} {}^{i+\Delta t}R - {}^i_0F \\ {}^i_0N \Delta t + \Delta t {}^i_0G {}^i_0 p^k \end{pmatrix}$$

and similarly for equations (VII.3.6) and (VII.3.7)

$$(VII.4.5) \quad \begin{pmatrix} ({}^iK_L + {}^iK_{NL}) & -{}^iL \\ -{}^iL^T & -\beta \Delta t {}^iG \end{pmatrix} \begin{pmatrix} \Delta_i u^k \\ \Delta_i p^k \end{pmatrix} = \begin{pmatrix} {}^{i+\Delta t}R - {}^iF \\ {}^iN \Delta t + \Delta t {}^iG {}^i p^k \end{pmatrix}$$

Volume integration - equations (VII.3.4), (VII.3.5) and (VII.3.6), (VII.3.7) must be integrated over the volume of each element. The integration function is, except for linear interpolation, very complex and is in most cases impossible to be integrated exactly. Hence, integration is evaluated approximately and numerically. There are many schemes for numerical evaluation of defined integrals; however the Gauss method has proved most useful for finite element work. The 4 to



8 variable-number-noded element has been used in the sample solutions in this work and the numerical integration is done using 2 x 2 Gauss points for any number of nodes per element.

### VII.5 Equilibrium Iteration

It is important to realise that the system of equations (VII.4.4) or (VII.4.5) are only approximations of the actual equations to be solved in each load-time step. Depending on the non-linearities of the system, the linearization of equations (VI.8.13), (VI.8.14) and (VI.9.6), (VI.9.7) may introduce errors which ultimately results in solution instability. For this reason it may be necessary to iterate for each load time step until, within the simplified assumptions of the material response and numerical time integration, equations (VI.8.13), (VI.8.14) or (VI.9.6), (VI.9.7) are satisfied to a required tolerance. The system of equations in the total Lagrange formulation is then

$$(VII.5.1) \quad \begin{pmatrix} {}^i_0K_I + {}^i_0K_{NL} & -{}^i_0L \\ -{}^i_0L^T & -\beta\Delta {}^i_0G \end{pmatrix} \begin{pmatrix} \Delta_0 u_i^k \\ \Delta_0 p_i^k \end{pmatrix} = \begin{pmatrix} {}^{i+\Delta t}R - {}^{i+\Delta t}_0F_{(i-1)} \\ \Delta t {}^{i+\Delta t}_0N_{(i-1)} + \Delta t {}^{i+\Delta t}_0G_{(i-1)} \delta p^k \end{pmatrix}$$

It should be noted that for  $i = 1$ , equation (VII.5.1) corresponds to equations (VII.3.4), (VII.3.5), i.e.  $\Delta_0 u_i^k = \Delta_0 u^k$ ,  $\Delta_0 p_i^k = \Delta_0 p^k$ ,  ${}^{i+\Delta t}_0F_{(0)} = {}^i_0F$ ,  ${}^{i+\Delta t}_0N_{(0)} = {}^i_0N$ ,  ${}^{i+\Delta t}_0G_{(0)} = {}^i_0G$ .

The vector of nodal point forces equivalent to the element stresses  ${}^{i+\Delta t}_0F_{(i)}$ , is the finite element evaluation of  $\int_{\Omega} {}^{i+\Delta t}_0\sigma_{ij(i)} \delta_0^{i+\Delta t}\epsilon_{ij(i)}^0 d\Omega$ , where the subscript (i) indicates that the stresses and strains are

evaluated using  ${}^{t+\Delta t}u_{(i)}$ .

Since  $\delta_0^{t+\Delta t}\epsilon_{ij} = \frac{1}{2}\left(\delta\frac{\partial\Delta u_i}{\partial a_j} + \delta\frac{\partial\Delta u_j}{\partial a_i} + \frac{\partial_0^{t+\Delta t}u_k}{\partial a_i}\delta\frac{\partial\Delta u_k}{\partial a_j} + \frac{\partial_0^{t+\Delta t}u_k}{\partial a_j}\delta\frac{\partial\Delta u_k}{\partial a_i}\right)$  the nodal point forces for the first two degrees of freedom are

$${}^0_{0}{}^{t+\Delta t}F_{(i)} = \int_{\Omega_0} {}^0_{0}{}^{t+\Delta t}B_{L(i)}^T {}^0_{0}{}^{t+\Delta t}\bar{\sigma}_{(i)} d\vartheta$$

in which the matrices  ${}^0_{0}{}^{t+\Delta t}B_{L(i)}^T$  and  ${}^0_{0}{}^{t+\Delta t}\bar{\sigma}_{(i)}$  correspond to the matrices  ${}^0_{0}B_L$  and  ${}^0_{0}\bar{\sigma}$  but are defined for time  $t+\Delta t$  and iteration  $(i)$ , respectively

The vector of nodal point forces for the third degree of freedom  ${}^0_{0}{}^{t+\Delta t}N_{(i)}$  and  ${}^0_{0}{}^{t+\Delta t}G_{(i)}{}^0p^k$  are

$${}^0_{0}{}^{t+\Delta t}N_{(i)} = \int_{\Omega_0} {}^0_{0}{}^{t+\Delta t}E {}^0_{0}{}^{t+\Delta t}D_{(i)} \nabla_0^{t+\Delta t}\bar{H}_{(i)} d\vartheta$$

$${}^0_{0}{}^{t+\Delta t}G_{(i)}{}^0p^k = \int_{\Omega_0} ({}^0_{0}{}^{t+\Delta t}E^T {}^0_{0}{}^{t+\Delta t}D_{(i)} {}^0_{0}{}^{t+\Delta t}E d\vartheta) {}^0p^k$$

where  ${}^0_{0}{}^{t+\Delta t}E = {}^0_{0}E$ ,  ${}^0_{0}{}^{t+\Delta t}D_{(i)}$  and  $\nabla_0^{t+\Delta t}\bar{H}_{(i)}$  correspond to the matrices  ${}^0_{0}D$  and  $\nabla_0\bar{H}$  but are defined for time  $t+\Delta t$  and iteration  $(i)$ , respectively.

In the updated Lagrange formulation the system of equations used for a single element with equilibrium iteration is:

$$(VII.5.2) \quad \begin{pmatrix} ({}^iK_i + {}^iK_{NL}) & -{}^iL \\ -{}^iL^T & -\beta\Delta t {}^iG \end{pmatrix} \begin{pmatrix} \Delta t u_i^k \\ \Delta t p_i^k \end{pmatrix} = \begin{pmatrix} {}^{t+\Delta t}R - {}^{t+\Delta t}F_{(i-1)} \\ \Delta t {}^{t+\Delta t}N_{(i-1)} + \Delta t {}^{t+\Delta t}G_{(i-1)} p_i^k \end{pmatrix}$$

in which the vector of nodal point forces equivalent to the element

stresses  ${}^{t+\Delta t}F_{i+\Delta t}^{(i)}$ , is the finite element evaluation of

$$\int_{{}^{t+\Delta t}\vartheta_{(i)}} {}^{t+\Delta t}\sigma_{ij}^{(i)} \delta_{{}^{t+\Delta t}\epsilon_{ij}^{(i)}} {}^{t+\Delta t}d\vartheta_{(i)}$$

i.e.

$${}^{t+\Delta t}F_{i+\Delta t}^{(i)} = \int_{{}^{t+\Delta t}\vartheta_{(i)}} {}^{t+\Delta t}B_{L(i)}^T {}^{t+\Delta t}\bar{\sigma}^{(i)} {}^{t+\Delta t}d\vartheta_{(i)}$$

where  ${}^{t+\Delta t}B_{L(i)}^T$  and  ${}^{t+\Delta t}\bar{\sigma}^{(i)}$  correspond to the matrices  ${}^iB_L$  and  ${}^i\bar{\sigma}$  respectively, but are defined for time  $t+\Delta t$  and iteration  $(i)$ , respectively.

The vector of nodal point forces for the third degree of freedom  ${}^{t+\Delta t}N_{i+\Delta t}^{(i)}$  and  ${}^{t+\Delta t}G_{i+\Delta t}^{(i)} p^k$  are

$${}^{t+\Delta t}N_{i+\Delta t}^{(i)} = \int_{{}^{t+\Delta t}\vartheta_{(i)}} {}^{t+\Delta t}E_{(i)}^T {}^{t+\Delta t}D_{(i)} {}^{t+\Delta t}E_{(i)} {}^{t+\Delta t}d\vartheta_{(i)}$$

$${}^{t+\Delta t}G_{i+\Delta t}^{(i)} = \int_{{}^{t+\Delta t}\vartheta_{(i)}} {}^{t+\Delta t}E_{(i)}^T {}^{t+\Delta t}D_{(i)} \nabla {}^{t+\Delta t}\bar{H}_{(i)} d\vartheta_{(i)}$$

where  ${}^{t+\Delta t}E_{(i)}^T$ ,  ${}^{t+\Delta t}D_{(i)}$ ,  $\nabla {}^{t+\Delta t}\bar{H}_{(i)}$

correspond to the matrices  ${}^iE$ ,  ${}^iD$ ,  $\nabla {}^iH$ , respectively, but are defined for time  $t+\Delta t$  and iteration  $(i)$ , respectively.

Procedure Iterative Calculation

Define the following constants:

$$tol \leq 0,01 \quad , \quad nit \geq 3 \quad , \quad \beta = 1 \quad .$$

A. Calculate displacement increment

1. If a new stiffness matrix is to be formed, calculate and triangularize  $\bar{K}$ , that is:

$$\bar{K} = \begin{pmatrix} ({}^iK_L + {}^iK_{NL}) & -{}^iL \\ -{}^iL^T & -\beta \Delta_i {}^iG \end{pmatrix} = \bar{L} \bar{D} \bar{L}^T$$

2. Form the effective load vector,

$${}^{i+1}R = {}^{i+\Delta i}R - {}^iF$$

3. Solve for displacement and pore-pressure increment,

$$\bar{L} \bar{D} \bar{L}^T \{\Delta u, \Delta p\}^T = {}^{i+1}R$$

4. If required, iterate for non-linearities, that is:

a.

$$i = i + 1$$

b. Evaluate the (i-1)st approximation to displacement

$${}^{i+1}\Delta u_{(i-1)} = {}^i\Delta u + \Delta u_{(i-1)}$$

c. Calculate (i-1)st effective out-of-balance loads,

$${}^{i+1}R_{(i-1)} = {}^iR - {}^{i+1}F_{(i-1)}$$

d. Solve for the  $i$ th correction to displacement and pore-pressure increment,

$$\mathbf{L} \mathbf{D} \mathbf{L}^T \{ \Delta \dot{u}_{(i)} + \Delta \dot{p}_{(i)} \}^T = {}^{i+r} R_{(i-1)}$$

e. Calculate new displacement and pore-pressure increments:

$$\Delta u_{(i)} = \Delta u + \Delta \dot{u}_{(i)} \quad \Delta p_{(i)} = \Delta p + \Delta \dot{p}_{(i)}$$

f. Check for convergence  $\| \Delta \dot{u}_{(i)} \| / \| \Delta u + \Delta \dot{u}_{(i)} \| < tol$

If it converges:

$$\Delta u = \Delta u_{(i)} , \quad \Delta p = \Delta p_{(i)} \quad \text{and go to B.}$$

If it does not converge and  $i < nit$  : go to 1; otherwise restart using the new stiffness matrix and/or a smaller time step.

B. Calculate new displacements, pore-pressure, strain, stress and return to new load-time step.

#### A few words about convergence

Equations (VII.5.1) and (VII.5.2) are now ready to be solved at discrete points and time for a specific load path.

Provided the chosen element for the sample solution satisfies the criteria of invariance, continuity of displacement and pore-pressure within the element, rigid body deformation modes, constant strain and

pore-pressure behaviour, inter-element compatibility of displacement and pore-pressure (which is the case when isoparametric 4 to 8 variable-number-noded element with constant thickness is used, integrated at 2 x 2 Gauss points) the only reason for errors which could make the absolute convergence requirement uncertain are those derived from the numerical integration and iterative calculation schemes adopted.

The iterative calculation procedure converges, however, to the right answer, if some care is taken with numerical time and volume integration schemes.

As far as time integration is concerned, the process is stable if the scalar  $\beta \geq 1/2$  is assumed (Booker and Small, 1975).

As far as volume integration is concerned, the 2 x 2 Gauss points for a four to eight noded, constant thickness, isoparametric element is nearly ideal to ensure the convergence of the process. (Pugh, Hinton and Zienkiewicz, 1978; Bicanic and Hinton, 1979).

These suggestions were used as an integration rule in the computer programme with great success.

CHAPTER VIIICONSTITUTIVE LOCAL STRESS-STRAIN RELATIONSHIPSVIII.1 Preliminaries

Whichever model one considers to simulate the stress-strain relationship for soil, determining the parameter definitions for feeding into such a model has proved to be the most difficult task. This is not surprising when one considers the number of variables which the soil response depends on, such as previous stress history, inherent anisotropy, induced anisotropy (influence of stress ratio direction or strain ratio direction), modulus of strain rate (or stress rate), irreversibility of deformation, mineralogical composition, laboratory technique etc... Extreme difficulties are encountered in distinguishing their different effects on the soil properties.

Innumerable laboratory investigations have been made to show these influences and a qualitative pictures of the soil response have been already achieved. For a quantitative analysis, however, they seem only to be applicable for the specific conditions (initial conditions, stress-path, stress rate ..., and type of soil under consideration). For a quantitative purpose a simplified model has to be assumed and in this respect innumerable stress-strain relationships for soils have been proposed. Some of these models are better supported by the

physical properties of the soil than others, however, the more realistic a model becomes the more costly is its practical application. The choice of the type of model is then a question of cost-benefit, though sometimes it becomes only a matter of preference.

Before presenting the various attempts to represent the stress-strain relationship, a brief description of soil properties will be given.

### VIII.2 Brief Description of Soil Properties.

As far as the modulus of strain rate (or stress rate) is concerned the soil properties can be classified into two distinct regions. One where the modulus of strain rate (or stress rate) considerably affects the soil properties and the other region in which the properties are reasonably insensitive to the modulus of strain rate (or stress rate). The limiting strain rate(stress rate) modulus which separates these two regions can be called the quasi-static strain rate(stress rate) modulus and the soil properties obtained for strain rate(stress rate) moduli smaller than (or equal to) the limiting one, are defined as quasi-static properties, while the properties for the higher range of rates are called kinematic properties. The existence of such an idealized classification is strongly supported by many laboratory investigations but only a few will actually be mentioned here, such as Smith et al(1969), Vaid and Campanella(1977), Gens(1982), De Campos (1982), Takashi(1981) and Hight(1982), Lacasse(1979), Bjerrum (1971), Ladd et al(1972), Buri(1978), Crawford(1968a,b), Lovenbury(1969), Shmertmann(1975).

Smith et al (1969) have carried out Ko-consolidation tests with pore-pressure measurement for three different soils at different constant



vertical strain rate moduli. The pore-pressures were measured at the base of the sample, therefore the expected non-homogeneity of pore-pressure was taken into account in order to evaluate the effective average vertical stress. By plotting the change in void ratio versus effective vertical stress, it could be seen that the compressibility ( $\lambda$  and  $K$ ) and the pre-consolidation pressure changed considerably for a certain range of strain rate moduli for calcium-montmorillonite and Massena clay. It was also noticed that compressibility and pre-consolidation pressure were not greatly affected by strain rate moduli lower than a certain value.

Although the influence of strain rate modulus considerably affects the properties of these two soils it does not seem to cause much influence on kaolinite. The latter's compressibility seems to be greatly insensitive to the strain rate modulus.

Similar consolidation tests under constant rate were carried out by Wissa et al(1971).

Undrained triaxial tests have been carried out on Lower Cramer Till by Takahashi (1981), Gens(1982), Hight(1982), De Campos(1984) where isotropic and anisotropic normally and overconsolidated samples have shown that the undrained stress- paths converge to one path when the strain rate(stress rate) modulus decreases.

Also Lacasse (1979) has carried out a comprehensive literature survey on the effect of shearing rates on the behaviour of clays. The behaviour of three materials was selected as prototypes of time-related behaviour observed in other soils. The selected three materials are: Drammen clay (Bjerrum,(1971)), Atchofalaya clay (Ladd

et al(1972)) and Haney clay (Vaid and Campanella,(1977)). It is clear that in all three soils the strain rate modulus effect tends to become negligible as the testing rate decreases.

Other investigators have also reported the influence of strain rate(stress rate) modulus in one way or another in their laboratory observations, however just a few of them like Singh and Mitchell(1968), Takahashi(1981), De Campos(1984) and Hight(1982) have systematically approached the effect of strain rate on the soil properties inside the kinematic region.

In the quasi-static region the mechanical properties of soils are better known than in the kinematic region. Most laboratory results are obtained for stress conditions restricted to triaxial or plane strain conditions, and just a few results has been obtained in more general stress state conditions. However, because most of the soil test are restricted to special conditions, i.e., triaxial compression, extension and plane strain, it is usually assumed that the behaviour of soil for a more general stress condition can be obtained by extrapolating from the properties of soil obtained in these simple conditions.

Bearing in mind this restriction the following simplified soil behaviour may be stated:

## VIII.2.1 Soil Properties on the Quasi-Static Region

### 1. Triaxial Test Conditions

#### 1.1 K-Consolidation Test and Swelling Test

Laboratory test results of constant  $k$  tests are concentrated in the  $J_2/J_1$  -plane with  $b=0$  (or  $\sigma_2 = \sigma_3 = \sigma_{min}$ ). Some laboratory results start from a slurry sample (null stress state) and consolidation at constant  $k$  is carried out until a high stress level is achieved. Others start from compacted samples.

Although in the early stage of a  $k$ -consolidation test on slurry some reorientation of strain occurs, as soon as considerable strain occurs the strain rate direction remains constant until the end of the test (Gens,1982). Most investigators (Ladd (1965), Whitman et al (1960), Danaghe and Townsend (1978), Khera and Krizek(1967), Mitachi and Kitago (1976), Olson (1962) and Henkel and Sowa (1963), Lewin and Burland (1970), and Gens (1982)) report that  $k$ -constant consolidation tests for different values of  $k$  plot parallel in the water content versus logarithm of mean stress space, and in this plot water content for a certain mean stress usually decreases when  $k$  decreases. However, Whitman et al(1960) and Henkel and Sowa(1963) found a unique relationship between water content versus mean stress for isotropically consolidated and  $k$  -consolidated specimens, but they started with compacted samples.

Also Yudhdir et al (1978) report that the slope of the virgin consolidation line depends on the stress ratio.

Some  $k$ -consolidated tests on specimens which have been previously prepared at a fairly low water content have been reported by Lee and Morrison (1970) and Broms and Ratnam (1963). They found a unique relationship between water content and vertical stress, which confirmed Rutledge's hypothesis for initially compacted samples.

Swelling tests on samples initially normally consolidated at different constant  $k$  seems to show an unique slope when plotted in water content-logarithm of mean stress space (Gens, 1982), (Burland, 1967).

### 1.2 Failure Envelope Line, Critical State Line (triaxial conditions)

The ultimate failure stress state for most soil in triaxial compression seems to lie on the Mohr-Coulomb envelope line, independently of whether the soil is normally consolidated isotropically or anisotropically (for any value of  $k$  constant). Furthermore it seems to be only slightly sensitive to stress rate (strain rate) modulus and direction. However, if cyclic loading is applied some difference is observed (Gens (1982), De Campos (1984), Takahashi (1981)).

In addition, the Mohr-Coulomb failure line seems to represent the locus of specimens which experience no additional change in volume when further shear is imposed (Gens, 1982). A line which represents the ultimate possible state of stress of soil specimens and where no further change in volume occurs under an increasing shear strain is called the critical state line. Strictly speaking, however, anisotropically consolidated specimens find more difficulty in

reaching this state than isotropically consolidated samples. Anisotropically consolidated samples seems to require much larger shear strain to achieve a true critical state, if it is ever achieved.

### 1.3 Peak Strength

#### 1.3.1 Peak Strength for a Stress Path Directed Towards the Hvorslev Line (triaxial conditions)

It seems that a specimen isotropically normally consolidated or anisotropically normally consolidated, isotropically over consolidated and anisotropically over consolidated which has its stress-path directed to the Hvorslev line in triaxial compression seems to find its stress peak on the Hvorslev Line (Gens, 1982). However, the path which specimens follow from the Hvorslev line to the critical state is not unique. Isotropically over consolidated samples have been tested under triaxial undrained conditions and many possible stress paths from the Hvorslev line to the critical state line were found. Thus two extreme stress path can be idealized:

a- Once reached the Hvorslev line the stress path drop almost vertically to find its final position on the critical state line.

b- Once reached the Hvorslev line the stress state moves on it until the interception point between the Hvorslev line and the critical state line is achieved.

Vaughan et al (1976) postulated two classes of clay to explain these two distinct stress path observed in some undrained laboratory tests.

a- Soil with a high proportion of clay particles.

b- soil with a low proportion of clay particles.

They suggested that an overconsolidated specimen of clay type a after reaching the failure (Hvorslev line) would orientate its predominantly clay particles if further strain is imposed. The orientation of particles would weaken the material rapidly on the way to the critical state line (or by reducing the effective stress friction angle). A good example of this kind of behaviour is observed on isotropically over consolidated Mucking clay as reported by Wesley (1975).

If a similar sample of clay type b is tested in undrained conditions, not much clay fraction is present to be orientated , therefore the stress path does not drop from the failure line (Hvorslev) but runs along it until the interception between the Hvorslev line and the critical state line is encountered. This kind of behaviour is observed in Weald and London clay as reported by Henkel (1958, 1959) and in Lower Cromer Till as reported by Gens (1982).

Two completely different idealized criteria for failure and or softening behaviour have therefore been defined. For clay type a, failure occurs at the moment of reaching the failure envelope (Hvorslev line). Softening (or hardening) occurs continuously and slowly until the failure envelope is reached and from this point the critical state line is reached rapidly, the material neither softening nor work hardening. In practice, however, it seems that if material reaches the failure envelope by softening then it work hardens until the critical state. If material reaches the failure line by working hardening, then it softens until it reaches the critical state line.

For clay type b the undrained strength is controlled by the water content, independently of whether the effective failure envelope is reached. In this kind of material softening and or hardening occurs continuously and slowly until the failure point (interception of the Hvorslev line with the critical state line) is reached.

There is, of course, scope for soils of intermediate behaviour in which both criteria have some influence.

It should be noted however that the previous explanation is applicable only for undrained conditions because the drained test would give the same peak strength in terms of  $(\sigma_1 - \sigma_3)$  for both types of idealized clay a and b. The drained peak strength would generally be closer to the undrained shear strength of the clay type a than that of clay type b, as reported by Gens (1982).

Although there is not much information available for anisotropically over consolidated soil of clay type a tested under undrained conditions it is expected that the previous simplified picture can also be applied. Gens (1982) carried out undrained triaxial compression test on over consolidated samples where the stress path went towards the Hvorslev line and found no peak strength. The stress path engaged the failure line (Hvorslev line) and ran along it until the critical state was reached. However, the Lower Cromer Till tested by Gens (1982) behaves more like clay type b than clay type a.

In conclusion, clay type a would present the same peak strength in drained and undrained tests while clay type b would present no peak strength in undrained tests but the drained peak, if in terms of

(  $\sigma_1 - \sigma_3$  ), would plot closer to the undrained peak strength of clay type a.

Also it can be concluded that the Hvorslev line seems to be applicable for any stress path which follows that direction, independently of the specimen conditions, but the stress path and the softening rule from the Hvorslev line to the critical state seems to have no simple way to be governed. The clay proportion in the material can be an indicator of the tendency of the material stress path (and softening rule) from the Hvorslev line to the critical state line.

### 1.3.2 Peak Strength for Stress-Paths which Go Beyond the Hvorslev Line (triaxial conditions).

It seems that isotropically consolidated samples do not show any peak strength for stress paths which do not go in the direction of the Hvorslev surface, which is the case of isotropically normally consolidated and slightly over consolidated specimens. Drained and undrained tests on isotropically normally consolidated samples which experience stress paths not in the direction of the Hvorslev line find their ultimate strength at the critical state line without any peak strength, independently of the clay type.

The hardening and softening rules seem to be a continuous function of stress state, and the transition between hardening and softening seems also to be a continuous function of stress state independently of the type of clay.

Anisotropically consolidated (normally and slightly over consolidated)



samples sheared in compression with the effective stress-path direction not towards the Hvorslev line, can present peak strength before the ultimate strength is achieved at the critical state. The peak strength seems to be more pronounced in low plasticity clays than in high plasticity ones. For example no peak is reported by Noorany and Seed (1965), and only a small one by Henkel and Sowa (1963) and Mitachi and Kitago (1979). However, a peak is reported by Donaghe and Townsend (1978), Koutsoftas (1981), Ladd (1965), Ladd and Lambe (1963), Vaid and Campanella (1974), Gens (1982). Also, Gens (1982) reported that the brittleness increases sharply for samples which have previously been consolidated at lower  $k$ -constant values.

Large differences between undrained peak and ultimate strength usually involve significant differences between the friction angles at peak and ultimate conditions. The reverse does not seem to be true. Soil like Atdrafalaya clay (Ladd and Edgers, 1972) and Kawasaki clay (Ladd, 1965) shows very little undrained brittleness but large differences between peak and ultimate friction angles. However, since the strain rate modulus in the different tests were different it is dangerous to come to any conclusive pattern of behaviour.

It seems also that the strength of isotropically normally and over consolidated samples and the ultimate strength of anisotropically normally and over consolidated samples all coincide for the clay type b as postulated by Vaughan et al(1976), independently of the stress rate (or strain rate) direction. In fact undrained and drained test carried out by Gens (1982) show that the previous statement holds. However, clay type a, as postulated by Vaughan et al(1976), would have to run along the critical state until it finds an ultimate strength common to all kind of soil conditions. This statement needs much more

experimental confirmation before any definitive conclusion can be achieved.

#### 1.4 Stress Path Effect on Soil Response

##### 1.4.1 General

Before discussing the stress path(strain path) influence on soil response a brief review of the critical state theory will be presented.

Rendulic (1936,1937) and later Henkel (1960) observed that the stress path followed by undrained tests on samples previously isotropically consolidated were very similar to the constant void ratio contours derived from drained tests carried out on the same types of sample.

Roscoe et al (1958) incorporated these observations into the concept of the state boundary surface which relates the stress states and void ratio observed in normally consolidated samples. Together with other contributions from Roscoe and Poorooshasb (1963), Roscoe and Burland (1968), Schofield and Wroth (1968), Atkinson and Bransby (1978) the basic postulate of the critical state theory becomes;

On the "wet" side:

1. All possible states of stress (usually defined by the stress invariants  $J_1$  ,  $J_2$  ,  $\theta$  ) and void ratio (or water content, or volume) forms a surface in the four-dimensional space and it is called the state boundary surface (SBS).

2. A Three-dimensional form of this surface for  $\theta_j = \text{constant}$ , particularly for  $\theta_j = \pi/6$  or  $b=0$  (or  $\sigma_2 = \sigma_3 = \sigma_{min}$ ) has the following properties:

- a. The interception of a family of planes  $J_2/J_1 = \text{constant}$  with the SBS, plot as parallel straight lines in water content- logarithm of mean stress space.
- b. The interception of a family of constant volume (or void ratio) planes with the SBS plot as a family of parallel curves in  $J_2, J_1$  space.
- c. Any sectional line in a surface find its locus in a two-dimensional representation of the surface. This is the case of drained, undrained or any other non-special stress path on the state boundary surface.
- d. The plastic potential in the two-dimensional representation coincides with the SBS, but does not coincide in three-dimensional representation. If the plastic potential coincides with the SBS in the three-dimensional plot ( $p, q, e$ ) the strain rate does not necessarily plot orthogonally in the two-dimensional representation.

On the "dry" side:

On the dry side the soil specimens fail at the Hvorslev line and the ultimate strength with no further change in volume is found when the sample reaches the so called critical state line. Here, soil specimens if further sheared (in the same direction), experience no further change in volume or in stress state.

The four-dimensional form of this surface is considered to be achieved

by interpolating the observed response in different  $\theta_j = \text{constant}$  section, i.e., test results on  $\theta_j = \pi/6$  ,  $\theta_j = 0$  ,  $\theta_j = \pi/6$  can be used to find the general form of the SBS function of  $J_1$  ,  $J_2$  ,  $\theta_j$  and void ratio.

#### Basic Corollaries:

1. A directly consequence of postulate 2.b. is that the state boundary surface is normalisable in the  $J_2$  ,  $J_1$  space, i.e., reducible to a two-dimensional curve in  $J_2$  ,  $J_1$  space. Particularly, reduction to a two-dimensional plot can be achieved by normalization in relation to water content or any other variable which can uniquely be related to the water content, for example, mean stress at virgin consolidation line (Pe).
2. A line on the SBS obtained by the interception of  $J_2/J_1$  constant planes with constant volume plane plot as a point on the same line in water content-logarithm of mean stress space as postulated in 2.a..
3. The  $J_2/J_1$  constant plane plotted in the two-dimensional representation of SBS, in the  $J_2$  ,  $J_1$  ,  $\theta = \text{constant}$  space, reduces to a point.

#### 1.5 Stress Path influence

Very few results strictly obey the idealised assumptions of the critical state theory. Innumerable discrepancies has been reported:

For example Roscoe and Thurairajah (1964) found important differences between normalized stress paths observed in undrained conventional triaxial test on kaolin, i.e., they do not obey the Rendulic principle.

Using a biaxial apparatus, Hambly (1972) tested anisotropically consolidated samples under plane strain conditions and when plotting equal volume change contours, he found that they were no longer geometrically similar to each other or to the undrained stress path.

Le Lievre and Wong (1970) reported that by using stress controlled tests on certain kinds of kaolin the normalised stress path differences could be reduced but not eliminated. Newland (1975) published a complete set of results concerning triaxial tests on kaolin and found that normalized stress paths in drained and undrained test are different. Lewin and Burland (1970) reporting results on slate dusts showed different normalized stress paths for drained and undrained tests. Gens (1982) reported quite different normalized stress paths obtained in drained and undrained (and many others paths) on isotropically consolidated samples of Lower Cromer Till.

The non-uniqueness of the normalized stress path can be at least partly attributed to the development of an anisotropic structure during consolidation (Gens, 1982).

The stress path has also a great influence on the direction of the strain rate, which will be discussed in the next section.

### 1.6 Strain Rate Direction

It is assumed in the critical state theory that the strain rate direction is normal to the SBS in the normalized  $J_2, J_1$  stress space, being a function of the stress state alone.

Many discrepancies in these assumptions have been reported. For  $k$  - constant consolidation tests innumerable variations in the ratio  $\eta = J_2/J_1$  when plotted against  $J_2/J_1$  have been reported by Roscoe and Pooroshasb (1963), Balasubramanian(1969), Le Lievre (1967), Namy (1970), Gens (1982).

Furthermore, many investigators have shown the strong influence of the previous consolidation history on the strain rate direction (Lewin (1973, 1975), Wood (1973, 1975, 1981) and Wood and Wroth (1977), Gens (1982)).

In general a sudden change in direction of the stress path makes the strain rate direction rotate with some delay from the previous established direction until it finally achieves a new direction corresponding to the imposed new stress ratio direction. Lewin (1973), Gens (1982) carried out many tests to show this and some of the stress paths used by them will be described:

First sequence of set of tests:

1. One set of samples was consolidated, each with constant  $k$  ( $k$  varying from 1 to  $k$  at critical state), to a high stress level. The direction of strain rate for each constant  $k$  was recorded.

2. One (or many) samples were consolidated uni-dimensionally ( $k=0.5$ ) and then sheared undrained until  $k=0.667$  was reached, from which further consolidation was carried out. The recorded strain rate ratio from  $k=0.667$  onwards was not the same as that corresponding to  $k=0.667$  obtained in the consolidation test where the stress rate direction was always steady (as obtained in the first item). However the strain rate direction seems to converge to the one corresponding to  $k=0.667$  (with steady stress ratio direction) at a higher mean stress. Usually convergence occurs for a mean stress twice or more that corresponding to the initial stage of the consolidation test with  $k=0.667$ .

3. One (or many) samples were consolidated uni-dimensionally ( $K=0.5$ ) and then unloaded until  $k=1$ , from which further consolidation was carried out. Again, the recorded strain rate ratio during  $k=1$  consolidation was no longer equivalent to the one corresponding to the consolidation with  $k=1$  as obtained in the first item. Strain rate directions for samples with a history of stress previous to  $k=1$  consolidation, as presented in this item, do not appear to converge to the one correspondent to  $k=1$  consolidation (as obtained in the first item) at least until the mean stress reaches four times the one at the initial stage of  $k=1$  consolidation. However, the tendency to do so can be observed.

Other stress histories have been imposed to show the effect on the strain rate direction. The effect on the strain rate for stress paths in the  $b=0$  plane has been reported by Lewin (1978), Gens (1982); and for  $b=1$  by Lewin (1978), and for stress paths in the deviatoric plane by Wood (1981).

Most observations on the influence of stress path direction on the

strain rate direction are for the following test pattern.

Strain rate ratio is observed for a steady stress path and then, after the stress ratio has suddenly changed to another direction, the rotation of strain rate is observed for a new steady stress ratio.

The general conclusion is that the change from one steady stress ratio direction to another steady stress ratio direction results in strain rate direction being no longer equivalent to that obtained if the sample were tested steadily with an unique stress ratio corresponding to the second stress ratio direction. However a clear tendency to converge to it is observed when the last steady stress path has reached a high level of mean stress. The value of mean stress depends on the material and the stress path under consideration, nevertheless, a mean stress twice or more the mean stress at the beginning of the last steady stress ratio is acceptable.

Also, whether the convergence occurs from higher or lower values than the convergent one depends on the sample stress history. For example, for specimens uni-dimensionally consolidated and then unloaded previous to subsequent consolidation with a higher constant  $k$  (for  $b=0$ ) the strain rate is shown to converge from a lower value than the convergent one. However, specimens consolidated at constant  $k=1$  and then loaded previously to a subsequent consolidation at higher value of constant  $k$ , show that the strain rate converges from a higher value than the convergent one.

Although important gains have been achieved in these researches; the influence of a more complex stress path on the strain rate direction is yet to be known.



## 2. Third Stress Invariant Effect

### 2.1 General

The soil behaviour described previously was concentrated on the behaviour observed in the plane  $\theta=0$  ( $\theta = \pi/6$ ). Soil in the field, however, presents a much more general stress path than those allowed in the  $\theta=0$  plane. Consequently it is highly desirable to find out how soil responds in a more general stress space.

An attempt to define the third stress invariant influence on the soil can be made by carrying out extension tests (triaxial test equipment) and plane strain tests (plane strain equipment). However, for a more systematic observation, a true triaxial equipment and/or hollow cylinder apparatuses is required. But, unfortunately a discussion of the advantages and disadvantages of these apparatus is out of the scope of this thesis.

Although most results are reported for triaxial extension (triaxial test equipment) and plane strain (plane strain equipment) some more general studies in the  $\pi$ -plane have been reported when using the true-triaxial and or hollow cylinder apparatus, these being: Krieg (1975) and Ladd et al (1977), Sekiguchi and Ohta (1977), Tavenas et al (1979), Tavenas and Leroueil (1977), Vaid and Campanella (1977), Wissa et al (1971), Hashiguchi (1977,1981).

## 2.2 Critical State Surface and Hovslev Surface.

There has been a lot of arguments as to whether the Mohr-Coulomb envelope represents the critical state or not. Innumerable test results have been carried out in order to measure the friction angle for extension and plane strain conditions and a few of these are reported here.

-Extension tests give similar angles to those measured in compression only for normally consolidated specimens. Even in this circumstance exceptions were found where the difference between the compression and extension friction angle can be, for example,  $13.6^\circ$ ,  $6.8^\circ$  or  $34^\circ$  as reported by Mitachi and Kitago (1979), Broms and Casbarian (1965) and Leon and Alberro (1972), respectively, the extension friction angle being greater. The difference between effective stress friction angles observed in the extension test on anisotropically consolidated samples and in compression is in general as high as  $1.6^\circ$ ,  $2.1^\circ$ ,  $2.5^\circ$ ,  $4^\circ$ ,  $5^\circ$ ,  $7.2^\circ$  as reported by Gens (1982), Mitachi and Kitago (1980), Koutsoftas (1981), Vaid and Campanella (1974), Ladd and Varallyay (1965), Parry and Nadarajah (1974), respectively. The same friction angle in compression and extension for anisotropic consolidated samples was reported by Andersen et al (1980). No pattern between the friction angle obtained in undrained extension and in undrained compression tests can be arrived at. Mitachi and Kitago (1980) found the friction angle for extension tests on isotropically consolidated sample greater by  $14^\circ$  whereas Parry and Nadarajah (1974) reported friction angle values lower by  $7.5^\circ$ . Friction angles obtained in undrained extension on samples anisotropically consolidated sample greater by  $1.3^\circ$  and

1.5° have been reported by Gens (1982) and Ladd and Varallyay (1965), respectively.

The value of friction angle obtained in undrained plane strain on samples consolidated isotropically have been reported to be higher when compared with the value of friction angle in triaxial compression. (Lade and Musante, 1977, 1978; Yong and Mckyes, 1967, 1971; and Wood, 1973). However, Pearce (1970, 1971) and Wu et al (1963) have found the Mohr-Coulomb failure criterion applicable, though the latter had to use Hvorslev parameters in order to do so.

A great number of studies involving plane strain tests on  $k$  - consolidated samples have been reported also. Duncan and Seed (1966), Roscoe et al (1959), Ladd et al (1971), Hambly (1972), Sketchley and Bransby (1973), Gens (1982) reported the same friction angles obtained in triaxial compression and in plane strain conditions on samples consolidated anisotropically, where the angle of friction under consideration is the maximum mobilized angle of friction.

However, observations reported by Mitachi and Kitago (1980) suggest a different friction angle for both cases. Larger difference exists if the angle of friction at peak is considered.

Furthermore, a series of drained test carried out by Gens (1982) on Lower Cromer Till show that no great error is involved in the assumption of a unique value for the ultimate friction angle corresponding to the critical state. Again, if the peak friction angle is considered then greater differences would be encountered. (Simons, 1960a; Gens, 1982).

Similar values of angle of friction in drained and undrained tests have also been reported by Amerasinghe and Parry (1975), Hambly and Roscoe (1969), Henkel (1956,1959), Parry (1960), Simons (1960a, 1960b).

From these observations it is clear that the Mohr-Coulomb failure envelope is not generally applicable.

Also, although the Hvorslev surface may be applicable for certain types of isotropic soil it does not seem to be so in extension for some anisotropically consolidated samples.

### 2.3 Undrained Shear Strength and Mean Stress at Failure for tests Other than the Compression Test.

#### 2.3.1 Isotropically Consolidated Specimens.

The undrained shear strength obtained in compression ( $C_u$ ) and extension ( $C_{ue}$ ) tests on isotropically consolidated soil does not exhibit any peak. The ratio  $C_u/C_{ue}$  is usually 1.15 or higher for most soils. Gens (1982) found the ratio  $C_u/C_{ue}$  to be 1.18, being strongly independent of the over consolidation ratio, although similar values for both strengths were reported by Parry and Nadarajah (1974), Mitachi and Kitago (1979), and Leon and Alberro (1972).

The value of mean stress at failure observed in extension  $P_{fe}$  and in compression  $P_{fc}$  on isotropically normally consolidated soil are not in general equal. For Lower Cromer Till the ratio  $P_{fe}/P_{fc}$  is equal to 1.18. However, almost equal mean stresses at failure for compression

and extension on normally consolidated soil have been reported by Parry (1971).

The normally consolidated stress path forms a kind of boundary for all the other stress paths for over consolidated sample.

Also, it can be observed that the initial undrained shear modulus for compression and extension on isotropically consolidated samples are almost the same.

### 2.3.2. Anisotropically consolidated specimens

Not many undrained triaxial compression and extension tests have been carried out on anisotropically consolidated soil. Actually, just a few have been reported for normally consolidated, such as Mitachi and Kitago (1979), Ladd and Varallyay (1965), Gens (1982) for reconstituted samples; and Koutsoftas (1981) and Vaid and Campanella (1974) for intact samples. From these results the following may be concluded:

Anisotropically consolidated samples sheared in triaxial compression present a peak in strength ( $C_p$ ) and an ultimate strength ( $C_u$ ) whilst when sheared in extension no peak is noticeable. However, no pronounced peak has been reported by Vaid and Campanella (1974). The peak characteristic of clay seems to be related to its plasticity index. The lower the plasticity index the more pronounced the peak. Furthermore, it is clear that the degree of undrained brittleness increases sharply for samples which have been previously consolidated at lower  $k$ -constant values. The magnitude of the anisotropy, as

suggested by comparison of the ultimate values in compression and extension, increases substantially as the k-constant consolidation ratio (carried out previous to the undrained shear) reduces. High stress levels during consolidation also appears to reduce the stiffness which is observed after the sample has gone into extension. (Gens, 1982).

Although the ultimate stress values of a series of anisotropic consolidation and isotropic consolidation tests coincide, they are quite distinct for samples sheared in extension. Part of this difference can be explained by the anisotropy effect, part by the change in  $b$ , and part by the difference in friction at the boundary introduced by the loading conditions.

Comparing results from isotropic and anisotropic tests, assuming the  $b$  effect will be the same in both, the effect of anisotropy on the ultimate undrained strength for anisotropically consolidated sample can be evaluated. By doing so Gens (1982) showed that the resulting horizontal/vertical ratio of critical state strengths turned out to be an approximately constant value of 0.79, against a value of 0.83 obtained from undrained tests on horizontal and vertical samples previously consolidated anisotropically. The strength ratio was found to be approximately constant for all over consolidation ratios (OCRs).

The normally consolidated stress path forms a kind of boundary for all the other stress paths and so it provides the envelope of the possible peak strength values. The resulting undrained brittleness defined as  $C_p/C_u$  is seen to depend strongly on the degree of overconsolidation.

Similar comments can be made in relation to the plane strain tests on

anisotropically consolidated samples.

### VIII.2.2 Properties of the Material in the Kinematics Region.

#### 1. Speculative Introduction

Because of the nature of the linking between particles, soil exhibit viscous effects. An static sample of clay achieves its internal mechanical equilibrium by balancing the various attractive and repulsive forces acting within its volume. Similarly for a static sample of sand to be in internal equilibrium it has to satisfy the contact and repulsive forces acting within its volume.

An external action on the soil mass boundary has to break this internal equilibrium before making the soil deform. The intensity of the resistive force offered to the action seems to depend on the rate of the actions and its direction is opposite to it. When deformation occurs the material goes on changing its structure either until a new stable structure for kinematics is achieved or until static boundary conditions are achieved. If, however, a material under a kinematic boundary condition experiences a sudden change in the boundary, such as a change of modulus and/or direction of the stress rate, new change in structure are observed until a new stable structure is achieved. Each change of the boundary conditions, from static to kinematic, from one kinematic state to another kinematic state seems to be accompanied by a change in structure. The change in structure, therefore, is a function of deformation and time (as explained elsewhere).

From the physical point of view this time dependent process occurs continuously and seems to be more important for strain rates higher than the quasi-static one. Special care must be taken when measuring the material properties in this range of strain rate (or stress rate) because of the degree of non-uniformity of the physical material response which seems to increase for higher strain rates.

Also, standard triaxial test equipment results, must be viewed with great care, particularly the comparison between compression and extension tests, because of the difference in the friction at the boundary, and this can generate a greater source of errors.

The influence of the strain rate (or stress rate) larger than the quasi-static on the soil properties will then be described as follows:

## **2. Failure Envelope Line (and surface)**

The friction angle obtained at the ultimate stress state in a triaxial compression test does not seem to be considerably affected by the strain rate intensity. Indeed, undrained compression tests carried out by De Campos (1984), Takahashi (1981), Hight (1982) on isotropically consolidated and overconsolidated specimens of Lower Cromer Till showed no great effect of the strain rate intensity on the effective stress friction angle. Also the majority of data presented by Lacasse (1979) agrees with this conclusion. Furthermore, undrained triaxial compression tests on sand carried out by Shelley (1984) on inherently anisotropic sand consolidated isotropically does not reveal any significant strain rate intensity effect on the friction angle obtained at the ultimate stress state.



Undrained triaxial extension tests carried out by Takahashi (1981) showed that the friction angle is somehow affected by the strain rate intensity.

More laboratory results for other materials and other conditions than triaxial compression or triaxial extension are necessary to show the influence on the Hvorslev surface.

### **3. Peak Strength, Pore Water Pressure Generation.**

Undrained triaxial compression tests on isotropically consolidated soil exhibit large undrained strength increases for larger strain rate intensities.

Certainly because less time has elapsed during the period when larger strain rates are applied in the undrained triaxial tests less relaxation in mean stress and consequently in generation of pore water pressure are observed, Lacasse (1979), Takahashi (1981), Hight (1982).

Several investigators (Vaid and Campanella (1977), Bjerrum et al (1958), Richardson and Whitman (1963), Crawford (1960), De Campos (1984)), showed that the effect of strain rate intensity on the soil strength is more pronounced in isotropically overconsolidated specimens than in isotropically normally consolidated ones. Richardson and Whitman (1963), however, point out that the water migration effects have an important influence on the measured strength of an overconsolidated sample.

The observed undrained peak strength in compression of anisotropically normally consolidated or slightly overconsolidated samples seems to be

greatly increased by an increase in the strain rate. (Hight , 1982; Gens, 1982; De Campos, 1984; Takahashi , 1981).

It should be mentioned that the ultimate undrained strength of anisotropically consolidated sample can be much less sensitive to the strain rate. (Gens, 1982; Takahashi, 1981; Hight, 1982).

Undrained triaxial extension test on isotropically normally consolidated and overconsolidated sample suggested similar trend of behaviour: Less pore-pressure generation and higher undrained strength with increase in strain rate. (Takahashi, 1981; De Campos, 1984)

By observing the laboratory test results it can be concluded that the increase in ultimate undrained strength for isotropically and anisotropically normally consolidated samples due to increase of strain rate, can not represent by itself the amount of decrease in pore-pressure generation for stress levels below the critical one. Indeed, decrease in water pressure generation with increase in strain rate at the earliest stage of an undrained test can be substantially higher than the increase in ultimate strength.

It will be seen that the decrease in pore-pressure generation with increase in strain rate in an undrained test can be, at least partially, explained by the decrease in the material compressibility due to the strain rate increase.

Many laboratory results such as Lacasse (1979), Takahashi (1981), De Campos (1984) , Hight (1982), have suggested some kind of power law or exponential function to represent the empirical relationship between strain rate and undrained strength. A typical function is that the

undrained strength obtained in compression tests increases linearly with the logarithm of strain rate. The overconsolidation ratio and the plasticity index also influences this empirical relationship.

Compressibility: Smith (1969) and Wissa et al (1971) carried out  $k$  - consolidation tests at a constant rate of deformation and reported substantial decreases in compressibility ( $\lambda, K$ ) and increase in pre-consolidation pressure when the strain rate intensity increases, the effect of change being more pronounced in more plastic material. No test including a change in the direction of action has been performed yet.

No information, however, can be obtained about the effect of a change in strain rate on the soil compressibility. A consolidation test changing its constant strain rate to another would show this influence.

In practice the effect of a change in strain rate on the soil properties is extremely important. For example, a normally consolidated soil (static conditions) when loaded to a certain stress rate will exhibit a compressibility characteristic different from that exhibited when loaded from static equilibrium to another stress intensity. Obviously innumerable rates will occur in engineering practice which will only add to the other difficulties in finding a proper model for soil.

In  $k$  -consolidation tests the Young's modulus obtained for effective stress can be shown to increase at higher strain rates.

Also a considerable increase in the Young's Modulus can be observed in

undrained tests on isotropically and anisotropically normally and overconsolidated sample when sheared at a higher strain rate. Obviously the increase in undrained shear modulus may be associated with the decrease in compressibility as discussed previously.

### VIII.2.3 Effect of the Strain Rate on the Stress-Strain Relationship Based on the Elasto-Plastic Theory.

#### **1. First Yielding.**

The first yield locus is dependent on the strain rate. Indeed as the first yield depends on the pre-consolidation pressure, it must be a rate function.

#### **2. Shape of the Yield Locus and Plastic Potential.**

One should remember that the yield locus shape, as obtained by the critical state theory, is based on Rendulic's Principle, i.e., all possible stress paths for normally consolidated samples can be reduced to an unique one when normalized with relation to the mean stress obtained in the isotropically consolidated test.

Also it has been mentioned previously that this principle does not seem to be applicable to most soils and it is much less applicable if the strain rate is taken into account. Many yielding surfaces exist, one for each initial condition, each stress path, each strain rate (or stress rate) intensity. In soil mechanics practice the shape of the

yield locus is obtained based on the undrained stress-path and as the undrained stress-path is a function of the rate, so will the yield locus be.

### 3. Elastic Constants

The elastic constants are functions of the strain rate (or stress rate). As the elastic constants can be expressed as a function of the slope of the reconsolidation line ( $k$ ) they will be rate functions.

To take into account all these influences, or any of these influences is not an easy task. Many simplified model taking strain rate into account have been proposed. The first, which corresponds to the observation described in item "a" and "c" above considers the material as viscoelastic-plastic, which means that the rate causes no effect on the plastic deformation. The difficulty here lies in defining the visco strain in the elastic region, which is usually assumed to be a function of time and stress level, and in defining the first yielding. Also, material points moving to the elastic region would be difficult to consider.

This kind of approach can be very useful when introducing the rate effect in an overconsolidated region by means of kinematic hardening.

Secondly, the consideration of the soil as an elasto-viscoplastic material, which means that the viscous effect occurs in the plastic region. This approach makes it easier to define the first yielding surface, which can be useful when introducing the rate effect for the normally consolidated region.

Many other approaches exist and they will be discussed in the next section. However, all of them are extremely rigid and can be applied only for each special circumstance.

In this work a more flexible approach will be suggested.

#### VIII.2.4 Material Behaviour for Rates Smaller than the Quasi-Static One:

It has been seen that the rate effect (creep law) in the kinematic region can be expressed by some empirical law. When, however, the strain rate becomes smaller than the quasi-static one, different values for the constant must be used, because it has been shown that the soil responds to the rate action in a completely different manner for this range of strain rates. A discussion in more detail will be given in the next section.

A material straining at very large strain rates would experience extremely small deformations, while the stress state changes dramatically because of the smaller compressibility of the material. Eventually, material straining at very high strain rates would fail at the Mohr-Coulomb type envelope after the occurrence of infinitesimally small strains. In other words, the material on the way towards the Mohr-Coulomb envelope would experience neither work hardening nor softening, and the response would be of a perfectly plastic material with a Mohr-Coulomb type envelope. In this sense, there would also be a strain rate where the material would experience virtually no deformation on the way towards the Von-Mises type envelope to finally

end at the Mohr-Coulomb type envelope. Also, there would be a strain rate where material would strain elasto-plastically through a yield surface dependent on second degree terms of mean stress.

Results of undrained tests on normally consolidated samples at higher strain rates consistently show the undrained stress-strain relationship to be stiffer, the pore-pressure generation to diminish and the undrained strength to increase, which agrees with the soil response as viewed from the consolidation test point of view, where the soil compressibility decreases and the pre-consolidation pressure increases at higher strain rate intensities.

The usual classifications of an idealized soil material are presented next, together with their respective difficulties and restrictions of applicability.

### VIII.3 Brief Comments on Various Attempts

In elasticity theory there are basically three approaches to define the constitutive behaviour of materials. Although retaining the concept of "elasticity" they provide constitutive equations which no longer produce the same results. In fact, three different types of generalization are obtained, which are named by Truesdell (1965) as elasticity, hyperelasticity and hypoelasticity.

Since the Eulerian stress tensor and the Eulerian-Almansi strain tensor are related uniquely to the Kirchhoff stress tensor and Green-Lagrange strain tensor respectively, these three "elastic" constitutive equations hold for small and finite strain conditions. However,

special difficulties are encountered in the concept of stress rate used in hypoelastic (or plastic) type materials. The difficulties come when the requirement of invariance of the stress rate is not satisfied by a unique relationship (Oldroyd (1950), Truedell (1953), Prager (1961), Cotter and Rivlin (1955)).

However, Oldroyd pointed out that the differences among the various definitions of stress rate are not important once they can be uniquely related to each other. In chapter IV all linear combinations of different stress rate definitions, were presented. (For more details see references above)

Next, the various attempts are going to be considered without discussing the derivations. The derivations for almost any idealized attempt will be discussed separately in a following section.

### VIII.3.1 Elasticity - Viscoelasticity

The first definition (elasticity) is based on Cauchy's approach and states that the current state of stress depends only on the current state of deformation (i.e., stress is a unique function of strain, independently of the stress (or strain) path history of the loading cycle (loading, unloading, etc...)) and time (viscous effect).

Elasticity (or linear elasticity) has been extensively used in the past to model clay skeleton behaviour by means of Biot's theory. The first consistent application was introduced by Sandhu and Wilson (1969), Hwang et al (1972), Verruijt (1972,1977), Matsumoto (1976) etc... Very few theoretical approaches , however, include the viscous



behaviour, except Biot (1956a), who has proposed a general viscoelasticity theory with a thermodynamic approach, and Mandel (1957) and Tan (1957a,b), who has proposed a general three dimensional theory where the rheological type model (Maxwell-type solid) was assumed to simulate the soil (clay) behaviour. Very few applications have included these models, but viscoelasticity has been used to some extent, Suklje (1977), Booker and Small (1977), Zienkiewicz and Corneau (1974), Smith (1982).

From a computer point of view visco-elastic models are very attractive since they provide a very simple and inexpensive solution.

From the physical point of view linear elasticity (or viscoelasticity) may be sufficient to predict behaviour of heavily overconsolidated clay, especially for the dry crust of a clay layer. If this crust has a substantial thickness, linear elasticity can be perfectly justified in the case of a simple surface loading, even if the subsoil is only slightly overconsolidated, the reason being that the additional stresses from the applied load decrease rapidly with depth and the deformation field for small stress changes will be of little significance even for strongly non-linear soil masses. Of course, this conclusion is not absolute and its validity has a compromise which lies between the variation of overconsolidation with depth and the absolute value of the additional stress level.

Although many non-linear models have been proposed, linear elasticity will always be used for soil because the more sophisticated models are restricted to a certain simple circumstances, for which linear elasticity can, to certain extent, provide similar answers in practical engineering for much less cost.

### VIII.3.2 Hyper and Hypoelasticity-Viscohyperelasticity

The second definition (hyperelasticity) is based on Green's method and assumes the existence of a strain energy density  $\epsilon$  (or a complementary energy function  $\Omega$ ) such that the current state of stress (or a current state of strain) is a function of the rate of change of the strain energy density (or the stress energy density) with respect to strain (or with respect to stress). In this  $\epsilon$  is, in general, an analytical function of strain but normally stipulated as a function of strain invariants and  $\Omega$  is, in general, an analytical function of stress but normally stipulated as a function of stress invariants.

### VIII.3.3 Hypo-Elasticity

The third definition (hypo-elasticity), also called the incremental model, embodies the rate theory and describes the mechanical behaviour of a class of materials in which the state of stress depends on the current state of strain as well as on the stress path followed to reach that state. This class of material is reversible for infinitesimally small increments, thus justifying the use of suffix "elastic" in the term hypoelastic used by Truesdell, but not reversible for *the whole strain increment*

The so called pseudo elasticity which is a hybrid form of hyper-hypoelasticity was first introduced by Duncan and Chang (1970).

In this a volume energy function is assumed to exist (hyperelasticity), but deviatoric strain-stress relations are of rate type, i.e., the bulk modulus is assumed to be a function of the mean stress (in practice often restricted to the initial mean stress), while the tangent shear modulus continuously decreases with mobilized shear stress and tends to zero when the deviatoric stress approaches a maximum value (asymptotically) determined by a Mohr-Coulomb failure criterion.

More recently, Duncan (1980) has extended the model to take into account volume change and cyclic loading but neither intermediate stress influence nor anisotropy are taken into account.

A more rigorous treatment for the hyperelastic model is given by Nelson and Baron (1971) for isotropic conditions and cyclic loading and Saleeb and Chen (1980) where only isotropic conditions and monotonically increasing loading are allowed. Both approaches, however, include the influence of the intermediate stress component, and provide invariant constitutive equations. Also volume change is taken into account.

Many applications of non linear elasticity of Duncan's type have been used: Cavodinis (1975), Osaimi (1977), Desai and Saxena (1977), etc...

As far as the author knows neither a consistent hyperelastic nor a visco-hyperelastic model has been applied yet.

From the computer point of view some advantages seems to exist in using hyper elasticity (or visco-hyperelasticity) when compared with

elasto-plastic (or elasto-viscoplastic) models. It seems that they can be less time consuming.

On the other hand hyperelasticity does not violate the thermodynamics law if treated consistently but it has no physical meaning because it assumes that the directions of stress rate and strain rate always coincide (at least incrementally). However, reasonable answers may be achieved in the prediction of clay behaviour if used consistently.

#### VIII.3.4 Elasto-Plasticity

The hyperelastic model may predict clay response with some realism for certain circumstances if applied consistently, although it is assumed that the direction of incremental strain and stress always coincide which in general is incorrect, particularly when the stress level approaches the critical state. One way to overcome these limitations is to use the plasticity theory. Although this theory is more flexible and to a certain extent has more foundation physically it is still restricted to applications in simple circumstances.

From the application point of view the main feature of interest in the flow theory of plasticity is a proper choice of a yield criterion (and/or critical state), a flow rule, and a hardening (and/or softening) rule.

The initial yield criterion may then be classified as:

1. Mean stress independent

This type of criterion, such as Von Mises's and Tresca's, involve assumptions which provide a pure  $J_2$  dependence and  $J_2, \theta_j$  combined dependence, respectively; where  $J_2$  and  $\theta_j$  are the second stress invariant and Lode angle with respect to stress, respectively. The bar means that the is a invariant function of deviator stress.

It might be argued that pure deviator dependence can be used in an undrained situation, in which a total stress analysis can sometimes be used instead of effective stress analysis. In this case the clay is then considered as a one phase medium (Hoeg, Christian and Whitman (1968)).

2. Linear mean stress dependence:

Examples of this type of yield criteria are Drucker-Prager, Mohr-Tresca and Mohr-Coloumb. The first of these criteria has a pure  $J_2$  dependence on the deviatoric stress whilst the other two have a combined  $J_2$  and  $\theta_j$  dependence. For discussion see Nayak and Zienkiewicz (1972).

A smooth curve in the deviatoric plane (where the dependence is, of course, due to  $J_2, \theta_j$ ) has been suggested by Lade and Duncan (1975), Zienkiewicz and Pande (1976), Gudehus et al (1977). For discussion see Eekelen (1980), Zienkiewicz and Pande (1975), Argyris et al (1974).

Some investigators have argued that associated flow rules should not be used when combined with linearly mean stress dependent yield conditions, Davis (1968), Potts and Gens (1982). Some effects of a non associative flow rule can be observed in Zienkiewicz et al (1975), Potts and Gens (1982). For soft clay it is quite obvious, because it is contractant whilst an associated flow rule generally implies dilatancy, the volume expansion will be overestimated, at least for deviator stresses approaching the critical ones. If such an analysis is used, the consequence is to produce a decrease in pore-pressure and less decrease in effective stresses, due to the plastic dilatance introduced. Thus, when the stress path moves towards the yield cone an overestimation of the deviatoric strength is implied. It must be emphasized that when linear mean stress dependent yield criteria are used in soft clay, they should be used as critical state (in the sense of critical state theory) rather than initial yield.

According to section VIII.2, the ultimate state of stress does not always satisfy the Mohr-Coulomb criteria. In that sense the general expression provided by Eekelen (1980) can be used where the constant of the equation should be calibrated to each soil characteristic.

As a non-associated flow rule implies a non-symmetric tangential stiffness matrix, a convenient solution technique may be the fictitious viscoplasticity approach, as suggested by Zienkiewicz et al (1975), Corneau (1975), in which plasticity is assumed to be a limiting stage of a stable creep process.

Consolidation analysis with a rigid-plastic model has been performed by Small et al (1976). The initial yield is that of Mohr-Coulomb type

and an associative flow rule was then assumed. Also Carter et al (1979) has presented a small strain large rotation consolidation analysis adopting the same rigid-plastic model.

### 3. Non-linear mean stress dependence:

The first attempt to use this kind of dependence was made by Drucker, Gibson and Henkel (1957) and later Jenike and Shield (1959). However, non-linear elasto-plasticity has also been assumed in the critical state theory at Cambridge where exhaustive work in this subject has been done by Roscoe and Schofield (1963), Roscoe, Schofield and Thurairajah (1963), Roscoe and Burland (1968), Palmer and Pierce (1973) etc...

The fundamental assumptions in the critical state theory are that Rendulic's Principle is applicable and the plastic potential depends only on the state of stress, where, particularly, associative flow rule is assumed (as in the most classical theory of plasticity).

As discussed in section VIII.2 there is strong evidence that neither Rendulic's Principle is applicable nor is the plastic potential a function of the state of stress only. Furthermore, normality is not a general property of the soil.

Because of these disagreements of real response and the proposed theory, innumerable elasto-plastic models have been proposed. The shape of yield surface and/or plastic potential in the  $J_2/J_1$  plane can assume several forms such as a straight line (Larsson, 1977), circle (Drucker, Gibson and Henkel, 1957; Jenike and Shield, 1959),

bullet shape (Roscoe and Schofield, 1963; Roscoe, Schofield and Thurairajah, 1963), ellipse (Christian, 1966; Roscoe and Burland, 1968; Hagmann, 1971), exponential (DiMaggio et al, 1971), cone (Prevost and Hoeg, 1975), and several other combinations of parabola, hyperbole, ellipse and straight line have been assumed. Each of these shapes fit one particular kind of soil for certain specific testing circumstances.

To recapitulate on section VIII.2, the soil property for the quasi-static region has been stated as:

1. There are almost as many yield surface as stress-paths, i.e., Rendulic's principle is not applicable. This soil characteristic can be, at least partially, explained by the induced anisotropy during the consolidation process.

In many soils the associative flow rule does not apply and the strain rate direction depends not only on the stress state but on the stress history also.

As rational and interesting attempt to unify the plasticity theory for soil without having to obey the Rendulic's principle was made by Calandine (1963) by applying the slipping theory. In this theory the material has one yield locus for each combination of mean stress and deviatoric stress, and consequently, the yield for each sample (or material point) is obtained by adding the yielding on each plane of the sample. Applying this approach is difficult and expensive for obvious reasons, however, it can provide a better framework, making possible the calibration of experimental data with reasonably justification



Innumerable empirical models have been proposed to accommodate the two previously described soil properties. Each empirical hardening law, and evolution rule for the yield surface and plastic potential, is valid only for the characteristics of the soil and the conditions under which it has been tested. Details of these empirical models are out of the scope of this research. However, a very flexible model will be assumed here, which will allow accommodation of most of the empirical models for each material, stress-path, etc... The fundamental procedure to arrive at these models in the  $J_2/J_1$  plane, particularly for compression triaxial tests at quasi-static strain rates, will be briefly presented as:

1. A yield locus is obtained from the undrained stress-path. This yield surface depends on the type of clay or sand, on the conditions of anisotropy, on the previous history of stress, etc...
2. Another yield surface is obtained from the drained stress path, or alternatively, the locus of water content and stress state is measured and adopted as one of the limiting conditions.

The normalized drained stress path depends on the type of clay or sand, on the conditions of anisotropy and on the previous stress history, while the normalized state of stress obtained by k-constant consolidation tests depends on the type of soil and the initial conditions of the sample.

3. The direction of strain rate is measured for k-constant consolidation tests. The direction of the strain rate for this simple kind of stress-path depends on the type of soil.

4. The yield surface for other simple stress-path are observed. For example, stress-paths lying between drained and undrained stress-paths.

5. The direction of strain rate for other stress-paths are observed. For example, a sample initially consolidated at  $k_1 = \text{constant}$  is sheared until  $k_2 = \text{constant}$  from which it is consolidated again at  $k_2 = \text{constant}$ . The variation in the strain rate direction during this last period of consolidation is observed and compared with the strain rate direction if the soil had been consolidated from slurry at  $k_2 = \text{constant}$ .

6. The evolution of the yielding surface for the particular soil being tested and for the range of stress-path under consideration is observed and an empirical rule is proposed.

7. The variation of strain rate for the soil, stress history and stress-path under consideration is observed and an empirical rule is proposed.

For more detailed information about different empirical models and influence of stress history, stress-path, the following work should be considered: Wong and Mitchell (1975), Tavenas (1981), Tavenas and Leroueil (1977, 1979a, 1979b), Tavenas et al (1979), Leroueil et al (1979), Namy (1970), Lewin (1971, 1973, 1975, 1978), Lewin and Burland (1970), Gens (1982), Ohmaki (1979, 1980, 1982), Wood (1973, 1975, 1981), Wood and Wroth (1977), Palmer and Pierce (1973), Lewin et al (1982).

The application of these empirical models to different conditions from those which they have been obtained for, seems to be inappropriate,

because of the strong dependence of the yielding surface and plastic potential on the stress history. The shape of the yield locus for natural clay has been found to be different in the field from those obtained for specific laboratory conditions (Mitchell, 1970; Wong and Mitchell, 1975; Crooks and Graham, 1976; Pender et al, 1975). In this sense if an elasto-plastic model is to be used the yield surface and plastic potential should be obtained from sample as natural as possible and applying the specific conditions of the field boundary conditions. There is no point in using an expensive model if its results are accompanied by an enormous degree of uncertainty.

Usually in the elasto-plasticity theory for soil, anisotropically consolidated soil have different model from the isotropically consolidated soil. Normally, the isotropic yield function is rotated, translated or both with no attention being paid to the principal stress direction in relation to the direction of anisotropy (Baladi and Sandler, 1980; Runesson, 1978; Kolymbas and Gudehus, 1980). One way to introduce the effect of the anisotropy would be to use the slip theory (Callandine, 1971). However, a different and interesting approach to introducing the anisotropy in where the principal stress direction is incorporated implicitly, as provided by Matsuoka (1974), Tatsuoka (1980); Yamada and Ishihara (1982).

The model proposed by Tatsuoka (1980) and Yamada and Ishihara (1982) is based on the postulate proposed by Matsuoka (1974), which assumes that any component of the principal strains in the three-dimensional deformation of sand can be represented as the summation of the two strains that are supposed to developed on two imaginary slip planes. To explain that let  $x$ ,  $y$  and  $z$  denote the direction of the three effective principal stresses  $\sigma_x$ ,  $\sigma_y$  and  $\sigma_z$ . In the case of the

stress conditions,  $\sigma_x > \sigma_y > \sigma_z$ , the imaginary slip planes are envisaged for three pairs of two-dimensional stress system,  $\sigma_x > \sigma_y$ ,  $\sigma_x > \sigma_z$  and  $\sigma_y > \sigma_z$ , as schematically shown in Figure VIII.1.

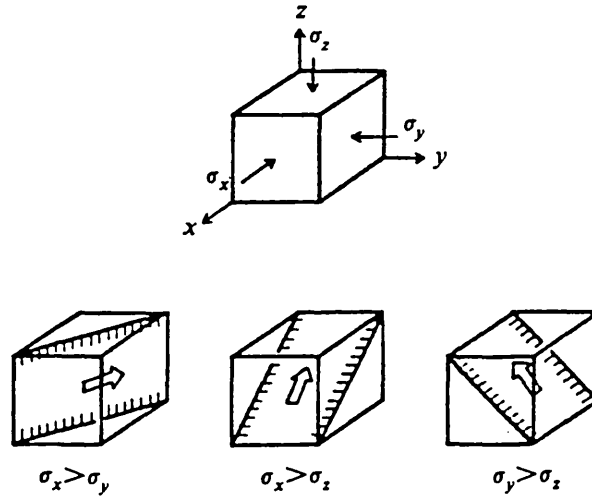


Figure VIII.1

Therefore, the three principal strains  $\epsilon_x$ ,  $\epsilon_y$  and  $\epsilon_z$  are broken down each into two components as follows,

$$\epsilon_x = f_{xy} + f_{xz}, \quad \epsilon_y = g_{xy} + f_{yz}, \quad \epsilon_z = g_{xz} + g_{yz}$$

where  $f_{xy}$  means compressive (positive) strain in the  $x$  direction and  $g_{xy}$  means expansive (negative) strain in the  $y$  direction, which are caused by the two-dimensional slipping in  $\sigma_x > \sigma_y$  stress system. Similarly  $f_{xz}$  and  $g_{xz}$  are compressive and expansive strains, respectively, for  $\sigma_x > \sigma_z$  stress system, and  $f_{yz}$  and  $g_{yz}$  are compressive and expansive strains, respectively, for  $\sigma_y > \sigma_z$  stress system.

This procedure seems to be powerful, in principle, to calibrate data with certain judgement.

Another approach is provided by Mizuno and Chen (1980) who suggested a general equation to be calibrated to the particular material to be analysed.

To analyse soil response under cyclic loading many models have been proposed. A basic formulation is presented by Mroz (1967), Dafalias and Popov (1975), and Prevost (1977). In this model a surface, called the bounding surface, encloses a family of nesting surfaces where each surface is defined by the actual stress state, and more, it can shrink, expand, rotate and distort with the motion of the stress state. Although the plastic potential can have its own rule of transformation, usually an associative flow rule is assumed.

A simplified version of this model called a two-surface model have been presented by Dafalias and Popov (1975), Krieg (1975), Prevost (1977), Dafalias et al (1980), Mroz et al (1978, 1979) where two surfaces are defined and are named bounding (or consolidation) surface and yielding surface. The bounding surface divides the space into two regions. In the region inside the bounding surface the material is in an elastic state if the stress state is inside the yield surface, but can be in a transitory elasto-plastic behaviour if the stress state is on the yield surface. A stress point on the bounding surface is in a fully elasto-plastic regime. The behaviour of the material in the transitory elasto-plastic region is obtained by an interpolation rule which is a function of the distance of the stress state from the bounding surface, measured in the direction of the stress increment. Although the plastic potential can have its own transformation rule, it is usually assumed to coincide with the bounding surface and the direction of the strain rate assumed is normal to a point on the

bounding surface which is obtained by the interception of the stress vector increment direction with the bounding surface (conjugate point).

Also, after the suggestion by Palmer and Pierce (1973), this kind of model was extended by Mroz et al (1979) to accommodate plasticity without a yielding surface as will be discussed later.

It should be mentioned that a delay function for the strain increment direction in relation to the stress increment direction can be incorporated into this kind of kinematic model.

Although this kind of model can be used to analyse cyclic loading if a realistic (experimental) hardening law and/or plastic potential evolution rule are used, it has not been yet applied successfully. This model will be seen here as a technique to analyse overconsolidated soil submitted to a simple stress path.

Van Eekelen and Potts (1978) extended the modified cam-clay model to accommodate cyclic loading, where one of the material properties is the pore-pressure generation in an undrained test.

The first convenient form for application of the critical state theory into finite elements was formulated by Zienkiewicz and Naylor (1972), Zienkiewicz et al (1975). At first the critical state line was considered to be of Drucker-Prager type, i.e., only  $J_2$  dependence on the deviatoric plane. Zienkiewicz et al (1975) introduced a  $\theta$  dependence by considering a Mohr-Coulomb section type for the linear and non-linear part of yielding. Lade and Duncan (1973), Zienkiewicz and Pande (1976), Gudehus et al (1977) have suggested a smooth yield

surface in the deviatoric plane for both the linear and non-linear sections of yielding.

To incorporate anisotropically consolidated soil the yielding surface has been rotated in the  $J_2/J_1$  plane and a simplified function is assumed in the deviatoric plane. For example, Baladi and Sandler (1980) and Runesson (1978) have assumed a rotated ellipse for the triaxial k-constant line and in the deviatoric plane another ellipse is assumed whose major axis is in the direction of the maximum effective stress. More experimental evidence, however, will be necessary to support the assumption of those models.

### VIII.3.5 Elasto-Viscoplasticity, Endochronic Theory

The notion of an elasto-viscoplastic material is reserved for those materials which shows viscous properties in the plastic region only. This idealization evidently simplifies the argument justifying the choice of an adequate initial yield criterion (i.e., the initial yield surface is time independent, although it does not reflect the soil material response). This idealization may be useful (or sufficient ) when creep effects are not significant below the preconsolidation stresses.

However, the endochronic theory, which is regarded as a special form of viscoplasticity (in which the strain rate is not only a function of the stress and strain states but also implicitly a function of the strain rate ) provides a better framework. The constitutive equations can be formulated in a form similar to viscoplasticity if the ordinary time variable is replaced by a fictitious time measure, called

intrinsic time, incorporating both the true time and the length of the (total) strain path traced. Also irrecoverable strains are obtained for every stress state except identically zero. This is contrary to the ordinary viscoplasticity approach, which defines a region bounded by a quasistatic loading surface within which strains are always recoverable. In that sense the endochronic theory provides a concept which could be said to be different from both viscoplasticity and elastic-viscoplastic theories. For more details see Bazant et al(1980).

The application of this theory, however requires much more information from the experimental field.

### VIII.3.6 Viscoelastic-Plastic and Viscoelastic-Viscoplastic Models

Additional difficulties are encountered in establishing the plastic state in a viscoelastic body. In order to discuss this let a load path in the nine-dimensional space of stresses be illustrated in Figure VIII.2.

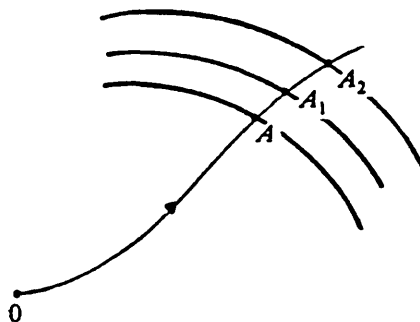


Figure VIII.2



In an elastic body the plastic state will be reached at the same point, represented by  $A$ , independent of the time taken in reaching that state, provided that the load path is the same in each case. If the material is viscoelastic the plastic state may be reached at different points  $A_1$  or  $A_2$ , say, depending on the time elapsing during the load path execution. It is also clear that by passing through the same path or in the same overall time but with different strain-rates, different yield limits will be obtained.

In order to describe the complicated problem of a viscoelastic material becoming plastic the notion of a flow surface will be introduced in agreement with Naghi and Murch (1963).

$$f^s = f^s(\sigma, \epsilon^p, \beta) = 0$$

The elastic-viscoplastic state is determined by the condition  $f^s = 0$ , while the viscoelastic states correspond to the condition  $f^s < 0$ .

Now consider the time-variability of a flow surface. The time derivative of the function  $f$  gives,

$$\dot{f}^s = \left(\frac{\partial f^s}{\partial \sigma}\right)^T \dot{\sigma} + \left(\frac{\partial f^s}{\partial \epsilon}\right)^T \dot{\epsilon}^p + \left(\frac{\partial f^s}{\partial \beta}\right)^T \dot{\beta}$$

If the state under consideration is elastic-viscoplastic and undergoes a change such that  $f^s < 0$ , this change leads to a viscoelastic state because  $f^s + \dot{f}^s dt$  gives a new value of  $f$  which lies below zero. Such a change of the stress state will be denominated an unloading process. During this process there is no increase in plastic strain, therefore  $\dot{\epsilon}^p = 0$ .

Since  $\beta$  can be expressed in terms of physical relations and particularly as a function of the stress rate or strain rate, the mathematical condition for unloading can now be written as

$$f = 0, \quad \left(\frac{\partial f^s}{\partial \sigma}\right)^T \dot{\sigma} + \left(\frac{\partial f^s}{\partial \beta}\right)^T \dot{\beta} < 0$$

A change of state of stress from one elastic-viscoplastic state to another elasto-viscoplastic state accompanied by no increase in plastic strain, the so called neutral process will be characterized by

$$f = 0, \quad \left(\frac{\partial f^s}{\partial \sigma}\right)^T \dot{\sigma} + \left(\frac{\partial f^s}{\partial \beta}\right)^T \dot{\beta} = 0$$

By considering the flow surface in the stress space it can be observed easily that the neutral process does not correspond to the direction of the stress increment  $\dot{\sigma} dt$  tangential to the flow surface at the point considered. This is different from flow theory. An active process which is accompanied by an increase of the plastic strain takes place if

$$f^s = 0, \quad \left(\frac{\partial f^s}{\partial \sigma}\right)^T \dot{\sigma} + \left(\frac{\partial f^s}{\partial \beta}\right)^T \dot{\beta} > 0$$

A neutral state will now be realized if the vector of stress increases  $\dot{\sigma} dt$  deviates from the direction normal to the flow surface by the angle  $d$ , where

$$d = \arccos \left[ -\left(\frac{\partial f^s}{\partial \beta}\right)^T \dot{\beta} / \left| \frac{\partial f^s}{\partial \sigma} \right| |\dot{\sigma}| \right]$$

which also is different from the classical theory of plasticity. Viscoelastic-plastic material presents viscous effects in the whole stress space, the viscous effect being incorporated into the elastic

part of the strain rate, while the viscoelastic-viscoplastic body presents viscous effect in the whole stress space but the viscous effect is part of both elastic and plastic strain rates.

### VIII.3.7 Elastic-Viscoplastic-Plastic Model

This idealized rheological model consists of springs, a Bingham body (or Maxwell body) and a frictional slider, coupled in some way. A typical 1-D arrangement is presented in Figure VIII.3 where the spring, Bingham body and frictional slider are coupled in series.

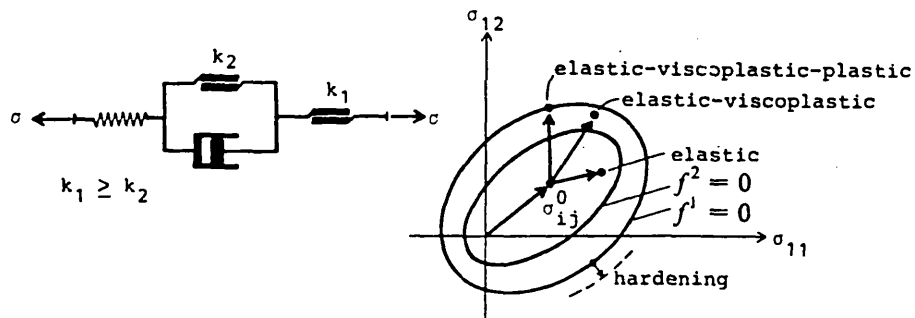


Figure VIII.3 a) 1D-rheological model

b) yield surface in stress space

The yield stresses associated with the slider are denoted by  $k_1$ , and  $k_2$ , where  $k_1 > k_2$  (otherwise the model has no meaning because the Bingham body will always be inactive). Associated with the sliders are two families of closed surfaces in stress space, see Figure VIII.3, the inviscid (dynamic) yield surface  $f^1$  and the quasi-static yield surface  $f^2$ . Associated to each of these surfaces there will be two

hardening (or softening) parameters . However it could be assumed that one or both of these parameters are independent of the plastic strain.

Depending on the position of the stress state in the stress space a different regime of strain is obtained (see Figure VIII.3). In the first region the material is in elastic conditions. In the second region the material under elasto-viscoplastic, i.e., there are two components of strain rate, one elastic strain and another viscoplastic strain, which is usually evaluated by means of a creep law. In the third region the material is assumed to be in a elastic-viscoplastic-plastic regime. The elastic-viscoplastic strain rate is evaluated as described previously and the plastic strain rate is evaluated by means of the usual plasticity theory.

In the existing versions of viscoplasticity it has been assumed, a priori, that the viscoplastic strain rate is normal to one (or more) of the loading surfaces, Perzyna (1966), Philips and Wu (1973), This restriction will also be adopted here.

The division of material states into three distinct regions simplifies very much the determination of the first inviscid yield surface and quasistatic yield surface but it is a mathematical fiction and there is little justification from a physical point of view. However, it could be applied to the case of a single loading condition or could be associated with a complementary model, such as the one which will be presented later.

**VIII.3.8 Elasto-Plastic Kinematic Hardening Model(Two Surfaces Model)**

This kind of model assumes that there are two distinct families of surfaces. The first family ( $f=0$ ), the yield surfaces, encloses the elastic region. The second family of surfaces,  $f^1=0$  define a region which also encloses the elastic region. Material with a state of stress that lies within the region defined by the yield and bounding surfaces experience elasto- and transitory plastic deformation. The materials with stress state on the bounding surface are under a regime of elasto- fully plastic deformation.

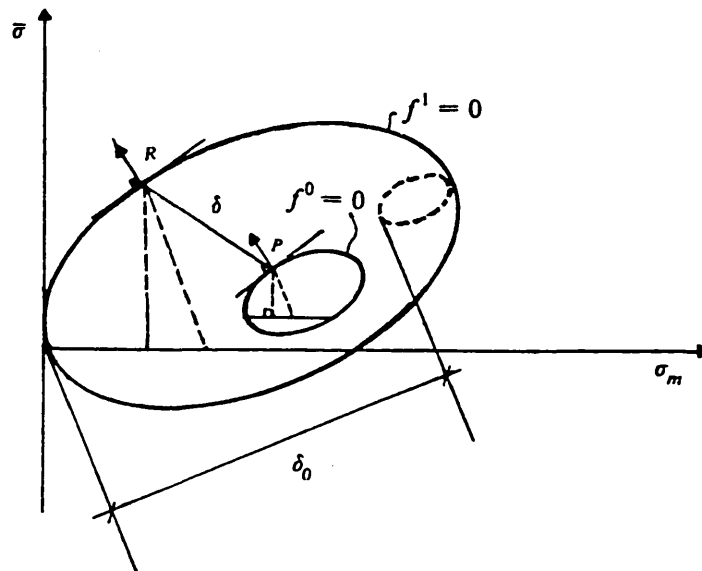


Figure VIII.4

The bounding or consolidation surface is defined as the locus of maximum loading stress. This surface may expand, contract, according to the stress rate direction.

The yield surface, always enclosed by the bounding surface, may

family of surfaces. The bounding surfaces can expand and contract while the yield surface can expand, contract and translate in the same way as for the elasto-plastic kinematic hardening. The third surface, bounding surface  $f^2$ , can expand and contract, accordingly with the expansion and contraction of the bounding surface  $f^1$ .

According to the stress state position, the material state is then defined as:

1. Stress states inside the yield surface  $f^0$  - The material produces only elastic deformation which is calculated by the usual Hooke's law.
2. Stress State on the yield surface- The material is in an elasto-transitory viscoplastic regime. The calculation is like that for the elasto-plastic kinematic hardening but in this case the bounding surface  $f$  is rate dependent and the strain rate direction can be either defined at  $R^1$  or any  $R$  as can be seen in Figure VIII.5.

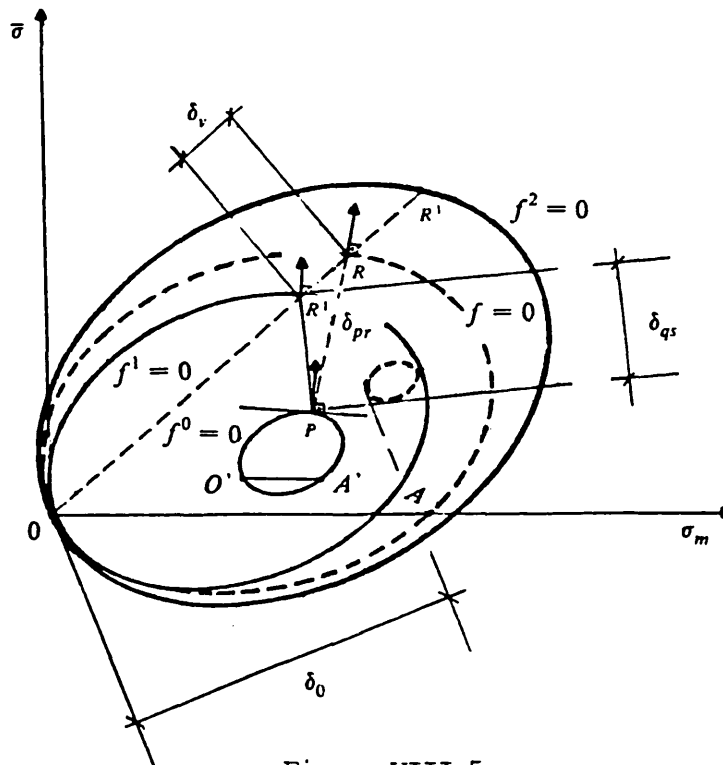


Figure VIII.5

expand, contract and translate kinematically, according to the stress rate movement.

The rules for the expansion of the bounding and yield surfaces are as in soil plasticity and the rule for contraction of the yield and bounding surfaces are calculated from the amount of plastic strain, which is interpolated from the plastic strain that would occur on the yield surface and that which would occur on the bounding surface. The translational rule for the yield surface is defined by imposing the condition that the yield and bounding surface apart from being similar they do not cross each other and are, similar. Also, the direction of plastic strain rate is assumed normal to the point on bounding surface obtained from the interception of this surface with the stress rate direction. See Figure VIII.4.

### VIII.3.9 Elasto-Viscoplastic Kinematic Hardening Model (Three Surfaces Model)

In this model three families of surfaces will be assumed, Figure VIII.5. The first family of surfaces, the yield surfaces,  $f^0 = 0$ , enclose the elastic region. The second family of surfaces, the bounding surfaces,  $f^1 = 0$ , define a region which encloses the elastic region and the elasto-transitory plastic region and they are defined for the quasi-static strain rate  $\dot{\epsilon}^1$  (or stress rate,  $\dot{\sigma}^1$ ). The third family of surfaces,  $f^2 = 0$  is the bounding surface  $f^2$ , obtained for strain rate  $\dot{\epsilon}^2$  (or stress rate,  $\dot{\sigma}^2$ ) in the kinematic range. Between the second and third family of surfaces lies many families of surfaces, bounding surfaces, for strain rates between quasi-static  $\dot{\epsilon}^1$  and the chosen kinematic strain rate  $\dot{\epsilon}^2$  corresponding to the third

The point  $R$  is evaluated by first evaluating the point  $R^1$  as in elasto-plastic kinematic hardening and  $R$  is then obtained by determining the interception of the bounding surface  $f$  for the actual stress rate  $\dot{\sigma}$  with the line that passes through the origin  $\emptyset$  and the point  $R^1$ .

3. Stress states on the region defined by the bounding surface  $f^1$  and  $f^2$  are in an elasto-viscoplastic state. Now the interpolation rule is radial only, that is, point  $R^1$  is at the end of the stress increment and the point  $R$  is obtained by the interception of the bounding surface  $f$  (defined by the actual stress rate) with the radial line that passes through the point  $R^1$ .

#### VIII.4 Explicitly Local Constitutive Stress-Strain Relationship

Two distinct formulations will now be presented. In the first formulation the material will be considered as an elasto-viscoplastic kinematic one. In fact a set of formulations are included in this model, that is, simplification to elasto-plastic kinematic, elasto-plastic and elastic can be obtained by introducing restrictions to the basic model.

In the second formulation the material is considered to be an elasto-viscoelastic-plastic body and restrictions can be imposed to obtain elasto-plastic, and elastic kinds of models.



## Basic Formulation

### 1. Elasto-viscoplastic kinematic (Three surface model)

In this elasto-viscoplastic kinematic model an associative flow rule is assumed, though it is not necessary to impose such a restriction. To introduce the non-associative flow rule, two more surfaces (quasi-static bounding plastic potential and viscoplastic bounding yield surface) , would be required. and, in this case the model would be called a five surfaces model. Despite this, the basic definition for non-associative flow rules are provided for both finite and vanishing elastic regions.

#### 1.1 Elastic behaviour

The elastic behaviour is defined by the generalized Hooke's law, that is,

$$\dot{\epsilon}^e = D^{-1} \dot{\sigma}$$

where  $D$  is the stiffness matrix of elastic constants which is defined explicitly in Appendix D.

#### 1.2 Viscoplastic behaviour on the bounding surface $f$ .

One must be reminded that  $f$  lies between  $f^1$  and  $f^2$  , according to the stress rate intensity  $\dot{\sigma}$  , that is  $f$  will be a type of surface defined by

$$f(\sigma_{ij}, \epsilon_{ij}^p, \dot{\sigma}_{ij}) = 0$$

and

$$\dot{\sigma} = \sigma / \sum t$$

where  $t$  is the actual time.

Because  $f$  is not generally normalized in relation to  $\dot{\sigma}$ , a numerical calculation to take into account the influence of  $\dot{\sigma}$  will be proposed. If for each iteration  $f$  is considered  $\dot{\sigma}$  independent, the flow rule is as in the classical theory of plasticity, that is to say, for non-associative flow rule

$$(VIII.4.1) \quad \dot{\epsilon}^p = \frac{1}{H_R} \frac{\partial g}{\partial \sigma} \left( \frac{\partial f}{\partial \sigma} \right)^T \dot{\sigma} \equiv \lambda^i \frac{\partial g}{\partial \sigma} \equiv \frac{1}{K_R} n \dot{\sigma}_m = \dot{\chi}^i n \quad \lambda^i \geq 0, \quad \dot{\chi}^i \geq 0$$

where

$$\lambda^i = \frac{1}{H_R} \left( \frac{\partial f}{\partial \sigma} \right)^T \dot{\sigma}, \quad \dot{\chi}^i = \frac{1}{K_R} \dot{\sigma}_m$$

where  $g$  is the plastic potential surface,

$f^i$  is the bounding surface,

$H_R$  is a positive constant,

$K_R$  is also a positive constant,

$n$  is the normal unit to the plastic potential and

$\dot{\sigma}_m = \dot{\sigma} \cdot m$  is the stress rate tensor projected onto the normal  $m$  to the bounding surface.

The rate of volumetric plastic change can be deduced from (VIII.4.1), to be:

$$(VIII.4.2) \quad tr \dot{\epsilon}^p = \dot{\lambda} \ tr \frac{\partial g}{\partial \sigma} = \dot{\lambda} \ tr n$$

which relates to the rate of change of plastic void ratio by:

$$(VIII.4.3) \quad \dot{\epsilon}^p = (1 + e) tr \dot{\epsilon}^p$$

Since  $f$  is iteration by iteration independent of  $\dot{\epsilon}$  for active loading, the consistency conditions provides,

$$(VIII.4.4) \quad \frac{\partial f}{\partial \sigma} \dot{\sigma} + \frac{\partial f}{\partial e^p} \dot{\epsilon}^p = 0$$

Substituting (VIII.4.2) into (VIII.4.3) and if the resulting equation is introduced into (VIII.4.4),  $H_R$  can be evaluated, that is,

$$(VIII.4.5) \quad H_R = -\frac{\partial f}{\partial e^p} (1 + e) \frac{\partial g}{\partial \sigma}$$

To relate  $H_R$  and  $K_R$  the definition of  $n$  and  $m$  will be considered.

$$(VIII.4.6) \quad n = \frac{\dot{\epsilon}^p}{\left[ (\dot{\epsilon}^p)^T \dot{\epsilon}^p \right]^{\frac{1}{2}}} \quad \text{and} \quad m = \frac{\partial f / \partial \sigma}{\left[ \left( \frac{\partial f}{\partial \sigma} \right)^T \frac{\partial f}{\partial \sigma} \right]^{\frac{1}{2}}}$$

By using (VIII.4.1) and the previous definition of the normal to the plastic potential and the normal to the bounding surface, respectively the required relation is achieved as,

$$(VIII.4.7) \quad K_R = \frac{H_R}{\left[ \left( \frac{\partial g}{\partial \sigma} \right)^T \frac{\partial g}{\partial \sigma} \right]^{\frac{1}{2}} \left[ \left( \frac{\partial f}{\partial \sigma} \right)^T \frac{\partial f}{\partial \sigma} \right]^{\frac{1}{2}}}$$

For an associative flow rule  $H_R$  becomes

$$(VIII.4.8) \quad H_R = -\frac{\partial f}{\partial e^p} (1 + e) \frac{\partial f}{\partial \sigma}$$

and

$$(VIII.4.9) \quad K_R = \frac{H_R}{\left( \frac{\partial f}{\partial \sigma} \right)^T \frac{\partial f}{\partial \sigma}}$$

### 1.3 Viscoplastic behaviour under the bounding surface $f$ .

It will be assumed that the viscoplastic strain rate on the yield surface (consequently under the bounding surface) is obtained by interpolating the hardening parameter from the point on the yield surface to the conjugate point obtained on the bounding surface by an convenient interpolation rule.

Because the shape of the yield surface and the bounding surface are not in general similar then the interpolation rule as proposed by Mroz et al (1978a) for the elasto-plastic kinematic model can not be used by itself, but a different option will be adopted here.

The rule for elasto-viscoplastic kinematic (three surfaces model) will be divided into two rules. An interpolation rule for the quasi-static plastic strain rate and another for the viscous strain rate. The quasi-static plastic strain rate will be calculated in the same way as

the elasto-plastic kinematic (two surfaces model), whilst for the viscous strain rate another rule will be given subsequently.

### 1.3.1 Quasi-static plastic strain rate interpolation rule.

The rule for translation, expansion or contraction of the yield and bounding surfaces for quasi-static stress rates is the same as that for the two surfaces model by Mroz et al (1978a). In this case the two surfaces are  $f^0$  and  $f^1$  of similar shape. According to Mroz (1978a) it will then be assumed that the surfaces  $f^0$  and  $f^1$  do not intercept but engage each other along a common normal. This assumption can be expressed mathematically by associating each point P on the yield surface  $f^0$  with the conjugate point  $R^1$  on the bounding surface  $f^1$  characterized by the same direction of exterior normal. (Figure VIII.5). Denoting the stresses at P and  $R^1$  by  $\sigma^P$  and  $\sigma^{R^1}$  and the stresses at a point which divides the line  $\overline{OA}$  and  $\overline{O'A'}$  in the same proportion as  $\alpha^P$  and  $\alpha^{R^1}$ , one has,

$$(VIII.4.10) \quad \frac{\sigma^P - \alpha^P}{a^0} = \frac{\sigma^{R^1} - \alpha^{R^1}}{a^1}$$

by similarity.

$a^1$  and  $a^0$  are respectively the middle point of the segment of stress  $\overline{OA}$  and  $\overline{O'A'}$

The equation (VIII.4.10) may be transformed to give

$$(VIII.4.11) \quad \sigma^{R^1} = \alpha^{R^1} + \frac{a^1}{a^0}(\sigma^P - \alpha^P) \quad \text{and} \quad \sigma^P = \alpha^P + \frac{a^0}{a^1}(\sigma^{R^1} - \alpha^{R^1})$$

Considering again that according to Mroz (1978a), the relative motion of "P" with respect to  $R^1$  to be directed along  $\beta = \overline{PR}$  ,

$$(VIII.4.12) \quad \beta = \sigma^{R^1} - \sigma^P = \frac{1}{a^0} [a^0 \alpha^{R^1} - a^1 \alpha^P + \sigma^P (a^1 - a^0)]$$

can be written.

By taking the time derivative of (VIII.4.11) and substituting (VIII.4.10) into the left equation from (VIII.1.1), one can write.

$$(VIII.4.13) \quad \beta \dot{\mu} = \dot{\sigma}^{R^1} - \dot{\sigma}^P = \dot{\alpha}^{R^1} + (\sigma^P - \alpha^P) \left( \frac{\dot{a}^1 - \dot{a}^0}{a^0} \right) - \dot{\alpha}^P$$

and

$$(VIII.4.14) \quad \dot{\alpha}^P = \beta \dot{\mu} + \dot{\alpha}^{R^1} + \frac{\dot{a}^1 - \dot{a}^0}{a^0} (\sigma^P - \alpha^P)$$

Now, assuming that the yield surface and the bounding surface are similar, the scalar  $\mu$  can be evaluated from the consistency conditions, that is,

$$(VIII.4.15) \quad \left( \frac{\partial f^0}{\partial \sigma} \right)^T \dot{\sigma} + \left( \frac{\partial f^0}{\partial \alpha^P} \right)^T \dot{\alpha}^P + \frac{\partial f^0}{\partial a^0} \dot{a}^0 = 0$$

By making use of equation (VIII.4.14) one finds:

$$(VIII.4.16) \quad \dot{\mu} = \frac{\left(\frac{\partial f^0}{\partial \sigma}\right)^T \dot{\sigma} + \frac{\partial f^0}{\partial \sigma} \dot{a}^0 - \left(\frac{\partial f^0}{\partial \sigma}\right)^T \left[ \dot{\alpha}^{R^1} + (\sigma^P - \alpha^P) \frac{\dot{a}^1 - \dot{a}^0}{a^0} \right]}{\left(\frac{\partial f^0}{\partial \sigma}\right)^T \beta}$$

where,

$$(VIII.4.17) \quad a^1 = a_i^1 \exp\left(\frac{e}{\lambda - k}\right), \quad \frac{a^0}{a^1} = I = \text{constant}$$

and

$$\dot{a}^1 = \frac{a_i^1}{\lambda - k} \dot{e}^P = \dot{\lambda}^1 \frac{a_i^1}{\lambda - k} \text{tr} \frac{\partial g}{\partial \sigma} = \dot{\chi}^1 \frac{a_i^1}{\lambda - k} \text{tr} n$$

$$(VIII.4.18) \quad \dot{a}^0 = \frac{a^0}{a^1} \dot{a}^1 = I \dot{a}^1$$

### 1.3.2 Viscous strain rate interception rule

To include the stress rate intensity influence it is now postulated that during the time period of application of the stress increment, the stress point P moves towards the stress point  $R^1$  on the quasi-static bounding surface  $f^1$  while the stress point  $R^1$  moves in a radial path, towards the stress point R on the viscoplastic bounding surface  $f$ . The stress rate intensity is approximately known at each iteration as the iteration by iteration stress computation progresses.

That is while P moves towards  $R^1$ , and defines  $R^1$  on the quasi-static bounding surface,  $R^1$  moves radially towards R during the stress increment, iteratively as the stress iteration progresses during the evaluation of the strain increment.

In mathematical form, the successive positions of the stress point

$\sigma^R$  is achieved by the interpolation of the radial line

$$(VIII.4.19) \quad \bar{\sigma} = \frac{\sqrt{3}}{3} \eta \sigma_m$$

with the successive shape of the rate-dependent surfaces

$$(VIII.4.20) \quad f(\sigma, \epsilon^p, \dot{\sigma}) = 0 \quad , \text{ for constant } \theta$$

which is defined at the stress point  $\sigma^{R'}$  .

$\eta = \sqrt{3} \frac{\bar{\sigma}}{\sigma_m}$  , defined at the conjugate stress point  $\sigma^{R'}$  and  $\bar{\sigma}$  is the second stress invariant, whilst  $\sigma_m$  is the first stress invariant.

### 1.3.3 Rule for the variation of $H_R$ .

To complete the model description it is necessary to specify the rule for the variation of  $H_R$  during the plastic deformation. Let it be assumed that  $H_R$  varies continuously from its value  $H_{p0}$  on the yield surface to the value of  $H_R$  , on the viscoplastic yield surface.  $H_R$  is computed by using equation (VIII.4.7) or (VIII.4.9) according to whether non-associative or associative rules are used.

The interpolation rule is similar to that suggested by Mroz et al (1978a), but  $H_R$  and  $\delta$  are now stress rate functions. Thus,

$$(VIII.4.21) \quad H_p = H_R + H_{p0} \left( \frac{\delta}{\delta_0} \right)^{\gamma+1}$$



$H_R$  is calculated iteratively according to the movement of the stress point  $\sigma^R$  which is governed by the stress rate intensity  $\dot{\sigma}^R$  and the plastic deformation  $\dot{\epsilon}^P$ . Also,  $\delta$  is calculated by adding the value  $\delta_v$  defined by the distance between the stress point  $\sigma^{R'}$  and  $\sigma^R$ , to the quasi-static  $\delta_{qs}$ ,  $\sigma^R$  being a function of the stress rate intensity  $\dot{\sigma}^R$ . (See Figure VIII.5). That is,  $\delta$  is equal to the distance  $\overline{PR}$ .  $\delta_0$  is the maximum value of the distances between the yield and the bounding surfaces for the quasi-static surfaces. That is,  $\delta_0$  is the maximum value of  $\delta_{qs}$ .

## 2. Elasto-Viscoplastic Kinematic- Vanishing elastic region

As the elastic behaviour in item 1.1 and the viscoplastic behaviour on the bounding surface  $f$  are as in item 1.2, the only pertinent aspect left to discuss is the viscoplastic behaviour under the bounding surface  $f$ .

### 2.1 Viscoplastic behaviour under the bounding surface $f$ .

The incremental relations derived for the viscoplastic behaviour under the bounding surface  $f$  in the previous section, describing the three-surfaces model, can be particularized for the case when  $a^0 = 0$ , that is, the elastic domain shrinks to a point. See Figure VIII.6. This hypothesis is convenient from the computational point of view as there is no need to make a distinction between elastic and viscoplastic domains nor is there the need to trace the variation in the size of the yield surface.

Two different interpolation rules for viscoelastic strain rate will be considered:

2.1.1 When the plastic potential bounding surface is  $\theta$ -independent

The plastic potential bounding surface is the plastic potential corresponding to the yield bounding surface which is the only bounding surface which has been used up till now.

In this case, it is assumed that for any increment  $d\sigma$ , the vector normal to the plastic potential bounding surface, coinciding with the direction of the viscoplastic strain increment, is parallel to the normal  $n_R$  at the conjugate point  $R$  at the intersection of the stress increment vector with the plastic potential bounding surface, see Figure VIII.6. Note that no restriction is imposed on the bounding yield surface which consequently may have any desired shape, and can be a function of  $\theta$  or not as required.

Obviously in the case where an associative flow rule is used the bounding yield surface must coincide with the plastic potential.

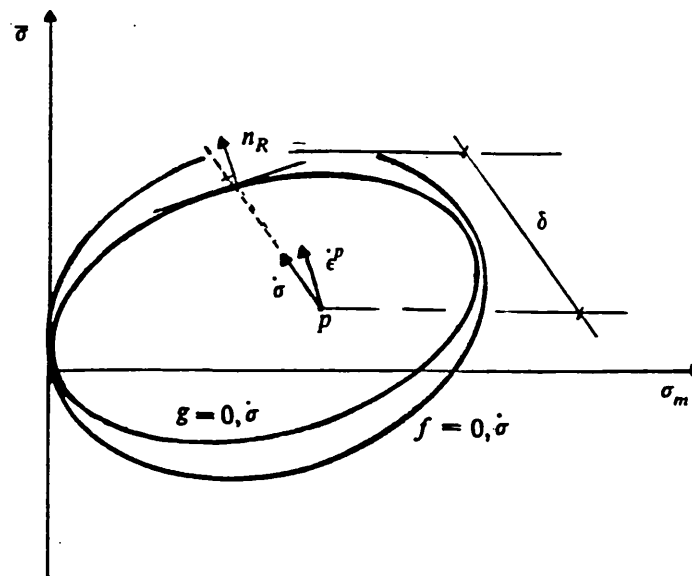


Figure VIII.6

When the plastic potential bounding surface is  $\theta$  independent the calculation is simpler, therefore it is easier to use a non-associative flow rule, that is to say:

$$(VIII.4.22) \quad \dot{\epsilon}^P = \frac{1}{K_p} n_R \dot{\sigma}_m = \dot{\chi}^1 n_R \quad \dot{\chi}^1 \geq 0$$

where  $n_R$  is the normal to the plastic potential bounding surface and  $\dot{\sigma}_m$  is the stress rate component in the direction normal to the yield bounding surface.  $\dot{\sigma}_m = \dot{\sigma} \cdot m$ ,  $n_R$  and  $m$  are defined by equation (VIII.4.6).

Therefore, as the yield surface reduces to a stress point  $\sigma^P$ , its centre reduces to  $\sigma^P$ , or in a rate form.

$$(VIII.4.23) \quad \dot{\alpha}^P = \dot{\sigma}^P$$

For the interpolation rule it is necessary to compute  $\delta$  as seen in Figure VIII.6. It must be clear that  $g$  is the viscoplastic bounding plastic potential and, consequently, only one interpolation rule is necessary now.

For each iteration  $\delta$  can be calculated as:

$$(VIII.4.25) \quad \delta = \left[ \frac{3}{M^2} (\bar{\sigma}^R - \bar{\sigma}^P)^2 + (\sigma_m^R - \sigma_m^P)^2 \right]^{\frac{1}{2}}$$

where:

$\bar{\sigma}^P$  and  $\sigma_m^P$  are the second and first invariants of stress at P, and  $\bar{\sigma}^R$  and  $\sigma_m^R$  are the second and first invariants at R. Because of the simplice shape assumed for the bounding plastic potential, explicit expressions for  $\bar{\sigma}^R$  and  $\sigma_m^R$  can be achieved. That is,  $\bar{\sigma}^R$  and  $\sigma_m^R$  are evaluated by the interception of the equation of the bounding plastic potential (to be defined as stress rate function) with the straight line

$$\bar{\sigma}^R = \bar{\sigma}^P + \frac{1}{\tan \beta} (\sigma_m^R - \sigma_m^P) \quad \text{where} \quad \tan \beta = \frac{d \sigma_m}{d \bar{\sigma}}$$

2.1.2 When the plastic potential bounding surface are  $\theta$ -dependent.

If it is assumed, as in the previous section, that the strain rate direction is defined by the normal to the bounding plastic potential at the stress point of interception between the stress increment direction and the bounding plastic potential, the calculation

procedure is as in the previous section. However in this case additional difficulties may be introduced because, in the general case it is not possible to find an explicit expression for the invariants  $\bar{\sigma}^R$  and  $\sigma_m^R$  at  $R$ .

To make the calculation procedure less expensive it will be assumed that the stress point  $R$  will be obtained at the interception between the bounding plastic potential and the projection of the stress rate direction in the  $\theta$  constant plane.

where, 
$$\theta = \theta^P + d\theta$$

$$(VIII.4.26) \quad d\theta = \tan 3\theta^P \left( \frac{dJ_3}{3J_3^P} - \frac{d\bar{\sigma}}{\bar{\sigma}^P} \right)$$

and  $\theta^P$  is the value of  $\theta$  before applying to the stress increment.

In this case the position of the stress point  $R$  can be determined explicitly for any surface function on  $\theta$ .

Once  $\bar{\sigma}^R$  and  $\sigma_m^R$  are evaluated, the calculation procedure reduces to that used in the previous section.

The stress point  $R$  will be defined by the interception of the bounding plastic potential (to be defined as stress rate function) with the straight line

$$(VIII.4.27) \quad \bar{\sigma}^R = \tan \gamma (\sigma_m^R - \sigma_m^P) + \bar{\sigma}^P \cos d\theta \quad , \text{ for the plane } \theta$$

where 
$$\tan \gamma = \frac{[(\bar{\sigma}^P \sin d\theta)^2 + (d\bar{\sigma})^2] - 2\bar{\sigma}^P \cos d\theta}{d\sigma_m}, \quad d\bar{\sigma} = \frac{\partial \bar{\sigma}}{\partial \sigma} \dot{\sigma},$$

$$d\theta = \frac{\partial \theta}{\partial \bar{\sigma}} \frac{\partial \bar{\sigma}}{\partial \sigma} \dot{\sigma} + \frac{\partial \theta}{\partial J_3} \frac{\partial J_3}{\partial \sigma} \dot{\sigma}$$

and  $\frac{\partial \theta}{\partial \bar{\sigma}}, \frac{\partial \theta}{\partial J_3}, \frac{\partial \bar{\sigma}}{\partial \sigma}, \frac{\partial J_3}{\partial \sigma}$  will be defined later.

### 3. Elasto-Viscoplastic-Plastic Model

This model, as described previously, assumes the existence of a yield surface  $f^1$  and a viscoplastic surface  $f^2$ , as seen in Figure VIII.3b.

$f^1$  is usually defined at a very high stress rate, and it is considered as time independent.  $f^2$  is usually obtained for a very low stress rate. In practice, however  $f^1$  and  $f^2$  are not in general similar.

Although this approach is inferior to the previous one, the application in Finite Element practice is straight forward.

In general the strain rate tensor is divided into three distinct components: Elastic, viscoplastic and plastic. The elastic component is defined by the Hooke's law and the plastic strain component as in the plasticity theory. As this model is more or less a mathematical fiction, the associative flow rule will be assumed. The only strain component left to be discussed is the viscoplastic strain.

#### 3.1 Viscoplastic strain rate.

The viscoplastic strain rate is defined by means of a flow rule (creep

law) similar to that for inviscid strain rate (high strain rate).

Thus, the creep law is defined by:

$$(VIII.4.28) \quad \dot{\epsilon}^{vp} = \Lambda(t) \langle \Phi(F) \rangle \frac{\partial f^2 / \partial \sigma}{\left[ \left( \frac{\partial f^2}{\partial \sigma} \right)^T \frac{\partial f^2}{\partial \sigma} \right]^{1/2}} = \lambda_2 \frac{\partial f^2}{\partial \sigma}, \quad F = f^2 / f_R^2$$

where

$$\lambda_2 = \frac{\Lambda(t) \langle \Phi(F) \rangle}{\left[ \left( \frac{\partial f^2}{\partial \sigma} \right)^T \frac{\partial f^2}{\partial \sigma} \right]^{1/2}}$$

$\Lambda(t)$  is the viscosity and assumed to be a time function only,  $\langle \Phi(F) \rangle$  means that  $\langle \Phi(F) \rangle = \Phi(F)$  for  $\Phi(F) \geq 0$  and  $\langle \Phi(F) \rangle = 0$  for  $\Phi(F) < 0$ . The reference parameter  $f_R^2$  may be chosen arbitrarily and is introduced only to make the argument of the scalar function  $\Phi$  non-dimensional.

#### 4. Constitutive Law in Stiffness Form

##### 4.1 Elasto-viscoplastic kinematic model.

Consider that  $f^0 \geq 0$ ,  $f^1 \geq 0$  and  $f = 0$ , that is, the yield and quasi-static bounding surfaces are in contact, and consequently the material is in an elasto-viscoplastic state. In this case:

$$(VIII.4.29) \quad \dot{\epsilon} = \dot{\epsilon}^e + \dot{\epsilon}^{vp}$$

By making use of (VIII.4.1), (VIII.4.2) and the consistency conditions the elasto-viscoplastic stiffness and flexibility matrices can be expressed as

$$(VIII.4.30) \quad D^{ep} = D - \frac{D \frac{\partial g}{\partial \sigma} \left( \frac{\partial f}{\partial \sigma} \right)^T D^T}{\left( \frac{\partial f}{\partial \sigma} \right)^T D \frac{\partial g}{\partial \sigma} - \left( \frac{\partial f}{\partial \rho} \right)^T \frac{\partial g}{\partial \sigma}}$$

$$(VIII.4.31) \quad C^{ep} = C - \frac{\frac{\partial g}{\partial \sigma} \left( \frac{\partial f}{\partial \sigma} \right)^T}{\left( \frac{\partial f}{\partial \rho} \right)^T \frac{\partial g}{\partial \sigma}}$$

where C and D are respectively the flexibility and stiffness matrices of elastic constants, and,

$$(VIII.4.32) \quad \left( \frac{\partial f}{\partial \rho} \right)^T \frac{\partial g}{\partial \sigma} = -H_R = - \left\{ \left[ \left( \frac{\partial f}{\partial \sigma} \right)^T \frac{\partial f}{\partial \sigma} \right] \left[ \left( \frac{\partial g}{\partial \sigma} \right)^T \frac{\partial g}{\partial \sigma} \right] \right\}^{\frac{1}{2}} K_R$$

$H_R$  is given by equation (VIII.4.6) and  $K_R$  is given by equation (VIII.4.8).

For an associative flow rule  $g$  and  $f$  are identical surfaces.

Note that the relations (VIII.4.30), (VIII.4.31) and (VIII.4.32) are similar to those for an elasto-plastic material, however, the gradient  $\frac{\partial g}{\partial \sigma}$ ,  $\frac{\partial f}{\partial \sigma}$  are now rate dependents.

#### 4.2 Elastic-viscoplastic-plastic.

Consider that  $f^1 > 0$  and  $f^2 = 0$ , that is, the material is an elastic-viscoplastic-plastic state. In this case:

$$(VIII.4.33) \quad \dot{\epsilon} = \dot{\epsilon}^e + \dot{\epsilon}^{vp} + \dot{\epsilon}^p$$



By making use of equations (VIII.4.1), (VIII.4.2), (VIII.4.28) and the consistency conditions the formal inversion of (VIII.4.33) can be achieved as:

$$(VIII.4.34) \quad \dot{\sigma} = D^{ep} [\dot{\epsilon} - h(\sigma, t)]$$

$h(\sigma, t)$  is the creep law vector as given by equation (VIII.4.28).

$$(VIII.4.35) \quad D^{ep} = D - \frac{D \frac{\partial f}{\partial \sigma} (\frac{\partial f}{\partial \sigma})^T D^T}{(\frac{\partial f}{\partial \sigma})^T D \frac{\partial f}{\partial \sigma} - (\frac{\partial f}{\partial \epsilon})^T \frac{\partial f}{\partial \sigma}}$$

$(\frac{\partial f}{\partial \epsilon})^T \frac{\partial f}{\partial \sigma}$  is given by (VIII.4.32) where  $g$  is replaced by  $f$ .

The special cases of elasticity, elasto-viscoplasticity and elasto-plasticity can be readily obtained from (VIII.4.34).

## 5. Yield and potential surfaces form

### 5.1 General shape for $f^s$ .

According to the review presented in section VIII.2 the yield surface and the plastic potential can in general assume almost any shape. The adoption of one of the shapes make the application of the model restricted to a particular soil type and physical conditions. To avoid this inconvenience a general equation is assumed which can be calibrated to most circumstances for which the other models are proposed for.

-On the  $J_2/J_1$  plane;

Before extending the model to the general state of stress the triaxial conditions will be analyzed, that is, when two principal effective stresses and strain are regarded as negative, the stress and strain states can be defined as:

$$p = -\frac{1}{3}(\sigma_1 + 2\sigma_2) \quad q = \sigma_2 - \sigma_1$$

(VIII.4.36)

$$\epsilon_v = -(\epsilon_1 + 2\epsilon_2) \quad \epsilon_q = \frac{2}{3}(\epsilon_2 - \epsilon_1)$$

The shape of the yield surface, plastic potential, boundary (or consolidation) surface, and nesting surfaces will be based on the general equation:

$$f^s = A p^2 + 2B pq + C q^2 + 2D p + 2E q + F = \varnothing \quad s = 1, 2, 3, ..$$

The parameters A, B, C, D, E and F will be determined from the following conditions:

1)  $p = \varnothing, \quad q = \varnothing$

2)  $p = 2a, \quad q = \varnothing, \quad dp/dq = -\overline{S}_a$

3)  $p = b, \quad q = b n_b$

4)  $p = c, \quad q = c n_c, \quad dq/dp = \overline{S}_c$

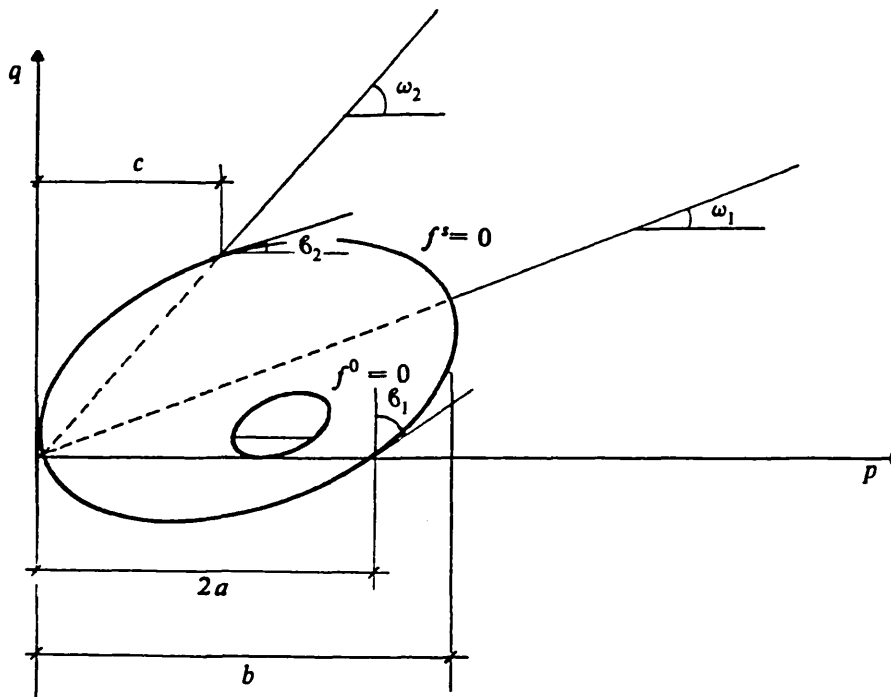


Figure VIII.7

These conditions imply the following from the upper portion of the surface ( $q > 0$ )

$$\begin{aligned}
 f^s = & \left\{ n_c + \bar{S}_c \left[ 1 - 2\bar{\xi}_2 + 2\frac{n_c}{n_b}(2\bar{\xi}_2 - 1) \right] \right\} p^2 + \\
 & 2 \left[ \bar{\xi}_2 - 1 - \frac{n_c \bar{S}_c}{n_b^2} (2\bar{\xi}_1 - 1 - 2\bar{\xi}_1 \bar{S}_a n_b + \bar{\xi}_2 \frac{n_b^2}{n_c} \bar{S}_a) \right] pq \\
 \text{(VIII.4.37)} \quad & + \frac{1}{n_b^2} \left\{ (1 - 2\bar{\xi}_1) \left[ \bar{S}_c (2\bar{\xi}_2 - 1) - n_c + 2n_b(1 - \bar{\xi}_2) \right] + 2\bar{S}_a n_b \left[ \bar{S}_c (\bar{\xi}_2 - \bar{\xi}_1) - \bar{\xi}_1 n_c \right] \right\} q^2 \\
 & - 2 \left\{ n_c + \bar{S}_c \left[ 1 - 2\bar{\xi}_2 + 2\frac{n_c}{n_b}(2\bar{\xi}_1 - 1) \right] \right\} ap \\
 & + 2 \left[ \bar{S}_c (\bar{S}_a - 2\frac{n_c}{n_b} \bar{S}_a - 2\frac{n_c}{n_b^2} + 4\bar{\xi}_1 \frac{n_c}{n_b^2}) + \bar{S}_a n_c + 2(1 - \bar{\xi}_2) \right] aq \quad q > 0
 \end{aligned}$$

where

$$\bar{\xi}_1 = \frac{a}{b}, \quad \bar{\xi}_2 = \frac{a}{c}, \quad n_b = \tan \omega_1, \quad n_c = \tan \omega_2, \quad \bar{S}_a = \tan \delta_1, \quad \bar{S}_c = \tan \delta_2$$

For  $q < 0$ ,  $q$  can be substituted by  $-q$  in the equation (VIII.4.37) and a proper value for  $\bar{\xi}_1, \bar{\xi}_2, \bar{S}_a, \bar{S}_c, n_b, n_c$  has to be chosen. An example will be given elsewhere.

In order to examine general kinematic types of models, an equation similar to (VIII.4.37) but with different dimensions will be required. The similarity of surfaces  $f^s$  and  $f^0$  can be represented mathematically by  $\bar{\xi}_0 = \frac{a^0}{d^0} = \frac{a}{d}, \bar{\xi}_1 = \frac{a}{b} = \frac{a^0}{b^0}, \bar{\xi}_2 = \frac{a}{c} = \frac{a^0}{c^0}$  and if the coordinate of point P are represented by  $\alpha_p, \alpha_q$  the equation for  $f^0$  is readily obtained; by changing  $p$  to  $p - \alpha_p + \frac{a^0}{\bar{\xi}_0}$  and  $q$  to  $q - \alpha_q$  in (VIII.4.37), that is:

$$f^0 = \bar{A}(p - \alpha_p)^2 + \bar{B}(p - \alpha_p)(q - \alpha_q) + \bar{C}(q - \alpha_q)^2 +$$

$$(VIII.4.38) \quad \frac{a^0}{\bar{\xi}_0}(2\bar{A} - \bar{D}\bar{\xi}_0)(p - \alpha_p) + \frac{a^0}{\bar{\xi}_0}(\bar{B} + \bar{E}\bar{\xi}_0)(q - \alpha_q)$$

$$+ \frac{a^{02}}{\bar{\xi}_0^2}(\bar{A} - \bar{D}\bar{\xi}_0) = 0$$

-In the general stress space.

To represent the surfaces  $f^s$  and  $f^0$  for a general state of stress, the stress invariant of the "translated" stress will be introduced in agreement with Pietruszczak and Mroz (1979), as follows

$$J_m = \frac{1}{3}(\sigma_{ii} - \alpha_{ii}) \quad \bar{\sigma} = \left[ \frac{1}{2}(\bar{\sigma}_{ij} - \bar{\alpha}_{ij})(\bar{\sigma}_{ij} - \bar{\alpha}_{ij}) \right]^{\frac{1}{2}}$$

$$(VIII.4.39)$$

$$J_3 = \frac{1}{3}(\bar{\sigma}_{ij} - \bar{\alpha}_{ij})(\bar{\sigma}_{ki} - \bar{\alpha}_{ki})(\bar{\sigma}_{kj} - \bar{\alpha}_{kj})$$

$\bar{\sigma}_{ij}$  is the deviator stress and  $\alpha_{ii}, \bar{\alpha}_{ij}$  denote the spherical and

deviatoric components of the translation tensor  $\alpha_{ij}$  of the  $f^0$  type of surface. The definition of the deviator stress and the Lode angle remained unchanged and were given by equations (IV.10.2.22) and (IV.10.2.25), respectively. Also the relationships between the invariants defined by the equations (IV.10.2.23) and (IV.10.2.24) still hold.

For the "triaxial" stress state, i.e.,  $\sigma_2 = \sigma_3$ , the following relations are applied:

$$p - \alpha_p = -J_m = -\sigma_m + \frac{1}{3}\alpha \quad q - \alpha_q = \sqrt{3}\bar{\sigma}_+$$

where  $\sigma_m = \frac{1}{3}\sigma_{ii}$ ,  $\alpha = \alpha_{ii}$  and  $\bar{\sigma}_+$  denote the value of  $\bar{\sigma}$  for  $\sigma_2 = \sigma_3$ ,  $\theta = \pi/6$ .

Thus, the expression for  $f^0$  can be rewritten as follows:

$$f^0 = \bar{A}(\sigma_m - \frac{1}{3}\alpha)^2 - \sqrt{3}\bar{B}(\sigma_m - \frac{1}{3}\alpha)\bar{\sigma}_+ + 3\bar{C}\bar{\sigma}_+^2$$

$$(VIII.4.40) \quad -\frac{a^0}{\bar{\xi}_0}(2\bar{A} - \bar{D}\bar{\xi}_0)(\sigma_m - \frac{1}{3}\alpha) + \sqrt{3}\frac{a^0}{\bar{\xi}_0}(\bar{B} + \bar{E}\bar{\xi}_0)\bar{\sigma}_+$$

$$+\left(\frac{a^0}{\bar{\xi}_0}\right)^2(\bar{A} - \bar{D}\bar{\xi}_0) = 0$$

Assuming that the yield curve in the  $\pi$ -plane can be expressed as

$$(VIII.4.41) \quad \bar{\sigma} = \bar{\sigma}_+ g_5 \quad \bar{\sigma}_+ = \bar{\sigma}/g_5$$

where

$$(VIII.4.42) \quad g_i = \frac{k_{i1}}{\left[ k_{i2} + k_{i3} \sin(k_{i4} + 3\theta) \right]^{k_{i5}}}, \quad g_i(\pi/6) = 1$$

and  $k_{i1}, k_{i2}, k_{i3}, k_{i4}, k_{i5}$ , are constants and  $i$  can assume the values  $0, 1, 2, 3, 4$ , or  $5$ . Similar expressions were proposed by Eeklen (1980), Argyris (1973), Gudehus (1973) and Zienkiewicz and Pande (1975).

If now the equation (VIII.4.41) is introduced into equation (VIII.4.40) it results in,

$$f^0 = A(\sigma_m - \frac{1}{3}\alpha)^2 - \sqrt{3}B(\sigma_m - \frac{1}{3}\alpha)\frac{\bar{\sigma}}{g_5} + 3C\frac{\bar{\sigma}^2}{g_5^2} - \frac{a^0}{\xi_0}(2A - D\xi_0g_0)$$

(VIII.4.43)

$$(\sigma_m - \frac{1}{3}\alpha) + \sqrt{3}\frac{a^0}{\xi_0}(B + E\xi)\frac{\bar{\sigma}}{g_5} + \left(\frac{a^0}{\xi_0}\right)^2(A - D\xi_0) = 0$$

Now considering that  $\xi_0, \xi_1, \xi_2, S_a, S_c$  for values of  $\theta$  different from  $\pi/6$  can be expressed as functions of  $\bar{\xi}_0, \bar{\xi}_1, \bar{\xi}_2, \bar{S}_a, \bar{S}_c$  defined at  $\theta = \pi/6$ , that is,

$$\xi_0 = \bar{\xi}_0 g_0 \quad \xi_1 = \bar{\xi}_1 g_1 \quad \xi_2 = \bar{\xi}_2 g_2$$

(VIII.4.44)

$$S_c = \bar{S}_c g_3 \quad \bar{S}_c \neq 0 \quad S_c = g_3, \quad \bar{S}_c = 0$$

$$S_a = \bar{S}_a g_4 \quad \bar{S}_a \neq 0 \quad S_a = g_4, \quad \bar{S}_a = 0$$

where  $g_i$  has been given by (VIII.4.42); expressions for  $f^0$  and  $A, B, C, D, E$  as a function of  $\theta$  can then be obtained as:

$$f^0 = A(\sigma_m - \frac{1}{3}\alpha)^2 - \sqrt{3}B(\sigma_m - \frac{1}{3}\alpha)\frac{\bar{\sigma}}{g_5} + 3C\frac{\bar{\sigma}^2}{g_5^2} - \frac{a^0}{\bar{\xi}_0 g_0}(2A - D\bar{\xi}_0 g_0)$$

(VIII.4.45)

$$(\sigma_m - \frac{1}{3}\alpha) + \sqrt{3}\frac{a^0}{\bar{\xi}_0 g_0}(B + E\bar{\xi}_0 g_0)\frac{\bar{\sigma}}{g_5} + \left(\frac{a^0}{\bar{\xi}_0 g_0}\right)^2(A - D\bar{\xi}_0 g_0) = 0$$

where

$$A = n_c + \bar{S}_c g_3 \left[ 1 - \frac{2n_c}{n_b} + 2\bar{\xi}_2 g_2 \left( \frac{2n_c}{n_b} - 1 \right) \right]$$

$$B = 2\{\bar{\xi}_2 g_2 - 1 - \frac{n_c}{n_b^2} \bar{S}_c g_3 [2\bar{\xi}_1 g_1 - 1 + 2\bar{\xi}_1 \bar{S}_a n_b g_1 g_4 + \frac{n_b^2}{n_c} \bar{\xi}_2 \bar{S}_a g_2 g_4]\}$$

$$C = \frac{1}{n_b^2} \left\{ (1 - 2\bar{\xi}_1 g_1) [\bar{S}_c g_3 (2\bar{\xi}_2 g_2 - 1) - n_c + 2n_b (1 - \bar{\xi}_2 g_2)] \right. \\ \left. + 2\bar{S}_a n_b g_4 [\bar{S}_c g_3 (\bar{\xi}_2 g_2 - \bar{\xi}_1 g_1) - \bar{\xi}_1 g_1 n_c] \right\}$$

(VIII.4.46)

$$D = 2\left\{ n_c + \bar{S}_c g_3 \left[ 1 - 2\bar{\xi}_2 g_2 + \frac{2n_c}{n_b} (2\bar{\xi}_1 g_1 - 1) \right] \right\}$$

$$E = 2\left\{ \bar{S}_c g_3 \left[ \bar{S}_a g_4 - 2\frac{n_c}{n_b} \bar{S}_a g_4 - 2\frac{n_c}{n_b^2} + 4\bar{\xi}_1 g_1 \frac{n_c}{n_b^2} \right] + \bar{S}_a n_c g_4 + 2(1 - \bar{\xi}_2 g_2) \right\}$$

In addition  $\bar{\xi}_0$ ,  $\bar{\xi}_1$ ,  $\bar{\xi}_2$ ,  $\bar{S}_a$ ,  $\bar{S}_c$  can also be functions of strain rate (or stress rate), stipulated by any empirical law.

Equation (VIII.4.45) is geometrically represented by a surface with, in general, variable cross-sectional shapes in each  $\pi$ -plane. More specific surfaces can be obtained by fixing the various constants for the specific physical problem under consideration.

The gradient tensor of this surface is given by:

$$(VIII.4.47) \quad \frac{\partial f^0}{\partial \sigma} = C_1 \frac{\partial \sigma_m}{\partial \sigma} + \left( C_2 + \frac{3\sqrt{3}J_3}{2\sigma^4 \cos 3\theta} C_3 \right) \left( \frac{\partial \bar{\sigma}}{\partial \sigma} \right) + \left( -C_3 \frac{\sqrt{3}}{2\sigma^3 \cos 3\theta} \right) \left( \frac{\partial \bar{J}_3}{\partial \sigma} \right)$$

where

$$C_1 = \frac{\partial f^0}{\partial \sigma_m}, \quad C_2 = \frac{\partial f^0}{\partial \bar{\sigma}}, \quad C_3 = \frac{\partial f^0}{\partial \theta}$$

Also, from (VIII.4.45)

$$\frac{\partial f^0}{\partial \bar{\sigma}} = 6C \frac{\bar{\sigma}}{g_3^2} - \frac{\sqrt{3}B}{g_5} \left( \sigma_m - \frac{1}{3}\alpha \right) + \frac{\sqrt{3}a^0}{\bar{\xi}_0 g_0 g_5} (B + E \bar{\xi}_0 g_0),$$

$$\frac{\partial f^0}{\partial \sigma_m} = 2A \left( \sigma_m - \frac{1}{3}\alpha \right) - \sqrt{3}B \frac{\bar{\sigma}}{g_5} - \frac{a^0}{\bar{\xi}_0 g_0} (2A - D \bar{\xi}_0 g_0),$$

$$\begin{aligned} \frac{\partial f^0}{\partial \theta} &= \frac{a^0}{\bar{\xi}_0^2 g_0^2 g_5} [2A \bar{\xi}_0 g_5 \left( \sigma_m - \frac{1}{3}\alpha \right) - \sqrt{3}B \bar{\xi}_0 \bar{\sigma} - D \bar{\xi}_0 a^0 - 2a^0 (A - D \bar{\xi}_0 g_0)] \frac{\partial g_0}{\partial \theta} \\ &+ \left\{ \frac{6\bar{\xi}_1}{n_b^2 g_3^2} [g_3 \bar{S}_c (1 - 2\bar{\xi}_2 g_2) + n_c + 2n_b (\bar{\xi}_2 g_2 - 1) + g_4 n_b n_c \bar{S}_a + g_3 g_4 n_b \bar{S}_a \bar{S}_c] \bar{\sigma}^2 \right. \\ &- 4\sqrt{3} \frac{n_c}{n_b^2} \frac{\bar{\xi}_1}{\bar{\xi}_1} \frac{g_3}{g_5} (1 + g_4 n_b \bar{S}_a) \left( \sigma_m - \frac{1}{3}\alpha \right) \bar{\sigma} + 4\sqrt{3} \frac{n_c}{n_b^2} \frac{\bar{\xi}_1}{\bar{\xi}_0 g_0} \frac{g_3}{g_5} (1 + g_4 n_b \bar{S}_a + 2\bar{\xi}_0 g_0 \bar{S}_c) a^0 \bar{\sigma} \\ &\left. + 8 \frac{n_c}{n_b} \frac{\bar{\xi}_1}{\bar{\xi}_1} a^0 \left( \sigma_m - \frac{1}{3}\alpha \right) - 8 \frac{n_c}{n_b} \frac{\bar{\xi}_1}{\bar{\xi}_0 g_0} a^0 \right\} \frac{\partial g_1}{\partial \theta} + \left\{ \frac{2\bar{\xi}_2}{n_b} g_3 \bar{S}_c (2n_c - n_b) \left( \sigma_m - \frac{1}{3}\alpha + \frac{a^0}{\bar{\xi}_0 g_0} \right)^2 \right. \\ &+ \frac{6\bar{\xi}_2}{n_b^2 g_3^2} [(1 - 2\bar{\xi}_1 g_1) (g_3 \bar{S}_c - 2n_b) + g_3 g_4 n_b \bar{S}_a \bar{S}_c] \bar{\sigma}^2 - 2\sqrt{3} \frac{\bar{\xi}_2}{g_5} (1 - g_3 g_4 \bar{S}_a \bar{S}_c) \left( \sigma_m - \frac{1}{3}\alpha \right) \bar{\sigma} \\ &\left. - 2\sqrt{3} \frac{\bar{\xi}_2}{\bar{\xi}_0 g_0 g_5} (2\bar{\xi}_0 g_0 - 1 + g_3 g_4 \bar{S}_a \bar{S}_c) a^0 \bar{\sigma} - \frac{2}{\bar{\xi}_0 g_0} (2\bar{\xi}_0 g_0 \bar{\xi}_2 g_3 \bar{S}_c + 1 - g_3 g_4 \bar{S}_a \bar{S}_c) a^0 \left( \sigma_m - \frac{1}{3}\alpha \right) + \frac{4\bar{\xi}_2 g_3 \bar{S}_c}{\bar{\xi}_0 g_0} a^0 \right\} \frac{\partial g_2}{\partial \theta} \\ &+ \left\{ \frac{2n_c - n_b}{n_b} \bar{S}_c (2\bar{\xi}_2 g_2 - 1) \left( \sigma_m - \frac{1}{3}\alpha + \frac{a^0}{\bar{\xi}_0 g_0} \right)^2 + \frac{3}{n_b^2 g_3^2} [(1 - 2\bar{\xi}_1 g_1) (2\bar{\xi}_2 g_2 - 1) \bar{S}_c + 2g_4 n_b \bar{S}_a \bar{S}_c (\bar{\xi}_2 g_2 - \bar{\xi}_1 g_1)] \bar{\sigma}^2 \right. \\ &+ 2\sqrt{3} \frac{\bar{S}_c}{g_5 n_b^2} [2\bar{\xi}_1 g_1 n_c - n_c + 2\bar{\xi}_1 g_1 g_4 n_b n_c \bar{S}_a + \bar{\xi}_2 g_2 g_4 n_b^2 \bar{S}_a] \left( \sigma_m - \frac{1}{3}\alpha \right) \bar{\sigma} + \frac{2\sqrt{3}}{g_5} \frac{\bar{S}_c}{\bar{\xi}_0 g_0 n_b^2} [\bar{\xi}_0 g_0 g_4 n_b^2 \bar{S}_a - 2\bar{\xi}_0 g_0 g_4 n_b n_c \bar{S}_a \\ &\left. - 2\bar{\xi}_0 g_0 n_c + 4\bar{\xi}_0 g_0 \bar{\xi}_1 g_1 n_c - 2\bar{\xi}_1 g_1 n_c + n_c - 2\bar{\xi}_1 g_1 g_4 n_b n_c \bar{S}_a - \bar{\xi}_2 g_2 g_4 n_b^2 \bar{S}_a] a^0 \bar{\sigma} \right\} \end{aligned}$$



$$\begin{aligned}
& + 2 \frac{\bar{S}_c}{n_b} \left[ (1 - 2\bar{\xi}_2 g_2) n_b + 2n_c (2\bar{\xi}_1 g_1 - 1) \right] a^0 \left( \sigma_m - \frac{1}{3} \alpha \right) - 2 \frac{\bar{S}_c}{n_b} a^0 \left[ (1 - 2\bar{\xi}_2 g_2) n_b + 2n_c (2\bar{\xi}_1 g_1 - 1) \right] \left. \right\} \frac{\partial g_3}{\partial \theta} \\
& + \left\{ \frac{6\bar{S}_a}{g_3^2 n_b} \left[ (\bar{\xi}_2 g_2 - \bar{\xi}_1 g_1) g_3 \bar{S}_c - \bar{\xi}_1 g_1 n_c \right] \bar{\sigma}^2 + \frac{4\sqrt{3} g_3}{n_b g_4} \bar{S}_a \bar{S}_c (\bar{\xi}_1 g_1 n_c + \bar{\xi}_2 g_2 n_b^2) \left( \sigma_m - \frac{1}{3} \alpha \right) \bar{\sigma} \right. \\
& \left. + \frac{2\sqrt{3} g_3}{n_b g_5} \frac{\bar{S}_a}{\bar{\xi}_0 g_0} \left[ \bar{\xi}_0 g_0 n_b \bar{S}_c + \bar{\xi}_0 g_0 n_b n_c - 2\bar{\xi}_0 g_0 n_c \bar{S}_c - 2\bar{\xi}_1 g_1 n_c \bar{S}_c - 2\bar{\xi}_2 g_2 n_b \bar{S}_c \right] a^0 \bar{\sigma} \right\} \frac{\partial g_4}{\partial \theta} \\
& - \frac{1}{\bar{\xi}_0 g_0 g_3^3} \left[ 6C \bar{\xi}_0 g_0 \bar{\sigma}^2 + \sqrt{3} g_5 (B + E \bar{\xi}_0 g_0) a^0 \bar{\sigma} - \sqrt{3} B \bar{\xi}_0 g_0 g_5 \left( \sigma_m - \frac{1}{3} \alpha \right) \right] \frac{\partial g_5}{\partial \theta}
\end{aligned}$$

and

$$\frac{\partial g_i}{\partial \theta} = - \frac{3k_{i1} k_{i3} k_{i5} \cos(k_{i4} + 3\theta)}{\left[ k_{i2} + k_{i3} \sin(k_{i4} + 3\theta) \right]^{k_{i5} + 1}}, \quad i = 0, 1, 2, 3, 4, 5.$$

To complete the kinematic hardening type of stress-strain relationship it will be necessary to derive  $\frac{\partial f^0}{\partial a^0}$ , that is:

$$\frac{\partial f^0}{\partial a^0} = - \frac{1}{\bar{\xi}_0 g_0} (2A - D \bar{\xi}_0 g_0) \left( \sigma_m - \frac{1}{3} \alpha \right) + \frac{\sqrt{3}}{\bar{\xi}_0 g_0 g_5} (B + E \bar{\xi}_0 g_0) \bar{\sigma} + 2 \frac{a^0}{\bar{\xi}_0^2 g_0^2} (A - D \bar{\xi}_0 g_0)$$

and from equations (IV.10.2.23), (IV.10.2.24) and the definitions of  $\sigma_m$ ,  $\bar{\sigma}$  and  $J_3$ ,

$$\frac{\partial \sigma_m}{\partial \bar{\sigma}} = \frac{1}{3} \begin{pmatrix} 1 \\ 1 \\ 1 \\ 0 \\ 0 \\ 0 \end{pmatrix}; \quad \frac{\partial \bar{\sigma}}{\partial \bar{\sigma}} = \frac{1}{2\bar{\sigma}} \begin{pmatrix} \bar{\sigma}_x - \bar{\alpha}_x \\ \bar{\sigma}_y - \bar{\alpha}_y \\ \bar{\sigma}_z - \bar{\alpha}_z \\ 2(\tau_{yz} - \alpha_{yz}) \\ 2(\tau_{xz} - \alpha_{xz}) \\ 2(\tau_{xy} - \alpha_{xy}) \end{pmatrix}$$

$$\frac{\partial J_3}{\partial \sigma} = \begin{pmatrix} (\bar{\sigma}_y - \bar{\alpha}_y)(\bar{\sigma}_y - \bar{\alpha}_z) - (\tau_{xy} - \alpha_{zy})^2 \\ (\bar{\sigma}_x - \bar{\alpha}_x)(\bar{\sigma}_z - \bar{\alpha}_z) - (\tau_{xz} - \alpha_{xz})^2 \\ (\bar{\sigma}_x - \bar{\alpha}_x)(\bar{\sigma}_y - \bar{\alpha}_y) - (\tau_{xy} - \alpha_{xy})^2 \\ 2\{(\tau_{xz} - \alpha_{xz})(\tau_{xy} - \alpha_{xy}) - (\bar{\sigma}_x - \alpha_x)(\tau_{yz} - \alpha_{yz})\} \\ 2\{(\tau_{yz} - \alpha_{yz})(\tau_{xy} - \alpha_{xy}) - (\bar{\sigma}_y - \alpha_y)(\tau_{xz} - \alpha_{xz})\} \\ 2\{(\tau_{yz} - \alpha_{yz})(\tau_{xz} - \alpha_{xz}) - (\bar{\sigma}_z - \alpha_z)(\tau_{xy} - \alpha_{xy})\} \end{pmatrix} + \frac{1}{3}\bar{\sigma}^2 \begin{pmatrix} 1 \\ 1 \\ 1 \\ 0 \\ 0 \\ 0 \end{pmatrix}$$

In addition by setting  $\bar{\alpha}_{ij} = 0$ ,  $\alpha_{ii} = -3\frac{a}{\bar{\xi}_0 g_0}$  and  $a^0 = a$  the equation for  $f^s$  for the general stress space can be obtained if equation (VIII.4.45) is used. The invariants defined by (VIII.4.39) now become:

$$J_m = \frac{1}{3}\sigma_{ii}, \quad \bar{\sigma} = \left(\frac{1}{2}\bar{\sigma}_{ii}\bar{\sigma}_{ij}\right)^{\frac{1}{2}}, \quad J_3 = \frac{1}{3}\bar{\sigma}_{ij}\bar{\sigma}_{ij}\bar{\sigma}_{ij}$$

and  $f^s$  as

$$f^s = A\left(\sigma_m + \frac{a}{\bar{\xi}_0 g_0}\right)^2 - \sqrt{3}B\left(\sigma_m + \frac{a}{\bar{\xi}_0 g_0}\right)\frac{\bar{\sigma}}{g_5} + 3C\frac{\bar{\sigma}^2}{g_3^2} -$$

(VIII.4.48)

$$\frac{a}{\bar{\xi}_0 g_0}(2A - D\bar{\xi}_0 g_0)\left(\sigma_m + \frac{a}{\bar{\xi}_0 g_0}\right) + \sqrt{3}\frac{a}{\bar{\xi}_0 g_0}(B + E\bar{\xi}_0 g_0)\frac{\bar{\sigma}}{g_5} + \left(\frac{a}{\bar{\xi}_0 g_0}\right)^2(A - D\bar{\xi}_0 g_0) = 0$$

with the gradient tensor defined by (VIII.4.48), where  $\frac{\partial f^s}{\partial \sigma_m}$ ,  $\frac{\partial f^s}{\partial \bar{\sigma}}$ ,  $\frac{\partial f^s}{\partial \theta}$  are now given by:

$$\frac{\partial f^s}{\partial \bar{\sigma}} = 6C\frac{\bar{\sigma}}{g_3^2} - \frac{\sqrt{3}}{g_5}B\left(\sigma_m + \frac{a}{\bar{\xi}_0 g_0}\right) + \frac{\sqrt{3}a}{\bar{\xi}_0 g_0 g_5}(B + E\bar{\xi}_0 g_0)$$

$$\frac{\partial f^s}{\partial \sigma_m} = 2A\left(\sigma_m + \frac{a}{\bar{\xi}_0 g_0}\right) - \sqrt{3}B - \frac{a}{\bar{\xi}_0 g_0}(2A - D\bar{\xi}_0 g_0)$$

$$\frac{\partial f^s}{\partial \theta} = \frac{\partial f^0}{\partial \theta}, \quad \text{but } \left(\sigma_m - \frac{1}{3}\alpha\right) = \left(\sigma_m + \frac{a}{\bar{\xi}_0 g_0}\right) \text{ and}$$

$$\sigma_m - \frac{1}{3}\alpha + \frac{a^0}{\bar{\xi}_0 g_0} = \sigma_m + \frac{a}{\bar{\xi}_0 g_0} + \frac{a}{\bar{\xi}_0 g_0} = \left(\sigma_m + \frac{2a}{\bar{\xi}_0 g_0}\right)$$

The variation  $\partial f^s / \partial a$  will be given by

$$\frac{\partial f^s}{\partial a} = D \left( \sigma_m + \frac{a}{\bar{\xi}_0 g_0} \right) + \frac{\sqrt{3}}{g_s} \bar{\sigma} + \frac{a}{\bar{\xi}_0^2 g_0^2} (A - D \bar{\xi}_0 g_0)$$

It will also be necessary to evaluate  $\text{tr} (\partial f^s / \partial \sigma)$  which is the same as  $\partial f^s / \partial \sigma_m$  given above.

It should be noted that  $a$ ,  $\bar{\xi}_1$ ,  $\bar{\xi}_2$ ,  $\bar{S}_a$ ,  $\bar{S}_c$  can be functions of the plastic strain (or stress) rate. Any empirical law, in principle, can be adopted.

The number of combinations of the surfaces  $f^s$ ,  $f^0$  which can be considered in order to form a model are enormous. Each particular condition provides elements to rule the arrangement and transformation of those surfaces. Restrictions can be introduced to those surfaces to fit almost any theoretical soil model and in principle, any set of soil test data can be used to calibrate and specifically define the surfaces  $f^s$ ,  $f^0$  and their transformation rule. The particular conditions and transformation rules to be imposed on those surfaces to represent any known model will be presented elsewhere. Here, just a few of them will be discussed.

The conditions necessary to be imposed on the general model to reduce to a particular one is presented together with the transformed equations in table I whilst the pertinent gradients and derivatives for each model are presented in table II.

TABLE I

$$f' = A(\sigma_m - \frac{1}{3}\alpha)^2 - \sqrt{3}B(\sigma_m - \frac{1}{3}\alpha)\frac{\sigma}{k_3} + 3C\frac{\sigma^2}{k_3} - \frac{\sigma^2}{\xi_0 k_0} (2A - D \xi_0 k_0)(\sigma_m - \frac{1}{3}\alpha) + \sqrt{3}\frac{\sigma^2}{\xi_0 k_0 k_3} (B + E \xi_0 k_0) \sigma + \left(\frac{\sigma^2}{\xi_0 k_0}\right)^2 (A - D \xi_0 k_0) + F = 0$$

DESCRIPTION	A	B	C	D
HUBER-MISES	0	0	0	0
DRUCKER-PRAEGER	0	0	0	$\frac{1}{3}$
TRESCA	0	0	0	0
MOHR-COULOMB	0	0	0	$\frac{1}{3}$
LARSSON	0	0	0	$\frac{1}{3}$
ORIGINAL CAM-CLAY	1	$\frac{(\sigma-2)(1-\sin\phi)}{6 \sin\phi}$	$\frac{(1-\sin\phi)^2}{36 \sin^2\phi} (\sigma^2 - 3\sigma + 1)$	2
MODIFIED CAM-CLAY	1	0	$\frac{(1-\sin\phi)^2}{36 \sin^2\phi}$	2
NOVA AND WOOD FIRST SURFACE	1	$\frac{1-\sin\phi}{3 \sin\phi} (\xi - 1)$	$\frac{(2+\sin\phi)^2}{36 \sin^2\phi} (1 - 2\xi)^2$	2
TRIAXIAL MODEL SECOND SURFACE	1	$\frac{2(1-\sin\phi)}{3 \sin\phi} (\xi - 1)$	$\frac{(1-\sin\phi)^2}{9 \sin^2\phi} (1 - 2\xi)^2$	2
PIETRUSZCZAK AND FIRST SURFACE	1	$\frac{(1-\sin\phi)}{3 \sin\phi} (\xi - 1)$	$\frac{(1-\sin\phi)^2}{36 \sin^2\phi} (1 - 2\xi)^2$	2
MROZ MODEL SECOND SURFACE	1	$\frac{(1-\sin\phi)}{3 \sin\phi} (\xi - 1)$	$\frac{(1-\sin\phi)^2}{36 \sin^2\phi} (1 - 2\xi)$	2
MODEL I FIRST SURFACE	1	$\frac{1-\sin\phi}{3 \sin\phi} \left( \frac{1-\sin\phi}{1-\sin\phi \sin M} \xi - 1 \right)$	$\frac{(1-\sin\phi)^2}{36 \sin^2\phi} \left[ \left( 1 - 2\xi \frac{1-\sin\phi}{1-\sin\phi \sin M} \right)^2 - 2 \frac{1-\sin\phi}{1-\sin\phi \sin M} M \xi S_0 k_0 \right]$	2
TWO-SURFACES MODEL SECOND SURFACE	1	$\frac{1-\sin\phi}{3 \sin\phi} \left( \frac{1-\sin\phi}{1-\sin\phi \sin M} \xi - 1 \right)$	$\frac{(1-\sin\phi)^2}{36 \sin^2\phi} \left[ \left( 1 - 2\xi \frac{1-\sin\phi}{1-\sin\phi \sin M} \right)^2 - 2 \frac{1-\sin\phi}{1-\sin\phi \sin M} M \xi S_0 k_0 \right]$	2

TABLE I--CONT.

$E$	$F$	$\xi_0$	$\xi_1$	$\xi_2$	$\xi_3$	$\xi_4$	$\xi_5$	$\overline{S}_a$	$\overline{S}_c$	$\xi_0$	$\xi_1$	$\xi_2$	$\alpha$
$\frac{1}{d}$	$-\sigma_y$	1	1	1	1	1	1	0	0	1	1	1	$-\frac{2d}{l}$
$\frac{3-\sin\phi}{6d'\sin\phi}$	$-c \cot\phi$	1	1	1	1	1	$\frac{1-\sin\phi}{6\sin\phi}$	0	0	1	1	1	$-\frac{2d'}{l}$
$\frac{1}{d'}$	$-\sigma_y$	1	1	1	1	1	$\frac{1}{2\cos\phi}$	0	0	1	1	1	$-\frac{2d'}{l}$
$\frac{3-\sin\phi}{6d'\sin\phi}$	$-c \cot\phi$	1	1	1	1	1	$\frac{1-\sin\phi}{3-\sin\phi \sin\phi}$	0	0	1	1	1	$-\frac{2d'}{l}$
$\frac{\overline{S}_c}{\sigma}$	$2a$	1	1	1	1	1	1	$\overline{S}_a$	0	1	1	1	$-\frac{2d'}{l}$
$(3-e)\frac{(1-\sin\phi)}{3\sin\phi}$	0	1	1	1	1	1	1	$\frac{1}{M}$	0	$\frac{1}{3}$	$\frac{1}{3}$	$\frac{1}{3}$	$-\frac{6d'}{l}$
0	0	1	1	1	1	1	1	0	0	1	1	1	$-3d'$
$\frac{2(1-\sin\phi)}{3\sin\phi}(1-\xi)$	0	1	1	1	1	1	1	0	0	$\xi$	$\xi$	$\xi$	$-\frac{2d}{l}$
$\frac{4(1-\sin\phi)}{3\sin\phi}(1-\xi)$	0	1	1	1	1	1	1	0	0	$\xi$	$\xi$	$\xi$	$-\frac{2d}{l}$
$\frac{2(1-\sin\phi)}{3\sin\phi}(1-\xi)$	0	1	1	1	1	1	$\frac{1-\sin\phi}{3-\sin\phi \sin\phi}$	0	0	$\xi$	$\xi$	$\xi$	$\alpha$
$\frac{2(1-\sin\phi)}{3\sin\phi}(1-\xi)$	0	1	1	1	1	1	$\frac{1-\sin\phi}{3-\sin\phi \sin\phi}$	0	0	$\xi$	$\xi$	$\xi$	$-\frac{2d}{l}$
$\frac{2(1-\sin\phi)}{3\sin\phi}\left(1 - \frac{1-\sin\phi}{3-\sin\phi \sin\phi} \xi + \frac{1-\sin\phi}{3-\sin\phi} \overline{S}_a \xi_4\right)$	0	1	$\frac{1-\sin\phi}{3-\sin\phi \sin\phi}$	$\frac{1-\sin\phi}{3-\sin\phi \sin\phi}$	1	$\xi_4$	$\frac{1-\sin\phi}{3-\sin\phi \sin\phi}$	$\overline{S}_a$	0	$\xi$	$\xi$	$\xi$	$\alpha$
$\frac{2(1-\sin\phi)}{3\sin\phi}\left(1 - \frac{1-\sin\phi}{3-\sin\phi \sin\phi} \xi + \frac{1-\sin\phi}{3-\sin\phi} \overline{S}_a \xi_4\right)$	0	1	$\frac{1-\sin\phi}{3-\sin\phi \sin\phi}$	$\frac{1-\sin\phi}{3-\sin\phi \sin\phi}$	1	$\xi_4$	$\frac{1-\sin\phi}{3-\sin\phi \sin\phi}$	$\overline{S}_a$	0	$\xi$	$\xi$	$\xi$	$-\frac{2d'}{l}$

By substituting into equation XVIII.4.45 the constants stipulated on Table I for each specific model, a field of equations representing any of those particular models are readily obtained, that is:

— HUBER-MISES

$$f^I = \sqrt{3}\bar{\sigma} - \sigma_y = 0$$

— DRUCKER-PRAGER

$$f^I = \sigma_m + \frac{\sqrt{3}(3-\sin\Phi)}{6\sin\Phi}\bar{\sigma} - c\cot\Phi - 0$$

— TRESCA

$$f^I = 2\bar{\sigma}\cos\Phi - \sigma_y = 0$$

— MOHR-COULOMB

$$f^I = \sigma_m + \frac{\sqrt{3}(3-\sin\Phi\sin 3\theta)}{6\sin\Phi}\bar{\sigma} - c\cot\Phi = 0$$

## — LARSSON

$$f^1 = \sigma_m + \sqrt{3} S_a \bar{\sigma} + 2a = 0, \quad \bar{\sigma} \leq -\frac{2\sqrt{3} \sin \Phi}{(3 - \sin \Phi \sin 3\theta)} \sigma_m$$

## — ORIGINAL CAM-CLAY

$$f^1 = \sigma_m^2 - \frac{\sqrt{3}(e-2)(3-\sin \Phi)}{6 \sin \Phi} \sigma_m \bar{\sigma} + \frac{(3-\sin \Phi)^2}{12 \sin^2 \Phi} (e^2 - 3e + 1) \bar{\sigma}^2 + 2a \sigma_m +$$

$$\frac{\sqrt{3}}{3}(3-e) \frac{3-\sin \Phi}{\sin \Phi} a \bar{\sigma} = 0, \quad \bar{\sigma} \leq -\frac{2\sqrt{3} \sin \Phi}{(3 - \sin \Phi \sin 3\theta)} \sigma_m$$

## — MODIFIED CAM-CLAY

$$f^1 = \sigma_m^2 + \frac{(3-\sin \Phi)^2}{12 \sin^2 \theta} \bar{\sigma}^2 + 2a \sigma_m = 0, \quad \bar{\sigma} \leq -\frac{2\sqrt{3} \sin \Phi}{(3 - \sin \Phi \sin 3\theta)} \sigma_m$$

## — NOVA AND WOOD TRIAXIAL MODEL

## FIRST SURFACE

$$f^1 = \sigma_m^2 - \frac{\sqrt{3}(3-\sin \Phi)}{3 \sin \Phi} (\bar{\xi} - 1) \sigma_m \bar{\sigma} + \frac{(3-\sin \Phi)^2}{12 \sin^2 \Phi} (1 - 2\bar{\xi})^2 \bar{\sigma}^2 + 2a \sigma_m +$$

$$\frac{2\sqrt{3}(3-\sin\Phi)}{3\sin\Phi}(1-\bar{\xi})a\bar{\sigma} = 0$$

$$\bar{\xi} = \frac{1}{2}\mu^{\frac{\mu}{\mu-1}}, \quad \mu \neq 1,$$

$$\bar{\xi} = \frac{e}{2}, \quad \mu = 1$$

SECOND SURFACE

$$f^2 = \sigma_m^2 - \frac{2\sqrt{3}(3-\sin\Phi)}{3\sin\Phi}(\bar{\xi}-1)\sigma_m\bar{\sigma} + \frac{(3-\sin\Phi)^2}{3\sin^2\Phi}(1-2\bar{\xi})^2\bar{\sigma}^2 + 2a\sigma_m +$$

$$\frac{4\sqrt{3}(3-\sin\Phi)}{3\sin\Phi}(1-\bar{\xi})a\bar{\sigma} = 0,$$

$$\bar{\xi} = \frac{1}{2}\sqrt{1+\mu},$$

$$\bar{\sigma} \leq -\frac{2\sqrt{3}\sin\Phi}{(3-\sin\Phi\sin 3\theta)}\sigma_m$$

— PIETRUSZCZAK AND MROZ

FIRST SURFACE

$$f^0 = 3\sin^2\Phi(\sigma_m - \frac{1}{3}\alpha)^2 - 6\sin^2\Phi\frac{1-\bar{\xi}}{\bar{\xi}}a^0(\sigma_m - \frac{1}{3}\alpha) -$$

$$\sqrt{3}(\bar{\xi}-1)\sin\Phi(3-\sin\Phi\sin 3\theta)\left[(\sigma_m - \frac{1}{3}\alpha) - \frac{1-2\bar{\xi}}{\bar{\xi}}a^0\right]\bar{\sigma} +$$

$$\left[\frac{1}{2}(1-2\bar{\xi})(3-\sin\Phi\sin 3\theta)\right]^2\bar{\sigma}^2 + 3a^{02}\sin^2\Phi\frac{1-2\bar{\xi}}{\bar{\xi}^2} = 0$$



## SECOND SURFACE

$$f^1 = 3 \sin^2 \Phi (\sigma_m + a)^2 - \sqrt{3}(\bar{\xi} - 1) \sin \Phi (3 - \sin \Phi \sin 3\theta) (\sigma_m + 2a) \bar{\sigma} +$$

$$\left[ \frac{1}{2} (1 - 2\bar{\xi}) (3 - \sin \Phi \sin 3\theta) \right]^2 \bar{\sigma}^2 - 3a^2 \sin^2 \Phi = 0$$

## — MODEL I

## FIRST SURFACE

$$f^0 = (\sigma_m - \frac{1}{3}\alpha)^2 - \sqrt{3} \frac{3 - \sin \Phi \sin \theta}{3 \sin \Phi} \left( \frac{3 - \sin \Phi}{3 - \sin \Phi \sin 3\theta} \bar{\xi} - 1 \right) (\sigma_m - \frac{1}{3}\alpha) \bar{\sigma} +$$

$$\frac{(3 - \sin \Phi \sin 3\theta)^2}{12 \sin^2 \Phi} \left[ \left( 1 - 2\bar{\xi} \frac{3 - \sin \Phi}{3 - \sin \Phi \sin 3\theta} \right)^2 - \frac{12 \sin \Phi}{3 - \sin \Phi \sin 3\theta} \frac{\bar{\xi} \bar{S}_a g_4}{\bar{\xi}} \right] \bar{\sigma}^2 - 2a^0 \frac{1 - \bar{\xi}}{\bar{\xi}} (\sigma_m - \frac{1}{3}\alpha) +$$

$$\sqrt{3} \frac{3 - \sin \Phi \sin 3\theta}{3 \sin \Phi} \frac{a^0}{\bar{\xi}} \left[ \frac{3 - \sin \Phi}{3 - \sin \Phi \sin 3\theta} \bar{\xi} - 1 + 2\bar{\xi} \left( 1 - \frac{3 - \sin \Phi}{3 - \sin \Phi \sin 3\theta} \bar{\xi} + \frac{3 \sin \Phi}{3 - \sin \Phi} \bar{S}_a g_4 \right) \right] \bar{\sigma} +$$

$$\frac{1 - 2\bar{\xi}}{\bar{\xi}^2} a^0{}^2 = 0$$

## SECOND SURFACE

$$f^1 = (\sigma_m + \frac{a^1}{\bar{\xi}})^2 - \sqrt{3} \frac{3 - \sin \Phi \sin 3\theta}{3 \sin \Phi} \left( \frac{3 - \sin \Phi}{3 - \sin \Phi \sin 3\theta} \bar{\xi} - 1 \right) (\sigma_m + \frac{a^1}{\bar{\xi}}) \bar{\sigma} +$$

$$\frac{(3 - \sin \Phi \sin 3\theta)^2}{12 \sin^2 \Phi} \left[ \left( 1 - 2\bar{\xi} \frac{3 - \sin \Phi}{3 - \sin \Phi \sin 3\theta} \right)^2 - \frac{12 \sin \Phi}{3 - \sin \Phi \sin 3\theta} \bar{\xi} \bar{S}_a g_4 \right] \bar{\sigma}^2 - 2a^1 \frac{1 - \bar{\xi}}{\bar{\xi}} \left( \sigma_m + \frac{a^1}{\bar{\xi}} \right) +$$

$$\sqrt{3} \frac{3 - \sin \Phi \sin 3\theta}{3 \sin \Phi} \frac{a^1}{\bar{\xi}} \left[ \frac{3 - \sin \Phi}{3 - \sin \Phi \sin 3\theta} \bar{\xi} - 1 + 2\bar{\xi} \left( 1 - \frac{3 - \sin \Phi}{3 - \sin \Phi \sin 3\theta} \bar{\xi} + \frac{3 \sin \Phi}{3 - \sin \Phi} \bar{S}_a g_4 \right) \right] \bar{\sigma} +$$

$$\frac{1 - 2\bar{\xi}}{\bar{\xi}^2} a^{1^2} = 0$$

TABLE II

DERIVATIVES

$$C_1 = \frac{\partial f}{\partial \sigma_m}, \quad C_2 = \frac{\partial f}{\partial \bar{\sigma}} + \frac{3\sqrt{3}J_1}{2\bar{\sigma}^4 \cos 3\theta} \frac{\partial f}{\partial \theta}, \quad C_3 = -\frac{\sqrt{3}}{2\bar{\sigma}^3 \cos 3\theta} \frac{\partial f}{\partial \theta}$$

DESCRIPTION	$C_1$	$C_2$
HUBER-MISES	0	$\sqrt{3}$
TRESCA	$2 \cos \theta (1 + \tan \theta \tan 3\theta)$	$\frac{\sqrt{3} \sin \theta}{\bar{\sigma}^2 \cos 3\theta}$
DRUCKER-PRAGER	1	$\frac{\sqrt{3}(1-\sin \theta)}{6 \sin \theta}$
MOHR-COULOMB	1	$\frac{\sqrt{3}(1-2 \sin \theta \sin 3\theta)}{6 \sin \theta}$
LARSSON	0	$\sqrt{3} S_e$
ORIGINAL CAM-CLAY	$2(\sigma_m + a) - \frac{\sqrt{3}}{6} \frac{1-\sin \theta}{\sin \theta} (\sigma - 2)$	$\frac{(1-\sin \theta)^2}{6 \sin^2 \theta} (\sigma^2 - 3\sigma + 1) \bar{\sigma} - \frac{\sqrt{3}}{6} \frac{1-\sin \theta}{\sin \theta} (\sigma - 2) \sigma_m + \frac{\sqrt{3}}{3} \frac{1-\sin \theta}{\sin \theta} (3-\sigma) a$
MODIFIED CAM-CLAY	$2(\sigma_m + a)$	$\frac{(1-\sin \theta)^2}{6 \sin^2 \theta} \bar{\sigma}$
NOVA AND WOOD FIRST SURFACE	$2(\sigma_m + a) - \frac{\sqrt{3}(1-\sin \theta)}{3 \sin \theta} (\xi - 1) \bar{\sigma}$	$\frac{\sqrt{3}(1-\sin \theta)}{3 \sin \theta} (1 - \xi)(\sigma_m + 2a) + \frac{(1-\sin \theta)^2}{6 \sin^2 \theta} (1 - 2\xi)^2 \bar{\sigma}$
TRIAXIAL MODEL SECONDSURFACE	$2(\sigma_m + a) - \frac{2\sqrt{3}(1-\sin \theta)}{3 \sin \theta} (\xi - 1) \bar{\sigma}$	$\frac{2\sqrt{3}(1-\sin \theta)}{3 \sin \theta} (1 - \xi)(\sigma_m + 2a) + 2 \frac{(1-\sin \theta)^2}{3 \sin^2 \theta} (1 - 2\xi)^2 \bar{\sigma}$
PIETRUSZCZAK FIRST SURFACE	$6 \sin^2 \theta (\sigma_m - \frac{1}{3} - \frac{1}{3} \sigma^0) - \sqrt{3}(\xi) \sin \theta (3 - \sin \theta \sin 3\theta) \bar{\sigma}$	$(2 \sin 3\theta \sin \theta + 3) \left[ \frac{1}{3} (1 - 2\xi)^2 (3 - \sin \theta \sin 3\theta) \bar{\sigma} - \sqrt{3}(\xi - 1) \sin \theta (\sigma_m - \frac{1}{3} - \frac{1}{3} \sigma^0) \right]$
AND MROZ MODEL SECONDSURFACE	$6 \sin^2 \theta (\sigma_m + a) - \sqrt{3}(\xi - 1) \sin \theta (3 - \sin \theta \sin 3\theta) \bar{\sigma}$	$(2 \sin \theta \sin 3\theta + 3) \left[ -\sqrt{3}(\xi - 1) \sin \theta (\sigma_m + 2a) + \frac{1}{3} (1 - 2\xi)^2 (3 - \sin \theta \sin 3\theta) \bar{\sigma} \right]$
MODEL I FIRST SURFACE		
TWO-SURFACES MODEL SECONDSURFACE		

These expressions can be obtained from the general gradient tensor given by equation (VIII.4.47).

TABLE II - CONT.

I, D - Constants

$C_3$	$\frac{\partial f}{\partial a}$	$\frac{\partial a}{\partial \xi}$	$\frac{\partial a}{\partial e}$
0	—	—	—
$\frac{\sqrt{3} \sin \theta}{2 \cos 3\theta}$	—	—	—
0	—	—	—
$\frac{1}{4\xi}$	—	—	—
0	2	$\frac{e}{\lambda-k}(1+e)$	—
0	$2\sigma_m + \frac{\sqrt{3} \sin \theta}{2 \cos 3\theta} (3-e) a$	$\frac{e}{\lambda-k}(1+e)$	—
0	$2\sigma_m$	$\frac{e}{\lambda-k}(1+e)$	—
0	—	—	—
0	$2\sigma_m + \frac{4\sqrt{3}(1-\sin \theta)}{3 \cos 3\theta} (1-\xi) \sigma$	$\frac{e}{\lambda-k}(1+e)$	$\frac{e^2}{\lambda-k}(1+e)$
$-\frac{2\sqrt{3}}{2\xi^2} \left[ (\xi-1) \sin^2 \Phi \left( \sigma_m - \frac{1}{3} - \frac{1-2\xi}{\xi} a^0 \right) - \frac{1}{2} \sigma (1-2\xi)^2 (3 - \sin \Phi \sin 3\theta) \sin \Phi \right]$	$6 \sin^2 \Phi \left[ \frac{1-2\xi}{\xi} a^0 - \frac{1-\xi}{\xi} (\sigma_m - \frac{1}{3} a) \right] + \sqrt{3} \sin \Phi \frac{(1-\xi)(1-2\xi)}{\xi} (3 - \sin \Phi \sin 3\theta) a^0 \sigma$	$\frac{e^2}{\lambda-k}(1+e)$	—
$-\frac{1\sqrt{3}}{2\xi^2} \left[ \sqrt{3}(\xi-1) \sin^2 \Phi (\sigma_m + 2b) - \frac{1}{2} (1-2\xi)^2 (3 - \sin \Phi \sin 3\theta) \sin \Phi \sigma \right]$	$6 \sin^2 \Phi \sigma_m - 2\sqrt{3}(\xi-1) \sin \Phi (3 - \sin \Phi \sin 3\theta) \sigma$	$\frac{e}{\lambda-k}(1+e)$	—
		$\frac{e^2}{\lambda-k}(1+e)$	—
		$\frac{e}{\lambda-k}(1+e)$	—

200

This expression is obtained by substituting the constants A, B ... F into the general expression  $\frac{\partial f}{\partial a}$  presented in section VIII.5.1

## 6. Practical Application of the Models

This section will be dedicated to compare the proposed models with some laboratory results. The triaxial test conditions will be chosen. For the elasto-viscoplastic-kinematic model the vanishing elastic region version will be the only one to be considered, but obviously the two surface model could be used.

### 6.1 Elasto-Viscoplastic-Kinematic with Vanishing Elastic Region:

For the triaxial conditions the general equation  $f'$  for the yield surface and/or plastic potential (see Figure VIII.8) can be simplified to a convenient form, that is,

$$f = p^2 + \frac{3-\sin\Phi}{3\sin\Phi}(\bar{\xi}-1)pq + \frac{(3-\sin\Phi)^2}{36\sin^2\Phi} \left[ (2\bar{\xi}-1)^2 - \frac{12\bar{\xi}\bar{S}_0\sin\Phi}{3-\sin\Phi} \right] q^2$$

$$- 2ap - \frac{3-\sin\Phi}{3\sin\Phi} \left[ 2(\bar{\xi}-1) - \frac{6\bar{S}_0\sin\Phi}{3-\sin\Phi} \right] aq = 0, \quad q > 0$$

where  $a = a(\epsilon_p)$ ,  $\bar{S}_0 = \bar{S}_0(\dot{q})$  and  $\bar{\xi} = \bar{\xi}(\dot{q})$ .

For  $q < 0$  it is necessary to substitute  $q$  by  $-q$ ,  $\bar{\xi}$  by  $\frac{3-\sin\Phi}{3\sin\Phi} \bar{\xi}$  and  $3-\sin\Phi$  by  $3+\sin\Phi$ .

To evaluate the function that relates  $\bar{S}_0$  and  $\bar{\xi}$  with the stress rate  $\dot{q}$ , the undrained standard triaxial test for different constant stress rate  $\dot{q}$  will be considered. This procedure is justified by the fact that the shape of the yield surface is obtained based on the normalised undrained stress-path and as the undrained stress path is

rate function so will be the yield surfaces. The change in the shape of the undrained stress- path together with the change of stress rate is justified by the change on the compressibility constants and the pre-consolidation pressure with the change of stress rate. Thus, another way to introduce the rate effect is by establishing the function that relates the compressibility constants and pre-consolidation pressure with the stress rate. However, this kind of procedure is more difficult because the effect of the stress rate on the compressibility constants and pre-consolidation pressure also seems to depend upon the stress ratio  $\eta = q/p$  .

Also the elastic constants is dependent on the stress rate. The bulk modulus for an isotropic material relates directly with the compressibility  $k$ , which justifies its dependence to stress rate. Laboratory results also shown that the initial elastic modulus seems to depend on the stress rate. In conclusion, it can be said that the Poisson ratio is a function of the stress rate. At the moment, however, it will be assumed that elastic constants are independent of the stress rate and that will explain the discrepancies between the model prediction and the laboratory results.

By analysing the undrained constant stress rate test (Takahashi, 1981) the relation between  $\bar{S}_0$  and  $\dot{q}$  ; and  $\bar{\xi}$  and  $\dot{q}$  are as plotted in Figure VIII.9.

The matrices of elastic constants are given by

$$D = \begin{bmatrix} 3G_s & 0 \\ 0 & K_s \end{bmatrix} \quad \text{and} \quad D^{-1} = \begin{bmatrix} \frac{1}{3G_s} & 0 \\ 0 & K_s \end{bmatrix}$$

for the following stress and strain invariants definition

$$q = \sigma_2 - \sigma_1, \quad p = -\frac{\sigma_1 + 2\sigma_2}{3}, \quad \epsilon_q = \frac{2}{3}(\epsilon_2 - \epsilon_1), \quad \epsilon_v = -(\epsilon_1 + 2\epsilon_2)$$

By making use of (VIII.3.1) the relation for the effective stress-controlled loading programme is given by (see Figure VIII.8):

For  $f < 0$

$$\begin{Bmatrix} \dot{\epsilon}_q \\ \dot{\epsilon}_v \end{Bmatrix} = \begin{bmatrix} A_1 & A_2 \\ A_2 & A_4 \end{bmatrix} \begin{Bmatrix} \dot{q} \\ \dot{p} \end{Bmatrix}$$

where

$$A_1 = \frac{1}{3G_s} + \frac{(\partial f / \partial q)^2}{K_p |\frac{\partial f}{\partial \sigma}|^2}$$

$$A_2 = \frac{(\partial f / \partial q)(\partial f / \partial p)}{K_p |\frac{\partial f}{\partial \sigma}|^2}$$

$$A_4 = \frac{1}{K_s} + \frac{(\partial f / \partial p)^2}{K_p |\frac{\partial f}{\partial \sigma}|^2}$$

$$|\frac{\partial f}{\partial \sigma}|^2 = \left(\frac{\partial f}{\partial q}\right)^2 + \left(\frac{\partial f}{\partial p}\right)^2$$

$$\frac{\partial f}{\partial q} = \frac{(3 - \sin \Phi)^2}{18 \sin^2 \Phi} \left[ (2\bar{\xi} - 1)^2 - \frac{12\bar{\xi}\bar{S}_0 \sin \Phi}{3 - \sin \Phi} \right] q_R + \frac{3 - \sin \Phi}{3 \sin \Phi} (\bar{\xi} - 1) p_R - \frac{3 - \sin \Phi}{3 \sin \Phi} \left[ 2(\bar{\xi} - 1) - \frac{6\bar{S}_0 \sin \Phi}{3 - \sin \Phi} \right] a$$

$$\frac{\partial f}{\partial a} = -2p_R - \frac{3 - \sin \Phi}{3 \sin \Phi} \left[ 2(\bar{\xi} - 1) - \frac{6\bar{S}_0 \sin \Phi}{3 - \sin \Phi} \right] q_R \quad \frac{\partial f}{\partial p} = 2(p_R - a) + \frac{3 - \sin \Phi}{3 \sin \Phi} (\bar{\xi} - 1) q_R$$

$$K_P = K_R + K_{P0} \left( \frac{\delta}{\delta_0} \right)^{\gamma+1} \quad K_R = -\frac{\partial f}{\partial a} \frac{1+e}{\lambda-k} a \frac{\partial f / \partial p}{|\frac{\partial f}{\partial \sigma}|^2} \quad q_R = (X^2 - Y)^{\frac{1}{2}} - X$$

$$X = \frac{1}{2} \frac{(p_P - q_P \tan \beta) \left[ 2 \tan \beta + \frac{3 - \sin \Phi}{3 \sin \Phi} (\bar{\xi} - 1) \right] - 2 \frac{3 - \sin \Phi}{3 \sin \Phi} \left[ (\bar{\xi} - 1) - \frac{3\bar{S}_0 \sin \Phi}{3 - \sin \Phi} + \tan \beta \right] a}{\tan^2 \beta + \frac{3 - \sin \Phi}{3 \sin \Phi} (\bar{\xi} - 1) \tan \beta + \frac{(3 - \sin \Phi)^2}{36 \sin^2 \Phi} \left[ (2\bar{\xi} - 1)^2 - \frac{12\bar{\xi}\bar{S}_0 \sin \Phi}{3 - \sin \Phi} \right]}$$

$$Y = \frac{(p_P - q_P \tan \beta)(p_P - q_P \tan \beta - 2a)}{\tan^2 \beta + \frac{3 - \sin \Phi}{3 \sin \Phi} (\bar{\xi} - 1) \tan \beta + \frac{(3 - \sin \Phi)^2}{36 \sin^2 \Phi} \left[ (2\bar{\xi} - 1)^2 - \frac{12\bar{\xi}\bar{S}_0 \sin \Phi}{3 - \sin \Phi} \right]}$$

$$p_R = p_P + \tan \beta (q_R - q_P) \quad \tan \beta = \frac{d p}{d q}$$

$$\delta = \left[ (q_R - q_P)^2 + (p_R - p_P)^2 \right]^{\frac{1}{2}}, \quad \delta_0 = 2a$$

$$d a = \frac{1}{K_P} \frac{1+e}{\lambda-k} a \frac{\partial f / \partial p}{|\frac{\partial f}{\partial \sigma}|^2} \left( \frac{\partial f}{\partial q} d q + \frac{\partial f}{\partial p} d p \right)$$

$$\bar{\xi}_c = \frac{a}{c_1}, \quad \bar{\xi}_c = \frac{a}{c_2} = \frac{3 - \sin \Phi}{3 + \sin \Phi} \bar{\xi}_c$$



$K_{p0}$  is the hardening modulus at the beginning of decompression in a  $e$ - $\ln p$  curve.  $\gamma$  represent the power necessary to calibrate the non-linearity of the decompression line  $e$ - $\ln p$ .

$\phi$  is the friction angle and  $e$  is the void ratio.

for  $f = 0$ , the same relations are valid, except that now

$$K_p = K_R, \sigma^R = \sigma^P$$

For a mixed loading programme where the volume changes and the deviator stress are prescribed, the deviator strain and mean stress change response are given by;

$$\begin{Bmatrix} \dot{\epsilon}_q \\ \dot{p} \end{Bmatrix} = \begin{bmatrix} B_1 & B_2 \\ B_2 & B_4 \end{bmatrix} \begin{Bmatrix} \dot{q} \\ \dot{\epsilon}_v \end{Bmatrix}$$

where

$$B_1 = A_1 - \frac{A_2^2}{A_4} \quad B_2 = -B_3 = \frac{A_2}{A_4} \quad B_4 = \frac{1}{A_4}$$

Now  $\tan \beta$  becomes

$$\tan \beta = \frac{B_3 d q + B_4 d \epsilon_v}{d q}$$

and the other relations are unchanged.

To show the accuracy of this model a series of constant stress rate undrained standard triaxial test will be analysed. The soil tested is lower Cromer Till (Takahashi, 1981) and the test procedure was as follows:

The material was first consolidated anisotropically and then swelled

back to an isotropic stress state. The undrained stress path is shown in Figure VIII.10 and the stress-strain relationship in Figure VIII.11. Note that neither the original cam-clay nor the modified cam-clay can predict the pore-pressure generation accurately. A much better prediction can be achieved by adopting  $\xi = 1.2$  and  $\bar{S}_0 = 0.2$  in the proposed model. The extension test could be improved if  $\bar{S}_0$  was adopted as function of  $\theta$  which is allowed in the general model.

The stress-strain relationship (Figure VIII.11) can also be reasonably predicted by the assumed model while the state of stress at failure ( $q_f$  and  $p_f$ ) are both very well predicted by the proposed model, while the modified cam-clay over-predict and the original cam-clay under-predict, both  $q_f$  and  $p_f$ .

The previous test corresponds to a low constant deviator stress rate. To calculate the undrained stress path for other stress rates it will be assumed that the value of  $\bar{S}_0$  and  $\xi$  for different stress rates are determined by a linear interpolation in the  $\bar{S}_0 - \ln \dot{q}$  space and  $\xi - \ln \dot{q}$  space, as presented in Figure VIII.9. In doing so the prediction of the pore-pressure in undrained constant stress rate test are presented in Figure VIII.12, and the stress-strain relationship in Figure VIII.13. It can be seen that the pore-pressure generation is quite good and the stress-strain relationship for the extreme stress rates are reasonably predicted. An improvement in the stress-strain relationship can be achieved if the elastic constants are considered as rate function. Also a non-associative flow rule may be necessary. However, the degree of strain is quite small and the accuracy of the laboratory test must be seen with a certain reserve in this range of strain level. The stress-strain relationship prediction for other

constants stress rate are presented separately in Figure VIII.14 so it would not overload Figure VIII.13. In this figure only compression test are presented.

Now some standard undrained tests are going to be simulated with variable stress rate in sample with the same stress history before the undrained test as presented in the constant stress rate tests.

It will be assumed that the stress rate invariant is given as a exponential function of the stress invariant as shown in Figure VIII.15.

The curve characteristics are given in Table 3. The first two curves represent tests which begin with high stress rate and then decrease exponentially until the end of the test. The initial stress rate and the rate of change of stress rate are shown in the Table 3. The third curve represents a test which begins with a small stress rate until a certain stress level when the stress rate increase until another stress level and then keep constant until the end of the test. The fourth curve represents a test which begins with high stress rate and decreases to a lower stress rate until a certain level of stress and from there the stress rate increase until another level of stress and then keeps constant until the end of the test. The fifth curve represent a test which starts with small stress rate and increase until certain level of stress and from there decreases until another level of stress and then keeps constant until the end of the test. The sixth curve represents a test which starts with a high stress rate and then reduces quickly to another level of stress rate which is kept constant until the end of the test. Finally the seventh curve

represents a test which starts with slow stress rate and then increases quickly to another stress rate and from there kept constant until the end of the test.

In table III  $\beta_i$  represent the initial tangent of the exponential function at the specified stress state and stress rate as given in table III. See also Figure VIII.15.

The undrained stress-path for each of those conditions is presented in Figure VIII.16. It can be seen that the increase in stress rate makes the pore-pressure generation to decrease while the decrease in stress rate makes the pore-pressure generation to increase, which are coherent with the laboratory results. However, to compare with real data more laboratory tests will be required. Also, a model which does not take the stress rate (strain rate) into account can have as many yield surfaces as the loading conditions (as stipulated by Figure VIII.15). As for the sake of curiosity, the loading conditions stipulated by the curve number 2 of Figure VIII.15 produce a yield surface which is an ellipse.

TABLE III

Curve no	Stress State	Stress Rate	$\beta_{i1}$	Stress State	Stress Rate	$\beta_{i2}$
1	0.	1.000	-0.0250	-	-	-
2	0.	14.12	-0.5430	-	-	-
3	0.	0.008	0.	100.0	0.008	0.0242
4	0.	1.	-0.05	100.0	0.008	0.00242
5	0.	0.008	0.00242	100.0	14.12	-4.278
6	0.	14.12	0.	200.0	14.12	-47.07
7	0.	0.008	0.	150.0	0.008	0.0266

$\beta_i$  represents the initial tangent of the exponential function at the specified stress state and stress rate.

It is more difficult to compare the prediction of the model with experimental results for the overconsolidation region because of the scarcity of test information.

The stress rate effect in this region seems to be much less important than in the normally consolidated region as seen in Figure VIII.18a. The test represented in this figure was carried out with displacement control but with the stress rate equivalent to 0.008 Kpa/sec and 0.11

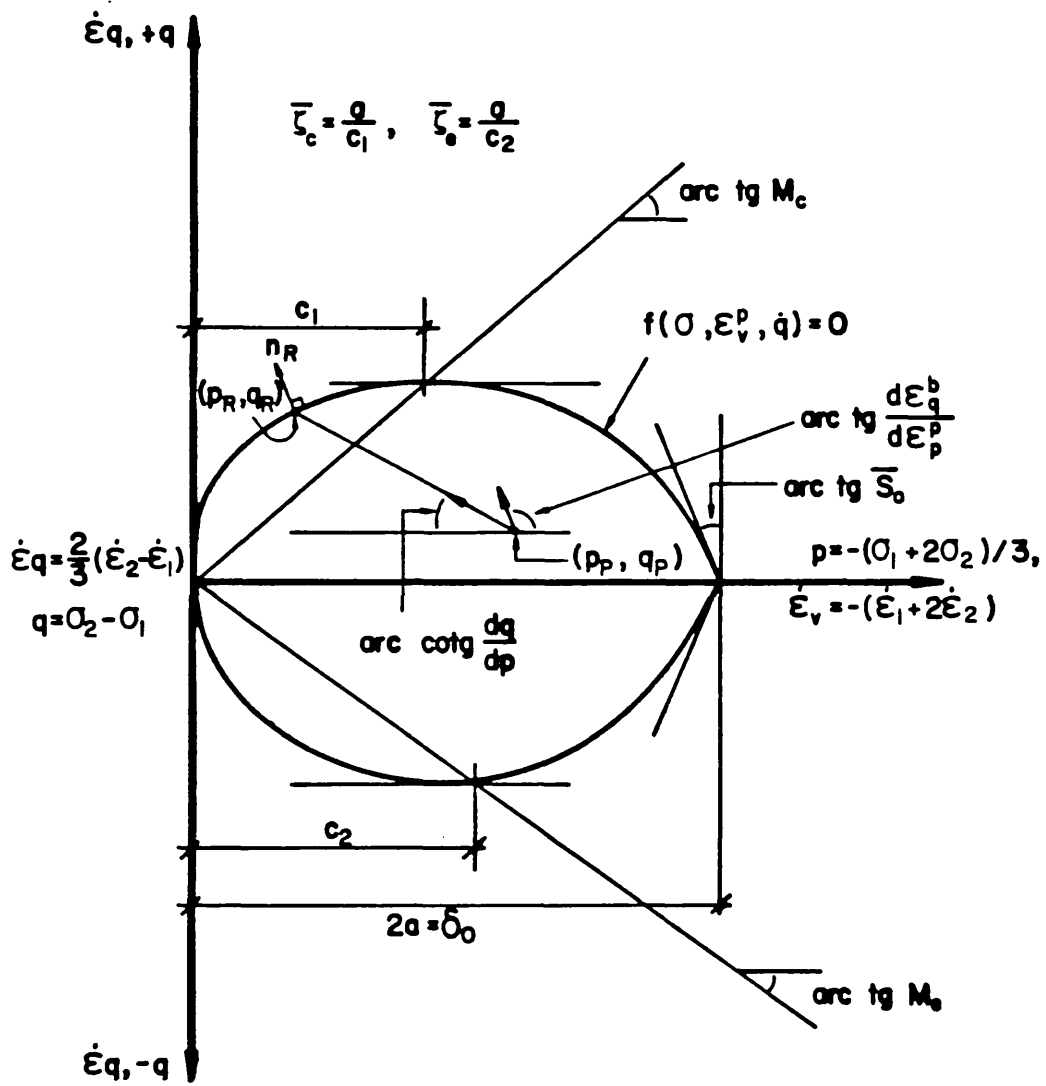


Figure VIII.8.

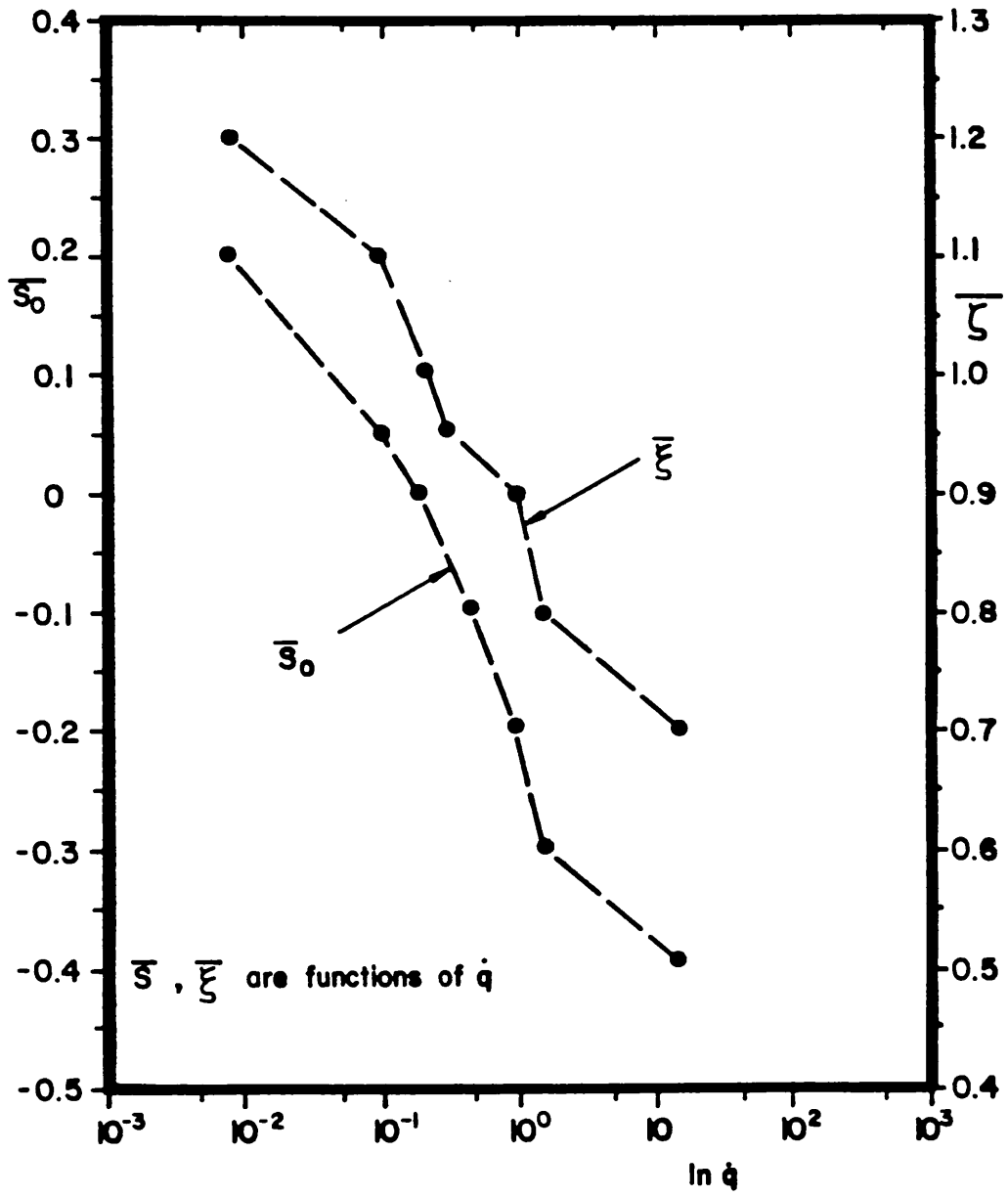


Figure VIII. 9.

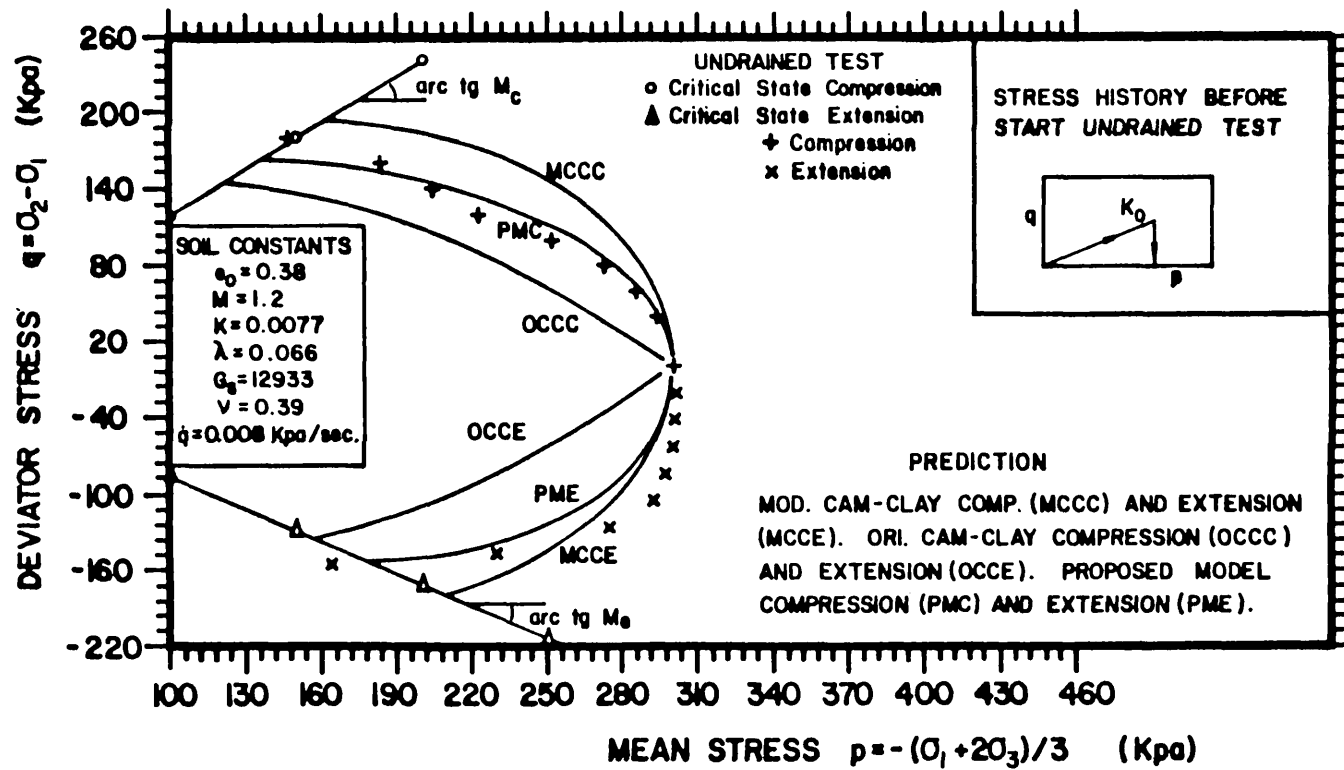


Figure VIII. 10.



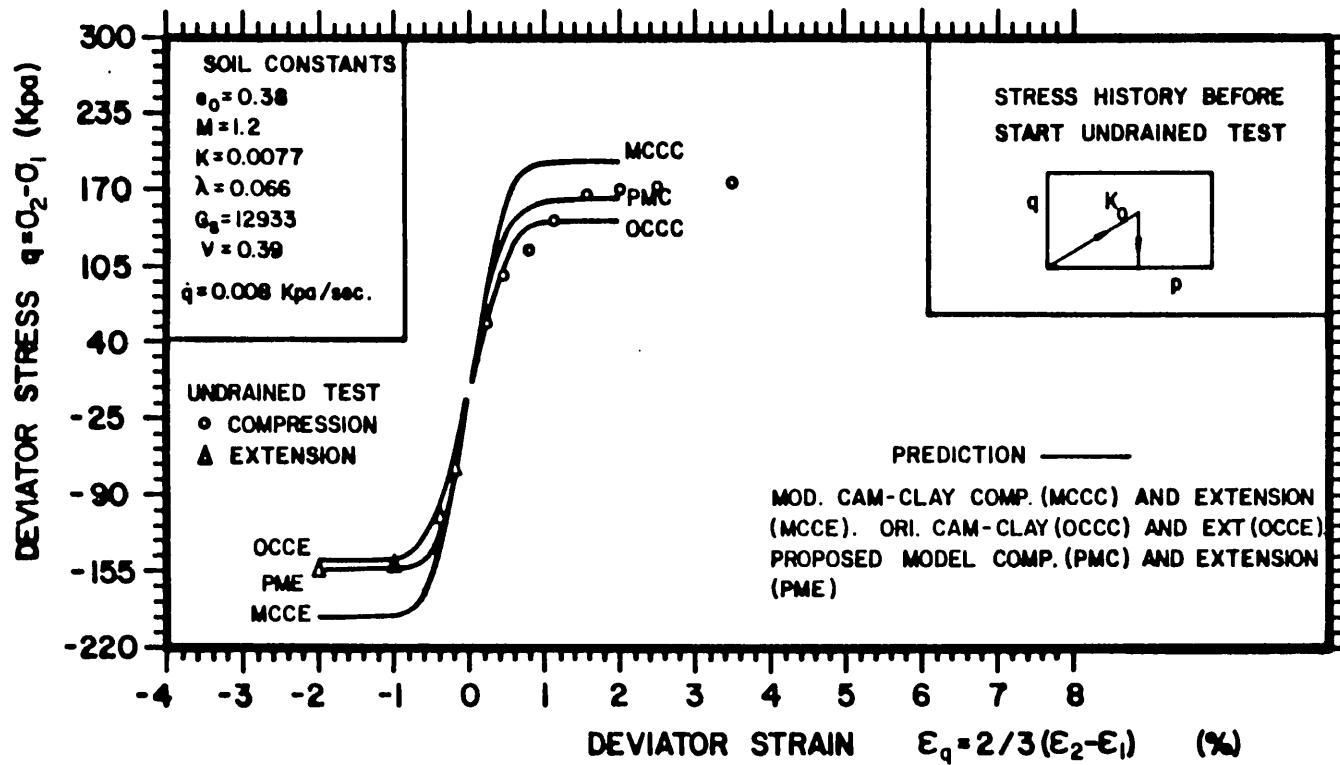


Figure VIII. II.

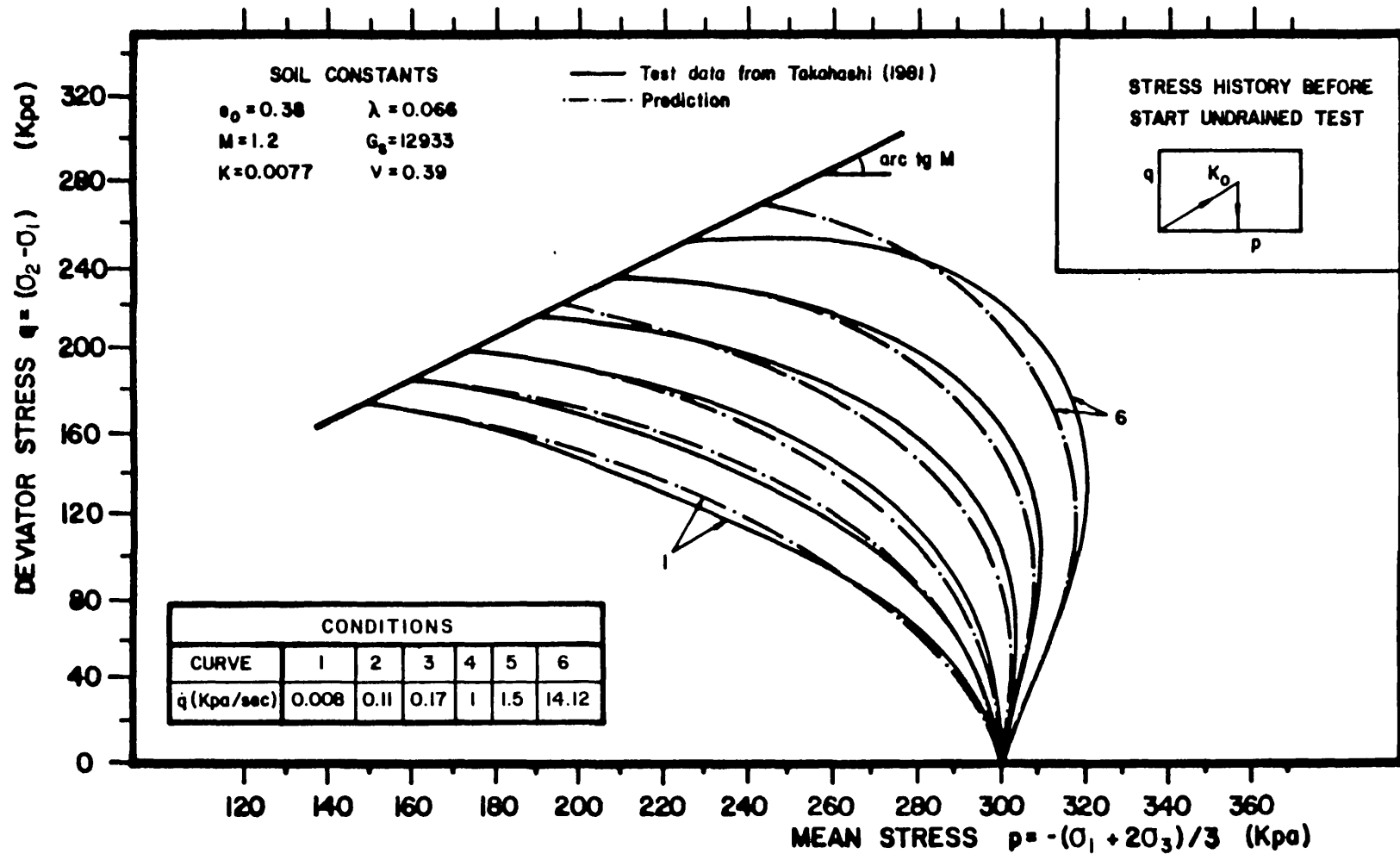


Figure VIII.12.

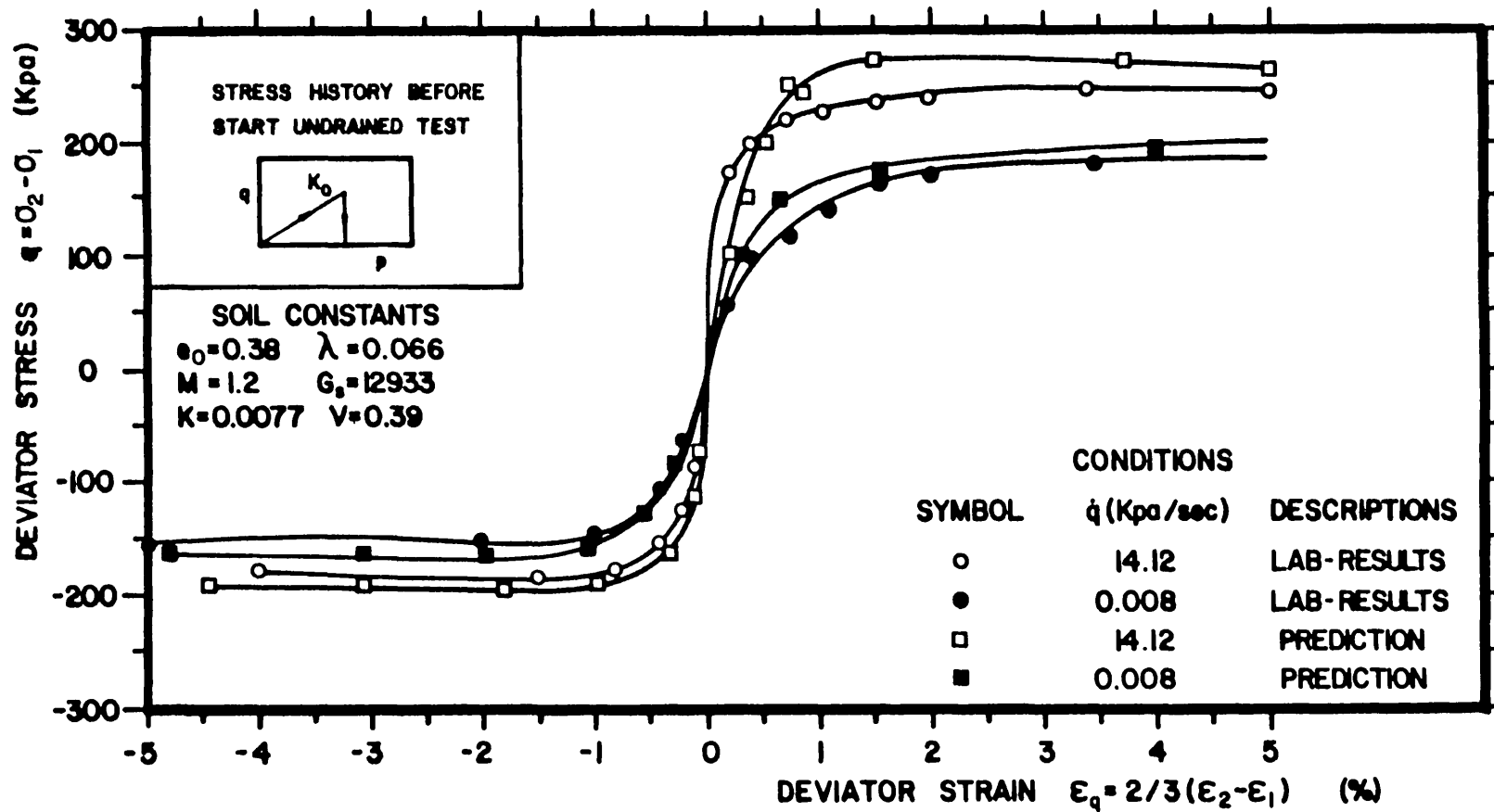


FIGURE VIII. 13.

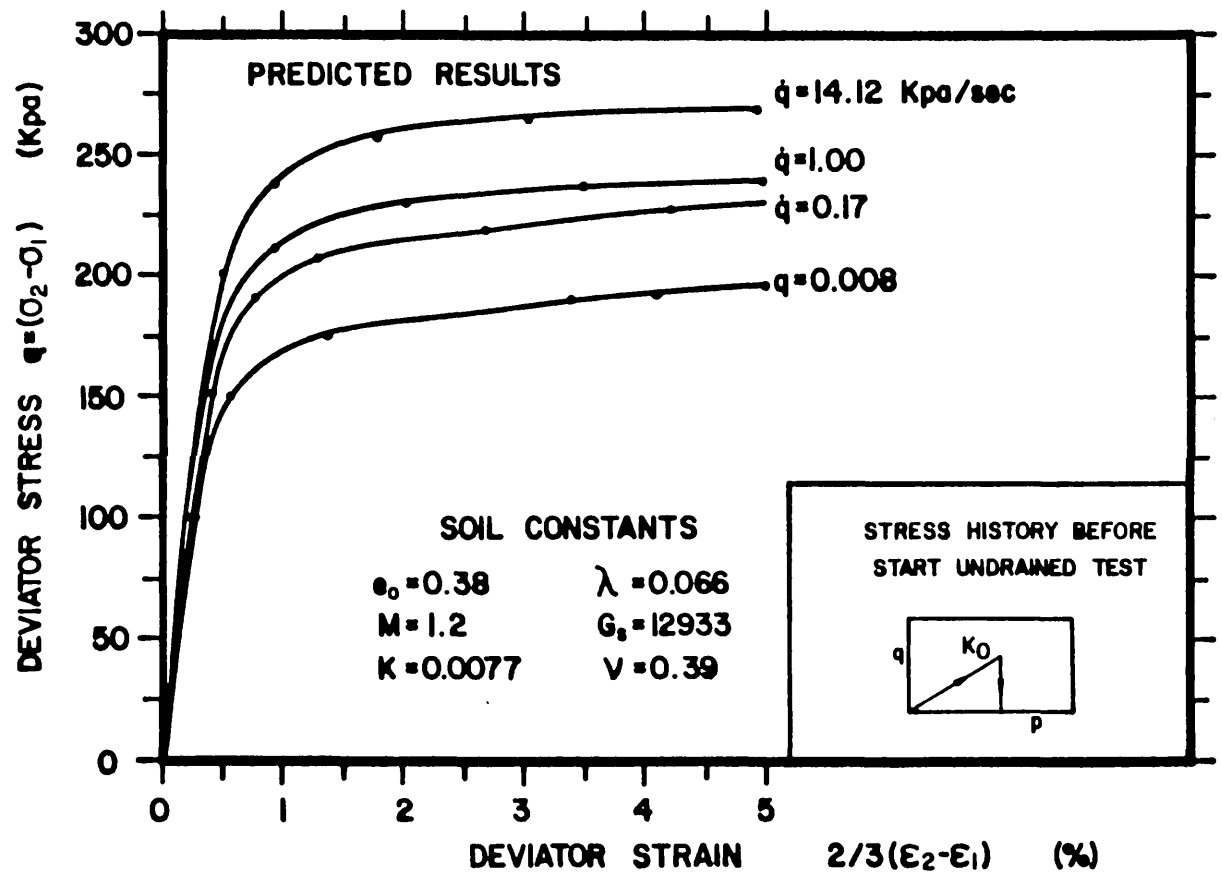


Figure VIII. 14.

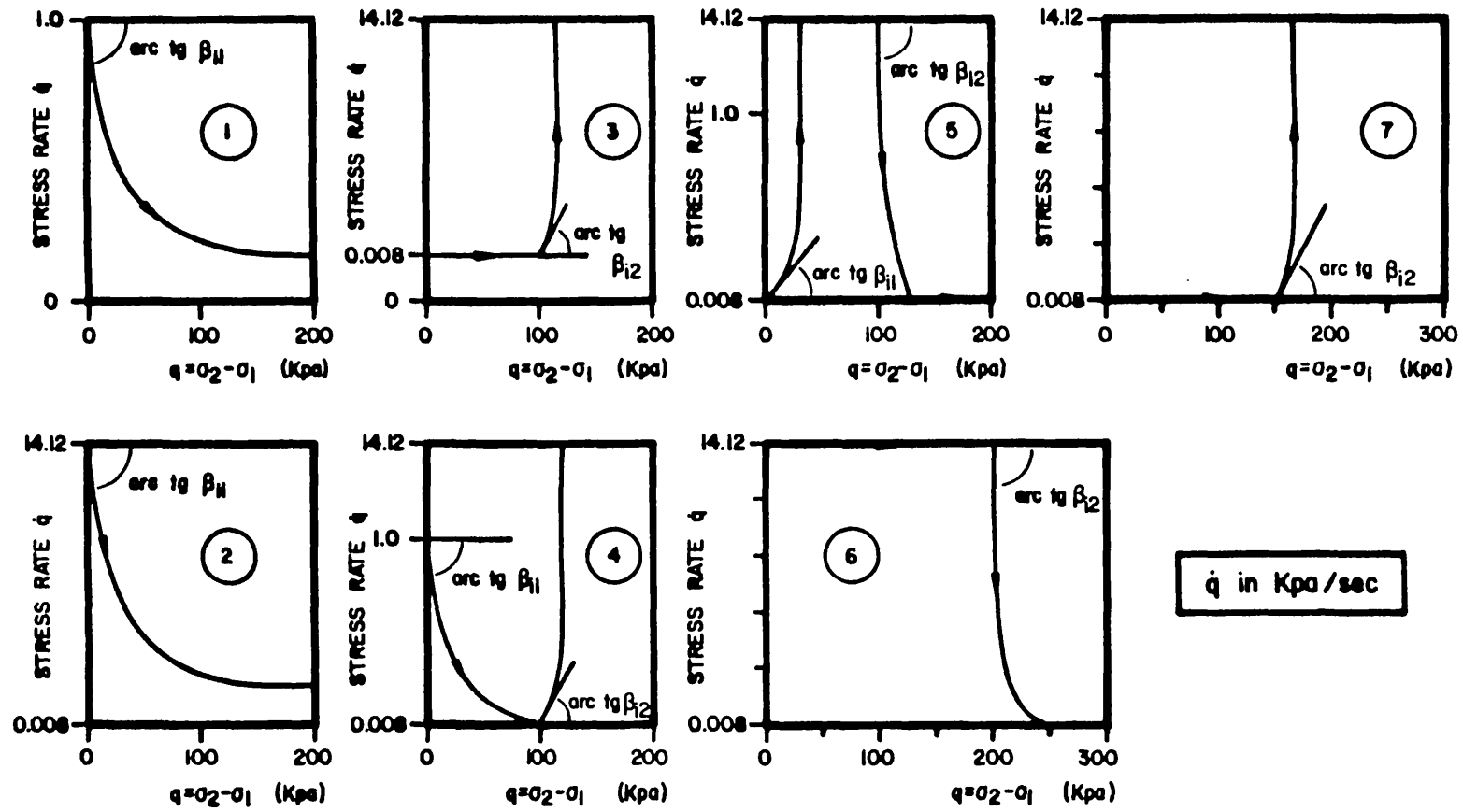


Figure VIII. 15.

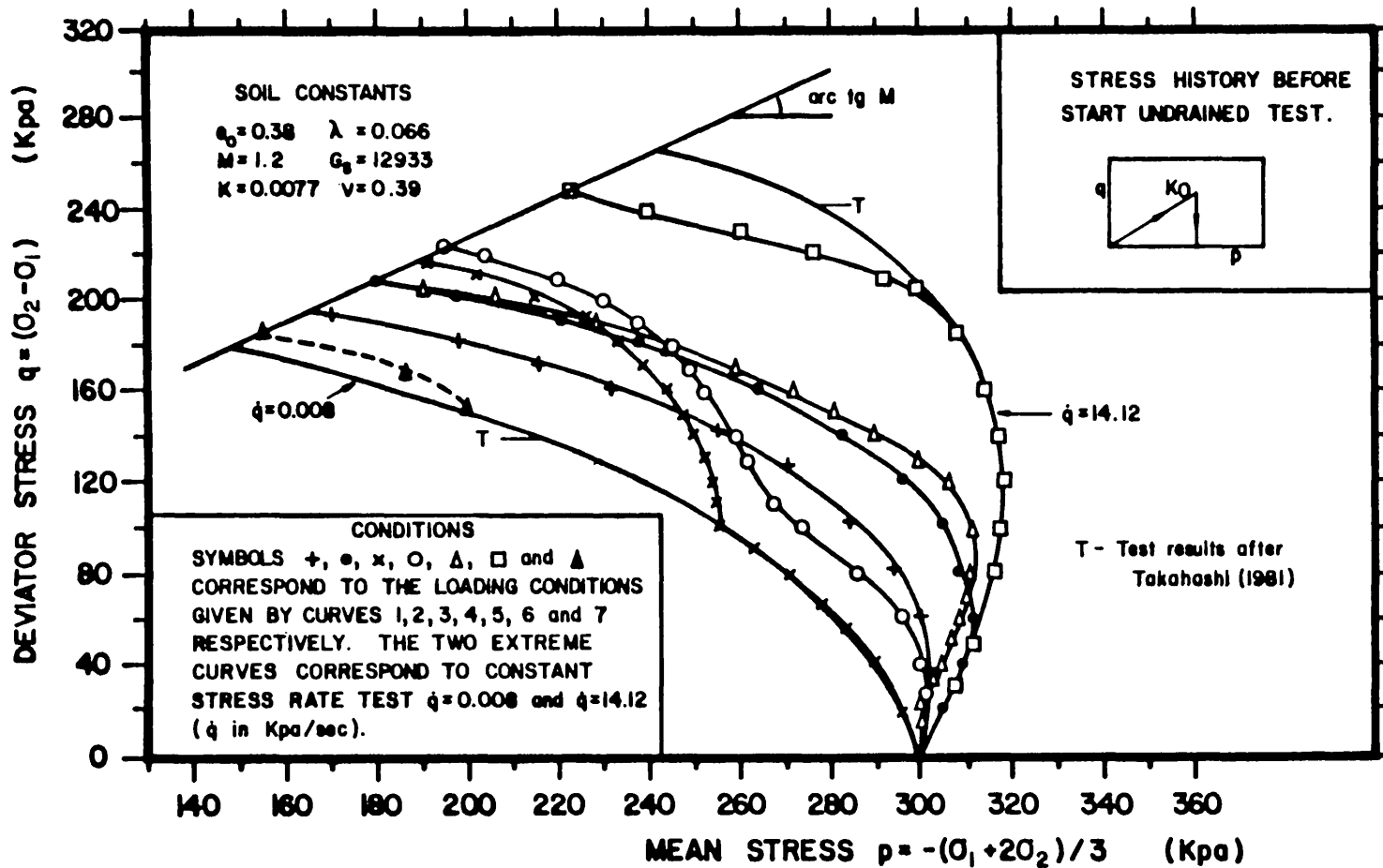


Figure VIII. 16.

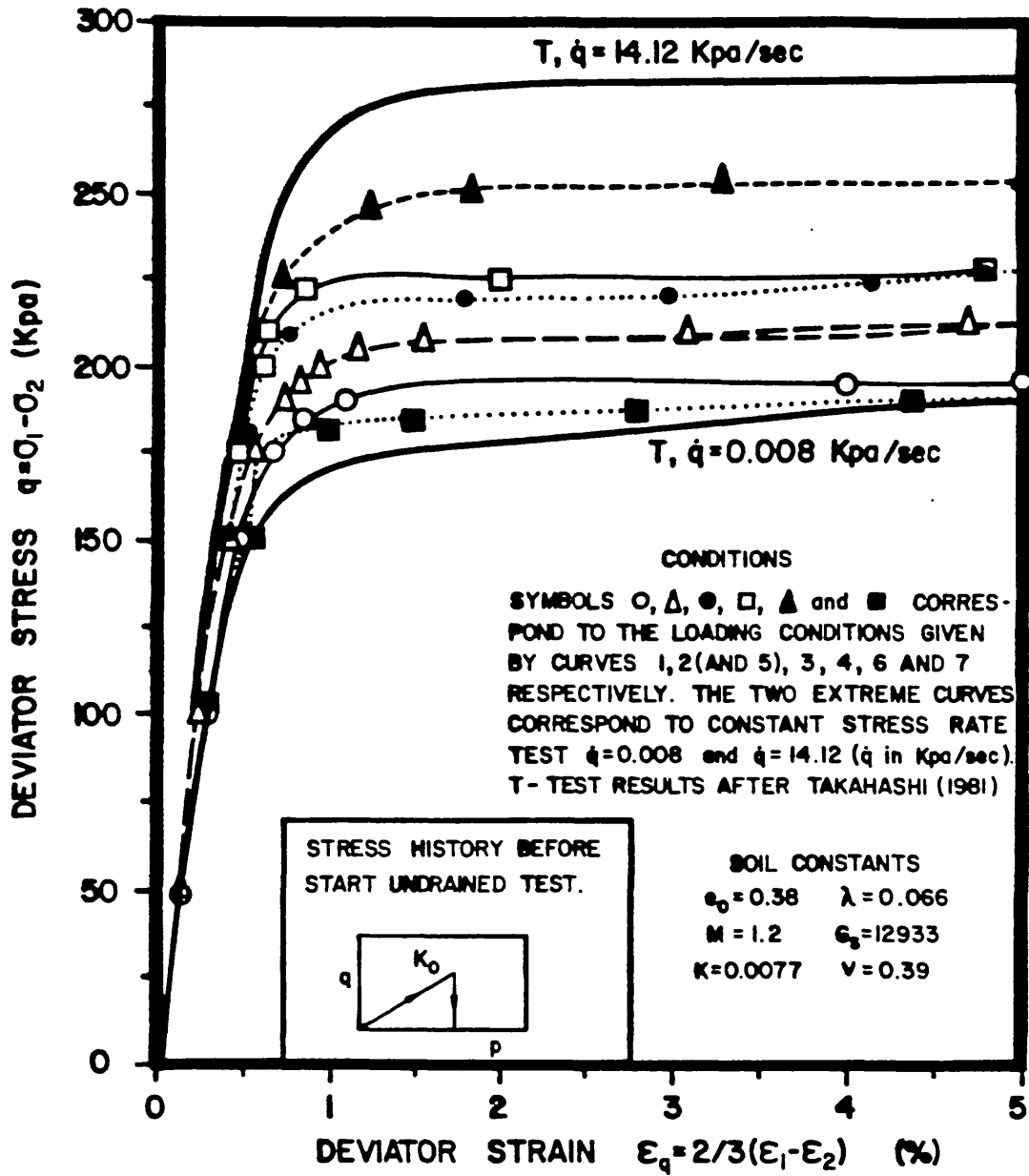


Figure VIII.17.

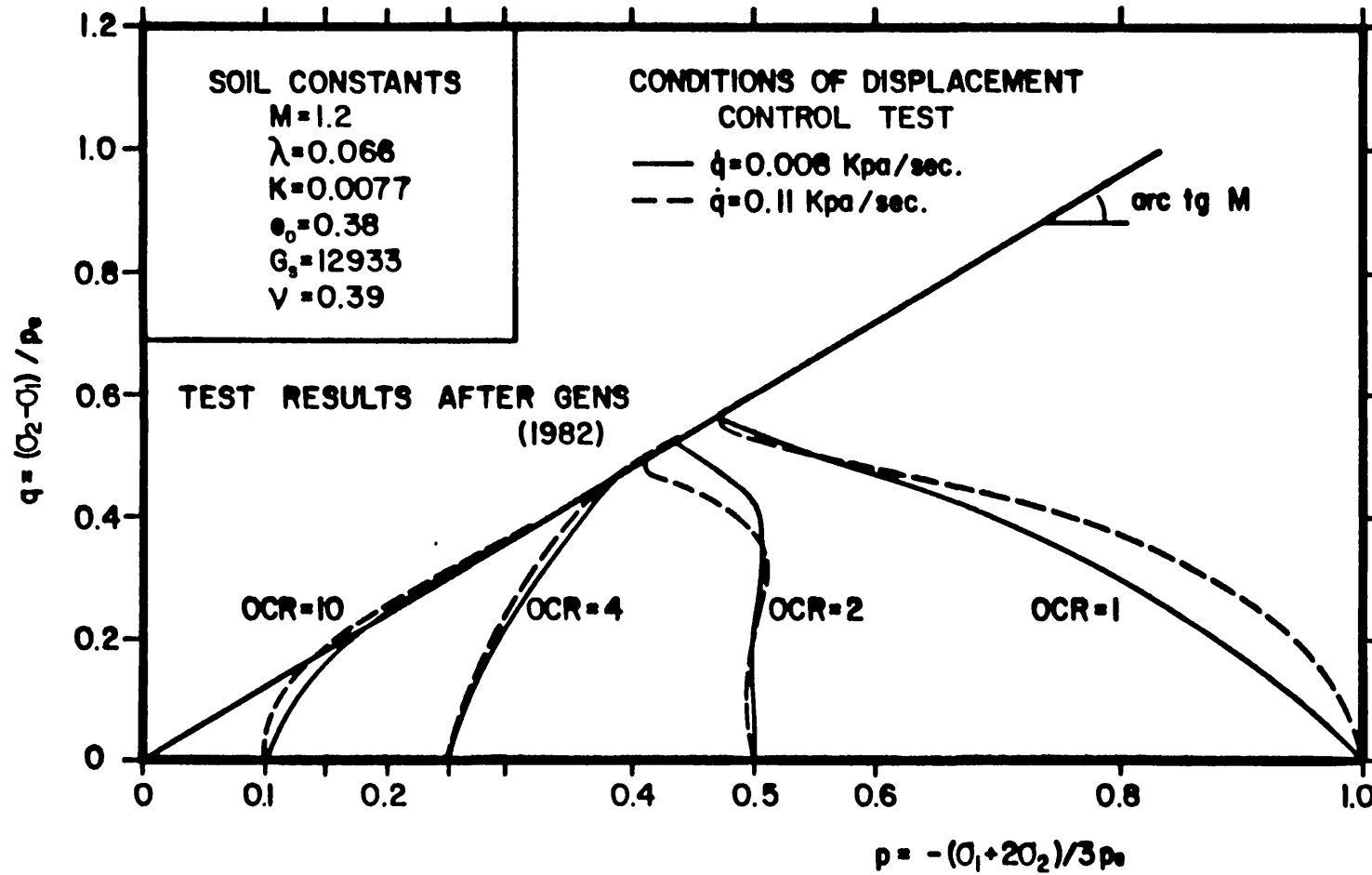


Figure VIII. 18 (a).



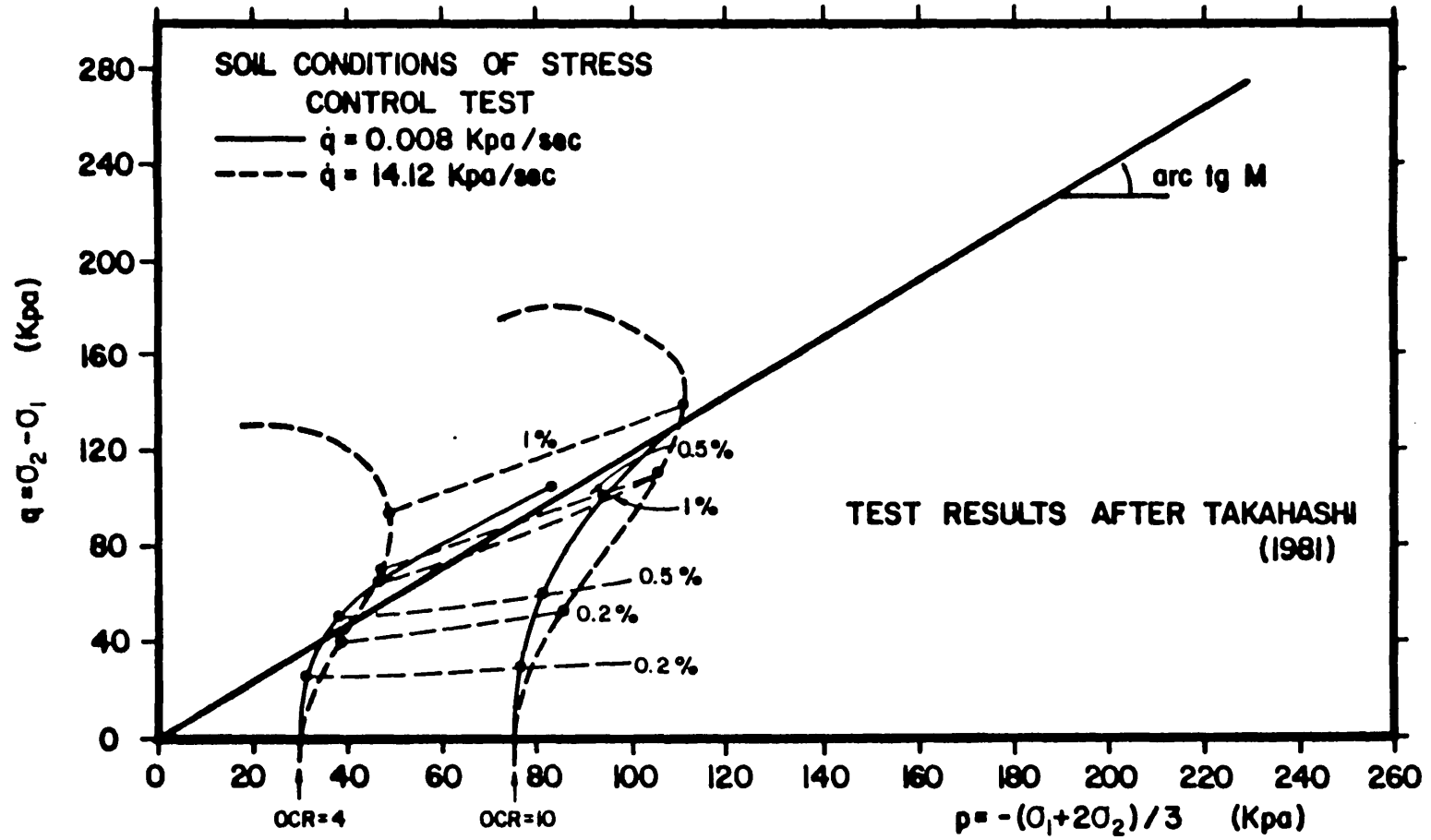


Figure VM. 18(b).

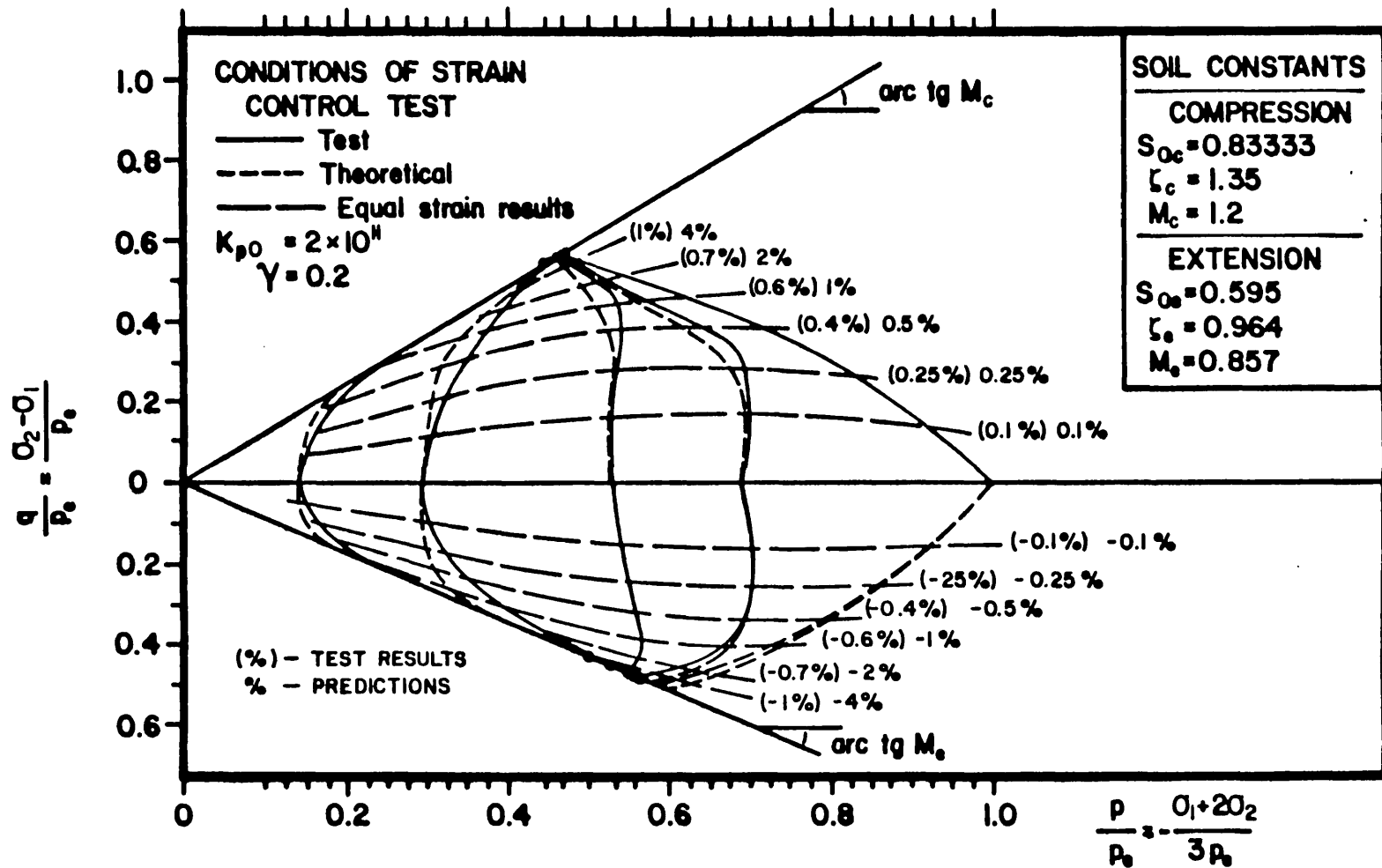


Figure VIII. 18(c).

Kpa/sec, therefore the difference in the stress path is not so pronounced. Additional difficulty will be encountered when analysing the laboratory results which considers the stress control test carried out on the same material with the constant stress rate of 0.008 Kpa/sec and 14.12 Kpa/sec as shown in the Figure VIII.18b. The influence of stress rate increase in this stress control test is the opposite when compared with the displacement control test of Figure VIII.18a. It is acceptable however that the displacement control test gives more reliable results, Hight (1981) and De Campos (1984).

The model can predict the two effects according to the parameters adopted but for the time being, the material behaviour in this region it is going to be considered stress rate independent and the prediction for any stress rate and its laboratory results are compared in Figure VIII.18c. The stress path predicted can be seen to be quite reasonable whilst the deformation prediction still need some improvement. However, considering that the deformation level is too small and the laboratory results' precision to this level of deformation is doubtful, the prediction can be acceptable.

## 6.2 Elasto-Viscoplastic-Plastic

In this model the viscoplastic strain rate is determined as function of the two independent variables: The stress level and time . This is completely fictitious since it is known that the viscoplastic strain rate is a function of the stress rate and stress level as presented in the previous section. The choice of such model for finite element application ,in the case of this thesis, is merely due to its

simplicity.

The elasto-viscoplastic model presented previously, however, can also be used in finite element method but its application is going to be a subject for future research.

Before presenting the experimental verification of this model for some restricted circumstances the introduction of the creep law is necessary.

#### Creep Law:

The creep law which is going to be presented here is similar to the one proposed by Singh and Mitchell (1968), Lovenbury (1969), Larsson (1977) for triaxial test conditions. The difference lies in that the creep law is decomposed into two components, according to the shape of the plastic potential. As normality is assumed, the creep law is broken into two components rate  $\dot{\epsilon}_q^{vp}$ ,  $\dot{\epsilon}_v^{vp}$ , according to the shape of the yield surface. Also as the shape of the yield surface depends on the stress level so will the viscoplastic strain rate components do too.

Note that the shape of the yield surface (triaxial condition) depend on the deviatoric stress level and mean stress which make the creep law dependent not only to the deviatoric stress but to the mean stress, too.

In addition, it seems reasonable to take explicit time hardening into

account.

The stipulation of the functional expressions  $\Phi(F)$  is still involved with great uncertainty because most of the available results are from undrained test with free development of pore-pressure. This means that the effective stresses were not kept constant and relaxation in mean stress and creep in deviatoric strain occurred simultaneously.

With these shortcomings in mind an explicit time hardening law can be proposed as:

$$(VIII.4.49) \quad \gamma(t) = A_c \left( \frac{t_r}{t_i + t} \right)^{m_c}$$

For the functional creep law  $\Phi(F)$  two expressions are suggested, a linear one for the overconsolidated region and an exponential one for the normally consolidated region, that is:

$$(VIII.4.50) \quad \Phi(F) = \begin{cases} F^{\frac{1}{2}}, & F \leq F_0 \\ F_0^{\frac{1}{2}} - 1 + \exp[\alpha_c(F^{\frac{1}{2}} - F_0^{\frac{1}{2}})] & F \geq F_0, \end{cases}$$

These expressions were suggested by laboratory results carried out by Lovenbury (1969), Larsson (1977), Singh and Mitchell (1968), and are some of the many suggested by Perzyna (1966)

$t_r$ , represent a reference time, often chosen as 60 sec.

The creep parameters  $A_c$ ,  $m_c$  and  $\alpha_c$  are determined from tests where the total effective stress state is kept constant and not only the

deviator stress.

The time hardening parameter  $m_c$  is determined by plotting  $\ln|\dot{\epsilon}^{\text{vp}}|$  versus  $\ln t$  from testing for  $t \gg t_i$  and an arbitrary but constant value of  $F$ . (see Figure VIII.19). The parameters must be chosen in a way that the initial conditions of no creep strain can be satisfied for an arbitrary development of stresses, say, in pure creep with constant stresses. For  $m_c$  to be arbitrary one must choose  $t_i > 0$ , otherwise the restriction  $m_c < 1$  must be imposed. Usually  $t_i$  is chosen as 1 sec. for pure creep test.

To completely define  $F$  the reference value  $f_2^r$ , as stated previously, must be chosen. It is convenient to adopt  $f_2^r$  equal to  $2a^2$ , that is the value for  $p^2$  which satisfy  $f^2$  for  $q^2 = 0$ . It also seems reasonable to consider that  $p^2 = 2a^2$  is the in situ mean stress, which means that the in situ stress lie in the quasi-static yield surface and consequently there is no creep occurrence in situ. Further  $F_0$  is defined as the value of  $F$  for stresses on the initial (dynamic) yield surface. Such stress state is defined by  $p = 2a^1$  and  $q = 0$ . Thus, for the triaxial test conditions and isotropic material  $F_0 = 2a^1 / 2a^2 = \frac{a^1}{a^2}$ . Assuming that  $f^2$  and  $f^1$  are of the same shape. The value of  $F_0$  can be estimated basically from two undrained test, one slow to define the shape of  $f^1$  and  $f^2$  and other fast to evaluate the constant  $F_0$ . See Figure VIII.20.

To determine  $A_c$  and  $\alpha_c$  the plot of  $|\dot{\epsilon}^{\text{vp}}|$  versus  $F^{\frac{1}{2}}$  should be considered for a certain time  $t = t_r - t_i$ . The value of  $A_c$  and  $\alpha_c$  are estimated as shown in Figure VIII.21.

### Experimental Verification:

The proposed creep law given by equations (VIII.4.49) and (VIII.4.50) will now be compared with laboratory test. The triaxial undrained test carried out by Larsson (1977) will be used. First the samples were consolidated to the in situ stress and then the deviatoric stress were increased to a certain level and kept constant. Relaxation in mean stress and creep for the vertical stress increases to three different levels in the overconsolidated region as shown in Figure VIII.22 and VIII.23. for Swedish clay.

Assuming linear elasticity for rapid loading, the stress path is pure deviatoric without any increase in the effective mean stress. Some deviation from this assumption was reported at the experiments. Relaxation in mean stress is demonstrated in Figure VIII.22 where the effective mean stress moves horizontally to the left along the stress paths. The vanishing stress rates reported will be the locus of the observed quasi-static yield surface which can be compared with the theoretical quasi-static yield surface obtained from the creep law given by equations (VIII.4.49) and (VIII.4.50).

It will be assumed that the quasi-static yield surface is isotropic and passes through the in situ stress point. Because the model is completely fictitious the shape of the quasi-static and inviscid yield surface will be considered as an ellipse. Thus, the following soil constants will be adopted:

$$\phi = 30^\circ, K_0 = 0,84, a^2 = 20.87Kpa, p = 40.65Kpa, q = 7.14Kpa, a^1 = 28.3Kpa,$$

$$K_s = 2500Kpa, G_s = 1154Kpa, t_i = 1sec., t_r = 60sec., m_c = 0,7, A_c = 1.10^5$$

Since only elastic and creep deformation occurs in this region, the stress strain relationship can be simplified to:

$$\dot{\epsilon}_q = \frac{\dot{q}}{3G_s} + \gamma(t) F^{\frac{1}{2}} \quad n_q = \frac{\dot{q}}{3G_s} + h_q(p, q, t), \quad \dot{\epsilon}_v = \frac{\dot{p}}{K_s} + \gamma(t) F^{\frac{1}{2}} \quad n_p = \frac{\dot{p}}{K_s} + h_p(p, q, t)$$

where

$$n_q = \partial f / \partial q \left[ \left( \frac{\partial f}{\partial q} \right)^2 + \left( \frac{\partial f}{\partial p} \right)^2 \right]^{\frac{1}{2}}$$

$$n_p = \partial f / \partial p \left[ \left( \frac{\partial f}{\partial q} \right)^2 + \left( \frac{\partial f}{\partial p} \right)^2 \right]^{\frac{1}{2}} \quad \frac{\partial f}{\partial q} = 2q/n^2, \quad \frac{\partial f}{\partial p} = 2(p-a^2)$$

For the mixed loading programme it becomes,

$$\dot{\epsilon}_q = \frac{\dot{q}}{3G_s} + h_q(p, q, t)$$

$$\dot{p} = K_s \left[ \dot{\epsilon}_v - h_p(p, q, t) \right]$$

In the undrained test, previously described, after the instantaneous deformation have occurred, the deviatoric creep strain and the relaxation in mean stress can be evaluated by considering the initial value problem.

$$\dot{\epsilon}_q = h_q(p, c, t) \quad p(0) = p_i$$

$$\dot{p} = K_s h_p(p, c, t) \quad \dot{\epsilon}_q(0) = 0$$

where  $c$  is the initial value of  $q$  and  $p_i$  is the initial value of  $p$ .

The result of this equation is plotted on Figure VIII.22 and Figure VIII.23.

Thus, it can be seen that the theoretical quasi-static surface lies on the left of the experimental one. This can be explained by the fact that the rapidly load increase makes the mean stress to increase and



in the theoretical calculation the effective initial mean stress has been considered constant.

In the Figure VIII.23 the theoretical prediction shows that for lower deviator stress level there is a tendency of the strain to decrease non-linearly while for higher deviatoric stress level this tendency is not observed at least for the time interval considered.

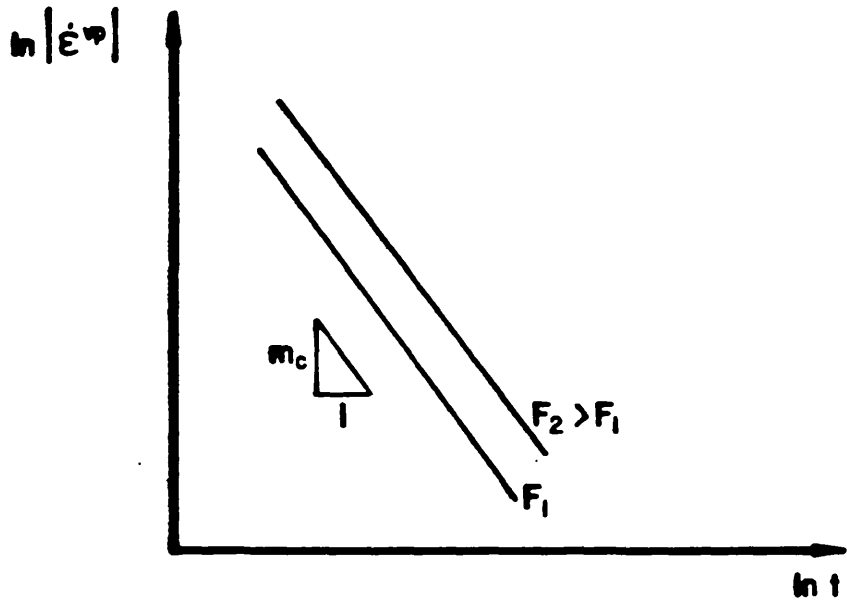


Figure VIII. 19.

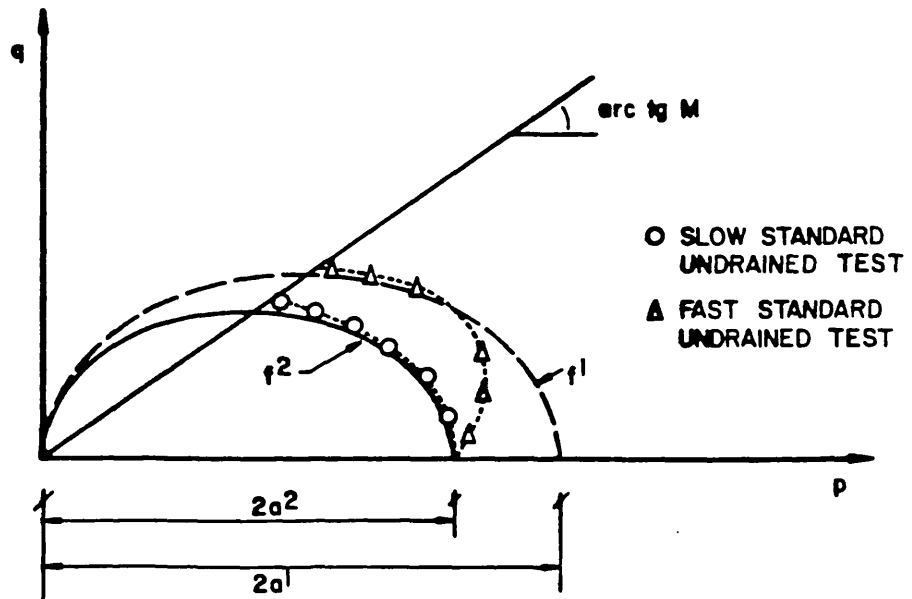


Figure VIII. 20.

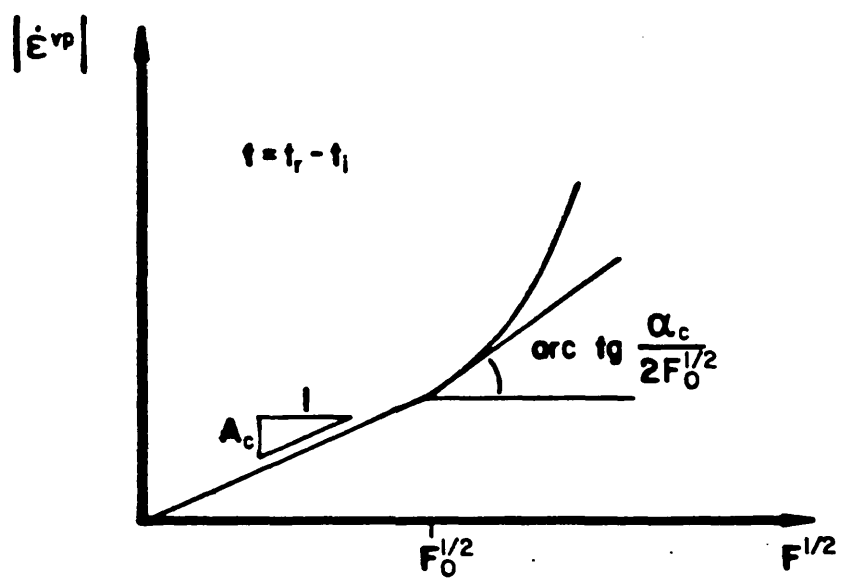


Figure VIII. 21.

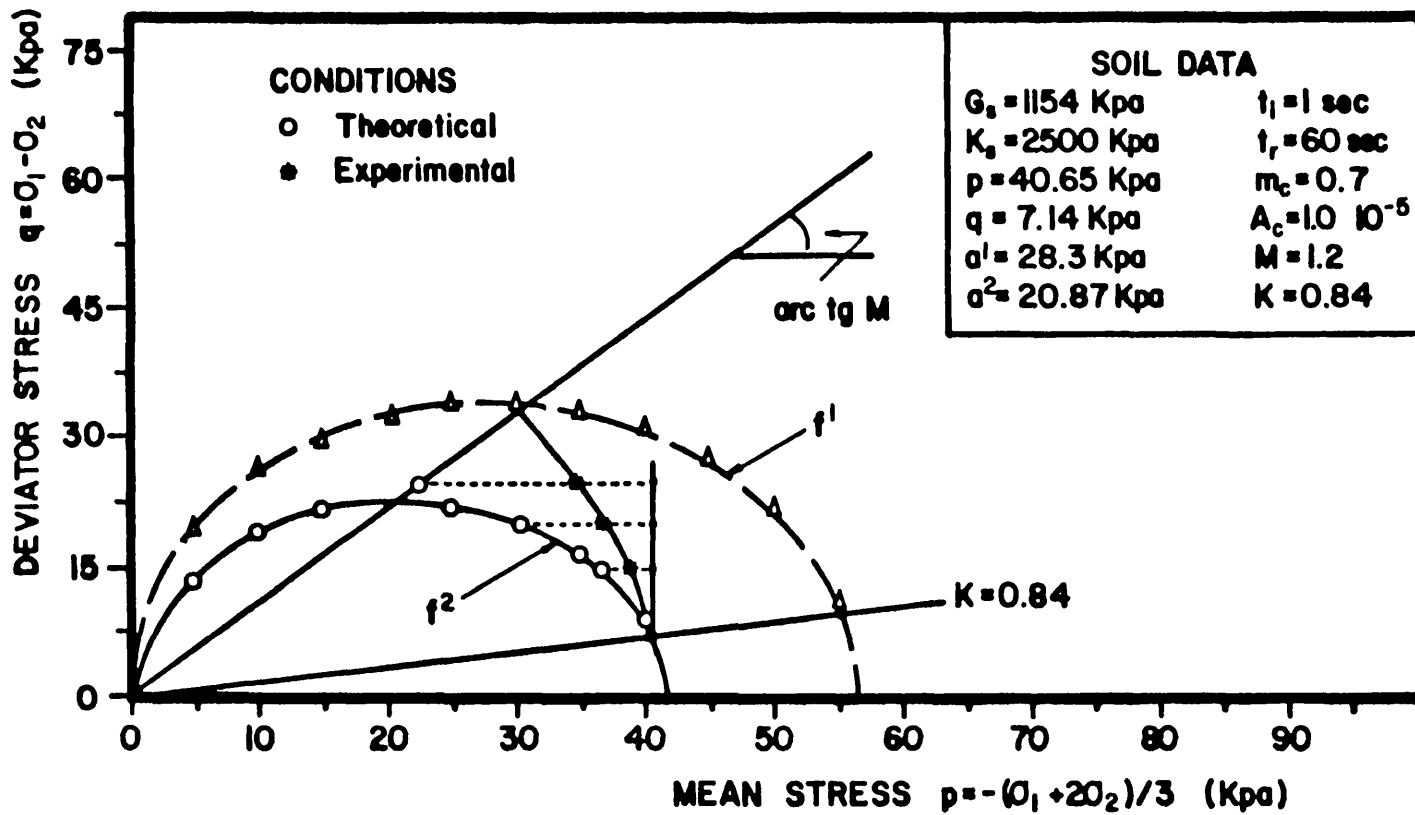


Figure VIII. 22.

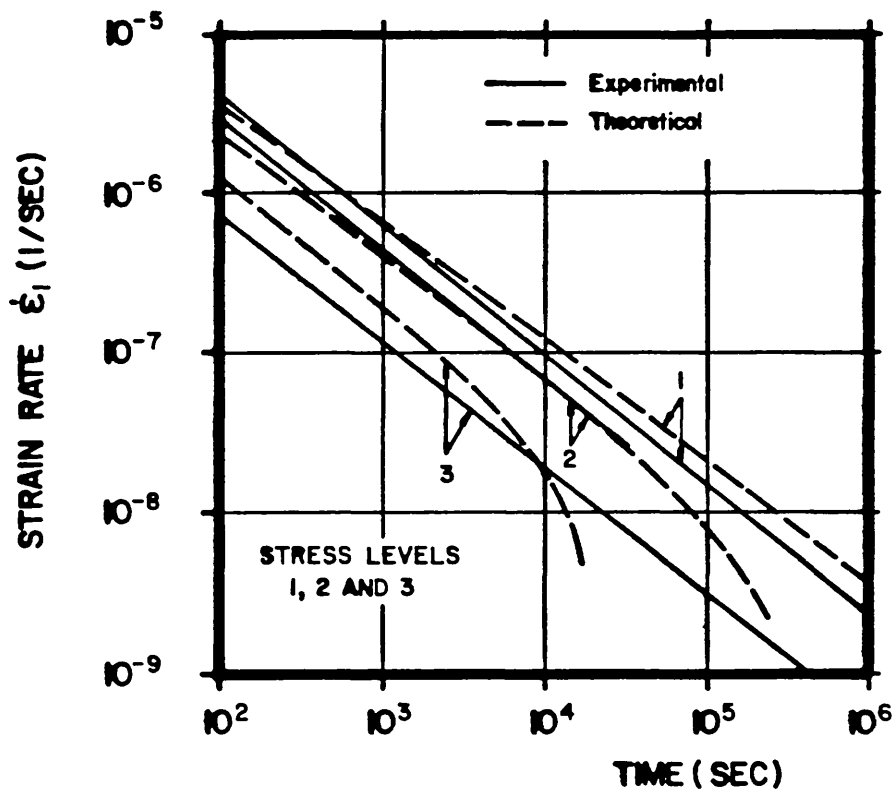


Figure VIII. 23.

CHAPTER IXSAMPLE SOLUTIONSIX.1 Introduction

Based on the assumptions discussed in previous chapters a computer program has been developed with the aim of evaluating stresses, strains, pore-pressure and displacement in plane strain and complete axi-symmetric conditions. Static analyses using non-linear geometry and material were allowed. Material non-linearity refers to the elasto-plastic, elasto-plastic-viscoplastic skeleton stress-strain relationship and the non-linear permeability matrix. The linear model considers isotropy and orthotropy and although the general elasto-viscoplastic-plastic model proposed includes orthotropy, the program is restricted to non-linear isotropy.

For the geometric non-linearity only up-dated Lagrange is considered.

Additional facilities such as field construction, dam reservoir filling and long term seepage through an earth dam are included. For the field construction the incremental loading scheme suggested by Clough and Woodward (1966) is used.

The program uses variable 3 to 8 nodes isoparametric elements and the active column solution techniques developed by Bathe and Wilson

(1973). Although the use of the same number of nodes for pore-pressure and displacement are not supported by the theory, because of the incompatibility of inter-element boundary conditions, it has not been noticed to have produced any harm. Furthermore, it has actually improved the accuracy for pore-pressure calculation. In the column solution technique the out-of-core stiffness matrix is stored in a block form, with a minimum of two.

The solution of the system of equations with an indefinite coefficient matrix is performed by a direct Crout method, Bathe and Wilson (1976).

No input data generation nor plotting output facilities are available.

Next, the sample analysis will be selected with some objectives in mind. The first aim is to present solutions which demonstrate some of the analysis capabilities of the present program. Therefore, linear and geometrically non-linear analysis are presented using the elements and material models available in the program.

A further objective is to study the accuracy and stability of the solutions. Therefore, a comparison between the theoretical solution and the respective responses predicted by other researchers is given. In this context, the importance of equilibrium iteration in some analysis is investigated.

The non-linear solutions have been obtained using the algorithm presented in chapter VII. For static non-linear consolidation, undrained analysis and long term settlement the equilibrium iteration depends on the load-time step. For example, the drained, undrained and partially drained standard triaxial test for geometric and material

non-linearity with 44 load-time steps requires one or two equilibrium iterations to converge to the required tolerance ( tolerance  $< 0.001$ ). However, a geometrically non-linear consolidation test with a very small time increment (time factor less than  $0.001$ ) requires changing the general stiffness to achieve the convergence requirement. Nevertheless, there is little practical interest in consolidation problems over such a small initial time.

An important problem is the optimization of the load steps in non-linear analysis. Although in this work no specific attention has been given so far to this problem, it should be noted that the order of all systems considered in this report was small and the computer time used rather negligible.

## IX.2 Static Linear Analysis

### IX.2.1 General

A few sample solutions will be chosen to be compared with closed analytical solutions and other investigators researchers.

First, the one-dimensional case and subsequently the two-dimensional case is analysed. In the one-dimensional case fixed boundary conditions are considered first and then variable boundary conditions are discussed.

The boundary conditions, the material profile, and the material constants are given separately in each example. For this section



linear elasticity and isotropy is assumed. As a consequence of the linear elasticity assumption the stresses and strains in situ are irrelevant. Also, the coupled theory and the uncoupled theory for one-dimensional analysis coincides. In the two-dimensional analysis the two theories will be shown to be distinct.

The Terzaghi case and the problem of two-contiguous finite layer with the same compressibility but with two different constant permeabilities are analysed.

The two-dimensional plane strain problem with infinite thickness is considered and compared to the closed analytical solution. One of the aims here is to show that the finite element solution, by being coupled, can detect the Mandel Cryer effect.

Finally, an axi-symmetric problem (deformation and flow in three-directions) with a finite continuous length is considered.

### IX.2.2 One-dimensional Tests.

**Fixed boundary conditions:**

1. Vertical deformation and flow of an axi-symmetric finite length geometry. (Terzaghi case)

A cylinder of length  $L$  cut out from a continuous layer is now considered. This cylinder is uniformly loaded with the intensity  $\bar{\sigma}$  given the uniform initial excess pore-pressure  $p_0 = \bar{\sigma}$  throughout the total length  $L$ . Free drainage is assumed at the top whilst the bottom

is considered impervious. Complete axi-symmetry is considered in the analysis.

If  $m_v$  is the compression modulus, the uniform compressive strain and total settlement are, respectively, given by

$$\epsilon'_z = \bar{\sigma}/m_v \quad \text{and} \quad w' = \bar{\sigma}L/m_v$$

The usual definition of consolidation factor is given by

$$U = 1 - \frac{1}{\bar{\sigma}L} \int_0^L p(z) dz$$

which is equivalent, in this one-dimensional case, to  $U = w/w'$ , where  $w$  is the current settlement. Care must be taken because the numerical errors in the space discretization may cause the two expressions not to coincide in the computation.

The set of graphics presented in Figure IX.1a, b represent, respectively, the pore-pressure generation  $p/\bar{\sigma}$  versus the depth ratio  $z/L$  and the average pore-pressure dissipation versus the time factor. The 8 equal element mesh was used in this example, though a 5 variable size element mesh, where the upper elements are thinner, could be used, and would give the same accuracy in the results (not presented here). The schematic problem with its boundary conditions is also included in Figure IX.1a and IX.1b.

The percentage of settlement  $U$  plotted against the vertical time factor  $T_v$  are both given by the equation,

$$T_1 = C_{v1} t / L^2 \quad \text{and} \quad C_{v1} = \frac{k}{\gamma_f} \frac{E(1-\nu)}{2(1+\nu)(1-2\nu)} = \frac{k}{\gamma_f m_v}$$

$t$  is the length of time,  $E$  is the elastic modulus,  $\nu$  is the Poisson ratio,  $k$  is the permeability and  $\gamma_f$  is the unit weight of water.

It can be seen that the finite element results approximate to the exact solution of this problem very closely. Though time steps decrease with the tolerance, almost indistinguishable results are obtained for a tolerance less or equal to 0.05 (not presented here).

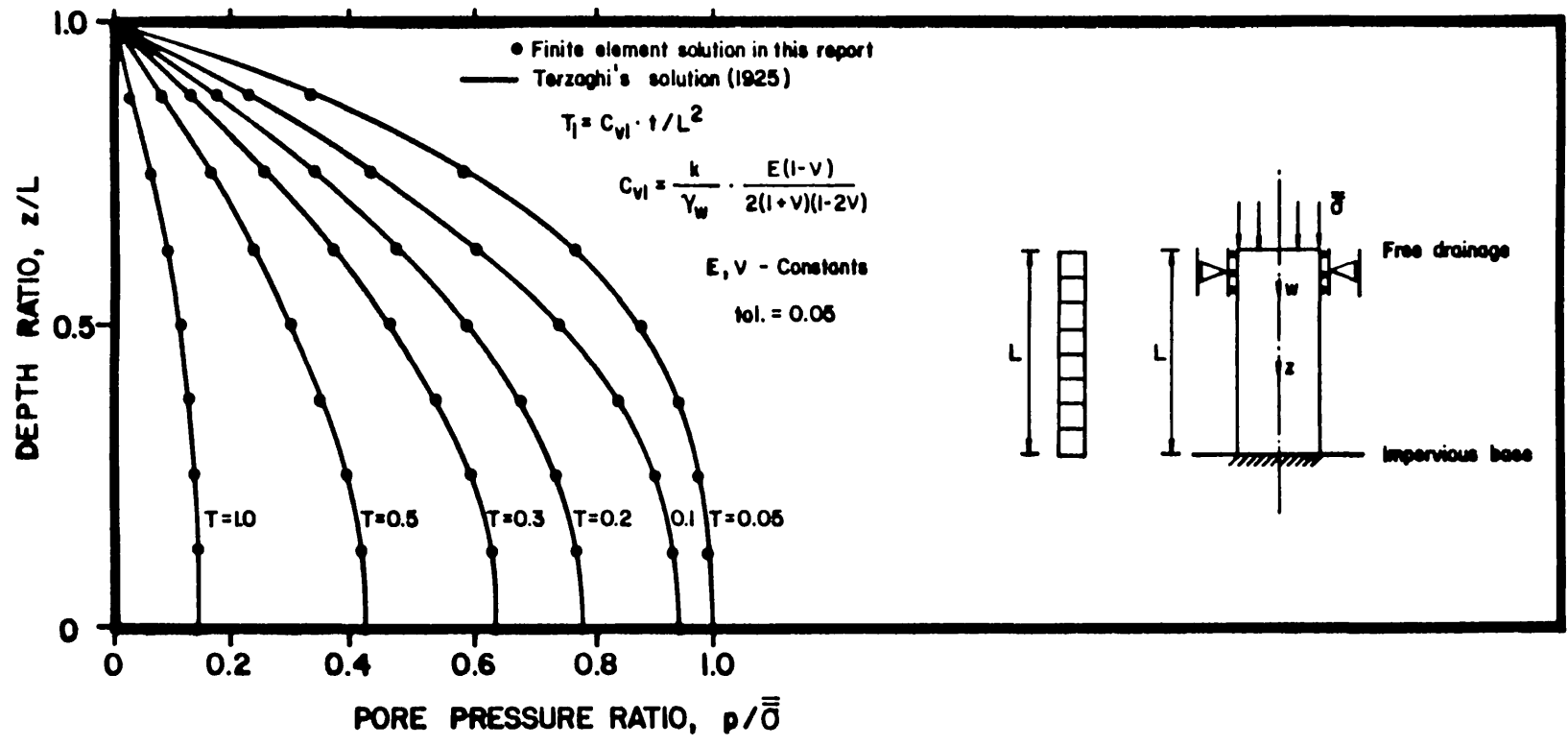


Figure IX. 1a.

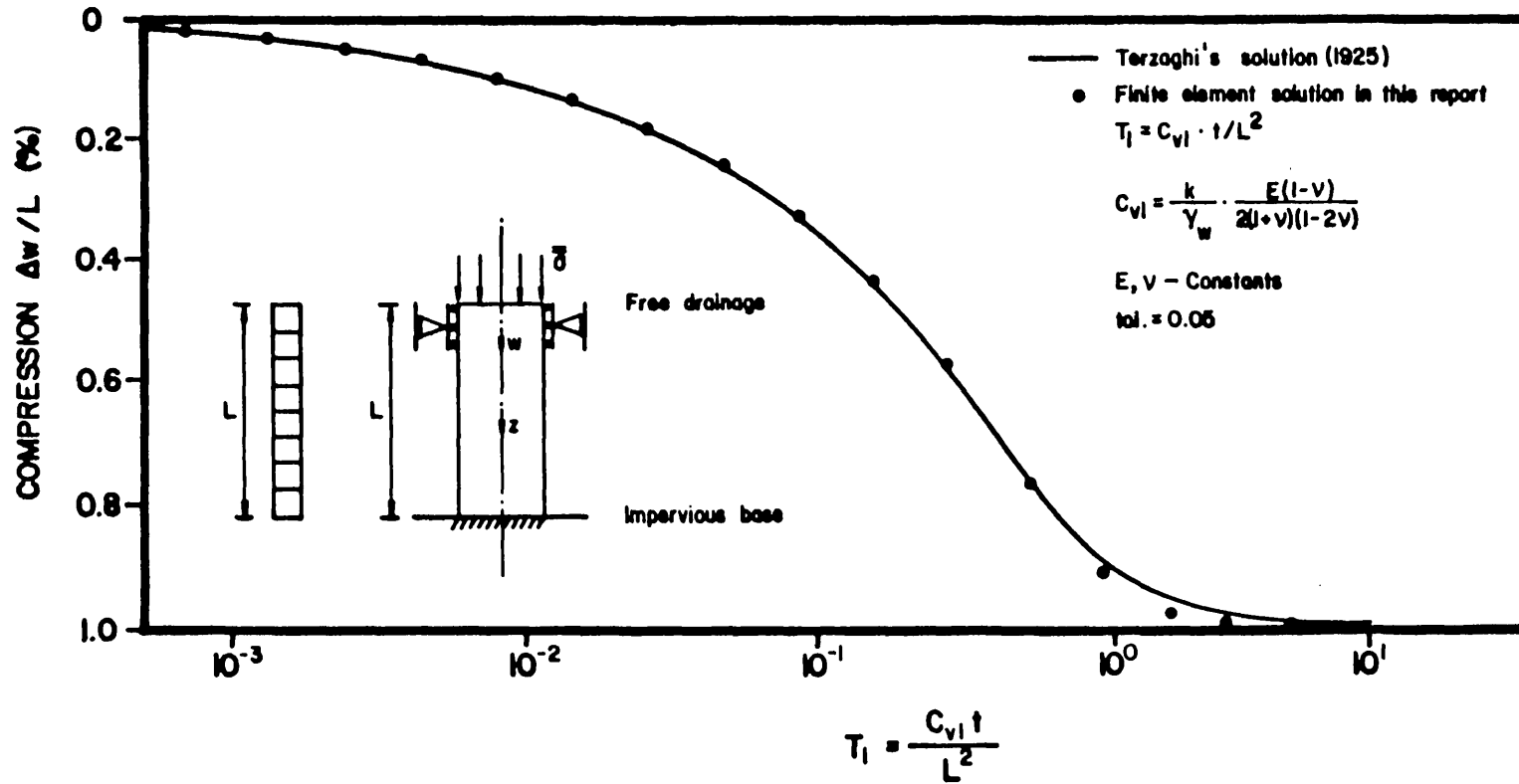


Figure IX. 1b.

## 2. Two contiguous layers

Two contiguous layers with the same compressibility, the upper being four times as permeable as the lower one, is now considered. Again free drainage is assumed at the top while the bottom is considered to be impervious.

Although no closed solution is known for this case, a few approximated solutions have been presented up to now. Schmidt (1924) presented a solution using a graphical procedure; Lusher (1965) proposed a solution using a computer analogy and Harr (1967) described a solution using the finite difference method. The first finite element solution were presented by Christian (1969).

Figure IX.2 presents the excess pore-pressure  $p/\bar{\sigma}$  against the depth ratio  $z/L$ , for the different solutions. In this case  $T_1$  is defined by

$$T_1 = C_{v1} t / L^2$$

and  $C_{v1}$  refer to  $C_{v1}$  of the drainage side, that is to say,

$$C_{v1} = \frac{4k_0}{\gamma_f} \frac{E(1-\nu)}{2(1+\nu)(1-2\nu)}$$

Thus, it can be seen that there is considerable spread among these results. Lusher (1965), because of the assumption involved, expected his results to be too slow. Harr's explicit finite difference procedure (computes values at the end of time steps) does not consider the compressibility of the nearby material at the interface between

two materials, and it therefore leads to a too fast consolidation. The correct solution is, therefore, expected to be between the two previous solutions. Christian's finite element solution, Schmidt's graphical procedure and the finite element solution achieved in this report coincide and lie between the two previous extreme solutions, and are believed to be accurate. However, it should be emphasized that all solutions to this problem are approximated solutions.

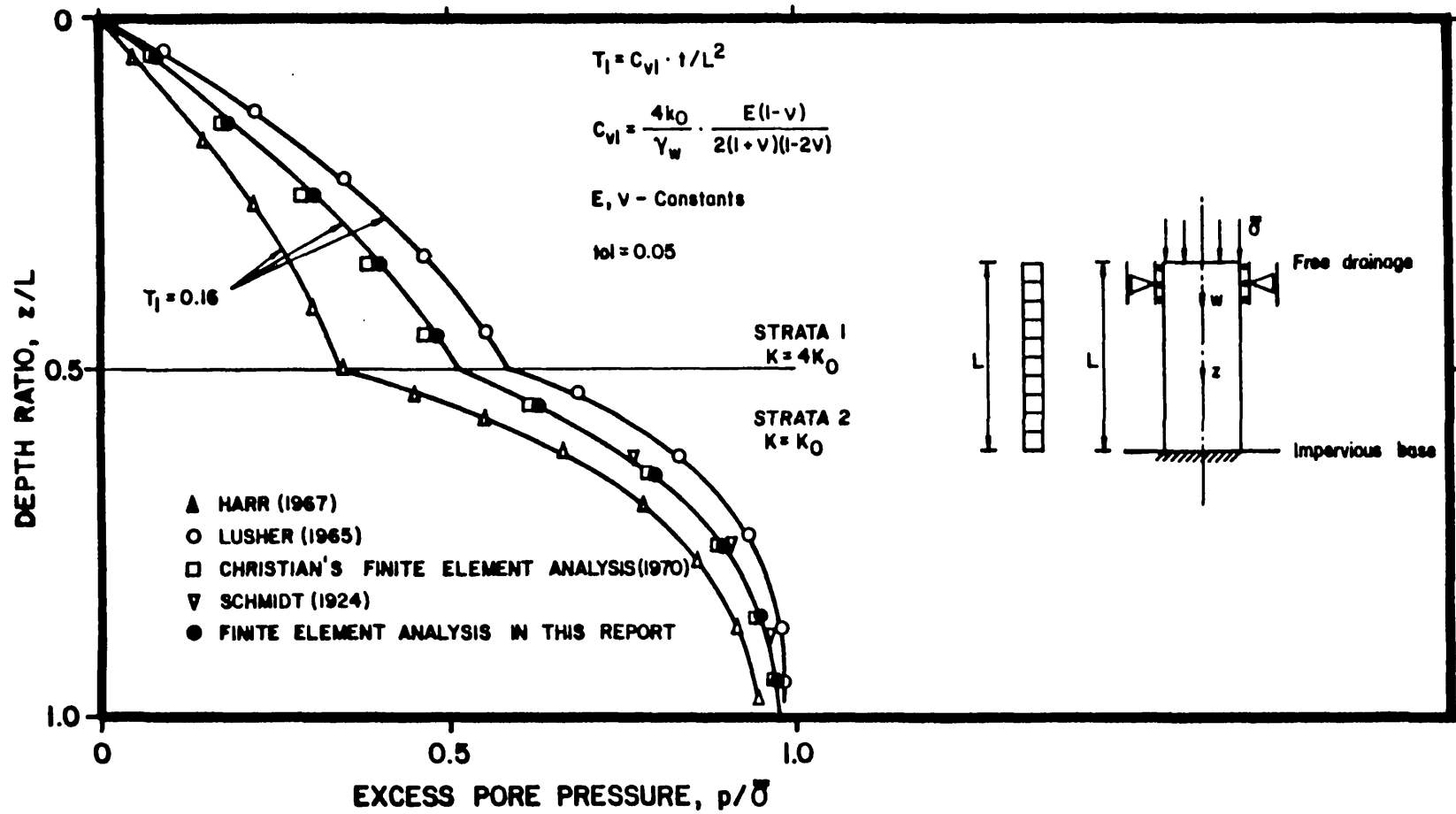


Figure IX. 2.



### 3. Variable loading conditions.

One-dimensional incremental deposition to simulate the time-dependent deposition and simultaneous consolidation of a saturated layer of material is now analysed. A closed analytical solution for the distribution of pore-pressure is given by Gibson (1958) for both impervious and permeable bases.

The time factor is defined by  $m^2 t / C_v$ , where  $m$  is the rate of deposition (units of length/time). When the time factor  $T$  is infinite, deposition is instantaneous and no consolidation occurs during deposition. When  $T$  is a finite value, it represents a finite rate of deposition, and consolidation occurs during deposition. To simulate the rate of deposition showed in Figure IX.3a and IX.3b, elements are added to the mesh at a certain time interval, as shown schematically in the right top position of Figure IX.3a and IX.3b, element number 2 is placed on top of element number 1, and element number 3 is placed on top of element number 2, and element number 4 is placed on top of element number 3 at a certain time interval.

In the Figure IX.3a the pore-pressure ratio defined by  $\bar{\sigma} / \gamma L$  ( pore-pressure by unit of total weight) is plotted against the weight ratio defined by  $z/L$  for an impermeable base and Figure IX.3b presents the same plot for the permeable base. It can be seen that the finite element solution shows good agreement with Gibson's analytical solution for both flow boundary conditions.

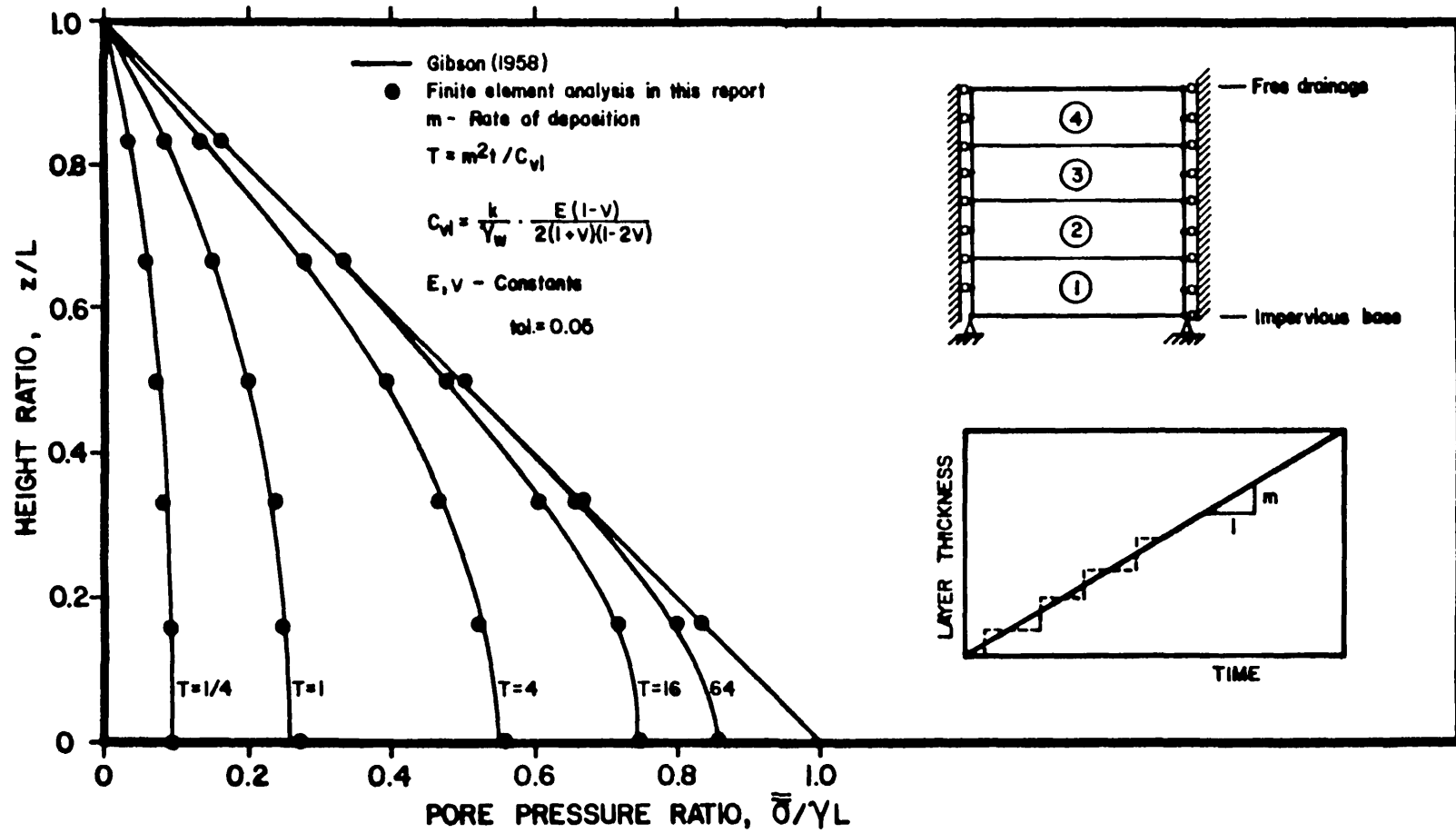


Figure IX.3a.

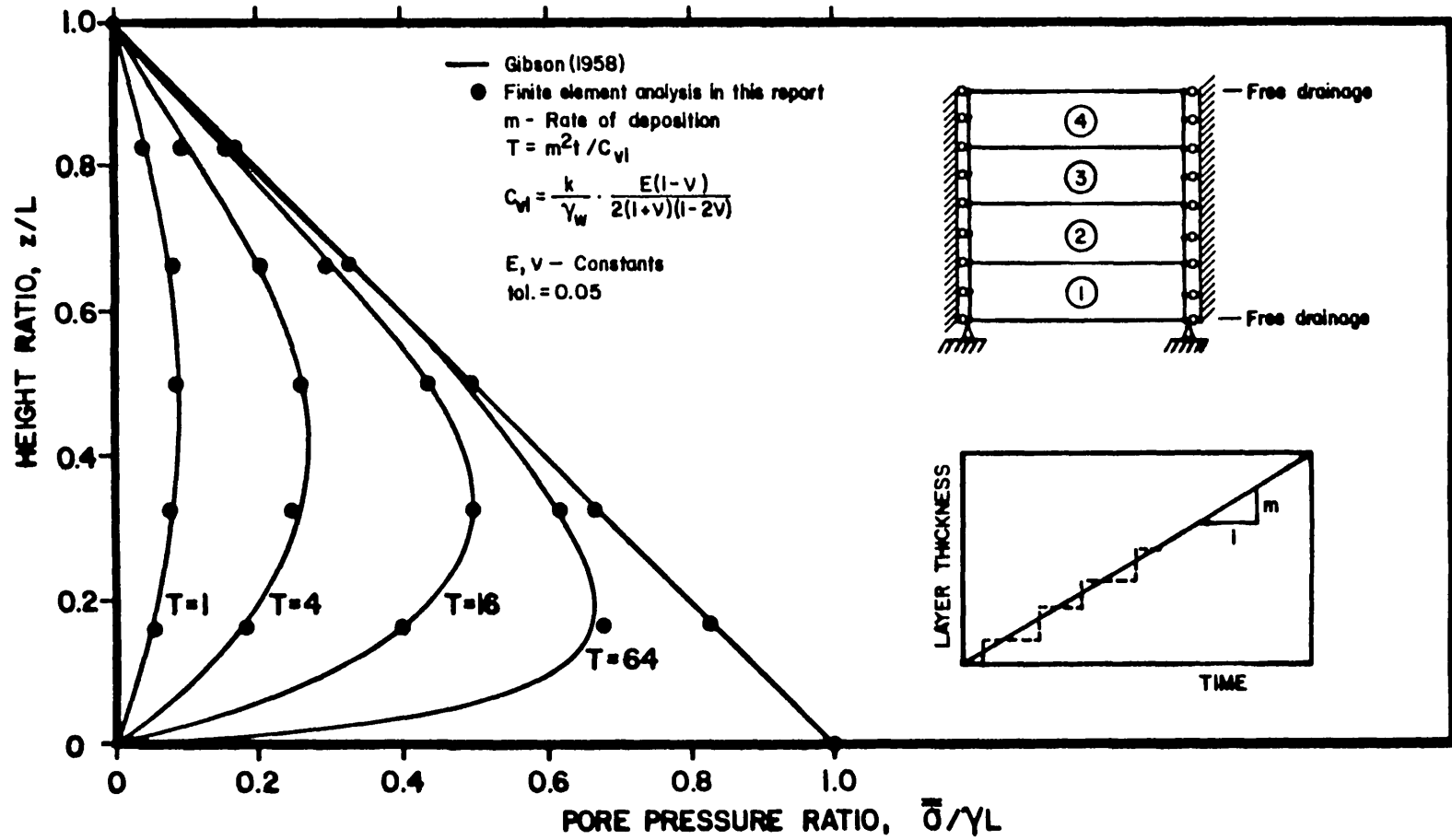


Figure IX. 3b.

### IX.2.3 Two-Dimensional Problem.

The only linear two-dimensional problem analysed here is the strip load on a half-plane where the uniform load  $\bar{\sigma}$  is applied over a width  $2a$ . Free drainage is assumed at the surface and because of the symmetry only a quarter-plane has to be analysed. Plane strain and plane flow are assumed. The general method for analytical solution for Biot's equations for complete isotropy (under the particular assumptions of this plane strain problem) is presented by McNamee and Gibson (1960a,b). Schiffman et al (1969) have evaluated numerically the stresses, pore-pressures and deformations for the uniformly loaded half-plane.

The choice of the boundary conditions for finite elements when analysing infinite regions is a difficult task. A few tentative tests are required until the boundary is sufficiently far away to ensure that they do not influence the results in the major zone of interest. The final tentative mesh, the schematic problem and its boundary conditions, and the pertinent results are presented in the Figure IX.4 and IX.5. Figure IX.4 shows the variation of excess pore-pressure beneath the centre of the loaded area, for a general  $T_2=0.1$  and Poisson ratio  $\nu = 0$ . Now  $T$  and  $C_v$  are defined by:

$$T = C_v t / a^2 \quad \text{and} \quad C_v = \frac{2G_s k}{\gamma_f}$$

where  $G_s$  is the shear modulus, and the other parameters are as already defined.

The tolerance chosen was 0.01 and the convergence can be seen to be

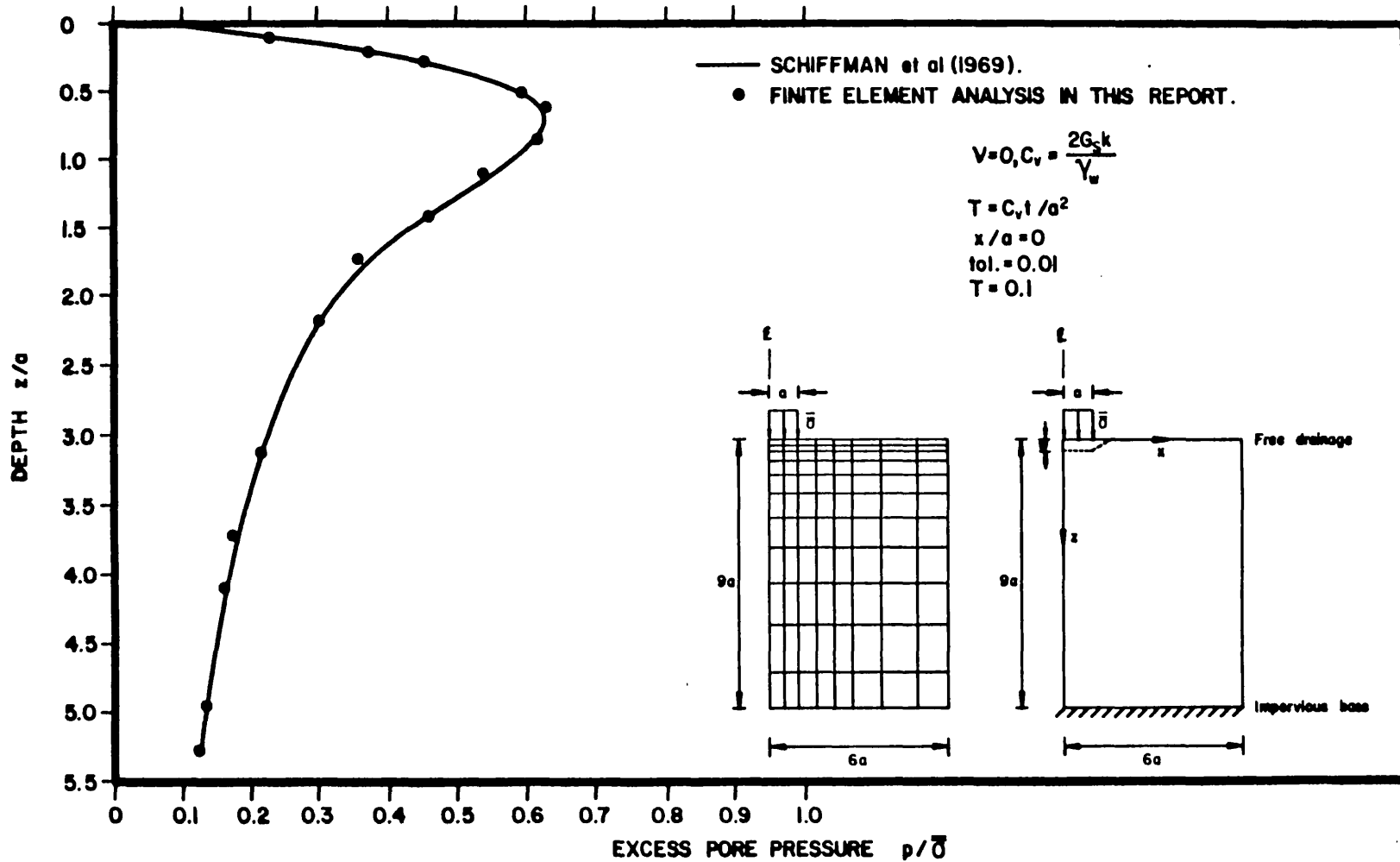


Figure IX. 4.

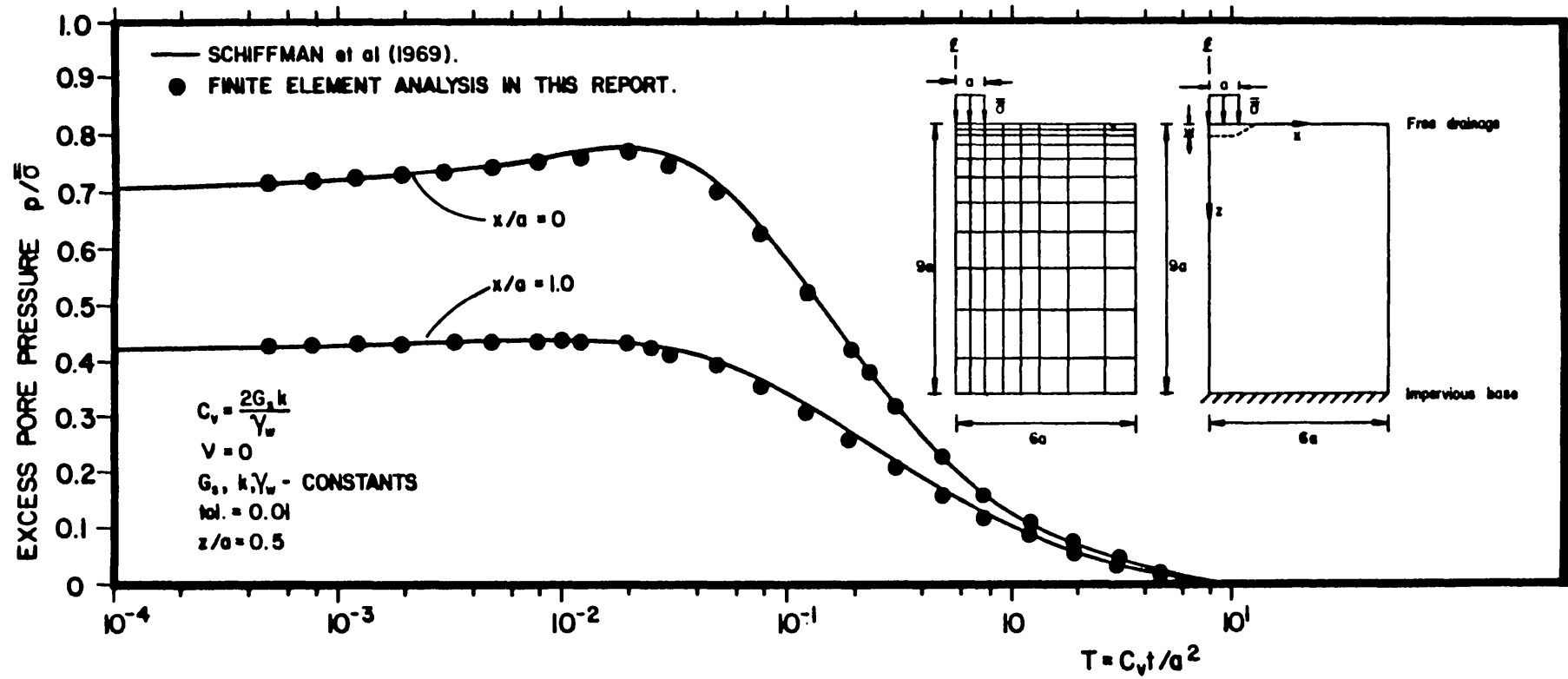


Figure IX. 5.

good for  $\beta = \frac{1}{2}$ . Certainly if the w-method (non-linear interpolation for the time integration) were used, the same degree of accuracy can be achieved with less element in the mesh. However, the accuracy is very good though this extreme situation (Poisson ratio equal to zero) is unrealistic in practice.

Figure IX.5 gives the variation of excess pore-pressure with time for two general chosen lines  $x/a = \text{constant}$  in the half-plane. Again the accuracy of the finite element program can be seen to be good. The Mandel-Cryer effect is demonstrated by both the analytical and the finite element solutions.

#### IX.2.4 Axi-symmetric Load on Finite Layer.

To show the ability of the proposed program to analyse axi-symmetric consolidation a circular area with diameter  $2a$ , uniformly loaded with an intensity  $\bar{\sigma}$ , over an finite thickness layer is now considered. Complete axi-symmetry of flow, load and deformation are assumed. Free drainage is assumed at the surface and an impervious base is considered at the bottom. The general solution for this problem (Biot's theory) is given by Gibson et al (1970).

The consolidation process at the center of the loaded area together with the schematic geometry, boundary conditions, and the final finite element mesh are given in Figure IX.6. In this figure  $s_z$  represents the settlement at the point

$$\frac{x}{a} = 0, \quad \frac{z}{a} = 0$$

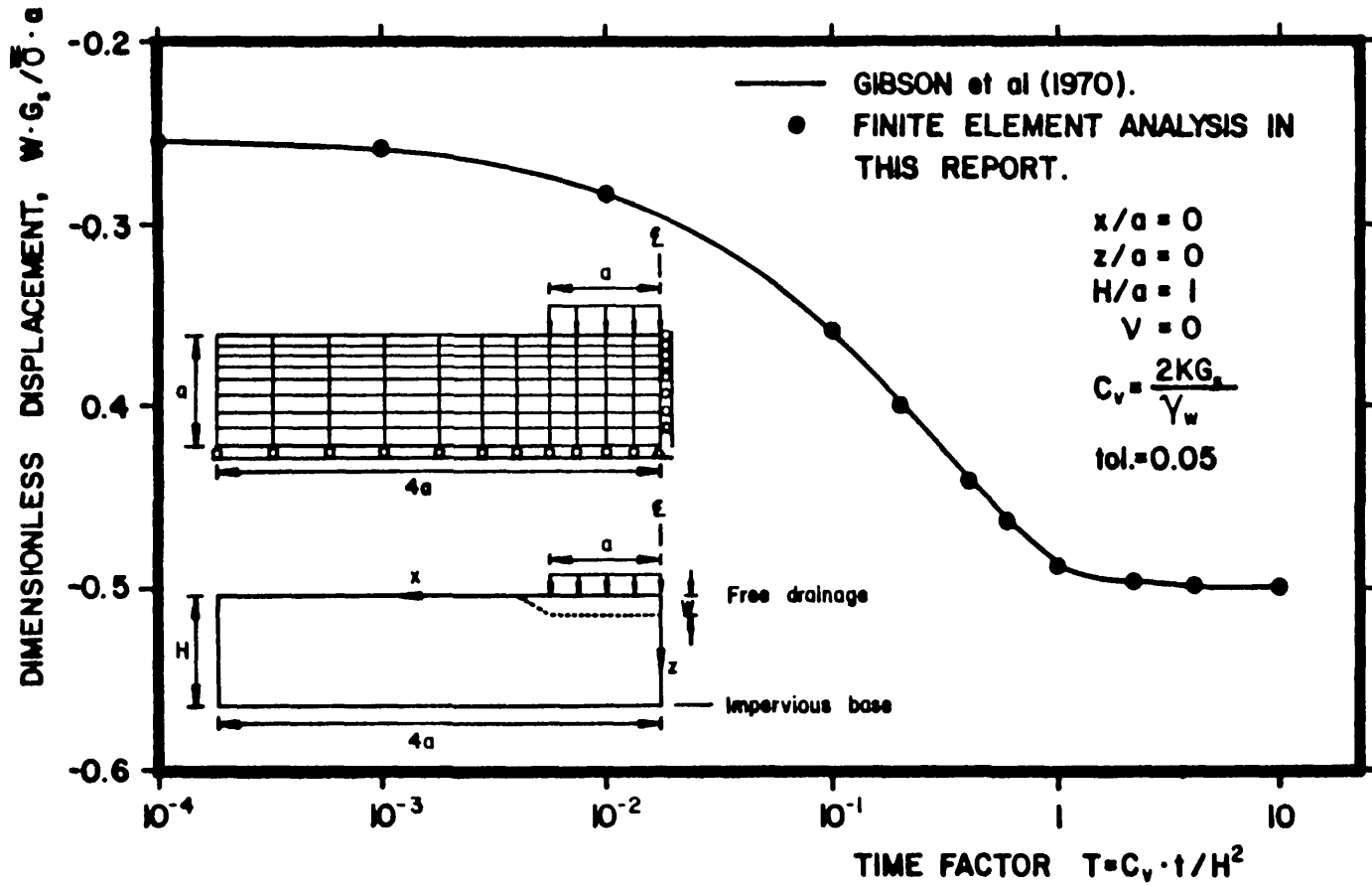


Figure IX.6.



for the conditions

$$\frac{H}{a} = 1., \quad \nu = 0.$$

The time factor  $T_3$  and coefficient on consolidation  $C_{v3}$  are given by

$$T_3 = \frac{C_{v3} t}{H^2} \quad \text{and} \quad C_{v3} = \frac{2G_s k}{\gamma_f}$$

It can be seen in this figure that the finite element solution approximates the theoretical solution very closely.

The value of  $\beta$  for the time integration was 1/2 and the tolerance 0.05.

#### IX.2.5 Creep Effect

The creep influence will be shown by comparing the finite element prediction with the laboratory test.

The oedometer test carried out by Buri (1978) on mucking clay is the one chosen to be compared with the elasto-viscoplastic-plastic model. The sample considered is a slightly overconsolidated one with OCR= 1.3. The vertical preconsolidation pressure  $\sigma_c = 65 \text{KN/m}^2$  and actual vertical stress level is at  $\sigma = 50 \text{KN/m}^2$ . The friction angle assumed is  $\Phi = 36^\circ$  and the elasticity modulus  $E = 190 \text{KN/m}^2$  and the Poisson ratio  $\nu = 0.3$  (corresponding to the Bulk modulus  $B = 238 \text{KN/m}^2$  and  $K_0 = 0.5$ ). The creep parameters are chosen as  $t_i = 1 \text{sec.}$ ,  $t_r = 60 \text{sec.}$ ,  $A_c = 1 \times 10^{-5}$ ,  $m_c = 0.75$  and the isotropic permeability is given by  $K = 1.373 \times 10^{-8} \text{ cm/seg.}$ .

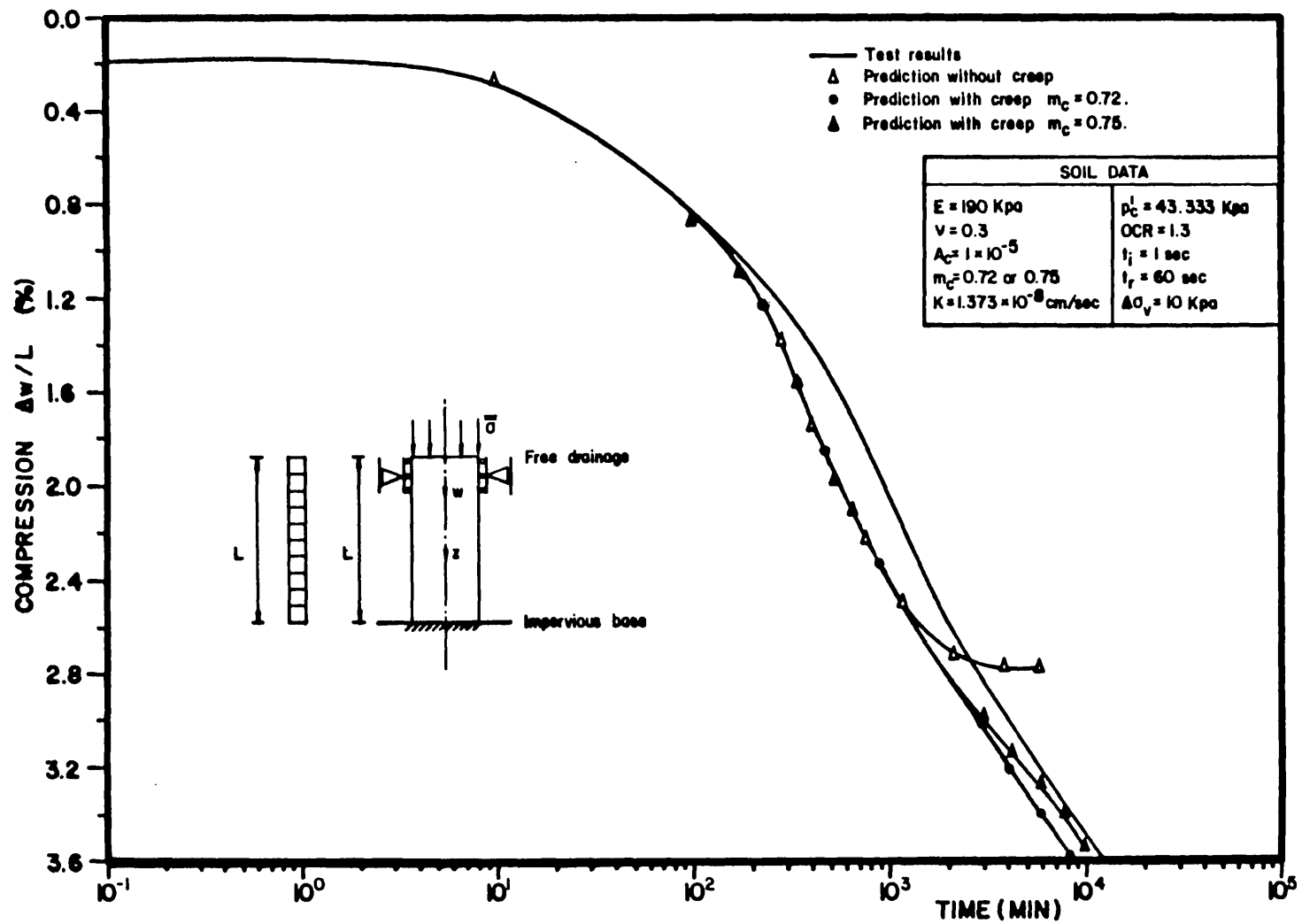


Figure IX.7.

The inviscid preconsolidation pressure can be estimated by the relation with the vertical preconsolidation pressure  $\sigma_c$  as

$$p_c^1 = \frac{1}{3}(1 + 2k_0)\sigma_c = 43.333 \text{KN/m}^2$$

As both the inviscid preconsolidation pressure  $p_c^1$  and the quasi-static preconsolidation pressure  $p_c^2$  are associated with loading along the  $k_0$ -line,  $p_c^2$  is calculated by

$$p_c^2 = p_c^1 / OCR = 33.333 \text{KN/m}^2$$

Because the additional load is  $\Delta \sigma_c = 10 \text{KN/m}^2$  the parameters associated with the behaviour in the past yield are not necessary.

The plot in Figure IX.7 shows the laboratory results of the odometer test and the finite element prediction in this report. The finite element mesh, geometric and boundary conditions are also displayed in this figure. It is demonstrated that the predicted and measured volume decrease due to creep are in good agreement. It should be emphasized that in the approach considered here no settlement can occur without volume change, and consequently without pore water flow. Finite water flow was observed in the calculation after the 'primary consolidation' had finished. The tolerance chosen was 0.05 and  $\beta = 1/2$ .

### IX.3 Static Non-Linear Analysis.

#### IX.3.1 General

Very few solutions have been developed for consolidation with the non-

linearity influence.

For geometric non-linearity some one-dimensional theories have been presented by Gibson et al (1967), Smiles and Poulos (1969), Monte and Krizek (1976) etc ... No multi-dimensional theory including the large strain effect is known to the author, and also, no material non-linearity effect has been considered in the analytical solution for consolidation (at least not to the author's knowledge). Computational results by finite element are only presented for elastic-perfectly plastic material (Carter et al (1979)).

Due to such restriction the comparison of the ability of this program with other solutions is possible only in a few cases.

For testing the geometric non-linearity effect two cases will be considered: One-dimensional flow and deformation with linear material and non-linear geometry, and secondly two-dimensional flow and deformation with elastic-perfectly plastic material and non-linear geometry.

To test the material non-linearity the only alternative is to compare with local stress-strain relationships obtained from the laboratory results. Drained, partially drained and undrained standard triaxial tests on weald clay will be considered.

The drained test is first shown and subsequently a consolidation test with drainage at both ends for different stress rate is considered. In this simulation the drained test result is achieved using a slow stress rate, the undrained test is achieved using a high stress rate and partial drained test using an intermediate stress rate.

Finally, to demonstrate the large deformation and creep influence in two-dimensional problems, the strip loading on an infinite half-plane has been considered.

### IX.3.2 Linear Material Non-Linear Geometry Analysis.

The one-dimensional flow and deformation field of an axi-symmetric load and geometry problem is now considered. Linear material behaviour and non-linear geometry are taken into account. Constant permeability and complete isotropy and null initial stress level are assumed. Different load/elastic modulus ratios ( $\bar{\sigma}/E$ ) are computed. The two extreme cases  $\bar{\sigma}/E \rightarrow 0$  and  $\bar{\sigma}/E = 1$  are plotted in Figure IX.8. The result obtained by Carter et al (1979), the finite element mesh and the initial geometry and boundary conditions are also displayed in this figure. The finite element result achieved in this report can be seen to have a very good agreement with results obtained by Carter et al (1979), despite the fact that the latter seems to have solved the problem only by updating the geometry, without iterating in each load-time step. Obviously many more load steps are necessary to converge to the right answer. Here only 44 load-steps are needed to converge, since  $\beta = 1/2$  and tolerance = 0.01 are chosen.

### IX.3.3 Elasto-Perfectly Plastic Material and Non-Linear Geometry

The two-dimensional elasto-perfectly plastic consolidation problem of a rigid strip loading on a finite layer of soil lying on a smooth rigid base is now considered.

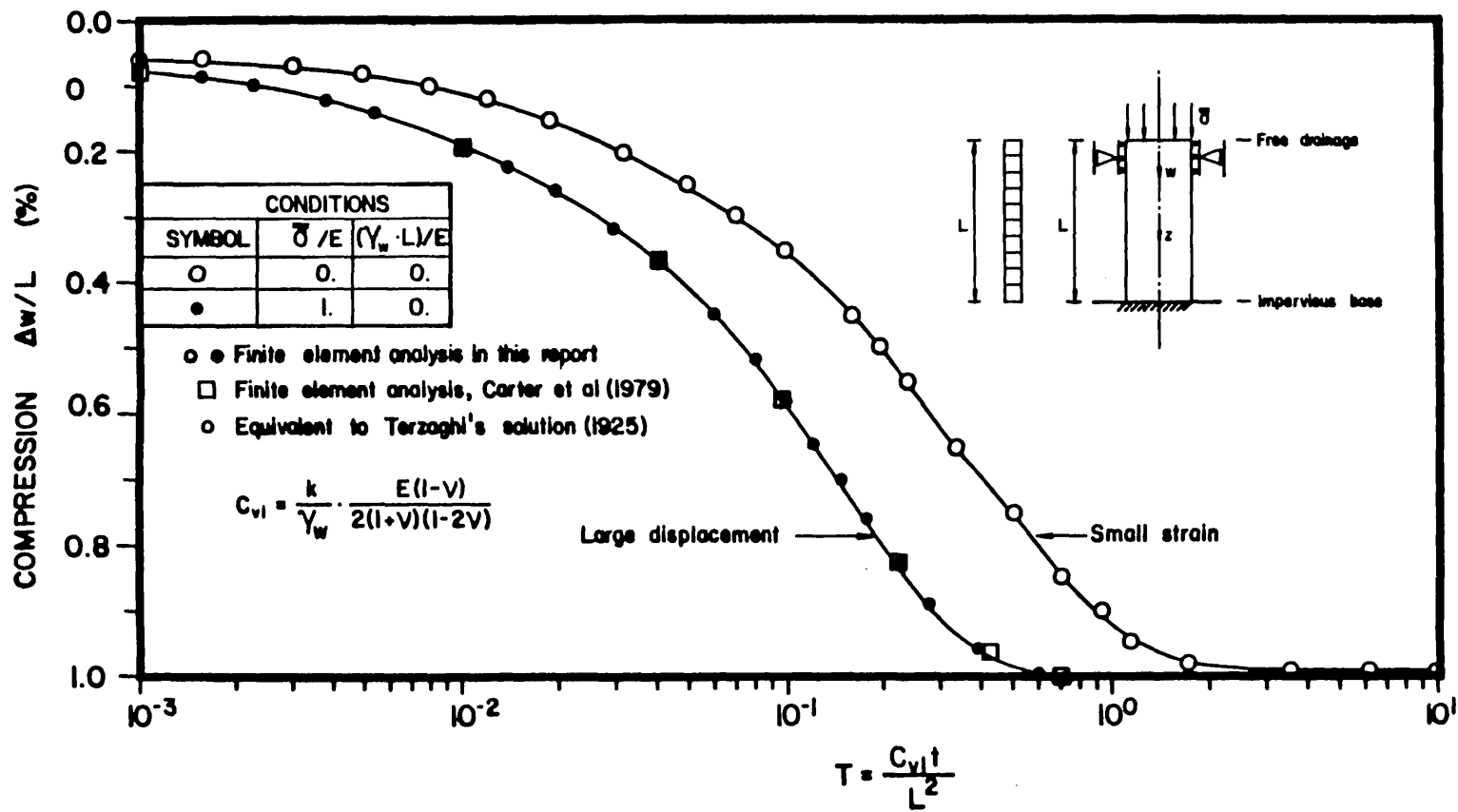


Figure IX. 8.

Constant permeability and full isotropy is assumed. Flow and deformation occur in two-dimension and free drainage is considered at the surface while the base is assumed impermeable. The soil constants are given as friction angle  $\phi = 30^\circ$ , Poisson ratio  $\nu = 0.3$  and the elasticity modulus/cohesion ratio  $E/c = 200$ . In addition the density influence is considered negligible, that is  $\gamma_f a/G_s \rightarrow 0$ . A few constant loading ratios defined by

$$\dot{\sigma} = \frac{d(\bar{\sigma}/c)}{dT} \quad \text{and} \quad T = C_v t / L^2$$

were chosen. Figure IX.9 show the finite element analysis obtained in this report and the one given by Carter et al (1979). The results for three loading rates are displayed ( $\dot{\sigma} = 0.143$ ,  $\dot{\sigma} = 1.43$  and  $\dot{\sigma} = 143$ ). Good agreement between the two finite element analyses are clear and basically no distinction between the small and large displacement analyses can be seen. The loading rate of 143 corresponds to the undrained test, the loading rate of 0.143 correspond to the drained analysis and the loading rate of 1.43 corresponds to a partially drained analysis.

#### IX.3.4 Elasto-Plastic Material and Linear Geometry.

To check the accuracy of the stress-strain relationship and the consolidation of non-linear material, a set of standard triaxial tests with different constant stress rates are now considered. Deformation, and flow occurs in three-dimensions and free drainage is considered at both ends. Constant permeability and complete isotropy is assumed.

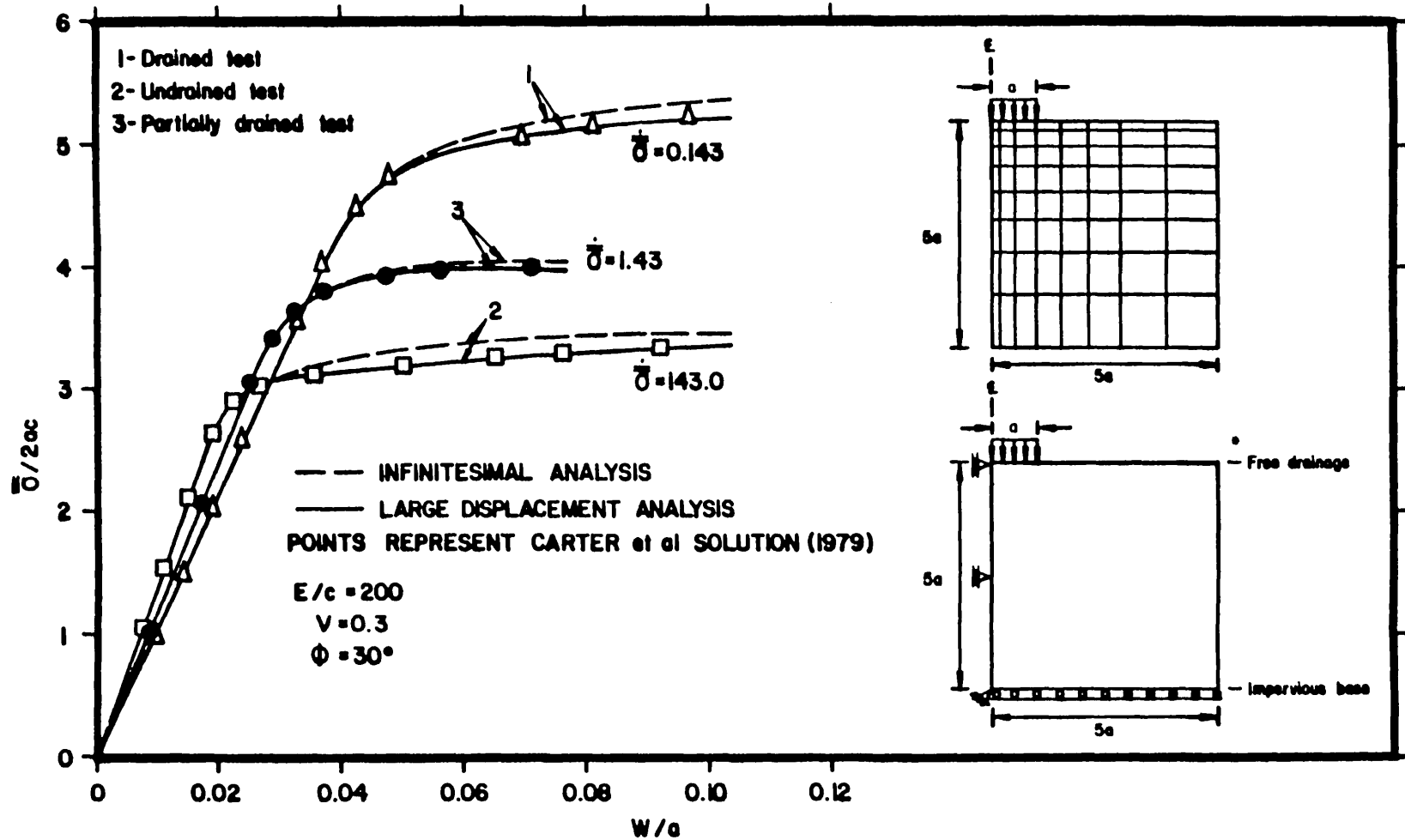


Figure IX.9.



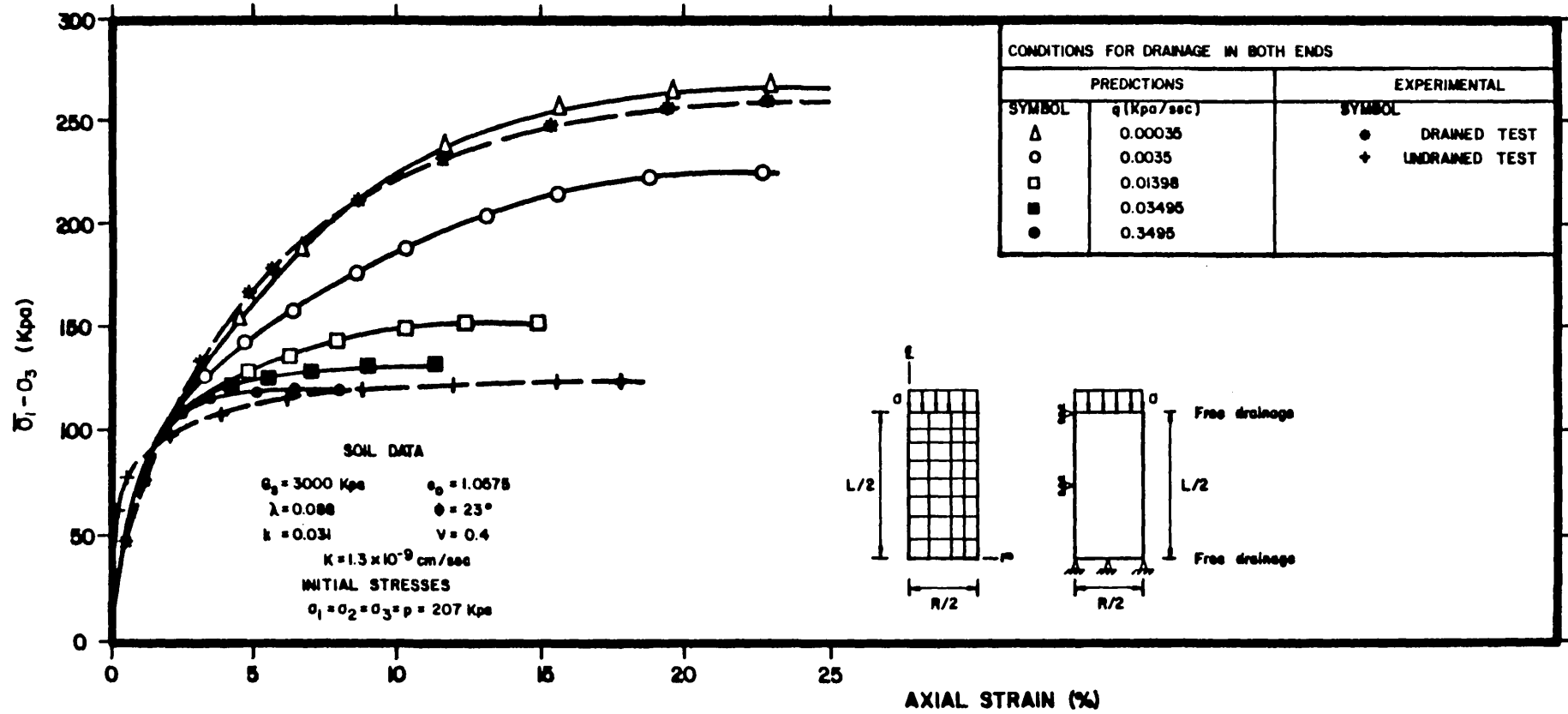


Figure IX. 10.

The soil chosen is weald clay (Bishop and Henkel (1971)) with the following parameters  $G_s = 3000 \text{ Kpa}$ ,  $\lambda = 0.088$ ,  $K = 0.031$ ,  $e_0 = 1.0575$ ,  $\phi = 23^\circ$ ,  $\nu = 0.4$ ,  $K = 1.3 \times 10^{-9} \text{ cm/sec}$ . and the initial effective stresses  $\sigma_1 = \sigma_2 = \sigma_3 = p = 207 \text{ Kpa}$ . The tests were carried out at constant displacement rates, however, the equivalent approximate stress rates in Kpa/sec are given as 0.00035, 0.0035, 0.01398, 0.03495, and 0.3495.

Figure IX.10 shows the finite element mesh, the schematic geometry and boundary conditions and the result obtained by the finite element analysis in this report and also the experimental results. Good agreement between the finite element analysis and the experiments is clearly shown by the figure. Again  $\beta = 1/2$  and tolerance of 0.05 are assumed.

### IX.3.5 Non-Linear Geometry and Creep Influence.

Strip loading on a half-plane where the uniform load has been applied over a width  $2a$  has been chosen to demonstrate the influence of large deformation and creep. Free drainage has been assumed at the surface and because of the symmetry only a quarter plane has to be considered. The finite element mesh, the schematic problem and its boundary conditions and pertinent results are presented in Figure IX.11. The dimensionless settlement  $w/a$  of the centre point of the strip load is also shown in the figure as a function of the time factor, for two ratios of  $\bar{\sigma}/G_s$  and  $\nu = 0$ ,  $\gamma_f = 0$ . The curves show that the difference between large deformation and small deformation theories is more pronounced for larger  $\bar{\sigma}/G_s$  ratios. For the creep analyses the parameters  $\alpha_c = m_c = 1$  and  $A_c = 1 \times 10^{-5}$  or  $A_c = 2.0 \times 10^{-5}$  have been chosen.

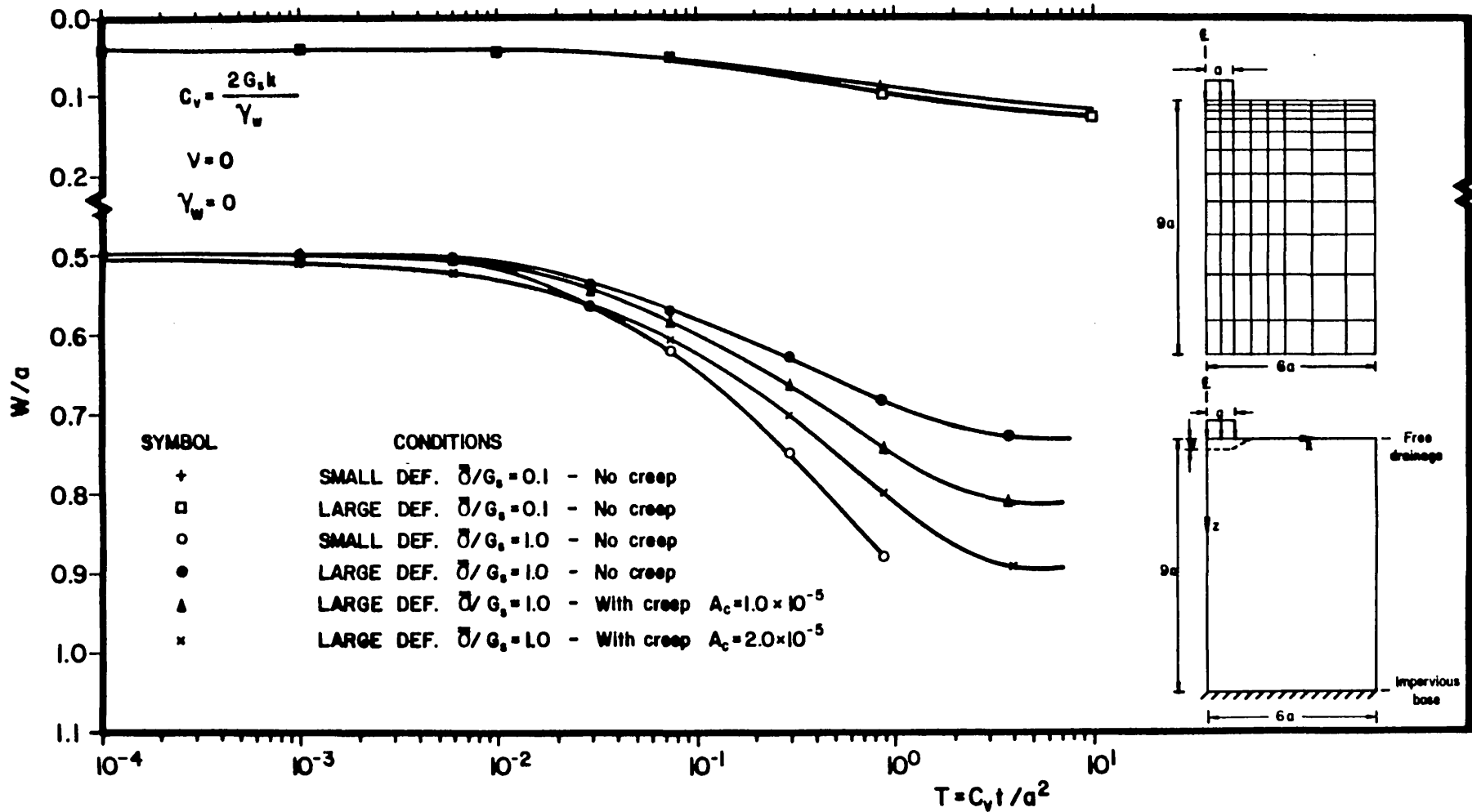


Figure IX. II.

The definition of  $C$ , and time factor are shown.

The integration constant  $\beta = 1/2$  and the tolerance level of  $0.01$  were chosen.

## CHAPTER X

### CONCLUDING REMARKS

#### X.1 General Results

Basically this report contains three main parts. These parts deal with the achievement of the finite element equations for geometric and material non-linear consolidation, with the constitutive equations for the soil skeleton and pore pressure fluid behaviour, and with the numerical solution of the differential equations, so produced.

Two sets of integral equations representing the geometric and material non-linear consolidation are arrived at, one based on the method known as the total Lagrange method and the other based on that known as the up-dated Lagrange method. The set of integral equations obtained on the basis of the up-dated Lagrange method is discretized in space and time and applied in the finite element program.

The constitutive behaviour of the soil is described using two distinct approaches. One considering the elasto-viscoplastic concept and the other involving the so called elasto-viscoplastic-plastic concept. The derived constitutive equation based on the first concept is compared with triaxial test results and exhibits quite good agreement.

It has been considered advantageous that the proposed model brings

together all basic known model into a unique equation and in addition allows a very large flexibility in calibrating almost any experimental data. The adoption of such a general model is justified by the non-uniqueness of the yield and plastic potential for soil and consequently the adoption of an rigid unified model is not justified and actually quite pretentious.

Although the elasto-viscoplastic model is more firmly based on physical concepts, only the elasto-viscoplastic-plastic model is used in finite element programming. The basic behaviour of the clay during undrained loading , consolidation and creep seems to be qualitatively well described by this elasto-viscoplastic-plastic constitutive model. The comparison with the triaxial test shows that the accuracy of the model shape is good in both hydrostatic and deviatoric planes.

The discrepancies between test results and the prediction for undrained creep may almost certainly be due to the linear elasticity assumption in the overconsolidated region at rapid loading. This is not in agreement with the experiments which sometimes show a pronounced non-linearity, depending on the stress rate (or strain rate) of testing.

Consideration of the effect of major variables influencing the consolidation problem will be presented separately as a main subject. This area requires more study because of the lack of full scale experimental data which make the judgement of the quantitative results incomplete and inconvenient, in particular, where it concerns the recording of horizontal displacements. Further difficulties are encountered when judging the time effect on the constitutive law because inviscid and viscous effect can hardly be separated in

observed deformations. In this respect the elasto-vicoplastic approach seems to be more convenient.

It is demonstrated that, because a purely rate-type constitutive equation has been adopted for undrained loading, the undrained loading algorithm and the consolidation process algorithm can be formulated very similarly. In the former case it is formulated as an initial value problem in "fictitious time"; and in the latter case it is formulated as an ordinary initial value problem.

In the solution of the initial problem the adopted load stepping procedure can be interpreted as an Euler extrapolation scheme. The time integration scheme is efficient and accurate because of the optimal choice of time step, based on an acceptable range of the local truncation error. Numerical sample solutions demonstrate that the accuracy is good and the sensitivity of the process of calculation for change in tolerance level is small.

The element mesh prepared to analyse initial value problem were designed to account for steep gradients. Though the computer program is coded in single precision (IBM 360/370) no problems due to ill-conditioning of the system of computed equations have become apparent.

To conclude, an important practical problem related to consolidation can be analysed based on the theory supported in this report. The presented numerical algorithm is applicable to practical problems such as: External loading on a footing, acceleration of consolidation by means of drains, calculation of secondary settlements in urban environments due to changes in the ground water hydraulics, dam construction, deformation, consolidation and long term seepage, and

slope stability.

## X.2 Future Development.

In the field of consolidation there is the need for research in three main related areas: Further development and verification of constitutive models, experimental test on laboratory-scale and full-scale conditions and additional development of numerical methods.

The constitutive model used in this report has been experimentally verified and numerically tested under rather restricted conditions. Experimentally the model has been verified for slow rate analyses in the hydrostatic planes. In fact it has been developed based on tests carried out by keeping the slow rate stress-path on the hydrostatic planes. To extend this model to predict for other paths, such as those which are more likely to happen in the field, is not yet recommended. It is known, however, that the isotropic version of this model is not able to predict the deformation obtained from stress-paths developed on the  $\pi$ -plane. This makes one believe that the model is only strictly applicable to analyse problems which experience the same restricted stress-path from which it was obtained.

Although some results have been achieved the investigation of very overconsolidated soils still remains to be done.

However, what is more serious is that the fundamental assumption of critical state theory has to be re-analysed because the Rendulic principle does not seem to be applicable at all. This can really cause serious inconvenience for the unification of the constitutive



model for soils. Perhaps a different approach such as the slipping theory, or the use of a more flexible model which would allow the calibration for any specific circumstances, as proposed in this report, should be adopted. In fact programming the general model as proposed in this report is recomendable and should be considered as one of the next tasks.

To investigate the anisotropy of the initial and subsequent loading surfaces it is not sufficient to investigate the behaviour in the principle stress space. In particular, it is not sufficient to conduct active and passive triaxial tests on samples which are taken vertically from the ground. Tests should be performed on samples taken vertically, horizontally and any other direction from the ground, because of the need to relate the direction of the anisotropy with the direction of the stress rate. No model which does not take the relation between the direction of action and the direction of anisotropy into account can be of practical value.

Creep and or rate effect must be studied much further with the intention of unifying these two effects. In the study of creep law it will be adequate to fix the effective stresses so that no relaxation occurs. This means in particular that during creep tests in a triaxial apparatus the pore-pressure change with time must be compensated so that the effective stress is held constant. If this procedure is adopted then there will be no elastic volume change and the observed amount of water which has drained is the volumetric part of creep strain.

However, it is the author's opinion that rate control in a partially drained and/or undrained test would be a preferable approach to

incorporate the time effect on the constitutive equations, although the calculation procedure is more complicated. The effect of both constant and continuously changing rates of testing should be analysed for undrained and partially drained tests. These would provide important reliable information about the influence of rate and change of rate on the compressibility parameters and preconsolidation pressure.

A major theoretical attempt should consider the interaction between subsoil and a flexible superstructure through a rigid footing or the interaction between the subsoil and a flexible raft resting on the ground should be considered as well. Also it is often necessary to take into account the three-dimensional effect. Theoretical development may be of minor practical importance if the computer calculation becomes progressively less expensive. In this context a more efficient algorithm such as the combination of implicit-explicit schemes could be conveniently adopted.

For the introduction of three-dimensional effect the facilities of mesh generation and plotting routine output would be indispensable.

APPENDIX AA BRIEF SUMMARY OF MATHEMATICS BACKGROUND

## -Basic Definitions

This appendix sets down some prerequisites mathematics that will be useful in subsequent developments of chapter number four and others.

Referring to Figure A.1 we can write the following basic relationship:

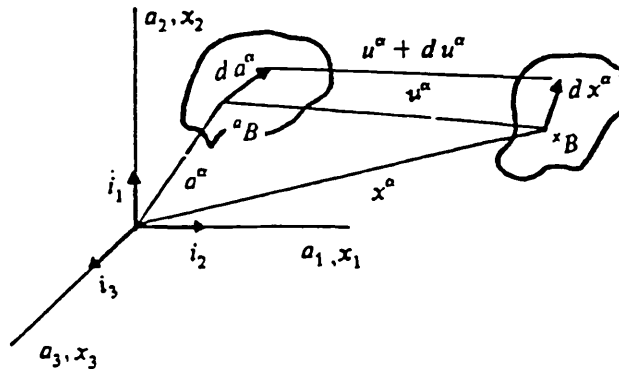


Figure A.1

The position vector of a two-phase material element in an initial configuration (I.C.) and in an actual configuration (A.C.) is represented as :

$$(A.1) \quad a^\alpha = a_k^\alpha i_k \quad , \quad x^\alpha = x_k^\alpha i_k$$

Where, and henceforth, except for  $\alpha$  , the usual summation convention

is understood over the repeated indices, i.e.  $a^\alpha = a_1^\alpha i_1 + a_2^\alpha i_2 + a_3^\alpha i_3$  or  $a^1 = a_1^1 i_1 + a_2^1 i_2 + a_3^1 i_3 = d^1 i_1 + b^1 i_2 + c^1 i_3$ . The infinitesimal differential vectors at I.C. and at A.C. are respectively

$$(A.2) \quad da^\alpha = da_k^\alpha i_k \quad , dx^\alpha = dx_k^\alpha i_k$$

The squares of the arc length at I.C. and at A.C. are given by

$$(A.3) \quad (d^a r^a)^2 = da^\alpha \cdot da^\alpha = da_k^\alpha \cdot da_k^\alpha = \delta_{kl} da_k^\alpha da_l^\alpha$$

and

$$(A.4) \quad (d^x r^a)^2 = dx^\alpha \cdot dx^\alpha = dx_k^\alpha \cdot dx_k^\alpha = \delta_{kl} dx_k^\alpha dx_l^\alpha$$

where  $\delta_{kl} = i_k \cdot i_l$  is the Kronecker Delta, which is equal to unity when the two indices are equal and otherwise zero. These differential vectors may be interpreted as a infinitesimal distance between two particles, i.e.,  $da^1$  is the distance between two fluid particles in the I.C. and  $dx^2$  is the distance between two solid particles in the A.C..

The interest, now, is to map the neighbourhood of the particle at  $a^\alpha$  in the I.C. into a particle  $x^\alpha$  at A.C. If  $da^\alpha$  is a spherical neighbourhood at,  $a^\alpha$

$$(A.5) \quad dx^\alpha = x^\alpha(a^\alpha + da^\alpha, t) - x^\alpha(a^\alpha, t)$$

is the spherical neighbourhood at  $x^\alpha$ .

By using Taylor's Theorem (Hildebrand (1976)) one may approximate to

the first order terms ( since, the magnitude  $|da^\alpha|$  of  $da^\alpha$  tends to zero),

$$(A.5) \quad x^\alpha(a^\alpha + da^\alpha, t) = x^\alpha(a^\alpha, t) + \frac{\partial x^\alpha}{\partial a^\alpha} da^\alpha$$

or in a parametric form

$$(A.6) \quad dx_k^\alpha = \frac{\partial x_k^\alpha}{\partial a_i^\alpha} da_i^\alpha, \quad da_i^\alpha = \frac{\partial a_i^\alpha}{\partial x_k^\alpha} dx_k^\alpha$$

where the linear transformation  $\partial x_k^\alpha / \partial a_i^\alpha$  is called deformation gradients

Sometimes it is appropriate to make use of so-called alternative tensor or permutation symbols defined by

$$(A.7) \quad e_{klm} = \begin{cases} 1 & \text{if } k,l,m \text{ are in cyclic order } 1,2,3,3,1,2,\dots \\ 0 & \text{if any two of } k,l,m, \text{ are equal} \\ -1 & \text{if } k,l,m \text{ are in anticyclic order } 3,2,1,1,3,2,\dots \end{cases}$$

provided one of the transformation  $\partial x^\alpha / \partial a^\alpha$  or  $\partial a^\alpha / \partial x^\alpha$  is known, it might be of interest to find the other. So, by the chain rule of differentiation, it may be written

$$(A.8) \quad \frac{\partial x_k^\alpha}{\partial a_m^\alpha} \frac{\partial a_m^\alpha}{\partial x_l^\alpha} = \delta_{kl}$$

This set consists of nine linear equations for the nine unknown  $\partial x_k^\alpha / \partial a_m^\alpha$  or  $\partial a_m^\alpha / \partial x_l^\alpha$ . A unique solution exists according to Cramer's rule of determinants, provided the jacobian does not vanish

and is given by

$$(A.9) \quad \frac{\partial a_k^\alpha}{\partial x_l^\alpha} = \frac{1}{J} \text{cofactor} \left( \frac{\partial x_l^\alpha}{\partial a_k^\alpha} \right) = \frac{1}{2J} e_{kmr} e_{lns} \frac{\partial x_n^\alpha}{\partial a_m^\alpha} \frac{\partial x_s^\alpha}{\partial a_r^\alpha}$$

where  $e_{kmr}$  and  $e_{lns}$  are the permutation symbols defined by (A.7), and

$$(A.10) \quad J = \det \left( \frac{\partial x_l^\alpha}{\partial a_k^\alpha} \right) = \frac{1}{3!} e_{kmr} e_{lns} \frac{\partial x_l^\alpha}{\partial a_k^\alpha} \frac{\partial x_n^\alpha}{\partial a_m^\alpha} \frac{\partial x_s^\alpha}{\partial a_r^\alpha}$$

(See Aris (1962))

By differentiating equation (A.9) and (A.10) two important identities are obtained

$$(A.11) \quad \frac{\partial}{\partial a_k^\alpha} \left( J \frac{\partial a_k^\alpha}{\partial x_l^\alpha} \right) = 0$$

$$(A.12) \quad \frac{\partial J}{\partial (\partial x_l^\alpha / \partial a_k^\alpha)} = \text{cofactor} \left( \frac{\partial x_l^\alpha}{\partial a_k^\alpha} \right) = J \frac{\partial a_k^\alpha}{\partial x_l^\alpha}$$

of which the latter is attributed to Jacobi.

At a later stage, we shall refer to time differentiation many times. For example, velocity acceleration, rate of deformation, stress rate, etc. However, at this stage it is appropriate to define what is understood by material time differentiation of material and spatial functions and to define time differentiation of basic functions, vectors and tensors, but firstly, let us set down the generalized Green-Gauss Theorem for a tensor field  $\tau_k$  over the surface  $S-\omega$  of the body  $\vartheta-\omega$  which states

$$(A.13) \quad \oint_{S-\omega} \tau_k ds_k = \int_{\vartheta-\omega} \frac{\partial \tau_k}{\partial x_k} d\vartheta + \int_S [\tau_k] n_k ds$$

where the volume  $\vartheta - \omega$  means the volume  $\vartheta$  of the body excluding the material points located on the discontinuity surface  $\omega$ . Similarly, the integral over the surface  $S - \omega$  excludes the line of intersection of  $\omega$  with  $S$ .

The material time of a vector (or tensor)  $f$  is defined by

$$(A.14) \quad \dot{f} = \frac{df}{dt} = \frac{\partial f}{\partial t} \Big|_x$$

where the subscript  $x$  indicates that  $x$  is held constant in the differentiation of  $f$ . If  $f$  is a function of material coordinates,

$$f(a, t) = f_k(a, t) i_k \quad , \text{ then} \quad \frac{df}{dt} = \frac{\partial f_k}{\partial t} i_k = \frac{\partial f}{\partial t}$$

If  $f$  is a function of spatial coordinates,

$$f = f(x, t) = f_k(x, t) i_k \quad , \text{ then} \quad \frac{df}{dt} = \left( \frac{\partial f_k}{\partial t} \Big|_x + \frac{\partial f_k}{\partial x_l} \frac{\partial x_l}{\partial t} \right) i_k = \frac{\partial f}{\partial t} + \frac{\partial f}{\partial x} \frac{\partial x}{\partial t}$$

so, one can write

$$(A.15) \quad \frac{d}{dt} f_k(x, t) = \frac{\partial}{\partial t} f_k(x, t) + \frac{\partial}{\partial x_l} [f_k(x, t)] \frac{\partial x_l}{\partial t}$$

which is called the material derivative of  $f_k$ . The first term on the right is called the local or non-stationary rate, and the second term

is the convective time rate. This expression is applicable also to material vectors and tensors. (Aris (1962))

Also, the material derivative obeys the ordinary rules of the partial differentiation involving sums and products, i.e.

$$\frac{d}{dt}(f_k + g_k) = \frac{df_k}{dt} + \frac{dg_k}{dt}, \quad \frac{d(f_k g_l)}{dt} = \frac{df_k}{dt} g_l + f_k \frac{dg_l}{dt}$$

Now follows some basic definitions:

Velocity: The velocity vector  $V$  is the time rate of change of the position vector

$$(A.16) \quad v^\alpha = v^\alpha(a^\alpha, t) = \frac{d}{dt}[x^\alpha(a^\alpha, t)] = \frac{\partial}{\partial t}[x^\alpha(a^\alpha, t)] = v_k^\alpha(a^\alpha, t) i_k$$

If one substitute equation (IV.3.3) into (A.16) one will get

$$(A.17) \quad v^\alpha = v^\alpha[a^\alpha(x^\alpha, t), t] = v^\alpha(x^\alpha, t) = v_k^\alpha(x^\alpha, t) i_k$$

Where the functional dependencies were changed, i.e. the velocity can be regarded as a time-dependent vector field. In fact, the acceleration and any time-dependent scalar, vector or tensor may be regarded either as a function  $\psi(a^\alpha, t)$  of the particle and time or as a function  $\psi(x^\alpha, t)$  of the place and time, provided that a defined motion (IV.3.3) is given. The material time rate of  $\psi(a^\alpha, t)$  and  $\psi(x^\alpha, t)$  are given by equation (A.15) where  $f_k$  is replaced by  $\psi_k$ .

Acceleration : The acceleration vector  $ac$  is the time rate of change



of the velocity vector, so,

$$(A.18) \quad ac = \frac{dv}{dt} \quad \text{and}$$

$$(A.19) \quad ac^\alpha(a^\alpha, t) = \frac{d}{dt} [v^\alpha(a^\alpha, t)] = \frac{\partial v_k^\alpha}{\partial t} i_k = ac_k^\alpha(a^\alpha, t) i_k \quad \text{and}$$

$$(A.20) \quad ac^\alpha(x^\alpha, t) = \frac{d}{dt} [v^\alpha(x^\alpha, t)] = \left( \frac{\partial v_k^\alpha(x^\alpha, t)}{\partial t} + \frac{\partial v_k^\alpha(x^\alpha, t)}{\partial x_m^\alpha} \frac{\partial x_m^\alpha}{\partial t} \right) i_k$$

The following are some fundamental lemmas ensuing directly from the basic definitions above.

The material derivative of the displacement gradient given by equation (A.5) or (A.6) is found to be

$$(A.21) \quad \frac{d}{dt} \left( \frac{\partial x_k^\alpha}{\partial a_l^\alpha} \right) = \frac{\partial}{\partial a_l^\alpha} \left( \frac{d x_k^\alpha}{dt} \right) = \frac{\partial v_k^\alpha}{\partial a_l^\alpha} = \frac{\partial v_k^\alpha}{\partial x_m^\alpha} \frac{\partial x_m^\alpha}{\partial a_l^\alpha}$$

since in the operation  $d|dt$ ,  $a_l^\alpha$  is fixed so that  $d|dt$  and  $\partial|\partial a_l^\alpha$  commute.

The material derivative of the distance between two points in A.C. is given by

$$(A.22) \quad \frac{d}{dt} (d x_k^\alpha) = \frac{d}{dt} \left( \frac{\partial x_k^\alpha}{\partial a_l^\alpha} d a_l^\alpha \right) = \frac{\partial v_k^\alpha}{\partial a_l^\alpha} d a_l^\alpha = \frac{\partial v_k^\alpha}{\partial x_m^\alpha} \frac{\partial x_m^\alpha}{\partial a_l^\alpha} d a_l^\alpha \quad \text{or}$$

$$\frac{d}{dt} (d x_k^\alpha) = \frac{\partial v_k^\alpha}{\partial x_m^\alpha} d x_m^\alpha$$

A corollary of this lemma is

$$(A.23) \quad \frac{d}{dt} \left( \frac{\partial a_l^a}{\partial x_k^a} \right) = - \frac{\partial v_k^a}{\partial x_m^a} \frac{\partial a_l^a}{\partial x_m^a}$$

proof: Taking the material differentiation of (A.8)

$$\frac{d}{dt} \left( \frac{\partial x_k^a}{\partial a_m^a} \frac{\partial a_m^a}{\partial x_l^a} \right) = \frac{d}{dt} \left( \frac{\partial x_k^a}{\partial a_m^a} \right) \frac{\partial a_m^a}{\partial x_l^a} + \frac{\partial x_k^a}{\partial a_m^a} \frac{d}{dt} \left( \frac{\partial a_m^a}{\partial x_l^a} \right) = 0$$

may be written. From this equation, together with (A.21) one can write equation(A.23)

The material derivative of the Jacobian is given by

$$(A.24) \quad \frac{d}{dt}(J) = \frac{d}{dt} \left[ \text{det} \left( \frac{\partial x_k^a}{\partial a_l^a} \right) \right] = \left( \partial J / \partial \left( \frac{\partial x_k^a}{\partial a_l^a} \right) \right) \frac{d}{dt} \left( \frac{\partial x_k^a}{\partial a_l^a} \right) = J \frac{\partial v_k}{\partial x_k}$$

where (A.12) and (A.21) were used

The material derivative of an infinitesimal volume is given by

$$(A.25) \quad \frac{d}{dt}(d^3\vartheta) = \frac{dJ}{dt} d^3\vartheta = J \frac{\partial v_k}{\partial x_k} d^3\vartheta$$

Time differentiation of a volume integral of a tensor field  $\psi$ . Consider a material volume  $\vartheta$  intercepted by a discontinuity surface  $\omega(t)$  moving with velocity  $\nu$ . The material derivative of the volume integral of a tensor field  $\psi$  over  $\vartheta - \omega$  is given by

$$(A.26) \quad \frac{d}{dt} \int_{\vartheta - \omega} \psi d\vartheta = \int_{\vartheta - \omega} \left[ \frac{\partial \psi}{\partial t} + \text{div}(\psi \nu) \right] d\vartheta + \int_{\omega} [\psi(\nu - \nu)] ds$$

The volume integral  $\vartheta - \omega$  means the volume  $\vartheta$  of the body excluding

A9

the material points located on the discontinuity.

Other function differentiations will be given after definition of strain and stress tensors.

APPENDIX BGeometric transforms in Deformation - area and volume

In this appendix considerations about the geometric transformation that takes place when a material point at the I.C. (initial configuration) moves to its corresponding point in the A.C. (deformed configuration), is given. The main concern is how an infinitesimal oriented surface element transforms during the deformation.

Area and Volume Change

An infinitesimal rectangular parallelepiped with edge vectors  $i_1 da_1^a$ ,  $i_2 da_2^a$ ,  $i_3 da_3^a$  at  $a^a$  after deformation becomes a rectilinear parallelepiped at  $x^a$  with corresponding edge  $\beta_1^a da_1^a$ ,  $\beta_2^a da_2^a$ ,  $\beta_3^a da_3^a$  (see Figure B.1)

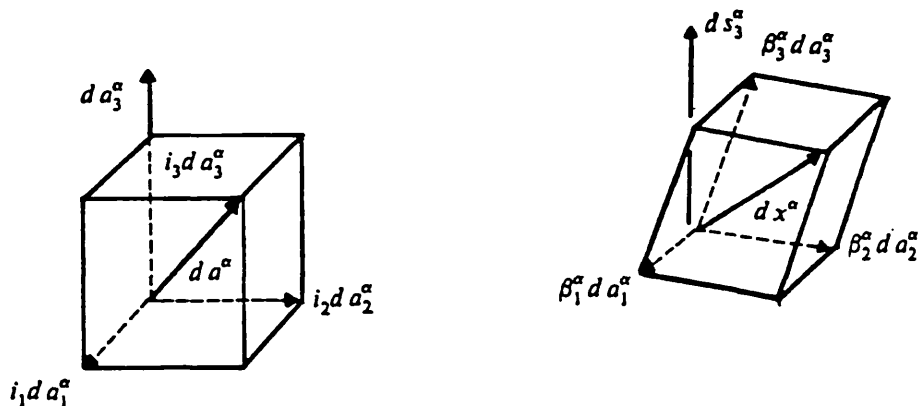


Figure B.1

Based on equations (A.5) and (A.6) the vectors  $da^a$  and  $dx^a$  may be written as:

$$(B.1) \quad d a^\alpha = d a_k^\alpha i_k, \quad d x^\alpha = \frac{\partial x_k^\alpha}{\partial a_l^\alpha} d a_l^\alpha i_k$$

where

$$\beta_l^\alpha = \frac{\partial x_k^\alpha}{\partial a_l^\alpha}$$

Now if the Figure B.1 is considered, where an element of area is built on the edge vectors  $i_1 d a_1^\alpha$  and  $i_2 d a_2^\alpha$  which after deformation becomes the area with the edge vectors  $\beta_1^\alpha d a_1^\alpha$  and  $\beta_2^\alpha d a_2^\alpha$  the deformed area is given by

$${}^x d s_3^\alpha = \beta_1^\alpha d a_1^\alpha \times \beta_2^\alpha d a_2^\alpha = \frac{\partial x_k^\alpha}{\partial a_1^\alpha} \frac{\partial x_l^\alpha}{\partial a_2^\alpha} i_k \times i_l d a_1^\alpha d a_2^\alpha = \frac{\partial x_k^\alpha}{\partial a_1^\alpha} \frac{\partial x_l^\alpha}{\partial a_2^\alpha} e_{klm} i_m d s_3^\alpha$$

where

$${}^a d s^\alpha = d a_1^\alpha d a_2^\alpha$$

.But from (A.9) we have

$$J \frac{\partial a_3^\alpha}{\partial x_m^\alpha} = e_{klm} \frac{\partial x_k^\alpha}{\partial a_1^\alpha} \frac{\partial x_l^\alpha}{\partial a_2^\alpha} \quad \text{so that,} \quad {}^x d s_3^\alpha = J \frac{\partial a_3^\alpha}{\partial x_m^\alpha} d s_3^\alpha i_m$$

where this expression represents the oriented area element  ${}^x d s_3^\alpha$  in relation to its components in the orthogonal reference system in which unit vector is represented by  $i_m$ .

Finding similar expressions for  ${}^x d s_1^\alpha$  and  ${}^x d s_2^\alpha$  one can write the Kth components as

$$(B.2) \quad {}^x d s_k^\alpha = J \frac{\partial a_l^\alpha}{\partial x_k^\alpha} d s_l^\alpha$$

To evaluate the deformed volume element, we make the scalar product of  $d s_j^\alpha$  with  $\beta_3^\alpha d a_3^\alpha$ , is made so:

B3

$$d^x \vartheta = d^a s_3^a \beta_3^a d a_3^a = J \frac{\partial a_3^a}{\partial x_k^a} i_k \cdot \left( \frac{\partial x_m^a}{\partial a_3^a} i_m \right) d^a s_3^a d a_3^a$$

$$d^x \vartheta = J \frac{\partial a_3^a}{\partial x_k^a} \cdot \frac{\partial x_m^a}{\partial a_3^a} \delta_{km} d^a \vartheta \quad \text{or}$$

(B.3)

$$d^x \vartheta = J d^a \vartheta$$

APPENDIX CEXPLICIT STIFFNESS MATRICESTOTAL LAGRANGIAN FORMULATION

-Incremental Strains

$${}^0e_{11} = \frac{\partial \Delta u_1}{\partial a_1} + \frac{\partial {}^i u_i}{\partial a_1} \cdot \frac{\partial \Delta u_1}{\partial a_1} + \frac{\partial {}^i u_2}{\partial a_1} \cdot \frac{\partial \Delta u_2}{\partial a_1} + \frac{1}{2} \left[ \left( \frac{\partial \Delta u_1}{\partial a_1} \right)^2 + \left( \frac{\partial \Delta u_2}{\partial a_1} \right)^2 \right]$$

$${}^0e_{22} = \frac{\partial \Delta u_2}{\partial a_2} + \frac{\partial {}^i u_1}{\partial a_2} \cdot \frac{\partial \Delta u_1}{\partial a_2} + \frac{\partial {}^i u_2}{\partial a_2} \cdot \frac{\partial \Delta u_2}{\partial a_2} + \frac{1}{2} \left[ \left( \frac{\partial \Delta u_1}{\partial a_2} \right)^2 + \left( \frac{\partial \Delta u_2}{\partial a_2} \right)^2 \right]$$

$${}^0e_{12} = \frac{1}{2} \left( \frac{\partial \Delta u_1}{\partial a_2} + \frac{\partial \Delta u_2}{\partial a_1} \right) + \frac{1}{2} \left( \frac{\partial {}^i u_1}{\partial a_1} \cdot \frac{\partial \Delta u_1}{\partial a_2} + \frac{\partial {}^i u_2}{\partial a_1} \cdot \frac{\partial \Delta u_2}{\partial a_2} + \frac{\partial {}^i u_1}{\partial a_2} \cdot \frac{\partial \Delta u_1}{\partial a_1} + \frac{\partial {}^i u_2}{\partial a_2} \cdot \frac{\partial \Delta u_2}{\partial a_1} \right) \\ + \frac{1}{2} \left( \frac{\partial \Delta u_1}{\partial a_1} \cdot \frac{\partial \Delta u_1}{\partial a_2} + \frac{\partial \Delta u_2}{\partial a_1} \cdot \frac{\partial \Delta u_2}{\partial a_2} \right)$$

$${}^0e_{33} = \frac{\Delta u_1}{a_1} + \frac{{}^i u_1 \Delta u_1}{(a_1)^2} + \frac{1}{2} \left( \frac{\Delta u_1}{a_1} \right)^2$$

-Linear Strain Displacement Transformation Matrix

Making

$${}^0e = {}^0 B_L \Delta_0 u^k$$

where

$${}^0e^T = ({}^0e_{11}, {}^0e_{22}, 2{}^0e_{12}, {}^0e_{33})$$

$$(\Delta_0 u^k)^T = (\Delta u_1^1, \Delta u_2^1, \Delta u_1^2, \Delta u_2^2, \Delta u_1^3, \Delta u_2^3, \dots, \Delta u_1^N, \Delta u_2^N)$$

$${}^0 B_L = {}^0 B_{L0} + {}^0 B_{L1}$$

and

$${}^0 B_{L1} = \begin{pmatrix} \frac{\partial \xi_1}{\partial a_1} & 0 & \frac{\partial \xi_2}{\partial a_1} & 0 & \frac{\partial \xi_3}{\partial a_1} & 0 & \dots & \frac{\partial \xi_N}{\partial a_1} & 0 \\ 0 & \frac{\partial \xi_1}{\partial a_2} & 0 & \frac{\partial \xi_2}{\partial a_2} & 0 & \frac{\partial \xi_3}{\partial a_2} & \dots & 0 & \frac{\partial \xi_N}{\partial a_2} \\ \frac{\partial \xi_1}{\partial a_2} & \frac{\partial \xi_1}{\partial a_1} & \frac{\partial \xi_2}{\partial a_2} & \frac{\partial \xi_2}{\partial a_1} & \frac{\partial \xi_3}{\partial a_2} & \frac{\partial \xi_3}{\partial a_1} & \dots & \frac{\partial \xi_N}{\partial a_2} & \frac{\partial \xi_N}{\partial a_1} \\ \frac{\xi_1}{a_1} & 0 & \frac{\xi_2}{a_1} & 0 & \frac{\xi_3}{a_1} & 0 & \dots & \frac{\xi_N}{a_1} & 0 \end{pmatrix}$$

where  $\bar{a}_1 = \sum_{k=1}^N \xi_k a_1^k$  ,

$a_1, a_2$  initial nodal coordinates

$N$  -number of nodes

$${}^0 B_{L1} = \begin{pmatrix} l_{11} \frac{\partial \xi_1}{\partial a_1} & l_{21} \frac{\partial \xi_1}{\partial a_1} & l_{11} \frac{\partial \xi_2}{\partial a_1} & l_{21} \frac{\partial \xi_2}{\partial a_1} \\ l_{12} \frac{\partial \xi_1}{\partial a_2} & l_{22} \frac{\partial \xi_1}{\partial a_2} & l_{12} \frac{\partial \xi_2}{\partial a_2} & l_{22} \frac{\partial \xi_2}{\partial a_2} \\ \left( l_{11} \frac{\partial \xi_1}{\partial a_2} + l_{12} \frac{\partial \xi_1}{\partial a_1} \right) & \left( l_{21} \frac{\partial \xi_1}{\partial a_2} + l_{22} \frac{\partial \xi_1}{\partial a_1} \right) & \left( l_{11} \frac{\partial \xi_2}{\partial a_2} + l_{12} \frac{\partial \xi_2}{\partial a_1} \right) & \left( l_{21} \frac{\partial \xi_2}{\partial a_2} + l_{22} \frac{\partial \xi_2}{\partial a_1} \right) \\ l_{33} \frac{\xi_1}{\bar{a}_1} & 0 & l_{33} \frac{\xi_2}{\bar{a}_1} & 0 \\ \dots & l_{11} \frac{\partial \xi_N}{\partial a_1} & l_{21} \frac{\partial \xi_N}{\partial a_1} & \\ \dots & l_{12} \frac{\partial \xi_N}{\partial a_2} & l_{22} \frac{\partial \xi_N}{\partial a_2} & \\ \dots & \left( l_{11} \frac{\partial \xi_N}{\partial a_2} + l_{12} \frac{\partial \xi_N}{\partial a_1} \right) & \left( l_{21} \frac{\partial \xi_N}{\partial a_2} + l_{22} \frac{\partial \xi_N}{\partial a_1} \right) & \\ \dots & l_{33} \frac{\xi_N}{\bar{a}_1} & 0 & \end{pmatrix}$$

where  $l_{21} = \sum_{k=1}^N \frac{\partial \xi_k}{\partial a_1} u_2^k$ ,  $l_{33} = \left( \sum_{k=1}^N \xi_k u_1^k \right) / \bar{a}_1$

$$l_{11} = \sum_{k=1}^N \frac{\partial \xi_k}{\partial a_1} u_1^k, \quad l_{22} = \sum_{k=1}^N \frac{\partial \xi_k}{\partial a_2} u_2^k, \quad l_{12} = \sum_{k=1}^N \frac{\partial \xi_k}{\partial a_2} u_1^k$$

-Non-linear Strain Displacement Transformation Matrix

$${}^0 B_{NL} = \begin{pmatrix} \frac{\partial \xi_1}{\partial a_1} & 0 & \frac{\partial \xi_2}{\partial a_1} & 0 & \frac{\partial \xi_3}{\partial a_1} & 0 & \dots & \frac{\partial \xi_N}{\partial a_1} & 0 \\ \frac{\partial \xi_1}{\partial a_2} & 0 & \frac{\partial \xi_2}{\partial a_2} & 0 & \frac{\partial \xi_3}{\partial a_2} & 0 & \dots & \frac{\partial \xi_N}{\partial a_2} & 0 \\ 0 & \frac{\partial \xi_1}{\partial a_1} & 0 & \frac{\partial \xi_2}{\partial a_1} & 0 & \frac{\partial \xi_3}{\partial a_1} & \dots & 0 & \frac{\partial \xi_N}{\partial a_1} \\ 0 & \frac{\partial \xi_1}{\partial a_2} & 0 & \frac{\partial \xi_2}{\partial a_2} & 0 & \frac{\partial \xi_3}{\partial a_2} & \dots & 0 & \frac{\partial \xi_N}{\partial a_2} \\ \frac{\xi_1}{\bar{a}_1} & 0 & \frac{\xi_2}{\bar{a}_1} & 0 & \frac{\xi_3}{\bar{a}_1} & 0 & \dots & \frac{\xi_N}{\bar{a}_1} & 0 \end{pmatrix}$$

-And The Second Piola-Kirchoff Stress Matrix and Vector

$${}^t \sigma = \begin{pmatrix} {}^t \sigma_{11} & {}^t \sigma_{12} & 0 & 0 & 0 \\ {}^t \sigma_{21} & {}^t \sigma_{22} & 0 & 0 & 0 \\ 0 & 0 & {}^t \sigma_{11} & {}^t \sigma_{12} & 0 \\ 0 & 0 & {}^t \sigma_{21} & {}^t \sigma_{22} & 0 \\ 0 & 0 & 0 & 0 & {}^t \sigma_{33} \end{pmatrix} \quad {}^0 \sigma = \begin{pmatrix} 0 & {}^t \bar{\sigma}_{11} \\ 0 & {}^t \bar{\sigma}_{22} \\ 0 & {}^t \bar{\sigma}_{12} \\ 0 & {}^t \bar{\sigma}_{33} \end{pmatrix}$$



-The matrix  ${}^0E = \nabla_0 \psi_p$  is

$${}^0E = \begin{bmatrix} \frac{\partial \xi_1}{\partial a_1} & \frac{\partial \xi_2}{\partial a_1} & \frac{\partial \xi_3}{\partial a_1} & \dots & \frac{\partial \xi_N}{\partial a_1} \\ \frac{\partial \xi_1}{\partial a_2} & \frac{\partial \xi_2}{\partial a_2} & \frac{\partial \xi_3}{\partial a_2} & \dots & \frac{\partial \xi_N}{\partial a_2} \end{bmatrix}$$

-The Matrix  ${}^0D = {}^0T^T {}^0K$  is

$${}^0D = \begin{pmatrix} {}^0\eta_{11} {}^0K_{11} + {}^0\eta_{21} {}^0K_{21} & {}^0\eta_{11} {}^0K_{12} + {}^0\eta_{21} {}^0K_{22} \\ {}^0\eta_{12} {}^0K_{11} + {}^0\eta_{22} {}^0K_{21} & {}^0\eta_{12} {}^0K_{12} + {}^0\eta_{22} {}^0K_{22} \end{pmatrix}$$

where

$${}^0\eta_{11} = \sum_{k=1}^N \frac{\partial \xi_k}{\partial a_1} x_1, \quad {}^0\eta_{12} = \sum_{k=1}^N \frac{\partial \xi_k}{\partial a_2} x_1, \quad {}^0\eta_{21} = \sum_{k=1}^N \frac{\partial \xi_k}{\partial a_1} x_2, \quad {}^0\eta_{22} = \sum_{k=1}^N \frac{\partial \xi_k}{\partial a_2} x_2$$

${}^0D$  is not in general symmetric.

The scalar  ${}^0H$  is  ${}^0H = b_i I_i = b_1 I_1 + b_2 I_2$  where  $I_i$  are the component of the unit vector in the gravitational direction relative to the adopted referencial frame. And,

$$\nabla_0 {}^0H = \left[ \sum_{k=1}^N \frac{\partial \xi_k}{\partial a_1} (b_1^k I_1 + b_2^k I_2), \quad \sum_{k=1}^N \frac{\partial \xi_k}{\partial a_2} (b_1^k I_1 + b_2^k I_2) \right]^T$$

UPDATED LAGRANGE FORMULATION

-Incremental Strain

$$e_{11} = \frac{\partial \Delta_i u_1}{\partial a_1} + \frac{1}{2} \left[ \left( \frac{\partial \Delta_i u_2}{\partial a_1} \right)^2 + \left( \frac{\partial \Delta_i u_1}{\partial a_1} \right)^2 \right]$$

$$e_{22} = \frac{\partial \Delta_i u_2}{\partial a_2} + \frac{1}{2} \left[ \left( \frac{\partial \Delta_i u_1}{\partial a_2} \right)^2 + \left( \frac{\partial \Delta_i u_2}{\partial a_2} \right)^2 \right]$$

$$e_{12} = \frac{1}{2} \left[ \frac{\partial \Delta_i u_1}{\partial a_2} + \frac{\partial \Delta_i u_2}{\partial a_1} \right] + \frac{1}{2} \left[ \frac{\partial \Delta_i u_1}{\partial a_1} \frac{\partial \Delta_i u_1}{\partial a_2} + \frac{\partial \Delta_i u_1}{\partial a_1} \frac{\partial \Delta_i u_2}{\partial a_2} \right]$$

$$e_{33} = \frac{\Delta u_1}{b_1} + \frac{1}{2} \left( \frac{\Delta_i u_1}{b_1} \right)^2$$

-Linear Strain Displacement Transformation Matrix

Making 
$$e = {}^t B_L \Delta_i u^k$$

where 
$$e^T = (e_{11}, e_{22}, 2e_{12}, e_{33})$$

and

$${}^t B_L = \begin{pmatrix} \frac{\partial \xi_1}{\partial b_1} & 0 & \frac{\partial \xi_2}{\partial b_1} & 0 & \dots & \frac{\partial \xi_N}{\partial b_1} & 0 \\ 0 & \frac{\partial \xi_1}{\partial b_2} & 0 & \frac{\partial \xi_2}{\partial b_2} & \dots & 0 & \frac{\partial \xi_N}{\partial b_2} \\ \frac{\partial \xi_1}{\partial b_2} & \frac{\partial \xi_1}{\partial b_1} & \frac{\partial \xi_2}{\partial b_2} & \frac{\partial \xi_2}{\partial b_1} & \dots & \frac{\partial \xi_N}{\partial b_2} & \frac{\partial \xi_N}{\partial b_1} \\ \frac{\xi_1}{b_1} & 0 & \frac{\xi_2}{b_1} & 0 & \dots & \frac{\xi_N}{b_1} & 0 \end{pmatrix}$$

where 
$$\bar{b}_1 = \sum_{k=1}^N \xi_k b_1^k \quad , \quad N \text{ -number of nodes}$$

## -Non-Linear Strain Displacement Transformation Matrix

$${}^iB_{NL} = \begin{pmatrix} \frac{\partial \xi_1}{\partial b_1} & 0 & \frac{\partial \xi_2}{\partial b_1} & 0 & \dots & \frac{\partial \xi_N}{\partial b_1} & 0 \\ \frac{\partial \xi_1}{\partial b_2} & 0 & \frac{\partial \xi_2}{\partial b_2} & 0 & \dots & \frac{\partial \xi_N}{\partial b_2} & 0 \\ 0 & \frac{\partial \xi_1}{\partial b_1} & 0 & \frac{\partial \xi_2}{\partial b_1} & \dots & 0 & \frac{\partial \xi_N}{\partial b_1} \\ 0 & \frac{\partial \xi_1}{\partial b_2} & 0 & \frac{\partial \xi_2}{\partial b_2} & \dots & 0 & \frac{\partial \xi_N}{\partial b_2} \\ \frac{\xi_1}{b_1} & 0 & \frac{\xi_2}{b_1} & 0 & \dots & \frac{\xi_N}{b_1} & 0 \end{pmatrix}$$

## -Cauchy Stress Matrix and Stress Vector

$${}^i\sigma = \begin{pmatrix} {}^i\sigma_{11} & {}^i\sigma_{12} & 0 & 0 & 0 \\ {}^i\sigma_{21} & {}^i\sigma_{22} & 0 & 0 & 0 \\ 0 & 0 & {}^i\sigma_{11} & {}^i\sigma_{12} & 0 \\ 0 & 0 & {}^i\sigma_{21} & {}^i\sigma_{22} & 0 \\ 0 & 0 & 0 & 0 & {}^i\sigma_{33} \end{pmatrix} \quad {}^i\bar{\sigma} = \begin{pmatrix} {}^i\bar{\sigma}_{11} \\ {}^i\bar{\sigma}_{22} \\ {}^i\bar{\sigma}_{12} \\ {}^i\bar{\sigma}_{33} \end{pmatrix}$$

-The Matrix  ${}^iE = \nabla_i \psi_p$  is

$${}^iE = \begin{pmatrix} \frac{\partial \xi_1}{\partial b_1} & \frac{\partial \xi_2}{\partial b_1} & \frac{\partial \xi_3}{\partial b_1} & \dots & \frac{\partial \xi_N}{\partial b_1} \\ \frac{\partial \xi_1}{\partial b_2} & \frac{\partial \xi_2}{\partial b_2} & \frac{\partial \xi_3}{\partial b_2} & \dots & \frac{\partial \xi_N}{\partial b_2} \end{pmatrix}$$

-The Matrix  ${}^iD = {}^iT {}^iK$  is

$${}^iD = \begin{pmatrix} K_{11} & K_{12} \\ K_{21} & K_{22} \end{pmatrix} = {}^iK$$

${}^iD$  is the symmetric, and the scalar  ${}^iH$  is  ${}^iH = b_i I_i = b_1 I_1 + b_2 I_2$

where  $I_i$  are the components of the unit vector in the gravitational direction relative to the adopted referencial frame. And,

$$\nabla_i H = [I_1, I_2]$$

APPENDIX DMATRICES OF ELASTIC CONSTANTS

For an orthotropic material and with the geometric axes coinciding with the anisotropic axes, the [D] matrix has the form:

$$[D] = \frac{1}{1 - \nu_{yz}^2 - \nu_{zx}^2 - \nu_{xy}^2 - 2\nu_{yz}\nu_{zx}\nu_{xy}} \begin{pmatrix} E_x(1 - \nu_{yz}^2) & E_x(\nu_{yz}\nu_{zx} + \nu_{xy}) & E_x(\nu_{yz}\nu_{xy} + \nu_{zx}) \\ E_y(\nu_{yz}\nu_{zx} + \nu_{xy}) & E_y(1 - \nu_{zx}^2) & E_y(\nu_{zx}\nu_{xy} + \nu_{yz}) \\ E_z(\nu_{yz}\nu_{xy} + \nu_{zx}) & E_z(\nu_{zx}\nu_{xy} + \nu_{yz}) & E_z(1 - \nu_{xy}^2) \\ 0 & 0 & 0 \\ 0 & 0 & 0 \\ 0 & 0 & 0 \end{pmatrix}$$

$$\left. \begin{matrix} 0 & 0 & 0 \\ 0 & 0 & 0 \\ 0 & 0 & 0 \\ (1 - \nu_{yz}^2 - \nu_{zx}^2 - \nu_{xy}^2 - 2\nu_{yz}\nu_{zx}\nu_{xy})G_{yz} & 0 & 0 \\ 0 & (1 - \nu_{yz}^2 - \nu_{zx}^2 - \nu_{xy}^2 - 2\nu_{yz}\nu_{zx}\nu_{xy})G_{zx} & 0 \\ 0 & 0 & (1 - \nu_{yz}^2 - \nu_{zx}^2 - \nu_{xy}^2 - 2\nu_{yz}\nu_{zx}\nu_{xy})G_{xy} \end{matrix} \right\}$$

Because of the symmetry requirement, it follows from [D] that,

$$E_x \nu_{yx} = E_y \nu_{xy} .$$

$$E_y \nu_{zy} = E_z \nu_{yz} .$$

$$E_z \nu_{xz} = E_x \nu_{zx} .$$

when,

$$\nu_{zx} = \nu_{yz} = \nu_h \quad \nu_{xy} = \nu_v,$$

$$E_x = E_y = E_h \quad E_z = E_v,$$

$$G_{zx} = G_{yz} = G_h \quad G_{xy} = G_v$$

The matrix [D] transform to:

$$[D] = \frac{1}{(1 + \nu_v)(1 - \nu_v - 2\nu_h^2)} \begin{pmatrix} E_h(1 - \nu_h^2) & E_h(\nu_v + \nu_h^2) & E_h\nu_h(1 + \nu_v) \\ E_h(\nu_v + \nu_h^2) & E_h(1 - \nu_h^2) & E_h\nu_h(1 + \nu_v) \\ E_h\nu_h(1 + \nu_v) & E_h\nu_h(1 + \nu_v) & E_v(1 - \nu_v^2) \\ 0 & 0 & 0 \\ 0 & 0 & 0 \\ 0 & 0 & 0 \\ 0 & 0 & 0 \\ 0 & 0 & 0 \\ 0 & 0 & 0 \\ (1 + \nu_v)(1 - \nu_v - 2\nu_h^2)G_h & 0 & 0 \\ 0 & (1 + \nu_v)(1 - \nu_v - 2\nu_h^2)G_h & 0 \\ 0 & 0 & (1 + \nu_v)(1 - \nu_v - 2\nu_h^2)G_v \end{pmatrix}$$

To obtain the matrix of elastic constants for an isotropic material the following conditions must be incorporated into the basic matrix [D], that is,

$$\nu_{zx} = \nu_{yz} = \nu_{xy} = \nu,$$

$$G_{zx} = G_{yz} = G_{xy} = G = \frac{E}{2(1 + \nu)},$$

$$E_x = E_y = E_z = E$$

APPENDIX EREFERENCES

ABDEL-HADY, M. and HERRIN, M., 1966. "Characteristics of Soil Asphalt as a Rate Process", J. of the Highway Divison, ASCE, Vol 92, No HW1, pp.49-69.

AMERASINGHE, S.F. and PARRY, R.H.G., 1975. "Anisotropy in Heavily Overconsolidated Kaolin." Journal of the Geo. Eng. Div., ASCE, Vol 101, pp 1277-1293.

ANDERSEN, K. H., POOL, J. H., BROWN, S.F. and ROSENBRAND, W.F., 1980. "Cyclic and Static Laboratory Tests on Drammen Clay". Journal of Geot. Eng. Div., ASCE, vol 106, GT5, pp 499-529.

ARGYRIS, J. H., FAUST, G., SZIMMAT, J., WARNKE, E. P. and WILLIAM, K. J., 1974. "Recent Developments in the Finite Element Analysis of PCVR", Nuclear Engineering and Design No 28, pp.42-75 North-Holland Publishing Co.

ARIS, R., 1962. " Vectors, Tensors, and The Basic Equations of Fluid Mechanics"

ATKINSON, J.H. and BRANSEY, P.L., 1978. "The Mechanics of Soils. An Introduction to Critical State Soil Mechanics." McGraw-Hill, London.

BALADI, G. Y., and SANDLER, I. S., 1980. "Examples of the use of the Cap Model for Stimulating the Stress-Strain Behaviour of Soils", Limit Equilibrium, Plasticity and Generalized Stress-Strain in Geotechnical Engineering, Raymond K. Yong and Hon-Yim Ko (eds), American Society of

Civil Engineering, pp.649.

BALASUBRAMANIAN, A.S., 1969. "Some factors influencing the Stress-Strain Behaviour of Clay." Ph.D.Thesis. University of Cambridge.

BANERJEE, P. K., and BUTTERFIELD, R., 1979."Developments in Boundary Element Methods-1", Appl. Science Publ.

BARRON, R. A., 1948. "Consolidation of Fine-Grained Soils by Drain Wells" , Am. Soc. of Civ. Eng., Transactions, pp. 718-754.

BATHE, K.J., and WILSON, E.L., 1973. "NONSAP- A General Finite Element Program for Non-Linear Dynamic Analysis of Complex Structures." Paper M3/1, Proc. of the 2nd Int. Conf. on Structural Mech. in Reactor Technology, Berlin.

BATHE, K.J., and WILSON, E.L., 1976. "Numerical Methods in Finite Element Analysis." Prentice-Hall, Englewood Cliffs, New Jersey.

BAZANT, Z. P., ANSAL, A. M., and KRIZEK, R. J., 1980. "Critical Appraisal of Endochronic Theory of Soils"; Limit Equilibrium, Plasticity and Generalized Stress-Strain in Geotechnical Engineering, Raymond K. Yong and Ho-Yim Ko (eds), American Society of Civil Engineering, pp.539.

BIOT, M. A., 1939. "Theory of Elasticity with Large Displacement and Rotations", Proc., Fifth Inter. Cong. Appl. Mech. (Cambridge, Mass., Sept. 1938), pp. 117-122, Wiley, New York.

BIOT, M. A., 1941a. "General Theory of Three-Dimensional



Consolidation", J. of Applied Physics, Vol. 12, pp. 155-164.

BIOT, M. A., 1941b. "Consolidation Settlement Under a Rectangular Load Distribution", J. of Applied Physics, Vol. 12, pp. 426-430.

BIOT, M. A., 1955. "Theory of Elasticity and Consolidation for a Porous Anisotropic Solid", J. of Applied Physics, Vol. 26, pp. 182-185.

BIOT, M. A., 1956a. "Theory of Deformation of a Porous Viscoelastic Anisotropic Solid", J. of Applied Physics, Vol. 27, pp.459-567.

BIOT, M. A., 1956b. "General Solution of the Equations of Elasticity and Consolidation for a Porous Material", Transactions, J. of Applied Mechanics, ASME, Vol. 78, pp.91-96.

BISHOP, A. W., 1966. "The Strength of Soils as Engineering Materials", Geotechnique, Vol. 16, pp.91-128.

BISHOP, A.W. and HENKEL, D.J., 1971. "The Measurement of Soil Properties in the Triaxial Test." Edward Arnold, London.

BJERRUM, L., 1971. "Recent Research on the Consolidation and Shear Behaviour of Normally Consolidated Clay." NGI, Internal Report 50302, Oslo.

BJERRUM, L., SIMONS, N. and TORBLAA, I., 1958. "The Effect of Time on the Shear Strength of a Soft Marine Clay." Brussels Conf. on Earth Pressure Problems, Proc. Vol 1.

BOOKER, J. R., 1973. "A Numerical Method for the Solution of Biot's Consolidation Theory", Quaterly J. of Mechanics and Applied Mathematics, Vol. 26, pp.457.

BOOKER, J. R., 1974. "The Consolidation of a Finite Layer Subject to Surface Loading", Int. J. of Solids and Structures, Vol. 10, pp. 1053.

BOOKER, J. R., and SMALL, J. C., 1975. "An Investigation of the Stability of Numerical Solutions of Biot's Equation of Consolidation", Inter. J. of Solids and Structures, Vol. 11, pp.907-917.

BOOKER, J. R., and SMALL, J. C., 1977."Finite Element Analysis of Primary and Secondary Consolidation", Inter. J. of Sollids and Structures, Vol. 13, pp.137-149.

BOOKER, J. R., and SMALL, J. C., 1977. "Methods for Numerical Solution of the Equations of Viscoelasticity", Inter. J. for Numerical and Analytical Methods in Geomechanics, Vol. 1, pp.139-150.

BORESI, A. P., 1965. "Elasticity in Engineering Mechanics". Prentice-Hall, Inc.

BOWEN, R. M., 1976."Theory of Mixtures", Continuum Physics, Vol. III (Ed. Eringen), Academic Press.

BROMS, B.B. and CASBARIAN, A.O., 1965. "Effects of Rotation of the Principal Stress Axes and of the Intermediate Principal Stress on the Shear Strength." Proc. of the 6th. ICSMFE, Montreal, Vol 1, pp 179-183.

BROMS, B.B. and RATNAM, M.V., 1963. "Shear Strength of an anisotropically Consolidated Clay." Div., ASCE, Vol 89, SM6, pp 1-26.

BUISMAN, A. S. K., 1936. "Results of Long Duration Settlement Tests", Inter. Conf. on Soil Mechanics and Foundation Engineering, (Cambridge, Mss.), Proceedings, Vol. 1, pp.103-106.

BURI, P. B., 1978. "Influence of Secondary Consolidation and Overconsolidation on the Behaviour of a Soft Alluvial Clay", Ph.D. thesis, University of London.

BURLAND, J.B., 1967. "Deformation of Soft Clay." Ph.D. Thesis. University of Cambridge.

CALLANDINE, C.R., 1971. "A Microstructural View of the Mechanical Properties of Saturated Clay." Geotechnique, Vol. 21, pp. 391-415.

CARRILLO, N., 1942. "Simple Two and Three-Dimensional Cases in the Theory of Consolidation of Soils", J. of Applied Physics, Vol. 21, pp. 1.

CARNAHAN, B., and others, 1969. "Applied Numerical Methods"

CARSLAW, and JAEGER, 1959. "Conduction of Heat in Solids", Oxford Press.

CARTER, J. P., 1975. "Discussion of Finite Elasto-Plastic Deformation"- I. Theory and Numerical Examples, Vol. 11, pp.1167-1169.

CARTER, J. P., SMALL J. C., and BOOKER J. R., 1977. "A Theory of

Finite Elastic Consolidation", Inter. J. of Solids and Structures, Vol. 13, pp.467-478.

CARTER, J. P., BOOKER J. R., and SMALL J. C., 1979. "The Analysis of Finite Elasto-Plastic Consolidation", Inter. J. for Numerical and Analytical Methods in Geomechanics, Vol. 3, pp.107-129.

CAVOUDINIS, S., 1979. "Two and Three-Dimensional Consolidation and its Solution by Finite Elements", Imperial College - Soil Mech. Section Internal Report.

CHANG, C. S., and DUNCAN, J. M., 1977. "Analysis of Consolidation of Earth and Rockfill Dams", College of Eng., Office of Research Services, University of California, Berkeley, California, 94720, September.

CHRISTIAN, J.T., 1966. "Plane Strain Deformation Analysis of Soils." Contract Report No 3-129, Contract DA-22-079-eng-471, U.S. Army Engineers Waterways Experiment Station, Corps of Engineers, Vicksburg, Mississippi, Dept. of Civil Eng., Massachusetts Inst. of Technology.

CHRISTIAN, J. T., 1968. "Undrained Stress Distribution by Numerical Methods", J. of Soil Mechanics and Found. Div., ASCE, Vol. 94, No. SM4, Proc. Paper 6243, pp.1333-1345.

CHRISTIAN, J. T., and BOEHMER, J. W., 1969. "Plane Strian Consolidation by Finite Element Methods", prepared for the United States Department of Transportation, Washington, D.C. under contract C-85-65, M.I.T., Dep. of Civil Eng., Research Report R.69-60, Soil Mechanics Publication No 243.

CLOUGH, R.W., and WOODWARD, R.J., 1967. "Analysis of Embankment Stresses and Deformations." J. of the Soil Mech. and Found. Div., ASCE, Vol. 93, No SM4, July.

COOK, D. R., 1974. "Concept and Applications of Finite Element Analysis." John Wiley & Sons, Inc.

CORMEAU, I. C., 1975. "Numerical Stability in Quasi-Static Elasto-Viscoplasticity", Int. J. for Num. Mth. in Eng., Vol. 9, pp109-127.

COTTER, B. A. and RIVLIN, R. S., 1955. "Tensor Associated with Time-dependent Stress." Quat. Appl. Math. No 13, pp.117.

CRAWFORD, C.B., 1960. "The Influence of Rate Strain on Effective Stresses in Sensitive Clay." American Society for Testing and Materials. Paper on soils 1959.

CRAWFORD, C.B., 1968a. "Discussion to Session 1, Shear Strength of Soft Clay." Geotec. Conf. on Shear Strength Properties of Natural Soils and Rocks, Oslo, 1967. Proc., Vol. 2, pp. 118.

CRAWFORD, C.B., 1968b. "Quick Clays of Eastern Canada." Eng. Geology, Vol. 2, No 4, pp. 239-265.

CROCKS, J.H.A., and GRAHAM, J., 1976. "Geotechnical Properties of the Belfast Estuarine Deposits." Geotechnique, Vol. 26, pp.293-315.

CROCHET, J., and NAGHDI, P. M., 1966. "On Constitutive Equations for Flow of Fluid Through and Elastic Solid", Int. J. of Eng. Sci., Vol.

4, pp.383-401.

CRYER, C.W., 1963. "A Comparisson of the Three-Dimensional Theories of Biot and Therzaghi." Quaterly J. Mech. and Appl. Math.

DAFALIAS, V. F., HERRMANN, L. R., and De NATALE, J. S., 1980. "Description of Natural Clay Behaviour by Simple Bounding Surface Plasticity Formulation"; Limit Equilibrium, Plasticity and Generalized Stress-Strain in Geotechnical Engineering, Raymond K. Yong and Ho-Yim Ko (eds), American Society of Civil Engineering, pp.711.

DAFALIAS, Y.F., and POPOV, E.P., 1975. "A model of Non-linearly Hardening Materials for Complex Loadings." Acta Mechanica, 21.

DESAI, C. S., and ABEL, J. F., 1972. "Introduction to the Finite Element for Engineering Analysis", van Nostrand Reyhold Company.

DESAI, C. S., and SAXENA, S. K., 1977. "Consolidation Analysis of Layered Anisotropic Foundations", Inter. J. for Numerical and Analytical Methods in Geomechanics, Vol. 1, No 1, pp.5-23.

De CAMPOS, T.M.P., 1984. " Two Low Plasticity Clay under Cyclic and Transient Loading" (2 vols.)- Ph.D. Thesis, University of London.

De SIMONE, P., and VIRGIANNI, C., 1976. "Consolidation of Thick Beds of Clay", Proc., Conference on Numerical Methods in Geomechanics, Ed. C. S. Desai, Blacksburg, U.S.A., pp.1067-1081.

De WET, J. A., 1962. "Three-Dimensional Consolidation", Highway Research Board Bulletin 342, pp.152-175.

Di MAGGIO, F.L. and SANDLER, I.S., 1971. "Material Model for Granular Soils." J. of the Eng. Mech. Div., ASCE, Vol. 97, No EM3, Proc. Paper 8212, June, pp. 935.

DONAGHE, R.T. and TOWNSEND, F.C., 1978. "Effects of Anisotropic Versus Isotropic Consolidation in Consolidated-Undrained Compression Tests of Cohesive Soils." Geotechnical Testing Journal, Vol 1, pp 173-189.

DRUCKER, D. C., GIBSON, R. E., and HENKEL, D., 1957. "Soil Mechanics and Work-Hardening Theories of Plasticity", ASCE Transactions, Vol. 122, Paper No. 2864.

DUNCAN, J. M. and CHANG, C. Y., 1970. "Non-Linear Analysis of Stress and Strain in Soils." ASCE, J. of Soil Mech. and Found. Div., Vol. 96, pp.1629-1653.

DUNCAN, M. J., 1980. "Hyperbolic Stress-Strain Relationships"; Limit Equilibrium, Plasticity and Generalized Stress-Strain in Geotechnical Engineering, Raymond K. Yong and Ho-Yim Ko (eds), American Society of Civil Engineers, pp.443

DUNCAN, J.M. and SEED, H.B., 1966a. "Anisotropy and Stress Reorientation in Clay." Journal of Soil Mech. and Found. Div., ASCE, vol 92, SM5, pp 21-50.

DUNCAN, J.M. and SEED, H.B., 1966b. "Strength Variation Along Failure Surfaces in Clay." Journal of the Soil Mech. and Found. Div., ASCE, Vol 92, SM6, pp 81-104.

DYM, C. L., and SHAMES, I. H., 1973. "A Variational Approach", McGraw-Hill, Inc.

ERINGEN, A. C., and SUHUBI, E. S., 1974. "Elastodynamics", Vol. I - Finite Motions, Academic Press.

ERINGEN, A. C., 1975. "Basic Principles, Continuum Physics", Vol. II, (Ed. Eringen), Academic Press.

FROLICH, O. K., 1934. "Druckverteilung im Baugrund", Springer-Verlag.

GENS, A., 1982. "Stress-Strain and Strength Characteristics of a Low Plasticity Clay", Ph.D. Thesis, University of London.

GHABOUSSI, J., and WILSON, E. L., 1971. "Flow of Compressible Fluid in Porous Elastic Media", Report SESM 71-12, Structural Engineering Laboratory, University of California, Berkeley.

GIBSON, R. E., and LUMB, P., 1953, "Numerical Solution of some Problems in the Consolidation of Clay", J. of Inst. Civil Engineers 1, Part 1, pp.182.

GIBSON, R. E., 1958. "The Process of Consolidation in a Clay Layer Increasing in Thickness with Time", Geotechnique, Vol. VIII, pp.171.

GIBSON, R. E., and LO, K. Y., 1961. "A Theory of Consolidation for Soils Exhibiting Secondary Compression", Norwegian Geotechnical Institute, Publication 41.

GIBSON, R. E., KNIGHT, K., and TAYLOR, P. W., 1963. "A Critical



Experiment to Examine Theory of Three-Dimensional Consolidation", Proc., European Conference on Soil Mechanics and Foundation Engineering, Wiesbaden, Vol. 1, pp.69-76.

GIBSON, R. E, SCHIFFMAN, R. L., and FU, S. L., 1970. "Plane Strain and Axial Symmetric Consolidation of a Clay Layer on a Smooth Impervious Base". Quarterly J. of Mechanics and Applied Mathematics, Vol 23, pp.505-520.

GIBSON, R. E., ENGLAND, G. L., and HUSSEY, M. J. L., 1967. "Theory of One-Dimensional Consolidation of Clays", Geotechnique 17, pp.261-273.

GURTIN, M., 1964. "Variational Principles for Linear Elastodynamics", Archives for Rational Mechanics and Analysis, Vol. 16, No.1, pp.34-50.

GREEN, A. E., and ATKINS, J. E., 1964. "A Contribution to the Theory of Non-Linear Diffusion", Arch. for Rational Mech. and Analysis, Vol. 15, pp. 235-246.

GREEN, A. E., and NAGHDI, P. M., 1965. "A Dynamical Theory of Interacting Continua", Int. J. of Eng. Sci., Vol. 3, pp.231-241.

GREEN, A. E., and STEEL, T. R., 1966. "Constitutive Equations for Interacting Continua", Int. J. of Eng. Sci., Vol. 4, pp.483-500.

GUDEHUS, G., GOLDSCHIEDER, M. and WINTER, H., 1977. "Mechanical Properties of Sand and Clay and Numerical Integration Methods", Ch. 3 of Finite Element in Geomechanics, G. Gudehus (ed), Wiley, London.

HAGMANN, A.J., 1971. "Prediction of Stress and Strain under Drained

Loading Conditions." Ph.D. Thesis, Massachusetts Inst. Technology.

HAMBLY, E.C., 1972. "Plane Strain Behaviour of Remoulded Normally Consolidated Kaolin." *Geotechnique*, vol 22, pp 301-317.

HAMBLY, E.C. and ROSCOE, K.H., 1969. "Observations and Predictions of Stress and Strains During Plane Strain of 'Wet' Clays." *Proc. of the 7th. ICSMFE, Mexico, Vol 1, pp 173-181.*

HARR, M. S., 1967. "Foundations of Theoretical Soil Mechanics", McGraw-Hill Book Company, New York.

HASHIGUCHI, K., 1977. "An Expression of Anisotropy in a Plastic Constitutive Equation of Soils (discussion to H. Sekiguchi and H. Ohta's paper)." *Constitutive equations of soils. Proc. Specialty Session 9, 9th. ICSMFE, Tokyo, pp 302-305.*

HASHIGUCHI, K., 1981. "Constitutive Equations of Elastoplastic Materials with Anisotropic Hardening and Elastic-Plastic Transition." *Journal of Applied Mechanics, ASME, Vol 48, pp 297-301.*

HENKEL, D.J., 1956. "The effect of Overconsolidation on the Behaviour of Clays During Shear." *Geotechnique, Vol 6, pp 139-150.*

HENKEL, D.J., 1958. "Correspondence". *Geotechnique, vol 8, pp 134-136.*

HENKEL, D.J., 1959. "The Relationships Between the Strength, Pore-Water Pressure and Volume Change Characteristics of Saturated Clays." *Geotechnique, Vol 9, pp 119-135.*

HENKEL, D. J., 1960. "The shear Strength of Saturated Remolded Clays", Research, Conf. Shear Strength of Cohesive Soils, ASCE, Boulder, pp.533-554.

HENKEL, D.J. and SOWA, V.A., 1963. "The Influence of Stress History on Stress Paths in Undrained Triaxial Tests on Clay. ASTM, STP 361, pp 280-291.

HERRMAN, L. R.,1965. "Elasticity Equations for Incompressible and Nearly Incompressible Materiala by a Variational Theorem", AIAA J., Vol.3, pp.1896-1900.

HIDELBRAND, F. B., 1976. "Advanced Calculus for Applications", Second edition, Prentice-Hall, Inc., pp.94.

HIGHT, D.W. ,1982. "Laboratory Investigations of Sea-Bed Clays. Ph.D.Thesis. University of London.

HOEG, K., CHRISTIAN, J. T., and WHITMAN, R., 1968. "Settlement of Strip Load on Elastic-Plastic Soil", ASCE, J. of Soil Mech. and Found. Div, Vol. 94 pp.431-435.

HUNTER, S. C., 1976. "Mechanics of Continuous Media", Ellis Horwood Ltd.

HWANG, C. T., MORGENSTERN, N. R., and MURRAY, D. W., 1971. "On Solutions of Plane Strain Consolidation Problems by Finite Element Methods", Canadian Geotechnical J., Vol. 8, pp.109-118.

HWANG, C. T., MORGENSTERN, N. R., and MURRAY, D. W., 1972.

"Applications of Finite Element Method to Consolidation on Problems", Proc., Symposium of Applications of the Finite Element Method in Geotechnical Engineering, Vol.2, pp.739-764.

IRONS, B.M. and AHRMAD, S., 1980. "Techniques of Finite Elements." Ellis Horwood Ltd., Chichester.

JEFFREYS, H., 1979. "Cartesian Tensors", Cambridge University Press.

JENIKE, A. W., and SHIELD, R. T., 1959. "On the Plastic Flow of Coulomb Solids Beyond Original Failure", J. of Applied Mechanics, December, pp. 599-602.

JOSSELIN DE JONG, G., 1957. "Application of Stress Functions to Consolidation Problems", Proceedings, Fourth International Conference on Soil Mechanics and Foundation Engineering", Vol. 1, pp.320-323.

JOSSELIN DE JONG, G., and VERRUIJT, A., 1965. "Primary and Secondary Consolidation of a Spherical Clay Sample" Proc., Sixth International Conference on Soil Mechanics and Foundation Engineering, Vol. 1, pp.190-195.

KHERA, R.P. and KRIZEK, R.J., 1967. "Strength Behaviour of an Anisotropically Consolidated Remoulded Clay." Highway Research Record, 190, pp 8-18.

KOLYMBAS, D., and GUDEHUS, G., 1980. "A Constitutive Law for Sands and Clays- Position, Prediction, and Evaluation"; Limit Equilibrium, Plasticity and Generalized Stress-Strain in Geotechnical Engineering,

Raymond K. Yong and Hon-Yim Ko (eds), American Society of Civil Engineers, pp.839.

KOPPEJAN, A. W., 1948. "A Formula Combining the Terzaghi Load Compression Relationship and the Buisman Secular Time Effect", Inter. Conference on Soil Mechanics and Foundation Engineering, Proc., Vol. 3, pp.32-37.

KOUTSOFTAS, D.C., 1981. "Undrained Shear Behaviour of a Marine Clay." Laboratory Shear Strength of Soil." ASTM, STP 740, pp 254-276.

KRAVTCHENKO, J., and SIRIEYS, P. M. (eds), 1966. "Rheology and Soil Mechanics" , Symposium Grenoble, April 1-8, 1964. Springer-Verlag Publ.

KRIEG, R.D., 1975. "A Practical Two Surface Plasticity Theory." Journal of Applied Mechanics, ASCE, vol.97, pp 641-646.

LACASSE, S., 1979. "Effect of Load Duration on Undrained Behaviour of Clay and Sand-Literature Survey." NGI, Oslo, Internal Report 40007-1.

LADD, C.C., 1965. "Stress-Strain Behaviour of Anisotropically Consolidated Clays During Undrained Shear." Proc. of the 6th. ICSMFE, Montreal, Vol.1, pp 282-286.

LADD, C.C., BOVEE, R.B., EDGERS, L. and RIXNER, J.J., 1971. "Consolidated-Undrained Plane Strain Tests on Boston Blue Clay." Dept. of Civil Eng., Research Report R71-13, MIT.

LADD, C.C. and EDGERS, L., 1972. "Consolidated-Undrained Direct-Simple Shear Tests on Saturated Clays." Dept. of Civil Eng., Research Report, R72-82, MIT.

LADD, C.C., FOOTT, R., ISHIHARA, K., POULOS, H.G. and SCHLOSSER, F., 1977. "Stress-deformation and Strength Characteristic." State-of-the-art Report for Session I. Proc. of the 9th ICSMFE, Tokyo, Vol. 2.

LADD, C.C. and LAMBE, T.W., 1963. "The Strength of 'Undisturbed' Clay Determined from Undrained Tests." ASTM, STP 361, pp 342-371.

LADD, C.C. and VARALLYAY, J., 1965. "The Influence of Stress System on the Behaviour of Saturated Clays During Undrained Shear." Dept. of Civil Eng. Research Report, 65-11, MIT.

LADD, C.C., WILLIAMS, C.E., CONNELL, D.H., and EDGERS, L., 1972. "Engineering Properties of Soft Foundation Clays at Two South Louisiana Levee Sites." Dept. of Civil Eng. Research Report R72-26, MIT.

LADE, P. V., and DUNCAN, J. M., 1973. "Cubical Triaxial Tests on Cohesionless Soil", J. of the Soil Mechanics and Found. Div., ASCE, Vol. 99, No. SM10, Proceedings Paper 10057, October, pp. 793-812.

LADE, P.V. and MUSANIE, H.M. , 1977. "Failure Conditions in Sand and Remoulded Clay." Proc. of the 9th. ICSMFE, Tokyo, Vol.1, pp 181-186.

LAMBE, T. W., 1967. "Stress Path Method", ASCE, J. of Soil Mech. and Found. Div., Vol. 93, No. SM6, pp.309-301.

LAMBE, T. W., and WHITMAN, R. V., 1979. "Soil Mechanics", Civil Engineering Library.

LEE, K.L. and MORRISON, R.A., 1970. "Strength of Anisotropically Consolidated Compacted Clay." J. of the Soil Mech. and Found. Eng. Div., ASCE, Vol. 96.

LE LIEVRE, B. 1967. "The Yielding and Flow of Cohesive Soils in Triaxial Compression." Ph.D.Thesis. Waterloo University.

LE LIEVRE, B. and WONG, B. , 1970. "Discussion to 'Stress-Probe Experiments on Saturated Normally Consolidated Clay' by P.I. Lewin and J. B. Burland. Geotechnique, Vol.20, pp 461-463.

LEON, J.L. and ALBERRO, J., 1972. "Extension and Compression Tests on Mexico City Clay." Proc. the 9th. ISCMFE, Tokyo, Vol.1, pp 193-196.

LEROUEIL, S., TAVENAS, F. and FRANCOISE, B., 1979. "Behaviour of Destructured Natural Clays." J. of the Geot. Eng. Div., ASCE. Vol. 105, GT6.

LEWIN. P.I., 1971. "Three-dimensional Anisotropic Consolidation of Clay and the Relationship between Plane Strain and Triaxial Test Data." RILEM Symposium on the Deformation and Failure of Solids Subjected to Multiaxial Stress, Cannes.

LEWIN, P.I., 1973. "The Influence of Stress History on the Plastic Potential." Symp. on 'The role of plasticity in Soil Mechanics',

Cambridge, pp 96-106.

LEWIN, P.I., 1975. "Plastic Deformation of Clay with Induced Anisotropy." Proc. of the Istanbul Conf. on SMFE.

LEWIN, P.I., 1978. "The Deformation of Soft Caly Under Generalized Stress Conditions." Ph.D.Thesis. University of London.

LEWIN, P.I., YAMADA, Y. and ISHIHARA, K., 1982. "Correlating Drained and Undrained Three-dimensional Tests on Loose Sand." IUTAM Conf. on Def. an Failure of Granular Materials, Delft. Aug/Sept.

LEWIN, P.I. and BURLAND, J.B., 1970. "Stress-Probe Experiments on Saturated Normally Consolidated Clay." Geotechnique, Vol. 20, pp 38-56.

LOVENBURY, H. T., 1969. "Creep Characteristics of London Clay", Ph.D. Thesis , London University.

LUSCHER, U., 1965. "Discussion on Eletric Analogs in Time Settlement Problems ", ASCE, J. of Soil Mechanics and Foundations Division, Vol. 91, No. Sml, pp.190-195.

MALVERN, L. E., 1969. "Introduction to the Mechanics of a Continuous Medium" , Prentice-Hall, Englewood Cliffs.

MANDEL, J., 1953. "Consolidation de Sols (Etude Mathematique)", Geotechnique, Vol. III, pp.287-299.

MANDEL, J., 1957. "Consolidation de Couches d'Argiles", Inter.



Conference on Soil Mechanics and Foundation Engineering, Proc., Vol. 1, pp.360-367.

MATSUOKA, H., 1974. "Stress-Strain Relationship of Sand Based on the Mobilized Plane, Soils and Foundations, Vol. 14, No 2.

MATSUMOTO, T., 1976. "Finite Element Analysis of Immediate and Consolidation Deformations Based on Effective Stress Principle", Soils and Foundations, Vol. 16, No. 4.

McNABB, A., 1960. "A Mathematical Treatment of One-Dimensional Soil Consolidation", Quaterly of Applied Mathematics, Vol. 17, No. 4, pp.337-347.

McNAMEE, J., and GIBSON, R. E., 1960. "Displacement Functions and Linear Transforms Applied to Diffusion Through Porous Elastic Media", Quaterly J. of Mechanics and Applied Mathematics, Vol. 13, pp.98-111 and pp.210-227.

MESRI, G. and ROKHSAR, A., 1974. "Theory of Consolidation for Clays", J. Geotechnical, Engineering Division, Proc., American Society of Civil Engineers, pp.889-904.

MITCHELL, J.K., 1970. "On the Yielding and Mechanical Strength of Leda Clays." Canadian Geotechnical Journals, Vol. 7.

MITCHELL, J. K., 1976. "Fundamentals of Soil Behaviour", John Wiley & Sons, Inc.

MITACHI, T. and KITAGO, S., 1976. "Change in Undrained Shear Strength Characteristics of Saturated Remoulded Clay due to Swelling." *Soils and Foundations*, vol.16, no.1, pp 45-58.

MITACHI, T. and KITAGO, S., 1979. "The Influence of Stress-Strain-Strength Properties of Saturated Clay." *Soils and Foundations*, vol.19, no.2, pp 45-61.

MITACHI, T. and KITAGO, S., 1980. "Undrained Triaxial and Plane Strain Behaviour of Saturated Remoulded Clay." *Soils and Foundations*, Vol. 20, no.1, pp 13-28.

MIZUNO, E., and CHEN, W. F., 1980. "Plasticity Models for Soils-Theory and Calibration"; *Limit Equilibrium, Plasticity and Generalized Stress-Strain in Geotechnical Engineering*, Raymond K. Yong and Hon-Yim Ko (eds), American Society of Civil Engineers, pp.553.

MONTE, L. L., and KRIZEK, R. J., 1976. "One-Dimensional Mathematical Model for Large Strain Consolidation", *Geotechnique*, No. 26, pp.495-510.

MROZ, Z., 1967. "On the Description of Anisotropic Work Hardening", *J. Mech. Phys. Solids* 15, pp.163-175.

MROZ, Z., MORRIS, V. A., and ZIENKIEWICZ, O. C., 1978a. "An Anisotropic Hardening Model for Soils and its Application to Cyclic Loading". *Int. J. Numerical Analyses Methods in Geomechanics* 2, pp.203-221.

MROZ, Z., MORRIS, V. A., and ZIENKIEWICZ, O. C., 1978b. "Stimulation of Behaviour of Soils under Cyclic Loading by Using a More General Hardening Rule", University College of Swansea Report.

MROZ, Z., NORRIS, V. A., and ZIENKIEWICZ, O. C., 1979. "Application of an Anisotropic Hardening Model in the Analysis of Elasto-Plastic Deformation of Soils", *Geotechnique* 29, No. 1, pp.1-34.

MURAYAMA, S., and SHIBATA, T., 1958. "On the Rheological Characteristics of Clays", Part I, Bulletin No. 26, Disaster Prevention Research Institute, Kyoto, Japan.

NAGDHI, P.M., and MURCH, S., 1974. "On the Mechanical Behaviour of Viscoelastic-Plastic Solids." *J. Appl. Mech.*, 30.

NAMY, D., 1970. "An Investigation of Certain Aspects of Stress-Strain Relationship for Clay Soils." Ph. D. Thesis. Cornell University.

NAYAK, G. C., and ZIENKIEWICZ, O. C., 1972. "A Convenient Form of Invariants and its Applications in Plasticity", *Proc. ASCE* 98 EM No. ST4, pp.949-954.

NAYLOR, D. J., PANDE, G. N., SIMPSON, B., and TABB, R., 1981. "Finite Element in Geotechnical Engineering", Pineridge Press.

NELSON, I. and BARON, M. L., 1971. "Application of Variable Moduli Models to Soil Behaviour", *Int. J. of Solids and Structures*, Vol. 7,

pp.399-417.

NEWLAND, P.L., 1975. "Experimental Study of the Stress Strain Characteristic of a 'Wet' Clay and Their Relevance to Settlement Analysis." Part 1. The State Boundary Surface. Australian Geomechanics Journal, Vol. G5, no.1, pp 10-19.

NOORANY, I. and SEED, H.B., 1965. "In-Situ Strength Characteristics of Soft-Clay." Journal of the Soil Mech. and Found. Div., ASCE, SM2, Vol. 91, pp 49-80.

OHMAKI, S., 1979. "A Mechanical Model for the Stress-Strain Behaviour of Normally Consolidated Cohesive Soil." Soils and Found., Vol. 19, No 3.

OHMAKI, S., 1980. "A Stress-Strain Relationship of Normally Consolidated Cohesive Soil under General Stress Condition." Soils and Found., Vol. 20, No 1.

OHMAKI, S., 1982. "Stress-Strain Behaviour of Anisotropically, Normally Consolidated Cohesive Soil." Proc. of the Int. Symp. on Numerical Models in Geomechanics, Zurich.

OLDROYD, J. G., 1950. "On the Formulation of Rheological Equations of State." Proc. Royal Society A, 200.

OLSON, R.E., 1962. "The Shear Strength Properties of Calcium Illite." Geotechnique, vol.12, pp 23-43.

OSAIMI, A. E., 1977. "Finite Element Analysis of Time Dependent Deformations and Pore-Pressure in Excavations and Embankments", Geotechnical Engineering Report, Dep. Civil Engineering, Stanford University, No. CE-216.

OVANDO-SHELLEY, E., 1984. "Internal Report in preparation." Imperial College.

PALMER, A. C., and PIERCE, J. A., 1973. "Plasticity Theory Without Yield Surfaces" , Proc. Symp. Plasticity and Soil Plasticity, Cambridge, pp. 108-126.

PANDE, G. N., and ZIENKIEWICZ, O. C., 1982. "Soil Mechanics- Transient and Cyclic Loads", John Wiley & Sons.

PARRY, R.H.G., 1960. "Triaxial Compression and Extension Tests on Remoulded Saturated Clay". Geotechnique, vol.10, pp 166-180.

PARRY, R.H.G., 1971. "Undrained Shear Strength in Clays." Proc. of the 1st. Australian-New Zealand Conf. on Geomechanics.

PARRY, R.H.G. and NADARAJAH, V., 1974. "Observations on Laboratory Prepared Lightly Overconsolidated Specimens of Kaolin." Geotechnique, Vol. 24, pp 345-358.

PEARCE, J.A. ,1970. "The Behaviour of a Soft Clay in a New True Triaxial Apparatus." Ph.D.Thesis. University of Cambridge.

PEARCE, J.A. , 1971. "A New True Triaxial Apparatus." Stress-Strain

Behaviour of Soils. Proc. of the Roscoe Memorial Symp., Cambridge, pp 330-339.

PENDER, M. J., 1978. "A Model for the Behaviour of Over-Consolidated Clay", Geotechnique 28, No. 1, pp.1-25.

PENDER, M.J., PARRY, R.H.G. and GEORGE, P.J., 1975. "The Response of a Soft Clay Layer to Embankment Loading." Proc. of the 2nd. Australian-New Zealand Conf. in Geom., Brisbane, pp. 169-183.

PERZYMA, P., 1966. "Fundamental Problems in Viscoplasticity", Advances in Appl. Mech., Vol. 9, pp.243-377.

PIETRUSZCZAK, St., and MROZ, Z., 1979. "Description of Mechanical Behaviour of Anisotropically Consolidated Clays", Proc. Euromech. Coll. Anisotropy in Mechanics, Grenoble, Noordhoff Int. Publ.

POTTS, D. M., and GENS, A., 1982. "The Effect of the Plastic Potential in Boundary Value Problems Envolving Plane Strain Deformation." Int. J. for Num. and Anal. Meth. in Geom., Vol. 8, pp. 259-286.

PRAEGER, W., 1961. "An Elementary Discussion of Definitions of Stress Rate", Quat. of Appl. Maths., Vol. XVIII, pp.403-407.

PREVOST, J.H. and HOEG, K., 1975. "Effective Stress-Strain-Strength Model for Soils." J. of the Geotechnical Eng. Div., ASCE, Vol. 101, No GT3, Proc. Paper 11157, March.

PREVOST, J. H., 1977. "Mathematical Modelling of Monotonic and Cyclic

Undrained Clay Behaviour", Int. J. Numerical Analysis Methods in Geomechanics 1, pp.195-216.

RENDULIC, L., 1936. "Porenziffer und Poren Wasserdruck in Tonen.", Der Bauingenieur, Vol. 17, pp. 559-564.

RENDULIC, L., 1936. "Relation Between Void Ratio and Effective Principal Stress for a Remoulded Silty Clay." Proc. of the 1st. ICSMFE, Harvard, Vol.3, pp 48-51.

RENDULIC, L., 1937. "Ein Grundgesetz der Tonmechanik und sein Experimenteller Beweis." Bauingenieur, 18, pp 459-467.

RICHARDSON, A.M. and WHITMAN R.V., 1963. "Effect of Strain-Rate upon Undrained Shear Resistance of a Saturated Remoulded Fat Clay." Geotechnique, Vol. 13, No 4.

RICHART, F. E. Jr., 1959. "Review of the Theory for Sand Drains", Transactions, ASCE, Vol. 124, pp.709-739.

ROSCOE, K.H. and BURLAND, J.B., 1968. "On the Generalized Stress-Strain Behaviour of 'Wet' Clay." Engineering Plasticity, Heyman, J. and Leckie, F.A. (eds), Cambridge University.

ROSCOE, K.H. and POOROOSHASB, H.B., 1963. "A Theoretical and Experimental Study of Strains in Triaxial Compression on Normally Consolidated Clays." Geotechnique, vol.13, pp 12-38.

ROSCOE, K.H., SCHOEFIELD, A.N. and WROTH, C.P. , 1958. "On the

Yielding of Soils." Geotechnique, Vol. 8, pp 22-53.

ROSCOE, K.H., SCHOFIELD, A.N. and WROTH, C.P. , 1959.  
"Correspondence". Geotechnique, vol 9, pp 72-82.

ROSCOE, K. H., and SCHOFIELD, A. N., 1963. "Mechanical Behavior of an Idealized 'Wet Clay'", Proc. of the 2nd European Conference on Soil Mechanics, Wiesbaden, Vol. I, pp.47-54.

ROSCOE, K. H., SCHOFIELD, A. N., and THURAIRAJAH, A., 1963. "Yielding of Clays in States Wetter than Critical", Geotechnique, Vol. 13, No. 13, No. 3, pp.211-240.

ROSCOE, K.H. and THURAIRAJAH, A. , 1964. "On the Uniqueness of Yield Surfaces for 'Wet' Clays." Proc. IUTAM Symp. on Rheology and Soil Mech., Grenoble, pp 364-384.

RUNESSON, K., 1978. "On Non-Linear Consolidation of Soft Clay", Publ. 78:1 Department of Structural Mechanics Chalmers University of Technology.

SALEEB, A. F., and CHEN, W. F., 1980. "Non Linear Hyperelastic (Green) Constitutive Models for Soils : Theory and Calibration", Limit Equilibrium , Plasticity and General Stress-Strain in Geotechnical Engineers, pp.492-527.

SANDHU, R. S., 1968. "Fluid Flow in Saturated Porous Elastic Media", University of California.



SANDHU, R. S., and WILSON, E. L., 1969. "Finite Element Analysis of Seepage in Elastic Media", J. of Engineering Mechanics Division, ASCE, Vol. 95, No. SM3, Proceeding Paper 6615, pp.641-652.

SANDHU, R. S., and PISTER, K., 1970. "A Variational Principle for Linear , Coupled Field Problems in Continuum Mechanics", Int. J. of Eng. Sci., Vol. 8, pp.989-999.

SANDHU, R. S., 1976."Variational Principles for Finite Element Analysis of Consolidation" , Sec. Int. Conf. on Num. Meth. in Geomech., Virginia Polytechn. Inst. and State Univ., pp.20-40.

SCHIFFMAN, R. L., 1959. "The Use of Visco-Elastic Stress-Strain Laws in Soil Testing", ASTM, Special Tech. Pub. No 254, pp.131-155.

SCHIFFMAN, R. L., CHEN, A., and JORDAN, J., 1964. "An Analysis of Consolidation Theories", ASCE, J. of Soil Mech. and Found. Div., Vol. 95, SM1, pp.285-312.

SCHIFFMAN, R. L., and GIBSON, R. E., 1964. "Consolidation of Non-Homogeneous Clay Layers", ASCE, J. of Soil Mechanics and Foundations Division, Vol. 90 No. SM5, pp.1-30.

SCHIFFMAN, R. L., et al, 1969, "An Analysis of Consolidation Theories", J. of Soil Mechanics, Foundation Division, ASCE, Vol. 95, pp.285-312.

SCHOFIELD, A.N. and WROTH, C.P., 1968. "Critical State Soil

Mechanics." McGraw-Hill, London.

SCHMIDT, E., 1924. "Über Die Anwendung der Differenzen Rechnung auf Technische Anheiz- und - Abkühlungs Probleme, A. Foppl Festschrift." Springer-Verlag OHG, Berlin.

SEKIGUCHI, H. and OHTA, H., 1977. "Induced Anisotropy and Time Dependency in Clays. Constitutive Equations of Soils." Proc. Specialty Session 9, 9th. ICSMFE, Tokyo, pp 229-238.

SHMERTMANN, J.H., 1975. "Measurement of in Situ Shear Strength; State-of-the-art report." American Soc. Civil Eng.. Specialty Conference on In Situ Measurement of Soil Properties. Raleigh, N.C. 1975. Proc., Vol. 2, pp. 57-138.

SIGH, A. and MITCHELL, J.K., 1968. "General Stress-Strain-Time Function for Soils", J. of the Soil Mech. and Found. Division-ASCE, Vol. 94, SM1.

SIMONS, N.E., 1960a. "Comprehensive Investigations of the Shear Strength of an Undisturbed Drammen Clay." Proc. Res. Conf. on Shear Strength of Cohesive Soils, ASCE, Boulder, pp 727-745.

SIMONS, N.E., 1960b. "The Effect of Overconsolidation on the Shear Strength Characteristics of an Undisturbed Oslo Clay." Proc. Res. Conf. on Shear Strength of Cohesive Soils, ASCE, Boulder, pp 747-763.

SKETCHLEY, C.J. and BRANSBY, P.L. , 1973. "The Behaviour of an Overconsolidated Clay in Plane Strain." Proc. of the 8th. ICSMFE,

Moscow, vol.1, pp 377-384.

SMITH, I.M., 1976. "Some Time-dependent Soil-Structure Interaction Problems." Proc. of NMSR 75, Inst. fur Bodenmech. und Felsmec. Univ. Karlsruhe, Karlsruhe.

SMITH, I.M., 1977. "Transient Phenomena of Offshore Foundations." Int. Symp. on Num. Meth. in Offshore Eng., Swansea.

SMITH, I.M. , 1982. "Programming the Finite Element Method with Application to Geomechanics.", John Willey & Sons.

SMITH, I.M., SIEMENIENIUCH, J.L., and GLADWELL, I., 1977. "Evaluation of Noersett Methods for Integrating Differential Equations in Time." Int. J. on Num. Meth. in Geomech.

SMITH, R.E. and WAHLS, H.E., 1969. "Consolidation under Constant Rate of Strain , Journal of the Soil Mech. and Found. Div., ASCE, vol.95, SM2, pp 519-539.

SPIEGEL, M. R., 1965. "Theory and Problems of Laplace Transforms", Schaum's Outline Series.

SPIEGEL, M. R., 1971. "Theory and Problems of Advanced Mathematics for Engineers and Scientists", Schaum's Outline Series.

SMALL, J. C., BOOKER, J. R., and DAVIS, E. H., 1976. "Elasto-Plastic Consolidation of Soil", Inter. J. of Solid Structures, Vol. 12, pp.431-448.

SKEMPTON, A. W., and BJERRUM, L., 1957. "A Contribution to the Settlement Analysis of Foundation on Clay", *Geotechnique*, Vol. VII, pp.168-178.

SMILES, D. E., and POULOS, H. G., 1969. "The One-Dimensional Consolidation of Columns of Soil of Finite Length", *Australian J. of Soil Research*, Vol. 7, pp.285-291.

SUKLJE, L., 1977. "Stresses and Strains in Non-Linear Viscous Soils", Civil Eng. Dep., University of Ljubljana, Ljubljana.

TABBADOR, F., and LITTLE, R., 1971. "Interacting Continuous Medium Composed on an Elastic Solid and an Incompressible Newtonian Fluid", *Int. J. of Solids and Struct.*, Vol. 7, pp.825-841.

TAKAHASHI, M., 1981. "Transient and Cyclic Behaviour of a Sand Clay." Ph.D. Thesis. University of London.

TAN, T. K., 1957a. "Three-Dimensional Theory on the Consolidation and Flow of Clay-Layers", *Scientia Sinica*, Vol. 6, No. 1, pp.203-215.

TAN, T. K., 1957b. "Two-Dimensional Problems of Consolidation and Flow of Clay Layers", *Acta Mechanica Sinica*, Vol. 2, No. 1.

TATSUOKA, F., 1980. "Stress-Strain Behaviour of an Idealized Anisotropic Granular Material." *Soils and Found.*, 20(3), pp. 75-90.

TAVENAS, F., 1981. "Some Aspects of Clay Behaviour and Their

Consequences on Modelling Techniques." Lab. Shear Strength of Soil, ASTM, STP 740, pp. 667.

TAVENAS, F., DES ROSIERS, J.P., LEROUEIL, S., LA ROCHELLE, P. and ROY, M., 1979. " The Use of Strain Energy as a Yield and Creep Criterion for Lightly Overconsolidated Clays." Geotechnique, Vol.29, pp.285-303.

TAVENAS, F., and LEROUEIL, S., 1977. "Effects of Stresses and Time on Yielding of Clays." Proc. of the 9th. ICSMFE, Tokyo, Vol.1, pp.319-326.

TAVENAS, F. and LEROUEIL, S.,1979a. "Clay Behaviour and the Selection of Design Parameters." Proc. of the 7th Eur. Conf. SMFE, Brighton, Vol. 1.

TAVENAS, F. and LEROUEIL, S., 1979b. "Les Concepts d'Etat Limite et d'Etat Critique et Leurs Applications Pratiques a l'Etude des Argiles." Revue Francaise de Geotechnique, No 6.

TAYLOR, D. N., 1942. "Research on Consolidation of Clays", M.I.T., Department of Civil and Sanitary Engineering(Cambridge, Mass.), Serial 82, pp.147.

TAYLOR, D. N., and MERCHANT, W., 1940. "A Theory of Clay Consolidation Accounting for secondary Compression" J. of Mathematics and Physics, Vol. 19, No. 3, pp.167-185, Department of Civil and Sanitary Engineering, M.I.T. (Cambridge, Mass.), serial 82.

TERZAGHI, K.,1923. "Die Berechnung Der Durchlasaiekut-Sziffer des

Tones aus dem Verlauf der Hydrodynamischen Spannungserscheinungen", original paper published in 1923 and reprinted to Theory and Practice in Soil Mechanics, New York, John Wiley & Sons, pp.133-146.

TERZAGHI, K., 1943. "Theoretical Soil Mechanics", Wiley & Sons.

TRUESDELL, C., 1955. "The Simplest Rate Theory of Pure Elasticity." Communications on Pure and Appl. Math., Vol. 8.

TRUESDELL, C., and NOLL, W., 1965. "The Non-Linear Field Theories of Mechanics ." Encyclopedia of Physics, Springer-Verlag, Berlin Vol III/3.

VAID, Y. P. and CAMPANELLA, R.G., 1974. "Triaxial and Plane Strain Behaviour of Natural Clays." Journal of the Geot. Eng. Div., ASCE, Vol 100, pp 207-224.

VAID, Y.P. and CAMPANELLA, R.G., 1977. "Time-Dependent Behaviour of Undisturbed Clay." Journal of the Geot. Eng. Div., ASCE, Vol 103, GT7, pp 693-709.

Van Eekelen, H.A.M., and POTTS, D.M., 1978. "The Behaviour of Drammen Clay Under Cyclic Loading". Geotechnique 28, No. 2, pp.173-196.

VAUGHAN, P.R., 1971. "Undrained Failure of Clay Embankments." Stress-Strain Behaviour of Soils. Proc. Roscoe Memorial Symp., Cambridge, pp 683-691.

VAUGHAN, P.R., DAVACHI, M.M., EL-GHAMRAWY, M.K., HAMZA, M.M., and HIGHT, D.W., 1976. "Stability Analysis of Large Gravity Structures."

Proc. of the 1st Int. Conf. Behaviour of Off-Shore Struct., Trondheim, Vol 1, pp 467-487.

VERRUIJT, A., 1972. "Solution of Transiente Groundwater Flow Problems by the Finite Element Method", Water Resources Research, Vol. 8, pp.725-727.

VERRUIJT, A., 1977. "A Variational Principle and a Computer Program for the Solution of Plane Strain Consolidation Problem", Finite Elements in Geomechanics, Edited by G. Gudehus.

WASHIZU, K., 1968. "Variational Methods in Elasticity and Plasticity", Int. Series of Monographs in Aeronautics and Astronautics, Div. I, Solid and Struct. Mech., Vol. 9.

WESLEY, L.D., 1975. "Influence of Stress Path and Anisotropy of the Behaviour of Soft Alluvial Clay. Ph.D.Thesis. University of London.

WHITMAN, R.V., LADD, C.C. and DACRUZ, P., 1960. "Discussion on Session 3," Res. Conf. on Shear Strength of Cohesive Soils, ASCE, Boulder, pp 1049-1056.

WISSA, A.E.Z., CHRISTIAN, J.T., DAVIS, E.H. and HEIBERG, S. , 1971. "Consolidation at Constant Rate of Strain," Journal of the Soil Mech. and Found. Div., ASCE, Vol. 97, SM10, pp 1393-1413.

WONG, P.K.K. and MITCHELL, R.J., 1975. "Yielding and Plastic Flow of Sensitive Cement Clay." Geotechnique, Vol. 25.

WOOD, D.M. , 1973. "Truly Triaxial Stress-Strain Behaviour of Kaolin."

Proc. Symp. on 'The Role of Plasticity in Soil Mechanics', Cambridge, pp 67-93.

WOOD, D.M. , 1975. "Explorations of Principal Stress Space with Kaolin in a True Triaxial Apparatus." Geotechnique, Vol 25, pp 783-797.

WOOD, D.M. , 1981. "True Triaxial Tests on Boston Blue Clay." Proc. of the 10th. ICSMFE, Stockholm, Vol 825-830.

WOOD, D.M. and WROTH, C.P., 1977. "Some Laboratory Experiments Related to the Results of Pressuremeter Tests." Geotechnique, Vol 27, pp 181-201.

WU, T.H., LOH, A.C. and MALVEN, L.E., 1963. "Study of Failure Envelope of Soils." Journal of the Soil Mech. and Found. Div., ASCE, Vol 89, SM1, pp 131-143.

YAMADA, Y. and ISHIHARA, K., 1982. "Modelling of Drained Deformation of Sand under Three-dimensional Stress Conditions." IUTAM Conf. on Deformation and Failure of Granular Materials, Delft.

YOKOO, Y., YAMAGATA, K., and NAGAOKA, H., 1974. "Finite Element Analysis of Consolidation Following Undrained Deformation", Soils and Foundations, Vol. 11, pp.37-58.

YONG, R.N. and MCKYES, E., 1967. "Yielding of Clay in a Complex Stress Field." Proc. of the 3rd. Pan Am. Conf. SMFE, Venezuela, Vol 1, pp 131-143.

YONG, R.N. and MCKYERS, E., 1971. "Yield and Failure of a Clay under



Triaxial Stresses." J. of the Soil Mech. and Found. Div., ASCE, Vol. 97, SM1.

YUDHBIR, MATHUR, S.K. and KUGANATHAN, V., 1978. "Critical State Parameters ." Journal of the Geot. Eng. Div., ASCE, Vol 104, GT4, pp 497-501.

ZARETSKII, Y.K., 1967." Theory of Soil Consolidation." Israel Program for Scientific Translations.

ZEEVAERT, L., 1958. "Consolidation de la Arcilla de la Ciudad de Mexico", American Society for Testing Materials, Special Technical Publication 232, pp.18-27.

ZIENKIEWICZ, O.C. and CORMEAU, I.C. 1974. "Viscoplasticity, Plasticity and Creep in Elastic Solids, A Unified Numerical Solution Approach." Int. J. for Num. Meth. in Eng., Vol. 8.

ZIENKIEWICZ, O. C., and NAYLOR, D. J., 1972. "Adaptation of Critical State Soil Mechanics for Use in Finite Elements", Stress-Strain Behavior of Soils, Parry, H. G., Poulos, G. T., and Co. (ed), pp.537-547.

ZIENKIEWICZ, O. C., HUMPHESON, C., and LEWIS, R. W., 1975. "Associated and Non-Associated Viscoplasticity in Soil Mechanics", C/R/ 249/75, Swansea.

ZIENKIEWICZ, O. C., and PANDE, G. N., 1975."Some useful Forms of Isotropic Yield Surfaces for Soil and Rock Mechanics", Int. Symp. Numerical Methods in Soil and Rock Mechanics (ed. Gudehus, G.), John

Wiley & Sons.

ZIENKIEWICZ, O. C., 1977. "The Finite Element Method", McGraw-Hill  
Book Co.